SCUOLA DI DOTTORATO
UNIVERSITÀ DEGLI STUDI *MEDITERRANEA* DI REGGIO CALABRIA
DIPARTIMENTO DI INGEGNERIA CIVILE, DELL'ENERGIA, DELL'AMBIENTE E DEI MATERIALI (DICEAM)

DOTTORATO DI RICERCA IN
INGEGNERIA DELLE INFRASTRUTTURE E DELLA MOBILITÀ
S.S.D. ICAR/04
XXIX CICLO

REVIEW OF DESIGN METHODS AND FEM ANALYSIS OF UNPAVED ROADS REINFORCED WITH GEOSYNTHETICS

PHD STUDENT:
Rocco Palamara

TUTOR:
Prof. Giovanni Leonardi

CO-TUTOR:
PROF. NICOLA MORACI
PHD. LIDIA SARAH CALVARANO

HEAD OF THE DOCTORAL SCHOOL
Prof. Felice Arena

REGGIO CALABRIA, 2017

This page has been intentionally left blank

ROCCO PALAMARA

REVIEW OF DESIGN METHODS AND FEM ANALYSIS OF UNPAVED ROADS REINFORCED WITH GEOSYNTHETICS

This page has been intentionally left blank

Abstract

The geosynthetics are widely used in mechanically stabilization of unpaved roads with a low volume of traffic. The practical use of geosynthetics above a weak subgrade or within a base course has demonstrated the benefit of reducing rut depths and prolonging pavement life. Alternatively, for the same traffic conditions and allowable rut depth, the use of geogrid reinforcement allows a reduction of the construction cost by decreasing the base layer thickness in comparison with the thickness required when the base layer is unreinforced (if the cost of the geosynthetic reinforcement is less than the cost of the base material).

The main purpose of this study is to analyze design criteria currently available for reinforced unpaved roads comparing the results obtained by different design procedures aimed at estimating the base thickness required for reinforced unpaved roads, underlining their improvements and limits. Furthermore, a parametric analysis varying design parameters such as soils and geosynthetics mechanical properties, allowable rut depth and traffic conditions, has been conducted.

Moreover, to predict the behavior of unpaved roads, both in unreinforced system and reinforced with geosynthetics configuration, a finite element models have been implemented in ABAQUS program. The focus of this approach is to assess the geogrid reinforcement contribution to reduce the rut depth under repeated wheel traffic load conditions.

This page has been intentionally left blank

Abstract (Italian)

I geosintetici sono ampiamente utilizzati nella stabilizzazione meccanica delle strade non pavimentate con un basso volume di traffico. L'utilizzo di geosintetici posti sopra un sottofondo debole o all'interno dello strato di base ha dimostrato il vantaggio di ridurre la profondità di ormaia e di prolungare la vita della pavimentazione. In alternativa, per le stesse condizioni del traffico e di profondità di ormaia consentita, l'uso dei geosintetici come rinforzo permette una riduzione del costo di costruzione diminuendo lo spessore dello strato di base rispetto allo spessore richiesto quando lo strato di base non è rinforzato (se il costo del geosintetico di rinforzo è inferiore al costo del materiale di base).

Lo scopo principale del lavoro svolto è stato quello di analizzare i metodi di progettazione attualmente disponibile per le strade non pavimentate rinforzate con geosintetici e di confrontare i risultati ottenuti dalle differenti procedure di progettazione volte a stimare lo spessore dello strato di base richiesto, sottolineando i loro miglioramenti e limiti. Inoltre, è stata condotta un'analisi parametrica variando i parametri di progetto quali le proprietà meccaniche dei terreni e dei geosintetici, la profondità di ormaia ammissibile e le condizioni del traffico.

Inoltre, per prevedere il comportamento di strade non pavimentate, sia nel sistema non rinforzato che in quello rinforzato con geosintetici è stato implementato in ambiente ABAQUS un modello agli elementi finiti. L'obiettivo di questa analisi è stato quello di valutare il contributo di rinforzo offerto dalla geogriglia nella riduzione della profondità dell'ormaia a seguito di carichi di traffico ciclici.

This page has been intentionally left blank

List of figures

List of tables

Introduction

In the last decades geosynthetics have been proposed and used as reinforcement for paved and unpaved roads in order to improve the performance and/or to allow for the reduction of the base course thickness.

The technique of soil-improvement using geosynthetics is extensively used in the construction of unpaved roads. Unpaved roads are usually used for temporary roads and they remain in service for only short periods (often less than 1 year), and are subjected to low volume traffic (less than 10000 load applications). Unpaved roads typically consist of an aggregate layer resting on the subgrade. When the subgrade is weak, due to its poor consistency and high compressibility, generally, a geosynthetic reinforcement is placed at the base/subgrade interface to improve the road performance.

The use of a geosynthetic as reinforcement material in the unpaved roads base course layer has been shown to improve the performance in terms of increased pavement service life, reductions in the base course thickness, rut depth and fatigue strain.

For properly designed unpaved roads, improvement is typically seen for all rut depths in addition to rut depths that make the pavement inoperable. Geosynthetics used in unpaved road are essentially geotextiles and geogrids.

The improvement has been attributed mainly to the prevention of lateral restraint of the aggregate base course. The interaction between the geosynthetic and the aggregate base course (interlocking) are required to prevent lateral spreading of base course soil. For this reason, geogrids offer a greater improvement in performance as compared to geotextiles.

The effect of interlocking with aggregate offered by a geogrid minimizes the lateral movement of aggregate particles and increases the modulus of the base course, which leads to a wider vertical stress distribution over the subgrade and consequently a reduction of vertical subgrade deformations. The degree of interlocking depends on the relationship between the geogrid aperture size and the aggregate particle size; the geogrid aperture shape; the ribs shape and stiffness. The effectiveness of interlocking depends on the in-plane stiffness (more than strength) of the geogrid and the stability of the geogrid ribs and junctions. Two are the main reinforcement mechanisms in unpaved roads: lateral confinement effect and tension membrane effect. They require different depth values of rutting in order to be mobilized. At small permanent deformation magnitudes, the lateral restraint mechanism is developed by the ability of the base aggregate to interlock with the geogrid. As the permanent deformations increase the tension membrane mechanism develops. If the geosynthetic has a sufficiently high tensile modulus, tensile stresses will be mobilized in the reinforcement, and a vertical component of this tensile membrane resistance will help to support the applied wheel loads.

In Chapter 1 of the present thesis the road pavement degradation in time has been talked about, highlighting the importance of the maintenance operation which should be planned and frequently done on the paved roads.

In Chapter 2 several geosynthetics types employed for civil engineering applications have been presented, focusing on those used for roads pavement, and the reinforce mechanisms offered by the

presence of geosynthetics in road pavement have been discussed. Therefore the researches and studies available in literature on the reinforcement of road pavement by means of geosynthetic have been briefly described.

In Chapter 3 several methods for the design of reinforced through geosynthetics unpaved roads have been reported and analyzed in details. All the considered methods aim at the determination of the base course layer thickness for an unpaved road. The phases to develop the model and to obtain as a result the base course layer thickness required for unpaved road have been schematized for the Barenberg (1975), Giroud and Noiray (1981), Giroud and Han (2004) and Leng and Gabr (2005) methods.

In Chapter 4 the previously described methods have been implemented in Matlab environment considering different values for the input variables. The obtained results have been then plotted in graphs aiming at better analyzing and understanding the reinforce mechanism taken into account for by each method, so to evaluate the improvement offered by the presence of the reinforcement in terms of surface vertical displacement reduction.

Furthermore it has been possible to evaluate the variables effect on the models and assess the reinforcement importance and the functionality.

Finally an unpaved road reinforced by a geogrid has been modelled through a 3D FEM model using the ABAQUS software.

A comparison has been done between an unreinforced road section and the same road section reinforced thanks to the presence of a geogrid in order to evaluate the improvement offered by the geogrid in terms of superficial rut reduction under the cyclic load.

CHAPTER 1

Pavement Deterioration and Pavement Management System

This page has been intentionally left blank

CHAPTER 1

1. Pavement Deterioration and Pavement Management System

1.1. Importance of road in modern society

Transportation infrastructure plays a vital role in the economic, social, and state of all countries and this role cannot be neglected. Roads are important infrastructures that play a very efficient role in populations' development, allowing the easy mobility of people and goods. This mobility create a better access to jobs, health, education, resources and markets, among other amenities, supporting the growth of quality of life and reducing poverty. The importance of roadways can be reassumed in the followings points:

1. Allow a comfortable, fast and cheap way to travel from one place to another;
2. Connect several different places not only inside the cities, shortening their distance, but also between cities as well as between different countries, easing the mobility of people;
3. Have a strong impact on the economic growth, due to the fact that roads promote tourism and supply a quick way for the distribution and trading of goods.

Transportation has always played an important role in influencing the formation of urban societies. Although other facilities like availability of food and water, played a major role, the contribution of transportation can be seen clearly from the formation, size and pattern, and the development of societies, especially urban centers. In fact, people depend upon the natural resources to satisfy the needs of life but due to non uniform surface of earth and due to difference in local resources, there is a lot of difference in standard of living in different societies. So, there is an immense requirement of transport of resources from one particular society to other. These resources can range from material things to knowledge and skills.

The quality and efficiency of road surface affects the quality of life, the health of the social system and the continuity of economic and business activities, but road pavement surface exhibits distresses due to their constant usage.

If an appropriate maintenance policy is not applied, the road security quality can be compromised of the road pavement surface degrades. Road pavement surfaces are often composed by asphalt, although there may be other types, like unpaved road with an unbound aggregate base course as surface. So, Several distinct types of pavement can be identified, based on their structure.

The primary functions of a pavement system are to provide a reasonably smooth riding surface that was essential for riding comfort, and over the years it has become the measure of how road users perceive a road. Roughness can arise from a number of causes, most often however it is from pavement distress due to structural deformation. In addition to a smooth riding surface the pavement must provide adequate surface friction, especially during wet conditions it can be linked to a loss of surface friction between the tire and the pavement surface. A pavement must therefore provide sufficient surface friction and texture to ensure road user safety under all conditions.

Pavements are complex structures involving many variables, such as materials, construction, loads, environment, performance, maintenance, and economics. Thus, various technical and economic factors

must be well understood to design pavements, to build pavements, and to maintain better pavements. Moreover, the problems relating to road maintenance are still more complex due to the dynamic nature of road networks where elements of the network are constantly changing, being added or removed. These elements deteriorate with time and have to, therefore be maintained in good condition and it requires substantial expenditure. Moreover, the preparation and evaluation of the best ways to direct this expenditure is an extremely difficult task due to many factors that affect the deterioration of these elements.

Hence, the maintenance of road networks is an essential task to ensure the correct pavement performance, taking into account all the principles involved in its project, resulting in loss of asset value, poor quality of service and failure to provide access to affected areas (like cities, villages, among others) in case of neglected maintenance policies. To this end, good maintenance policies of road networks are required, relying on adequate management of rehabilitation procedures (Muhamma Mubarak,2010).

There are also many negative effects of transportation. There are three principal categories into which the environmental effects have been categorized:

- Safety;
- Pollution (noise, air);
- Energy consumption.

1.2. Factors affecting pavement system

There are many factors that affect pavement design which can be classified into four categories as drainage, environmental, traffic and loading and subgrade .

1.2.1. Drainage

Moisture sources are typically rainwater, runoff and high groundwater. These sources are prevented from entering the pavement structure or accumulating in the subgrade through surface drainage and subsurface drainage. This factor is important and have a significant impact on the pavement condition, in particular on the urban network, in fact the availability of a drainage system can affect the condition of a pavement.

Correct drainage is important to ensure a high quality long lived pavement; moisture accumulation in any pavement structural layer can cause problems. Moisture in the subgrade and aggregate base layer can weak these materials by increasing pore pressure and reducing the materials' resistance to shear. Additionally, some soils expand when moist, causing many deteriorations.

Excess moisture presence in pavement structures usually results in accelerated pavement distresses, In particular when combined with heavy axle loads. Both fiel observations and laboratory based research studies have shown that proper drainage can greatly improve pavement performance and increase its service life.

It is expected that pavement sections with a drainage system will have a better condition than pavement sections without a drainage system.

1.2.2. Environmental

Pavement structures and environment are in continuous interaction. Environmental conditions have been found to exert significant impact on the performance of flexible pavements.

The environment factors in pavement system can be divided in:

1) External factors: such as precipitation, temperature, humidity, freeze-thaw cycles, and depth of water table are the main environmental factors that exerted principal influences on the pavement system performance.
2) Internal factors: such as the susceptibility of the pavement materials to moisture and freeze-thaw damage, infiltration potential of the pavement.

These parameters undergo daily and seasonal variations as well as a spatial distribution as they are interconnected to the constantly evolving environment that surrounds the pavement system. The two main environmental factors in pavement engineering are temperature and moisture content.

Both internal and external factors are associated with the seasonal variation.

The effect of environmental conditions on performance can be broken in two separate categories:

- weather conditions when the marking is placed
- year-round climate.

Each of the above factors may affect marking performance. Air and pavement temperatures are important because most pavement marking materials require a minimum temperature for proper drying or curing. Humidity also affects the drying and curing times. Wind velocity affects drying times, but more importantly it affects the drop-on bead dispersion. Strong winds can prevent a high percentage of the drop-on beads from uniformly reaching the binder material. Pavement surface moisture at the time of application can have a severe effect on the bonding capabilities of the marking material to the pavement surface. Most materials require that the pavement surface be devoid of surface moisture prior to application to achieve bonding. Year-round climatic conditions can also affect the long-term performance of a pavement materials. Area that receive heavy snowfall are often exposed to heavy abrasion on their pavement markings due to snowplow, sanding, and chemical activity. States in sun-belt regions due to intense ultraviolet exposure may experience color fading and cracking of certain pavement marking materials (Lopez, 2004).

1.2.3. Traffic and loading

Traffic loading is considered as the primary factor that affects both pavement design and performance. The performance of pavements is mostly influenced by the loading magnitude, configuration and the number of load repetitions by heavy vehicles. The service lives of nearly all pavement marking materials are decreased when exposed to higher traffic volumes. Under extremely high-traffic conditions or other locations where a high number of wheel hits on the markings are likely to occur, such as weaving areas or transverse markings, materials of the utmost durability are desirable.

Loads are the vehicle forces exerted on the pavement (e.g., by trucks, heavy machinery, airplanes). Since one of the primary functions of a pavement is load distribution, pavement design must account for the

expected lifetime traffic loads. Traffic loading, the vehicle forces exerted on the pavement (e.g., by trucks, heavy machinery, airplanes), include tire loads, axle and tire configurations, load repetition, traffic distribution across the pavement and vehicle speed.

Tire loads are the fundamental loads at the actual tire-pavement contact points. For most pavement analyses, it is assumed that the tire load is uniformly applied over a circular area. Moreover, it is generally assumed that tire inflation and contact pressures are the same.

Generally, the design of the roadways requires that the areas of influence of wheels loads is no longer relating to two isolated single tire, but rather the combined effect of all the interacting tire load. Of course, slower speeds and stop conditions allow a particular load to be applied to a given pavement area for a longer period of time resulting in greater damage.

The damage caused per pass to a pavement by an axle is defined relative to the damage per pass of a standard axle load, which is defined as an 80 kN single axle load. This approach converts wheel loads of various magnitudes and repetitions to an equivalent number of "standard" or "equivalent" loads based on the amount of damage they do to the pavement. The commonly used standard load is the 18,000 lb. equivalent single axle load. Using the ESAL method, all loads are converted to an equivalent number of 18,000 lb. single axle loads and this number is then used for design. A "load equivalency factor" (Figure 1.1) represents the equivalent number of ESALs for the given weight-axle combination.

Thus, a pavement is designed to withstand a certain number of standard axle load repetitions that will result in a certain terminal condition of deterioration. Since loadings are one of the most important factors that affects damages of most pavement section, it is often used as an independent variable in developed condition prediction equations.

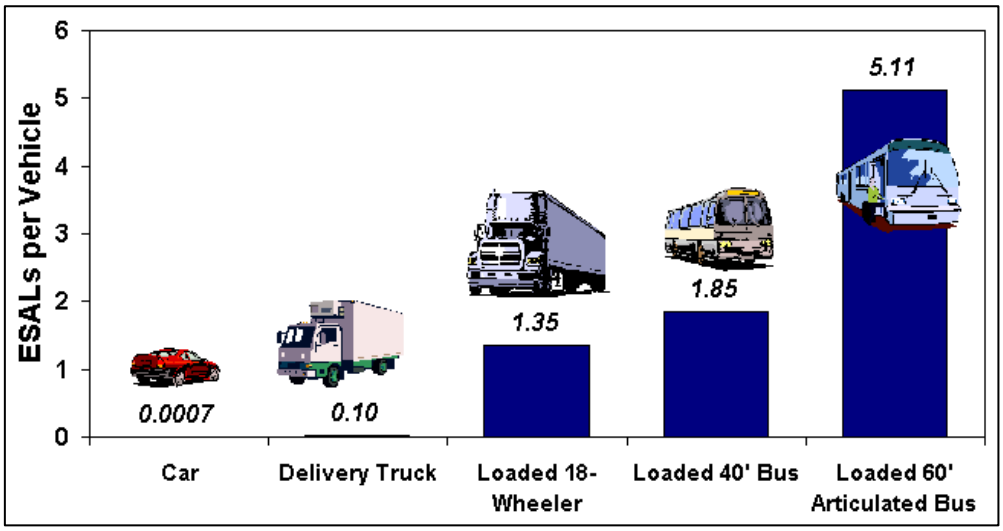

Figure 1.1 Load equivalency factor (www.pavementinteractive.org)

1.2.4. Subgrade

The "subgrade" is the in situ material upon which the pavement structure is placed. The subgrade is the underlying soil that supports the applied wheel loads. If the subgrade is too weak to support the wheel

loads, the pavement system will flex excessively which ultimately causes the pavement to fail. If natural variations in the composition of the subgrade are not adequately addressed by the pavement design, significant differences in pavement performance will be experienced, so it can often be the overriding factor in pavement system performance. Properties of the subgrade soil and its water content are not directly considered in assessing the performance or serviceability of pavements. However was recognize that the increased water content in subgrade soils (especially the cohesive ones) combined with increased traffic volumes and loads often leads to premature pavement distresses. Subgrade strength has the greatest effect in determining pavement thickness, weaker subgrades require thicker layers in pavement system to adequately bear traffic loads. A subgrade's strength generally depends on two interrelated characteristics:

- Load bearing capacity: the subgrade must be able to support loads transmitted from the pavement structure. This load bearing capacity is often affected by degree of compaction, moisture content, and soil type. A subgrade that can support a high amount of loading without excessive permanent deformation is considered good.
- Volume changes: most soils undergo some amount of volume change when exposed to excessive moisture or freezing conditions. Some clay soils shrink and swell depending upon their moisture content, while soils with excessive fines may be susceptible to frost heave in freezing areas.

Subgrade materials are typically characterized by their resistance to deformation under load. In general, the more resistant to deformation a subgrade is, the more load it can support before reaching a critical deformation value. There are two basic subgrade stiffness/strength characterizations commonly used:

- California bearing ratio (CBR): a simple test that compares the bearing capacity of a material with that of a well-graded crushed stone (thus, a high quality crushed stone material should have a CBR of about 100%). The CBR rating was developed for measuring the load-bearing capacity of soils used for building roads but it can also be used for measuring the load-bearing capacity of airstrips. The harder the surface, the higher the CBR rating. A CBR of 3 equates to tilled farmland, a CBR of 4.75 equates to turf or moist clay, while moist sand may have a CBR of 10. High quality crushed rock has a CBR over 80. The standard material for this test is crushed California limestone which has a value of 100, meaning that it is not unusual to see CBR values of over 100 in well compacted areas.
- Resilient Modulus (Mr) is a fundamental material property used to characterize unbound pavement materials. It is a measure of material stiffness and provides a mean to analyze stiffness of materials under different conditions, such as moisture, density and stress level. A material's resilient modulus is actually an estimate of its modulus of elasticity (E). While the modulus of elasticity is stress divided by strain for a slowly applied load, resilient modulus is stress divided by strain for rapidly applied loads (cyclic loads), like those experienced by pavements.

Resilient modulus is determined using the cyclic triaxial test. The test applies a repeated axial cyclic stress of fixed magnitude (amplitude) and load cycle duration (frequency) to a cylindrical test

specimen. While the specimen is subjected to this dynamic cyclic stress, it is also subjected to a static confining stress provided by a triaxial pressure chamber. It is essentially a cyclic version of a triaxial compression test; the cyclic load application is thought to more accurately simulate actual traffic loaging.

1.3. Pavement deterioration

Pavement deterioration is the process by which defects develop in the pavement under the combined effects of traffic loading and environmental conditions. Deterioration of pavement greatly affects on serviceability, safety, and riding quality of the road. After construction, roads deteriorate with age as a result of use and therefore, they need to be maintained to ensure that the requirements for safety, efficiency and durability are satisfied. Typically, pavement deteriorates at an ever-increasing rate. .Normally, new paved roads deteriorate very slowly in the first ten to fifteen years of their life and the pavement stays in relatively good condition, but as it ages more distresses develop with each distress making it easier for subsequent distresses to develop. Therefore, deterioration of asphalt pavements can also be due to factors that go beyond just normal wear and tear causing premature deterioration. The premature deterioration of asphalt pavement is usually due to failures in construction or human error. This can be due to a number of factors including:

- insufficient or improperly compacted base below the asphalt;
- over or under compaction of asphalt;
- improper temperature of asphalt when applied;
- poor drainage;

Pavement surface distresses can be divided using four classes. For each class several distress types can be considered, and for almost all distress types several criteria and parameters (some quantitative and others of qualitative nature), are used to grade them into severity levels but in some cases, only the distress type is important to record, as grading them into severity levels is not relevant.

The five classes considered for distresses are:

- Cracking;
- Surface deformation;
- Disintegration;
- Surface defects;

1.3.1. Cracking

Cracking is the most common distress class that appears in asphalt pavement surfaces roads (Hot-Mix Asphalt, HMA) and for this reason in many countries, the cracking performances are incorporated into pavement road design and maintenance systems. The causes are due mainly to the fatigue of the asphaltic pavement layers but other important causes include: adverse atmospheric conditions (shrinkage due to extremely low atmospheric temperatures); bad quality in the asphaltic mixtures production; weakness in the structural pavement resistance.

Cracking distresses can be subdivided into five types:

1) Fatigue cracking

2) Longitudinal cracking
3) Transverse cracking
4) Block cracking
5) Reflective cracking

1.3.1.1. Fatigue cracking

Fatigue cracking (Figure 1.2) is the principal structural distress which occurs in asphalt pavements with granular and weakly stabilized bases. It is a single crack or a series of interconnected cracks caused by fatigue failure of the asphalt concrete and it is commonly called alligator cracking. An important parameter associated with this crack type is the mesh width. This type of cracking is a consequence of a cracking ramification process, since the evolution of several isolated cracks comes to make several connections among themselves over time.

Factors which influence the development of alligator cracking are:

- the number and magnitude of applied loads;
- the structural design of the pavement like layer materials and thicknesses;
- the quality and uniformity of foundation support;
- the air voids;
- the climate of the site.

Alligator Cracking is measured in square feet. The major difficulty in measuring this type of distress is that more levels of severity often exist within one distressed area. Different criteria are used for the classification of alligator cracking into severity levels. Three severity levels can be defined according to the cracks width and the presence of degraded edges. The three levels of classification are:

1. low severity level, for alligator pattern cracking with crack widths lower than 2 mm;
2. moderate severity level, for alligator pattern cracking with crack widths higher than 2 mm and an initial state of degraded edges;
3. high severity level, for alligator pattern cracking with crack widths higher than 2 mm, plus degraded edges or the beginning of potholes formation.

The causes of fatigue cracking are the repetitive traffic loads and high deflection often due to wet bases or subgrade but also maybe present anywhere in the lane due to traffic wander. Alligator cracking may progress further, In particular in areas where the support is weakest to potholes and localized failures.

Figure 1.2 Fatigue cracking

1.3.1.2. Longitudinal Cracking

Longitudinal cracks (**Errore. L'origine riferimento non è stata trovata.**Figure 1.3) are long racks that usually occur near the pavement shoulder or sometimes near the pavement centerline. Longitudinal cracks are usually caused by fatigue failure under repeated traffic loading and it can consist of a single crack or as a series of parallel cracks.. In thin pavements, cracking starts at the bottom of the bituminous layer where the tensile stress is the highest and then it spreads to the surface as one or more longitudinal cracks. Understanding the cause of this phenomena is critical to selecting the proper repair. Multiple parallel cracks may be eventually formed by the initial crack. The principal causes for this phenomena are:

- The reflection of a crack or joint in the road pavement;
- Poorly constructed joints in the asphalt surface;
- Asphalt hardening;
- Diurnal temperature fluctuations.

Location within lane is significant to understand the phenomena

There are two types of longitudinal cracking: wheel path and non-wheel path longitudinal cracking. While wheel path Longitudinal cracking may also be produced in the wheel paths by the application of heavy loads or high tire pressures. Non-wheel path longitudinal cracking in an asphalt pavement, instead ,may reflect up from the edges of an underlying old pavement or from edges and cracks in a stabilized base, or may be due to poor compaction at the edges of longitudinal paving lanes.

Should be noted that only wheel path longitudinal cracking should be considered along with alligator cracking in assessing the extent of load-related damage.

a) b)

Figure 1.3 Longitudinal cracking in a) Non wheel path b) wheel path

1.3.1.3. Transverse cracking

Transverse cracking (Figure 1.4) is cracks that are predominantly perpendicular to pavement centerline. Transverse cracks are essentially caused by shrinkage of the HMA pavement surface due to low temperatures or asphalt binder hardening, reflective crack caused by cracks beneath the surface HMA layer and top-down cracking. When the tensile stress due to shrinkage exceeds the tensile strength of the asphalt pavement surface, the crack occurs (Ainalem Nega,2015).

As in fatigue cracking cases, the classification into severity levels takes into account the crack width and the presence of degraded edges. The three severity levels are:

1. Low severity level, for transversal joints cracks with a width lower than 2 mm;
2. Moderate severity level, for transversal joints cracks with a width higher than 2 mm;
3. High severity level, for transversal joints cracks with a width higher than 2 mm, plus degraded edges.

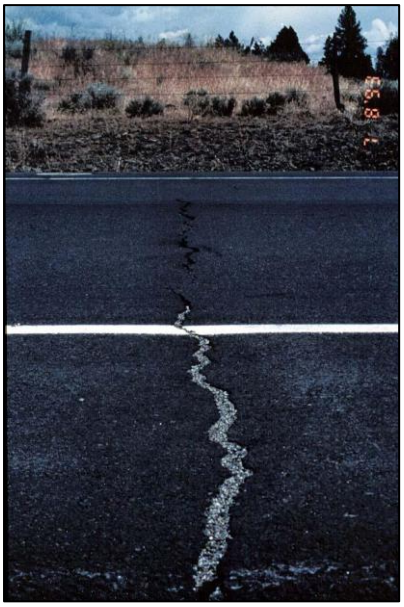

Figure 1.4 Transverse cracking (www.pavementinteractive.org)

The reasons for transverse cracking, and their repairs, are similar to those for longitudinal cracking. In addition, thermal issues can lead to low-temperature cracking if the asphalt is too hard.

1.3.1.4. Block cracking

Block cracking is an interconnected series of cracks that divides the pavement into rectangular pieces with cracks that intersect at about 90 degrees. The blocks usually range from 30 by 30 cm to 300 by 300 cm (**Errore. L'origine riferimento non è stata trovata.**Figure 1.5).Block cracking, unlike fatigue cracking, will occur throughout of the pavement width, not only in the wheel paths and this phenomena is sometimes the result of transverse and longitudinal cracks intersecting.

Furthermore this type of distress differs from alligator cracking in that alligator cracks form smaller, irregular shaped pieces with sharp angles. Moreover, alligator cracks are caused by repeated traffic loadings and are, therefore, generally located in traffic areas. These cracks are the result of age hardening of the asphalt coupled with shrinkage during cold weather, and can be effectively treated with crack sealants, or they can also be due to lack of compaction during construction. So, it is not a load-associated distress, although load can increase the severity of individual cracks.

In particular, block cracking can be caused by oxidative hardening of the asphalt if mixed too long in the mill, mixed too hot, or stored too long in silos. All these above reasons make the asphalt cement especially susceptible to tensile strains, which can exceed the tensile strain capacity of the asphalt mixture and cause the block cracking.

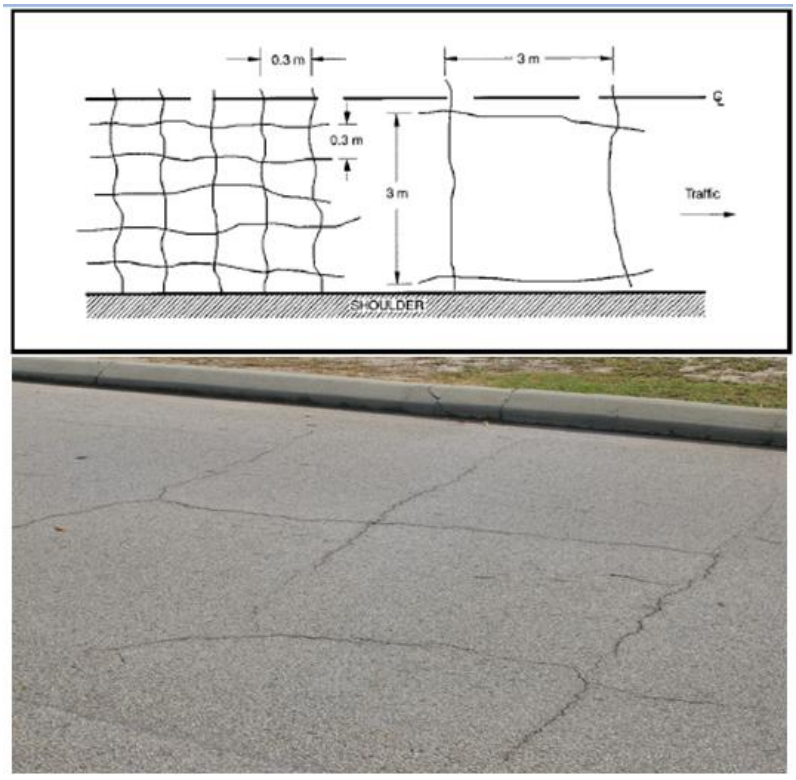

Figure 1.5 Block cracking (www.lgam.info)

Low severity block cracking may be repaired by a thin wearing course but if the cracking gets more severe overlays or recycling may be needed; if base problems are found, reclamation or reconstruction may be needed. Because the cracks can be closely spaced, the underlying layers can be exposed to significant quantities of infiltrating surface water. These cracks should be sealed to prevent or minimize intrusion of water.

1.3.1.5. Reflective cracking

Asphalt overlays are commonly applied on existing flexible and rigid pavements when pavement conditions (structural and functional) have reached an unacceptable level of service. Overlays are designed to resist fatigue and/or rutting failure mechanisms; however, overlays may still show cracking patterns similar to the ones, which existed in the old pavement after a short period of time. This distress is known as 'reflection cracking' (Nirmal Dhakala, 2016).

Reflection cracking (Figure 1.6) is one of the most important factors causing premature failure of asphalt layer overlays and hence the pavements. Reflection cracking occurs in asphalt layer because of their inability to withstand (or resist) tensile and shear stresses created by vertical and horizontal movements of cracked or jointed pavements underneath. The vertical movement of the pavement is mainly caused by moving traffic and the horizontal movement of cracks and joints is caused by temperature and/or moisture changes. The vertical movement in the overlay induces a shear stress in the asphalt overlay while the horizontal movement of cracked or jointed slabs causes high tensile stresses and strains at the bottom of the asphalt overlay and results is reflection cracking. The factors that influence the rate at which reflection cracks deteriorate are the number and magnitude of applied loads. The mechanism of reflective cracking is show in **Errore. L'origine riferimento non è stata trovata.**

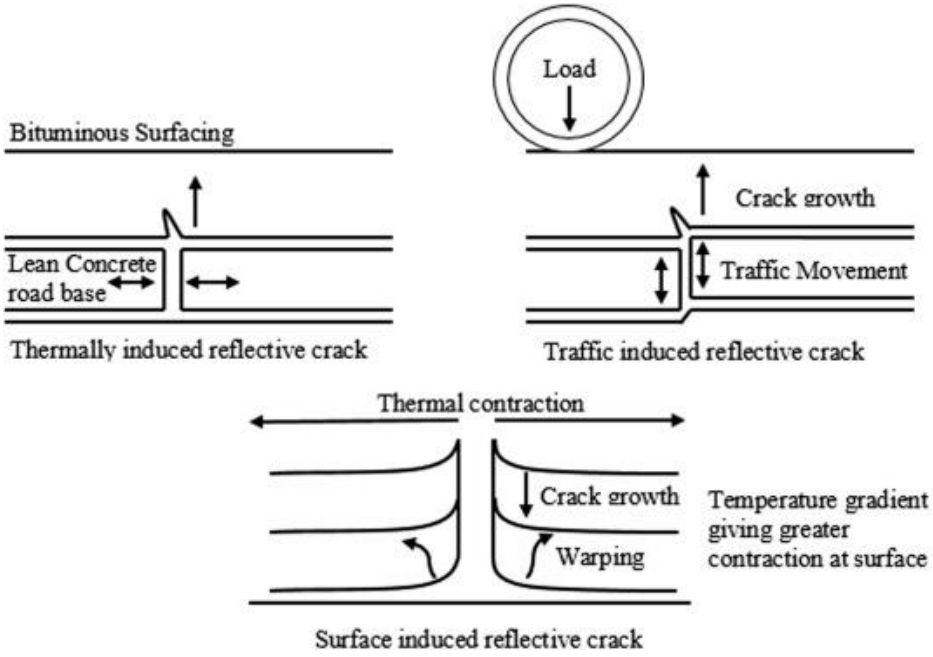

Figure 1.6 mechanism of reflective cracking

In another attempt to understand the process of reflection cracking, Francken et al. (1997) described different factors contributing to the development of reflection cracking. Traffic load can produce two types of movement in the cracked concrete slab that generate shear stresses (Figure 1.7a and Figure 1.7c) due to relative vertical movement of cracked slabs and flexural stresses (Figure 1.7b) in the HMA overlay. In addition, due to temperature and/or moisture changes, the cracked concrete slab contracts and expands, inducing large tensile stress at the bottom of asphalt overlay and causing progressive opening-up of joints and cracks (Figure 1.7d).

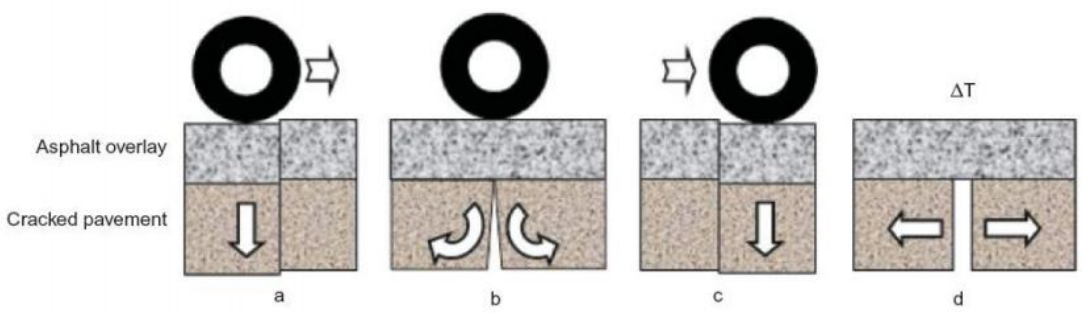

Figure 1.7 Propagation of cracking

Reflection cracking is a serious challenge associated with pavement rehabilitation as it leads to premature failure of the overlay and allows water infiltration through the cracks, which causes stripping in asphalt layers and weakening and deterioration in the base and/or subgrade.

The systems in order to delay reflection cracking are based on two mechanisms: (i) reflection cracking can be retarded by using reinforcement systems, which are stiffer than surrounded materials, such as geosynthetics or steel reinforcement and (ii) a low modulus material is used to create a stress absorption layer.

The major types of treatment methods that have been evaluated to control reflection cracking are:

- use of geosynthetic or geogrid as reinforcement;
- use of steel as reinforcement;
- stress absorbing membrane as an interlayer between overlay and concrete or old asphalt layer;
- using modified asphalt for overlay;
- using large thickness of asphalt overlay.

1.3.2. Surface deformation

Pavement deformation is the result of weakness in one or more layers of the pavement that has caused by traffic load after construction or to failures during construction. Surface distortions can be a traffic hazard and they interest both paved and unpaved roads.

The major types of surface deformation are:

1. Rutting
2. Shoving and corrugations

3. Depressions
4. Potholes

1.3.2.1. Rutting

Rutting is one of the major distress mechanisms in flexible pavements (both paved Figure1.8a**Errore. L'origine riferimento non è stata trovata.** and unpaved **Errore. L'origine riferimento non è stata trovata.**Figure 1.8b). Because of the increase in tire pressure and axle loads in recent years, rutting has become the dominant mode of failure of flexible pavements in many countries.

Rutting is defined as the longitudinal permanent deformation or plastic movement of the surface pavement under the action of repeated loadings over the wheel path but also a inadequate compaction can lead to rutting. Rutting can occur in all layers of the pavement structure and results from lateral distortion and densification. The width of the rut is a sign of which layer has failed, a very narrow rut is usually a surface failure, while a wide one is indicative of a subgrade failure. The width and depth of the rutting profile usually depends highly by the pavement structure (layer thickness and quality), traffic volume and composition as well as on the environment.

a) b)

Figure 1.8 Rutting in a)paved road, b) unpaved road

Deformation which occurs only in the asphalt layer may be the result of either consolidation or plastic flow. Consolidation is the continued compaction of asphalt layer by traffic loads applied after construction. Consolidation may produce significant rutting in asphalt layers which are very thick and which are compacted during construction to initial air void contents considerably higher than the long-term air void contents for which the mixes were designed.

According to Eisemann and Hilma (1987) that studied asphalt pavement deformation phenomenon using wheel tracking device and measuring the average rut depth as well as the volume of displaced materials below the tires and in the zones adjacent to them it is possible say that in the initial stages of trafficking the increase of irreversible deformation below the tires is distinctly greater than the increase in the failed zones. Therefore, in the initial phase, traffic compaction or densification is the primary mechanism of rut development. After the volume decrease below the tires is approximately equal to the volume increase in the adjacent failed zones. This indicates that most of the compaction under traffic is

completed and further rutting is caused essentially by shear deformation. Thus, it can consider the shear deformation the primary mechanism of rutting for the greater part of the lifetime of the pavement.

Generally there are three causes of rutting in asphalt pavements:

- Accumulation of permanent deformation in the asphalt surfacing layer: Rutting resulting from accumulation of permanent deformation in the asphalt layer is now considered to be the principal component of flexible pavement rutting. Rutting in asphalt layers is caused by an asphalt mixture that is too low in shear strength to resist the repeated heavy loads to which it is subjected. It is thus abundantly clear that rutting caused by accumulation of permanent deformation in asphalt layers is the primary cause of flexible pavement deterioration. To reduce this form of deterioration it is necessary to pay more attention to the selection of materials and mix design.
- Permanent deformation of subgrade: In this type of rutting, the permanent deformation occurs in the subgrade. Thus this type of rutting is considered to be more of a structural problem than a materials problem and is often referred to as structural rutting. Intrusion of moisture can also be the cause for weakening of the subgrade.
- Wear of pavements caused by studded tires: Studded tires damage hot mix asphalt and concrete pavements, wearing away the pavement and eventually forming ruts on the pavement surface. This type of rut damage is called "raveling." The studded tires, used in nordic countries, cause significant wear of the pavements, which results in longitudinal depression in the wheel path. Because of this, wear resistance mixtures, which are usually of high binder content and low void content are specified for high volume roads of studded tires. Therefore the observed rutting in the field would most probably be the combined effect of wear and permanent deformation.
-

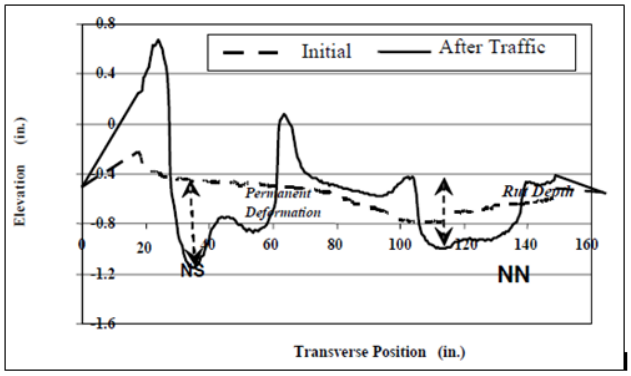

Figure 1.9 Permanent deformation vs rutting

Permanent deformation and rutting are sometimes used interchangeably, because they are both depressions that occur on a wheel path after traffic loading, the difference is accounted by the measurement method. Permanent deformation is measured as the depth of depression with reference to the original profile, while rutting is measured using a straight bar, as the depth between the highest and deepest points on a profile (**Errore. L'origine riferimento non è stata trovata.**Figure 1.9). For this dissertation, permanent deformation measurement method is referred.

To analyze the rutting importance three severity levels can be consider for HMA paved roads:

1. low severity level, for rutting distresses with a depth lower than 10 mm;

2. moderate severity level, for rutting distresses with a depth between 10 mm and 20 mm;
3. high severity level, for rutting distresses with a depth higher than 20 mm.

It is important to underline that rutting is a serious safety issue for drivers. When water accumulates in the ruts, there is a potential for hydroplaning. The hydroplaning phenomenon consists of the buildup of a thin layer of water between the pavement and the tire and results in the tire losing contact with the surface, with the consequent loss of stability control.

1.3.2.2. Shoving and corrugations

Shoving and corrugation are terms which refer to longitudinal displacement of asphalt concrete in a localized area. Shoving and corrugation are produced by traffic loading, but are indicative of an unstable liquid asphalt mix.

It is a form of plastic surface movement typified by ripples across the bituminous pavement surface. The cause of corrugations is usually lack of stability in the bituminous mix. Lack of stability can be caused by the aggregate having excessive amounts of fines, mix contamination, rounded or smooth textured particles, poor bond between material layers, or the use of soft binder.

Figure 1.10 Corrugations in asphalt layer

1.3.2.3. Depression

Depression (Figure 1.11) is associated to a defective support capacity in pavement aggregate layers (structural layers). Depressions may be caused by traffic heavier than that for which the pavement was designed, by settlement of the underlying pavement layers, or by poor construction methods. Depressions are small, localized bowl-shaped areas that may include cracking. it causes roughness, are a hazard to motorists, and allow water to collect. In opposition to the rutting distress type, depressions may appear not only in the wheel path area, but in any area of the pavement surface, in an isolated way (localized and with small dimensions), or may present significant horizontal dimensions, occupying almost the entire road lane width.

This distress type can be classified using three severity levels:

1. Low severity level for depressions with maximum depth between 0.5 and 1.5 cm;
2. Moderate severity level for depressions with maximum depth between 1.5 and 3 cm;

3. High severity level for depressions with maximum depth higher than 3 cm.

Figure 1.11 Depressions in asphalt layer

1.3.2.4. Potholes

Potholes (Figure 1.12) are what most people think of when they think of pavement failures.

The potholes are related with the development of a high severity level alligator pattern and the disappearance of portions of the top pavement layers and usually are caused by a localized weakness in the pavement resulting from a combination of such factors as too little asphalt, thin surface thickness, too many fines, too few fines, or poor drainage. These are usually non-functional pavement areas where the pavement has completely failed, exposing the base aggregate beneath it. Potholes are formed when the pavement disintegrates under traffic loading, due to inadequate strength in one or more layers of the pavement.

The occurrence of potholes often coincides with a period of heavy rainfall during which water penetrates the asphalt layer through cracks and softens the granular base course. Fine material is pumped through the cracks so that the underlying base support is weakened resulting in removal of the adjacent material by traffic. Once the first piece is dislodged, the pothole grows rapidly since all other pieces are more easily dislodged that the first piece.

Areas in which many potholes occur become suspect for fundamental problems such as inadequate drainage, pavement strength, or base/subgrade problems.

Potholes usually pose liability issues such as causing vehicular suspension damage, or tripping hazards if they reside within pedestrian walkways.

Figure 1.12 Pothole distress

1.4. Road Pavement Maintenance

The principal function of a road is to provide a surface with shape and frictional characteristics that permit vehicles to be controllable and, along with their contents, to remain undamaged while travelling at the desired speed. Pavements system are constructed to ensure that roads will fulfill this function reliably and durably.

Pavements are complex structures involving many variables, such as materials, construction, traffic loads, environment, performance and maintenance furthermore the problems that influence the road maintenance are still more complex due to continuous changing of road elements.

Deterioration and failure of roadway may occur because of overuse, and mismanagement and therefore maintained in good condition requires substantial expenditure furthermore the need for maintenance increases as road infrastructure ages, since it becomes more fragile, less resilient and journeys are more susceptible to disruption. Moreover, the preparation and evaluation of the best ways to direct this expenditure is an extremely difficult task due to many factors that affect the deterioration of these elements. So the maintenance that a pavement road needs can be predicted from a set of structural characteristics, such as age, climate, traffic, design standards, construction quality, and subsequent maintenance. Too often, decision makers are left unaware of the importance of road maintenance because justification for funding is based only on a narrow range of considerations and is not described in terms of the impacts on users and wider society. Robinson, Danielson and Snaith (1998) explain that ”maintenance reduces the rate of pavement deterioration, it lowers the cost of operating vehicles on the road by improving the running surface, and it keeps the road open on a continuous basis", so pavement maintenance activities represents those treatments that preserve pavement condition, safety, and ride quality, and therefore aid a pavement in achieving its design life.

The principal reasons that underline the important of pavement maintenance are:

- safety and security impacts;

- environmental impacts;
- economic impacts;
- accessibility and social inclusion impacts.

To obtain a good operations in road maintenance is important focusing on three subjects:

- Finding the constraints of capital;
- Understanding the common failures and the best and most cost effective treatment methods;
- Using the results of research in real projects to improve productivity.

Maintenance can also involve different approaches, based on whether the emphasis is on repairing distresses or preventing them before they happen. For this reasons the pavement maintenance can be divided in three types of pavement maintenance operations (Figure 1.13):

- Preventive Maintenance;
- Corrective Maintenance;
- Emergency Maintenance.

Many pavement rehabilitation can be used for preventive, corrective, or emergency maintenance. Pavement Rehabilitation consists of structural enhancements that extend the service life of an existing pavement and/or improve its load carrying capacity. Rehabilitation techniques include restoration treatments and structural overlays.

Pavement rehabilitation can be divided into two categories: minor rehabilitation that provides non-structural enhancements to the existing pavement and would be placed in the category of pavement preservation and major rehabilitation that provides structural enhancements that increase the life of the pavement or improve the load carrying capacity.

When the pavement rehabilitation is impossible for pavement state it's necessary the operation on reconstruction, that include the removal of all surface layer materials and possible substantial changes to base and subbase layer materials.

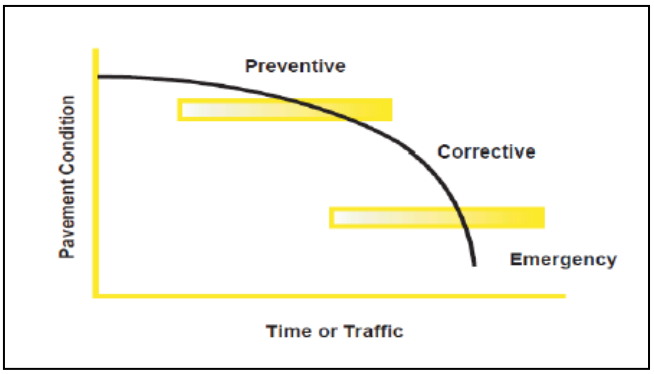

Figure 1.13 Categories of pavement maintenance (Johanns and Craig, 2002)

1.4.1. Preventive Maintenance

Although all three types of maintenance are important the preventive maintenance activities it essential because is the most cost effective and offer the best means for prolonging pavement service life (Figure 1.14). According to AASHTO Standing Committee on Highways, the preventive maintenance is "the planned strategy of cost-effective treatments to an existing roadway system and its appurtenances that preserves the system, retards future deterioration, and maintains or improves the functional conditions of the system, without increasing structural capacity" (U.S. Federal Highway Administration, 2000).

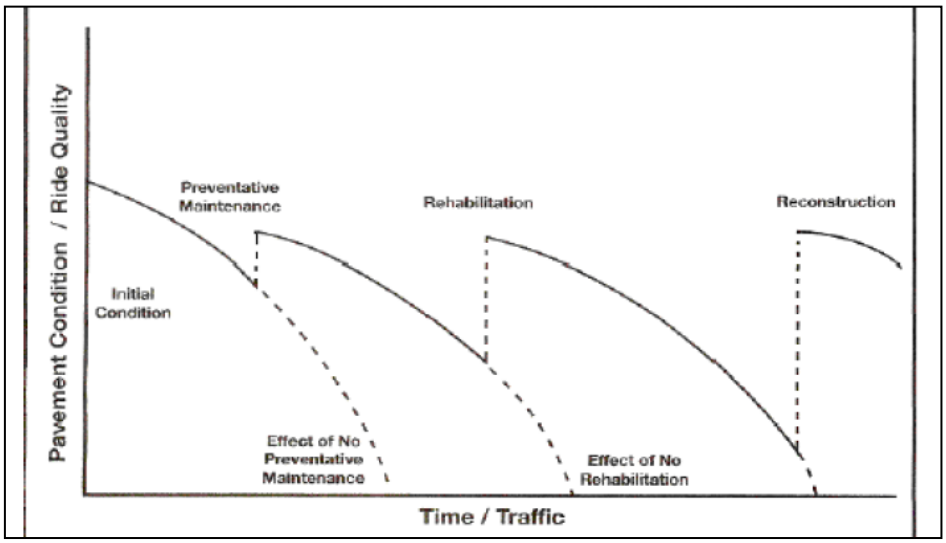

Figure 1.14 Pavement maintenance vs. time deterioration

Preventive maintenance is a planned pavement preservation strategy and not a single specific treatment, so it is defined as a planned strategy of cost-effective treatments and for this reason it needs to be viewed in the context of the overall management of municipal infrastructure. Waiting until after a failure occurs is not cost-effective or preventive maintenance. The effectiveness of a preventive maintenance treatment is directly related to the condition of the pavement in fact conducting an inappropriate repair can actually accelerate the rate of distress development (M. Johnson, 2000).

It is important discern preventive maintenance (a strategy) from a preventive maintenance treatment (an action). Preventive maintenance treatment should be applied to pavements in good condition having significant remaining service life and have the objective is to slow down the rate of pavement deterioration. The key is to apply the treatment when the pavement is still in relatively good condition with no structural damage.

Preventive maintenance treatment include:

- Waterproofing: preventing water from entering the pavement structure from above through cracks and joints, porous pavement surface materials and unsealed shoulders;
- Drainage: removing water from the pavement structure and subgrade by improved drainage;

- Strengthening: strengthening of those pavement sections that show local weakness (for example, due to poor local soil conditions or poor local construction) before major distresses appear on the pavement surface;
- Resurfacing: protecting pavement surface from progressive ravelling and coarse aggregate loss that can lead to potholing (also related to waterproofing);

The use of preventive maintenance does not mean that other pavement preservation treatments are not required. All types of maintenance treatments and rehabilitation treatments are needed as part of a comprehensive cost-effective pavement preservation program.

Critical elements of a successful for preventive maintenance are:

- Selecting the roadway;
- Determining the cause of the problem;
- Identifying and applying the correct treatment;
- Determining the correct time to do the needed work;
- Observing performance.

1.4.2. Routine maintenance

According to AASHTO Highway Subcommittee on Maintenance, routine maintenance "consists of work that is planned and performed on a routine basis to maintain and preserve the condition of the highway system or to respond to specific conditions and events that restore the highway system to an adequate level of service."

Routine maintenance may be defined as those treatments that are applied day-to-day a pavement system, to maintain and preserve the pavement at a satisfactory level. As such, routine maintenance is sometimes referred to as “reactive maintenance.” This suggests that it is work that is performed as a reaction to a specific distress.

Depending on the timing of application, the nature of the distress, and the type of activity, certain routine maintenance activities may be classified as preservation.

Routine maintenance is performed on pavements as they begin to show signs of deterioration, but is generally considered to be a wasted effort on pavements that are severely distressed (Wilde et al. ,2014).

Field observations will determine the type and schedule for much of the daily routine maintenance necessary to keep pavement system, including signs and markings, in acceptable condition. Routine maintenance can involve the following activities. Examples of important routine maintenance for pavement system are:

Repairs: Signs and devices should be repaired in a timely manner primarily to provide safe driving conditions for the public. Poorly maintained signs and markings may result in lessened respect for these devices and their messages. These routine repairs might also include sign supports.

Cleaning: This activity might be based on localized need and budget considerations. Dusting conditions in certain areas, mud splashing in construction areas, and snow and ice buildup in the winter can adversely affect sign and marking visibility. Rain can act to naturally clean traffic control devices, but certain signs and markings, In particular regulatory, may merit human extra attention.

1.4.3. Corrective Maintenance

Corrective maintenance differs from preventive maintenance primarily in cost and timing. While preventive maintenance is performed when the pavement is still in good condition, corrective maintenance is performed when the pavement is in need of repair, and for this reason is more costly.

Corrective Maintenance consists of activities carried out for the purpose of slowing the rate of pavement deterioration and keeping the pavement in a safe and operational condition. Adoption of this strategy requires that the pavement is structurally sound.

Then Corrective maintenance is not likely to increase the life of the pavement section but it will ensure safe operation. Furthermore, it will be necessary to perform many life cycle cost analyses on different projects. Therefore, it is recommended that a study of extended pavement life due to preventive maintenance types is carried out in order to draw a family of curves, like those show in Figure 1.14, for every possible treatment and to select the critical levels based on a scientific approach and engineering judgment rather than only on engineering judgment. Infact with scientific approach, through many methods like genetic algorithms and fuzzy logic it is possible to optimized the operations of maintenance and reduce costs.

1.4.4. Emergency Maintenance

Such discussed in precedent paragraphs there are several types of pavement distresses that contribute in different ways to pavement failure. Some distresses can be corrected with treatments used for preventive or routine maintenance treatments, while in other cases the treatment would serve as a corrective or emergency treatment.

Emergency maintenance is performed during an emergency situation, such as a important pothole that needs repair immediately. This also describes temporary treatments designed to hold the surface together until more permanent repairs can be performed. Emergency repairs may be necessary for both old and new pavements. Emergency maintenance treatment costs may be the least important consideration, after safety and time of application are considered.

Given the importance of strategic road asset management there is a need to investigate issues around road rehabilitation and maintenance with a view to establishing a framework for improved performance in the planning and monitoring process, all this process represents the base of pavement management system that is essential for:

- The use of a systematic approach to decision-making within a consistent and defined framework.
- To assess budget needs and resource requirements.
- To adopt consistent standards for maintenance and for the design of associated works.
- To allocate resources effectively.
- To review policies, standards and the effectiveness of programs on a regular basis.

1.5. Pavement management system

Pavement Management Systems (PMS) are widely used to maintain safe, durable and economic road networks. PMS prioritize the maintenance and rehabilitation of pavement sections by evaluating pavement performance at the network level.

A pavement management system consists of a coordinated set of activities, all directed toward achieving the best value possible for the available capital and must serve different management needs or levels. In fact the primary benefit of a pavement management system is that it helps users select cost-effective alternatives for pavement maintenance and rehabilitation, however, sometimes due to lack of budget and experience many local agencies don't have a formal pavement management system, but use an informal method for determining which pavements receive a specific maintenance treatment at any time..

According to Hass (1994) "Good pavement management is not usual business , it requires an organized and systematic approach to the way we think and in the way we do day to day business. Pavement management, in its broadest sense, includes all activities involved in the planning and programming, design, construction, maintenance, and rehabilitation of the pavement portion of a public works program". A pavement management system was then described by Federal Highway Administration (FHWA) as "a set of tools or methods that can assist decision makers in finding cost-effective strategies for providing, evaluating and maintaining pavements in serviceable conditions" (FHWA 1989).

Some of the possible benefits using Pavement Management Systems are:

- Facts and data let decision-makers know the impact of their decisions when developing long-range plans and annual budgets, thus reducing reliance on guesswork and political pressures.
- Show the current condition of the pavement network based on systematic and engineering procedures for obtaining objective pavement condition information.
- The consequences of past and future maintenance and rehabilitation decisions can be determined, hence, enhancing the Life of the road network by adapting different maintenance strategies suitable in terms of conditions pre-specified and any budget constraints.
- Performance of roadway conditions can be predicted along with maintenance activities saving money for future needs, and assisting policy and decision makers to effectively utilize the founds for roads under consideration by using various optimization techniques readily available in pavement management system.
- Produce a list of maintenance and rehabilitation projects.

Two major levels of pavement management decisions should be included in a PMS: network and project level.

Network-level decisions are concerned with programmatic and policy issues for an entire network. These decisions include: establishing pavement preservation policies, identifying priorities, estimating funding needs, and allocating budgets for maintenance, rehabilitation, and reconstruction (MR&R).

The network level deals with the pavement network as a whole and is generally concerned with high-level decisions relating to network-wide planning, policy and budget.

Specific products required to meet the objectives of a network level PMS include the following: information concerning the condition or health of the pavement network, establishment of MR&R policies, estimation of budget requirements, determination of network priorities.

Then its advantages are that it can:

- Optimize solutions for the entire network
- Quickly and accurately produce conditional scenarios.
- Prioritize broad areas of MR&R
- Use consistent inputs in scenario comparisons.
- More easily obtain top management attention

The project level deals with smaller constituent sections within the network and is generally concerned with lower-level decisions relating to condition; maintenance, reconstruction and rehabilitation (MR&R) assignment and unit costs.

Furthermore the network-level approach is characterized by top-down logic, system optimization, aggregate data, large data and resource requirements, and sophisticated models, while project-level decisions address engineering and technical aspects of pavement management, i.e., the selection of MR&R actions for individual projects and groups of projects. The project-level approach is characterized by simpler models respect to network-level, less data aggregation, fewer data and resource requirements, less reliance on feedback for success and better understanding.

The primary components of a pavement management system are:

1. Inventory data;
2. Pavement condition assessment;
3. Prediction models for pavement deterioration;
4. Optimization model and program implementation;

1.5.1. Inventory data

Inventory data (Table 1.1) includes geometric, lane, and crossing route data and are required for even the simplest pavement management system. Project identification including pavement type, route, functional classification, location is essential and in order to efficiently select.

Identifying pavement sections within the network using a common referencing method is one of the first tasks for developing the pavement management system. The most basic information about the road is included to reference the pavement, such as the road name or route number, location, number of lanes, and pavement type. Other inventory data may include:

- type of pavement (asphalt, concrete, composite),
- width of road,
- number of lanes,
- thickness of pavement layers, and
- drainage conditions.

Furthermore the history of the construction, rehabilitation, and maintenance of the pavement is very desirable and may be required for the systems with more complex analysis procedures.

Table 1.1 Type of inventory data

Shoulder type	Layer thickness	Material sources
Construction history	Shoulder width	Joint spacing
Functional classification	Rehabilitation history	Load transfer
Length	Maintenance history	Resilient modulus
Pavement type	Sub-grade classifications	Provision for drainage
Pavement width	Material properties	Climatic factors (precipitation, freeze-thaw)

1.5.2. Pavement condition assessment

One of the key components of an effective pavement management system is an accurate assessment of the condition of the existing pavement network. Accurate historical pavement condition information is absolutely essential for operation of the pavement management system, because all system recommendations are ultimately based on past and present condition data. Because of its vital importance and because pavements can deteriorate quickly from year to year, condition data should be collected frequently.

The assessment has historically been accomplished by an annual visual pavement condition survey. The surface cracking of a pavement represent the dominant distress for each segment of the pavement network . However, the complete condition and performance of a pavement is broader than just an assessment of the surface distress. Other factors, such as ride quality, structural capacity and friction are also important components.

However, objective pavement condition data can be expensive to obtain.

For this reason more sophisticated PMS databases contain four different types of condition data: physical distress data, roughness data, structural capacity data, and friction data. Usually an index represent the overall pavement condition. The pavement condition score is generally expressed on a scale of 0 to 100, with 100 representing the best pavement condition and 0 representing the worst pavement condition.

Pavement condition Rating (PCR) is an indicator that rates the surface condition of the pavement. It is built based on visual inspection of road section. PCR is used to quantify the road condition (FHWA, 1998). The inspection period for road might vary from segment to another depending on the type of road and the volume of traffic. PCR provides a method for regular rating of road deterioration.

Alternate methods can be used to develop a combined index or score. A combined index has several useful applications:

- It is a relatively simple way to communicate the health of the system to upper management, planners, and legislators
- Used as one factor, or the only factor, in a priority rating scheme
- Used as a technique for estimating average costs to maintain, rehabilitate, or reconstruct a candidate project;

The aims of pavement condition assessment are :

- Ranking of all pavement segments according to types of distress and condition scores as a function of traffic or road classification;
- Identification of MR&R strategies, which define a set of criteria for assigning a particular action to each pavement segment;
- Estimates of funding needs for the selected treatments.

1.5.3. Prediction models for pavement deterioration

The deterioration models can be classified into three main categories: deterministic, stochastic, and artificial intelligence models . Deterministic models are best fitted if a large amount of data is available. These models could vary from the straight-line extrapolation to regression analysis models . Markovian models are the most common stochastic techniques and have been widely used due to their need for less data. They are able to combine observed performance data with expert opinion (Elhakeem and Hegazy 2005) . The Artificial Neural Networks also work well with noisy data and enable carrying out parallel computation for multiple tasks, such as optimization and prediction.

1.5.4. Optimization models

Optimization models provide the capability for a simultaneous evaluation of an entire pavement network. The objective is to identify the network MR&R strategies which maximize the total network benefits, or minimize total network costs subject to such network-level constraints, such as available budget and desired performance standards.

A variety of methods are available to analyze pavement performance and cost data to identify cost-effective MR&R treatments and strategies. Pavement prediction performance models are used at both the network and project level to analyze the condition and determine maintenance and rehabilitation requirements. At the network level, they are used for condition forecasting, budget planning, inspection schedule, and working planning. At the project level, they are used to select rehabilitation alternatives to meet expected traffic and climate conditions, and to perform life-cycle cost analysis to compare various M&R alternatives. The aim is obtain the optimal treatment for each possible combination of performance variables such as: roughness, physical distress, traffic, environment, and functional class.

The optimization method requires identification of an objective function, decision variables and constraints. For the PMS analysis, the objective for optimization method can be:

- Maximization of user benefits.
- Maximization of network performance standards.
- Minimization of total present worth costs.

Decision variables are the set of MR&R treatments. The constraints may include the total available budget, minimum network performance standards and/or minimum performance standards for different areas. The optimization method identifies estimates of both short-term and long-term budgets needed in order to preserve the pavement network at or above prescribed standards.

An important optimization models is the life-cycle cost method that selects the MR&R treatments based on the least life cycle cost of a combination of treatments required during the analysis period. Alternative strategies can be evaluated as part of this method. The cost components included in this method of analysis are construction, maintenance between major rehabilitation treatments, cost of rehabilitation treatment and salvage value at the end of the analysis period.

In order to compare alternative strategies, life cycle costs are calculated using either present worth or equivalent uniform annual costs.

CHAPTER 2

Mechanism of geosynthetic reinforcement in road pavement

This page has been intentionally left blank

2. Mechanism of geosynthetic reinforcement in road pavement

2.1. Geosynthetics in civil engineering

In the past decades, considerable development has taken place in the area of geosynthetics and their applications (Table 2.1**Errore. L'origine riferimento non è stata trovata.**). Geosynthetics are now an accepted civil engineering construction material and have unique characteristics like all other construction materials such as steel, concrete, timber, etc.

The term 'Geosynthetics' has two parts: the prefix 'geo', referring to an end use associated with improving the performance of civil engineering applications. The American Society for Testing and Materials (ASTM) (ASTM, 1986) defines geosynthetics as "a planar product manufactured from polymeric materials used with soil, rock, earth, or other geotechnical engineering related material as an integral part of a man-made project, structure, or system."

Table 2.1 Geosynthetic products most used.

Geosynthetics	Material	Application	Function
Geotextiles	Polypropylene (PP), Polyster (PET), Polyethylene (PE)	retaining walls, slopes, embankments, pavements, landfills, dams	separation, reinforcement, filtration, drainage, containment
Geogrids	PP, PET, highdensity Polyethylene (HDPE)	pavements, railway ballasts, slopes, embankments, bridge abutments	reinforcement, separation
Geonets	Medium density Polyethylene (MDPE), HDPE	dams, pipeline and drainage facilities	drainage
Geomembranes	PE, polyvinyl Chloride (PVC)	containment ponds, reservoirs, and canals	fluid barrier
Geocomposites	depending to geosynthetics combination	embankments, pavements, slopes, landfills, dams	separation, reinforcement, filtration, drainage

They are available in a wide range of forms and manufactured using different materials and processes. They have been used for a wide range of applications in civil engineering including roads, airfields, railroads, embankments, earth retaining structures, canals, dams and coastal protection.

The materials used in the manufacture of geosynthetics are primarily synthetic polymers generally derived from crude petroleum oils; although rubber, fiberglass, and other materials are also sometimes used for manufacturing geosynthetics. Geosynthetics is, in fact, a generic name representing a broad range of

planer products manufactured from polymeric materials; the most common ones are geotextiles, geogrids, geonets, geomembranes and geocomposites.

2.1.1. Geotextile (GTX)

According to the definition of ASTM 4439, a geotextile is defined as "a permeable geosynthetic comprised solely of textiles. Geotextiles are used with foundation, soil, rock, earth, or any other geotechnical engineering-related material as an integral part of human-made project, structure, or system."

The ASAE (Society for Engineering in Agricultural, Food, and Biological Systems) defines a geotextile as a "fabric or synthetic material placed between the soil and a pipe, gabion, or retaining wall: to enhance water movement and retard soil movement, and as a blanket to add reinforcement and separation." A geotextile should consist of a stable network that retains its relative structure during handling, placement, and long-term service. Geotextiles have many applications and currently support many civil engineering applications including roads (Figure 2.1), airfields, railroads, embankments, retaining structures, reservoirs, canals, dams, bank protection, coastal engineering and construction site silt fences or geotube. Usually geotextiles are placed at the tension surface to strengthen the soil. Geotextiles are also used for sand dune armoring to protect upland coastal property from storm surge, wave action and flooding.

Figure 2.1 Geotextile in road application

Currently available geotextiles are made of polypropylene or polyester and are classified into the following categories based on the manufacturing process:

- Woven geotextile: A geotextile produced by interlacing, usually at right angles, two or more sets of yarns (made of one or several fibres) or other elements using a conventional weaving process with a weaving loom (Figure 2.2a);

- Nonwoven geotextile: A geotextile produced from directionally or randomly oriented fibres into a loose web by bonding with partial melting, needle-punching, or chemical binding agents (glue, rubber, latex, cellulose derivative, etc.) (Figure Figure 2.2b);
- Knitted geotextile: A geotextile produced by interlooping one or more yarns (or other elements) together with a knitting machine, instead of a weaving loom (Figure 2.2c);
- Stitched geotextile: A geotextile in which fibres or yarns or both are interlocked/ bonded by stitching or sewing.

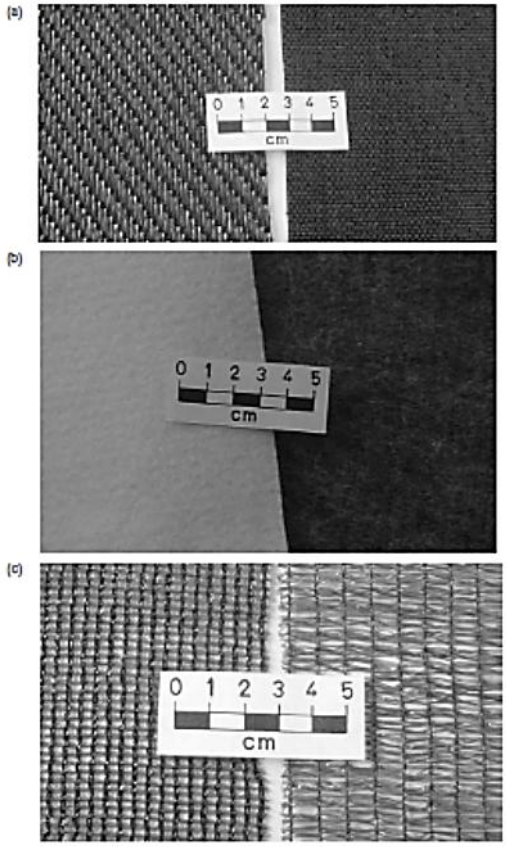

Figure 2.2 Typical geotextiles: (a) woven; (b) nonwoven; (c) knitted

Relatedly road applications, geotextiles are mainly the function of separation and reinforcement (or stabilization). Applying nonwoven geotextile directly on subgrades extends road life by preventing fine subgrade soil particles from migrating and intermixing into the aggregate and ballast base course. What it does is that acts as a filter/separator to maintain the integrity of the subbase by preventing movement of subgrade particles into the subbase. Roadway pavements are basically structures for taking the high contact pressures from the vehicle tires and reducing that pressure through the depth of the pavement to a level that can be supported by the underlying soil. Pressure is dissipated down through the various layers of materials within the pavement. Recently, for temporary road construction in environmentally sensitive areas, a biodegradable woven jute geotextile has been developed. These fabrics will totally biodegrade after one to two seasons, eliminating the need to remove a synthetic geotextile from under the roadbed. It is economical for use on roads that will be decommissioned after use. Moreover, reinforcement composite geotextile

(geocomposites) are used for laying railway tracks over weak grounds or ground with loose soil foundation or structure.

2.1.2. Geogrid (GG)

A geogrid is a polymeric product consisting of a mesh or net-like regular openings with longitudinal and transverse ribs joined at the junctions. The ribs can be linked by extrusion, bonding or interlacing: the resulting geogrids are respectively called extruded geogrid (Figure Figure 2.3a-i and Figure Figure2.3a-ii), welded geogrid (Figure Figure 2.3b) and woven geogrid (Figure Figure 2.3c), respectively.

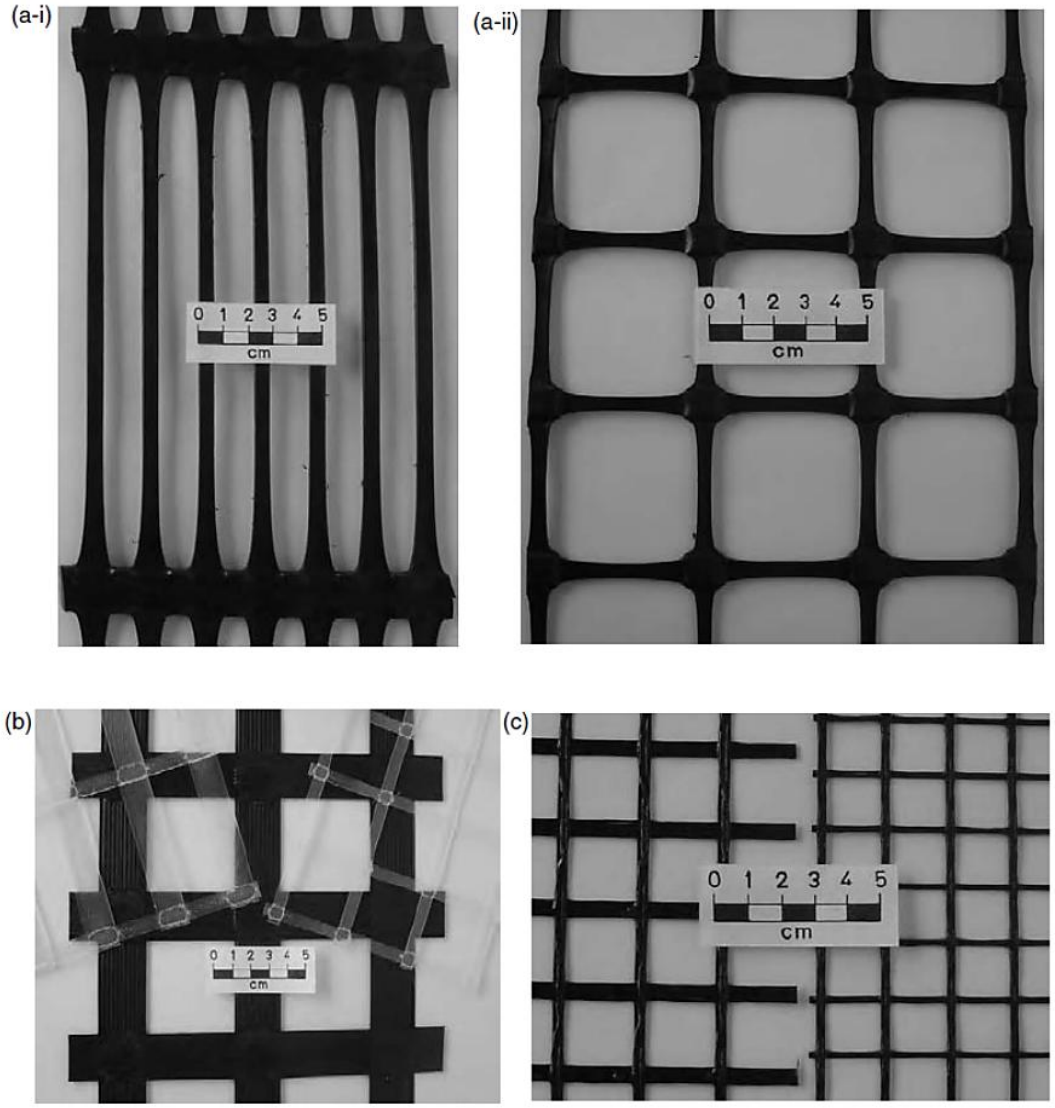

Figure 2.3 Typical geogrids: (a) extruded – (i) uniaxial; (ii) biaxial; (b) welded; (c) woven.

Extruded geogrids are classified into the following two categories based on the direction of stretching during their manufacture:

- Uniaxial geogrid: A geogrid produced by the longitudinal stretching of a regularly punched polymer sheet, and therefore it possesses a much higher tensile strength in the

longitudinal direction (machine-direction, MD) than the tensile strength in the transverse direction (TD) (Figure 2.3a-i).

- Biaxial geogrid: A geogrid produced by stretching in both the longitudinal and the transverse directions of a regularly punched polymer sheet, and therefore it possesses equal tensile strength in both the longitudinal and the transverse directions (Figure 2.3 a-ii).

The key feature of geogrids is that the openings between the longitudinal and transverse ribs, called apertures, are large enough to create interlocking with the surrounding soil particles (Figure 2.4). The shapes of the apertures are either elongated ellipses, near-squares with rounded corners, squares or rectangles. The dimensions of the apertures vary from about 2· 5 to 15 cm. The ribs of geogrids are often quite stiff compared to the fibres of geotextiles. Moreover, the junction strength is important in the case of geogrids because, through these junctions, loads are transmitted from one type of rib to the other when placed into the soil.

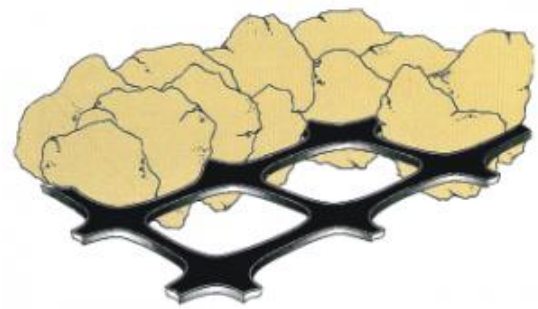

Figure 2.4 Geogrid with interlocking phenomena (www.tenax.net)

2.1.3. Geocell (GCL)

Geocell is three-dimensional, permeable, polymeric honeycomb or web structure, assembled from geogrids and special bodkins couplings in triangular or square cells or produced in the factory using strips of needle-punched polyester or solid high density polyethylene (HDPE). Geocells consisting of a series of interconnected single triangular or square cells completely encase the soil. In road applications (Figure 2.5) they have reinforcement functions because provide all-around confinement, thus preventing the lateral spreading of the infill material. Due to the confinement of the soil the geocells increase the stiffness and the load-deformation behaviour of gravel base layers and thereby reduce the deformation of the soil. The soil-geocell layers act as a stiff mat, thus distributing the vertical traffic loads over a much larger area of the subgrade soil.

Figure 2.5 Geocells in road application

2.1.4. Geonet (GN)

Geonets are extruded polymer meshes and look like geogrids (Figure 2.6Figure). They are different from geogrids, not in the material or configuration, but in their functions to perform the in-plane drainage of liquids or gases. In particular, geeonets have a polymeric structure, in the form of manufactured sheet, consisting of a regular network of integrally connected overlapping ribs, whose openings are usually larger than the constituents, used in geotechnical, environmental, hydraulic and transportation engineering applications. The manufacture of geonets begins with blending of the raw materials, which are fed into an extruder where the polymeric material is melted. It then passes into a counter rotating former which produces ribs at acute angles to one another; pressure is used to push the extrudate forward over a steel spreading mandrel which opens the ribs in a relatively large diamond-shaped apertures, typically 12 mm long by 8 mm wide, and 5 to 7 mm thick. The resulting angles are of the order of 70° and 110°.

There are three categories of geonets. The following are illustrated:

- Biplanar geonets: .these are the original and most common types and consist of two sets of intersecting ribs at different angles and spacings. The ribs themselves are of different sizes and shapes for different styles (Figure 2.6a).
- Triplanar geonets: these have parallel central ribs with smaller sets of ribs above and beneath mainly for geometric stability (Figure 2.6b).
- Other geonets: These newer geonet structures have either box shaped channels or protruding columns from an underlying support network.

Geonets are used almost exclusively for their drainage capability. As such, they are single-function geosynthetics.

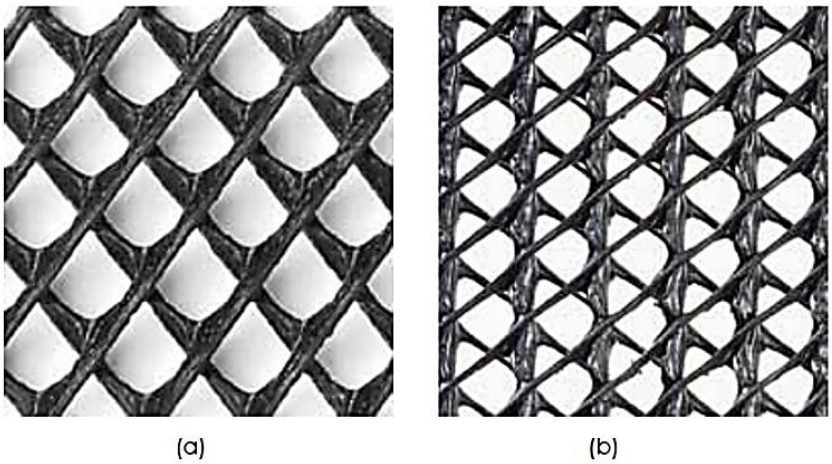

Figure 2.6 - Geonets structure types: a) biplanar; b) triplanar.

2.1.5. Geomembrane (GM)

A geomembrane (Figure 2.7) is very low permeability synthetic membrane liner or barrier used with any geotechnical engineering related material so as to control fluid (or gas) migration in a system. Geomembranes are waterproofing polymeric sheets and constitute the most significant group within the geosynthetics. They are used in a wide and growing range of applications (landfills, lagoons, channels, ornamental ponds), so geomembranes are present in environmental applications, geotechnical, transportation, hydraulic and other engineering works. The materials may be polymeric or asphaltic or a combination thereof. The term barrier applies when the geomembrane is used inside an earth mass. The term liner is usually reserved for the cases where the geomembrane is used as an interface or a surface revetment.

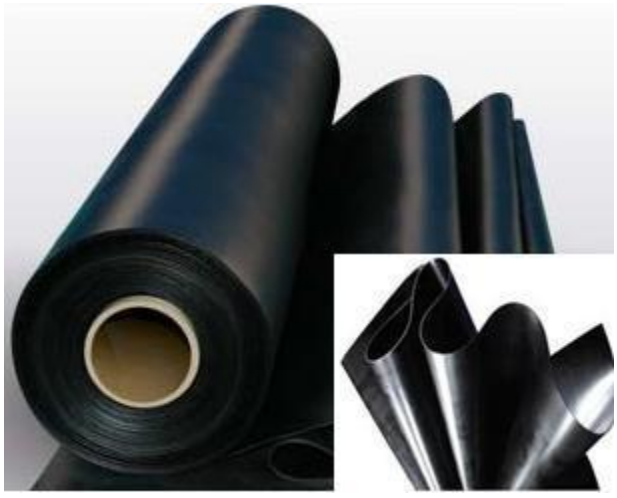

Figure 2.7 - Geomembrane

2.1.6. Geocomposite (GC)

Geocomposite (Figure 2.8) are, as the name suggests, basically combinations of two or more different types of geosynthetic in such a way that specific applications are addressed in the optimal manner and at minimum cost. There is almost no limit to the variety of geocomposites that are possible and the

development of these materials results from the anticipated usefulness of their multifunctionalities and the opportunity for more rapid installation than by using the individual components. In particular five basic functions that can be provided were individuated: separation, reinforcement, filtration, drainage, and containment.

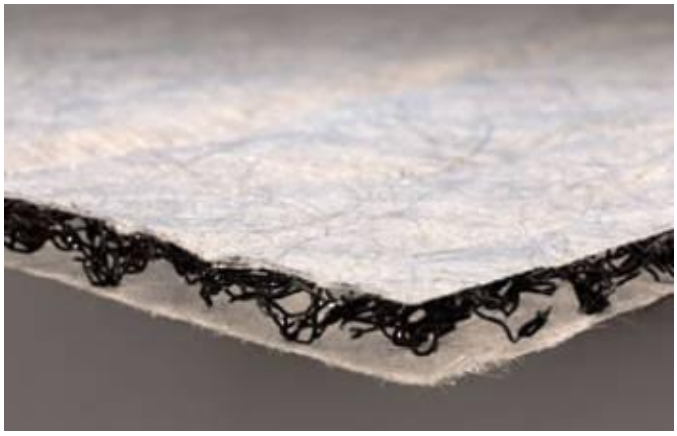

Figure 2.8 Geocomposite (www.geofabrics.co.nz)

2.2. Geosynthetics in pavement road application

During the past decades, the use of geosynthetics in pavements has widely increased. The attraction of this application lies in the possibility to increase pavement service life and to reduce the base course thickness (Perkins and Ismeik, 1997). The first alternative is beneficial if the cost of the geosynthetic is less than the combined cost of the replaced base course material and any construction related costs associated with a reduced base thickness (such as excavation, relocation of utilities, and purchase of right-of-way). Benefits are seen with the second alternative when maintenance and replacement costs are offset by the cost of the geosynthetic. Both alternatives are In particular attractive in areas where quality gravel sources are scarce, in urban areas where these sources have become depleted, or in environmentally sensitive areas where the siting of gravel quarries is not permitted (Palomino et al. , 2010).

The Federal Highway Administration has identified the following benefits of using geosynthetics in roadways:

- Reducing the intensity of stress on the subgrade and preventing the base aggregate from penetrating into the subgrade;
- Preventing subgrade fines from pumping or otherwise migrating up into the base;
- Allowing an increase in subgrade strength over time;
- Preventing contamination of the base materials, which may allow more open-graded, freedraining aggregates to be considered in the design;
- Reducing the depth of excavation required for the removal of unsuitable subgrade materials;
- Reducing the thickness of aggregate required to stabilize the subgrade;
- Reducing disturbance of the subgrade during construction.
- Reducing maintenance and extending the life of the pavement;

Another optimal benefit that is not included in the above list is the reinforcement of asphalt concrete surface.

A large type of deterioration factors affect the service life of roads and pavements including environmental factors, subgrade conditions and traffic loading. These factors contribute to an equally wide variety of pavement conditions and problems which must be addressed in the maintenance or rehabilitation of the pavements system. Furthermore pavement maintenance treatments are often ineffective and short lived. Therefore, to obtain a long service life there are various performance safeguards like include stabilizing the subgrade against moisture intrusion and associated weakening; strengthening road base aggregate without preventing efficient drainage of infiltrated water; and, as a last resort, enhancing the stress absorption and moisture proofing capabilities of selected maintenance treatments.

Geosynthetics are the most cost effective tools for safeguarding roads and pavements in these ways.

Geosynthetics provide significant improvement in pavement construction and performance. The three primary uses of a geosynthetic in a road application are: to serve as a construction aid over soft subgrades, extend the pavement service life and reduce the thickness of various layer for a given service life. Then the geosynthetics have traditionally been used in three different pavement applications: mechanical subgrade stabilization, aggregate base reinforcement and asphalt concrete (AC) overlay reinforcement.

The primary functions that geosynthetic materials may provide in pavement applications are separation, filtration and reinforcement.

2.2.1. Separation

When a geosynthetic is used with a separation function (Figure 2.9), its role are to preventing the intermixing of particles from two soil layers with different properties. Furthermore as separation function there are various material properties that must be taken into account to determine quantitatively which geosynthetic is suitable for a specific application, such as tensile strength, and resistance to tear and impact.

All design theories of layered pavement systems assume that the construction materials will remain as they are initially placed and with the same thickness. However, there are a mechanisms that may effectively reduce the thickness of the base course layer if it is constructed over a soft subgrade soil (Al-Qadi et al., 1994).

One of these is the tendency for the subgrade fines to move into the aggregate particles via subgrade pumping, In particular when the soil is wet. Pumping results in the accumulation of fines beginning near the bottom of the base course and continuing upward. This results in reduced base layer modulus and effective thickness, potentially leading to structural failure of the pavement system. The second mechanism is the penetration of aggregate stone particles into soft subgrade soil as local shear failure of the soil occurs and that was generated by the vehicle load pressure. The degradation is greatly accelerated if the aggregate is compacted over a wet subgrade or if the subgrade remains wet for extended periods during road use (Salman Ahmed Bhutta, 1998).

Reduction of the base thickness results in a decrease in the load-carrying capacity of the pavement system and a reduction in the pavement life.

Figure 2.9 Separation function (Stephen Archer, 2013)

2.2.2. Filtration

The filtration function, which is closely related to the separation function, prevents fine particles being washed from the subgrade into the road base material under the effects of traffic loads. The prevention of particles moving due to the action of water is similar to the prevention of piping in the filter function, except that in separation, it is in connection with a flow of water induced by the sudden application of an external load. Usually, this load will be a wheel load form some mode of transport. This process of erosion of the subgrade and movement of soil particles by water flow induced by a rapidly applied wheel load is frequently referred to as "pumping".

Pumping may occur when stresses are applied to a base course material, if water is present at the loose base course - subgrade interface, and when the subgrade is a fine grained soil.

Filtration is one of the functions most widely performed by geotextiles. The filtration function has two concurrent objectives: to retain the particles of the filtered soil, while permitting water to pass through the plane of the geotextile from the filtered soil. These two parallel roles are the key to filtration design. The use of geotextile filters can be subdivided into three categories based on the flow conditions. These are listed below in ascending order of severity (Sigurdsson, 1991):

- fairly steady unidirectional flow;
- reversing flow with a moderate cycle time;
- reversing flow with a very short cycle time.

The permeability criterion is one of the main factors in selecting an appropriate geotexile, in fact in the filtration function, the volume of water moving through the fabric is a key design element specifically addressed in the design and selection of the geotextile. It must be able to convey a certain quantity of water across the plane of the fabric through-out its design life to prevent the buildup of water pressure.

2.2.3. Reinforcement

Reinforcement is define as the synergistic improvement of a total system created by the inclusion of a geosynthetic (that is good in tension) into a soil (that is usually poor in tension) (Koerner, 1990). The geosynthetic reinforcement has generally been placed at the interface between the base and sub-grade layers or the interface between the base and subgrade layers for paved and unpaved road or within the base course layer or asphalt layer for the flexible pavement.

Two areas of reinforcement have found a great deal of success in pavement applications: subgrade and granular layer reinforcement, and HMA layer and overlay reinforcement.

The effectiveness of geosynthetics reinforcement of the subgrade and granular layers depends on three contributing mechanisms:

- Bonding between the reinforcement and the surrounding pavement materials defines the mobilized portion of the interlayer strength that may contribute to the reinforcement. This mechanism is essential for a solid interlayer (e.g., geotextile).
- Interlocking between the reinforcement and the surrounding aggregates. This mechanism, which is essential for interlayer products with openings, results from the protrusion of aggregates through the openings of the interlayer.
- Confinement of the reinforced layer results in a reduction of the horizontal deformation by lateral restraint. This mechanism is In particular important with relatively non-weak subgrade soils (Al.Qadi et al., 2008).

Some studies (Siriwardane, 2010; Canestrari, 2013; Montestruque, 2004) has established that vertical displacements have decreased with the inclusion of the geogrid within the asphalt layer with an improvement of approximately 38%. Observations showed that the inclusion of a geosynthetic reinforcement spreads the circular load over larger area in the lower layers of the pavement section reducing vertical stresses.

Three fundamental reinforcement mechanisms have been identified involving the use of geosynthetic to reinforce pavement materials:

1) lateral restraint;
2) improved bearing capacity;
3) tensioned membrane effect

2.2.3.1. Lateral restraint

The primary mechanism associated with the reinforcement function for pavement system is lateral restraint or confinement (Figure 2.10).

A spreading effect occurs when pressure from the wheel load creates shear stresses. Vertical strain resulting from the spreading effect can eventually cause rutting, or channelized depression in the wheel paths of highway pavement. One solution to limit this vertical strain would be through geosynthetics restraint of lateral movement due to frictional force between the geosynthetic and base course proportionally of the compaction of the base material into the geosynthetics.

Interaction between the base aggregate and the geosynthetic through the interlocking allows transfer of the shearing load from the base layer to a tensile load in the geosynthetic.

The tensile stiffness of the geosynthetic limits the lateral strains in the base layer. Furthermore, a geosynthetic layer confines the base course layer thereby increasing its mean stress and leading to an increase in shear strength.

The modulus of the base is expected to increase along with the developed shear interaction between the aggregate and geogrid since the granular base course is stress-dependent. The increase in base layer modulus results in an improved vertical stress distribution (more widely distributed) above subgrade, subsequently reducing subgrade deformation (Perkins, 1999).

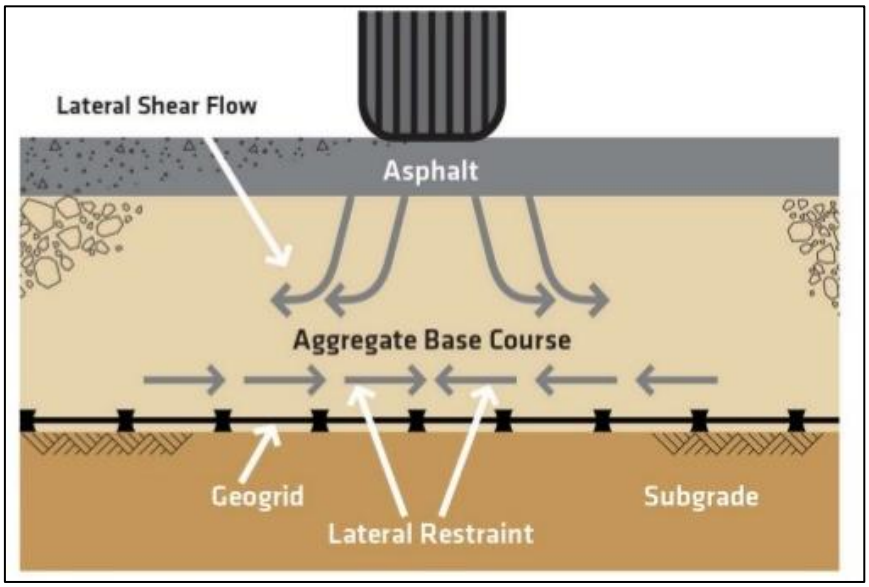

Figure 2.10 Lateral restraint reinforcement mechanism (Stephen Archer, 2013)

2.2.3.2. Improved bearing capacity

The second mechanism, improved bearing capacity, is attributed to the “forced” initiation of the potential failure surface along an alternate plane, with modified configuration, providing a higher total resistance.

As illustrated in Figure 2.11 the increased bearing capacity mechanism leads to soil reinforcement when the presence of a geosynthetic imposes the development of an alternate failure surface, furthermore the failure envelope of the pavement system is achieved by shifting from the relatively weak subgrade to the relatively strong base course material. This new alternate plane provides a higher bearing capacity. The geosynthetic reinforcement can decrease the shear stresses transferred to the subgrade and provide vertical confinement outside the loaded area. The bearing failure mode of the subgrade is expected to change from punching failure without reinforcement to general failure with reinforcement.

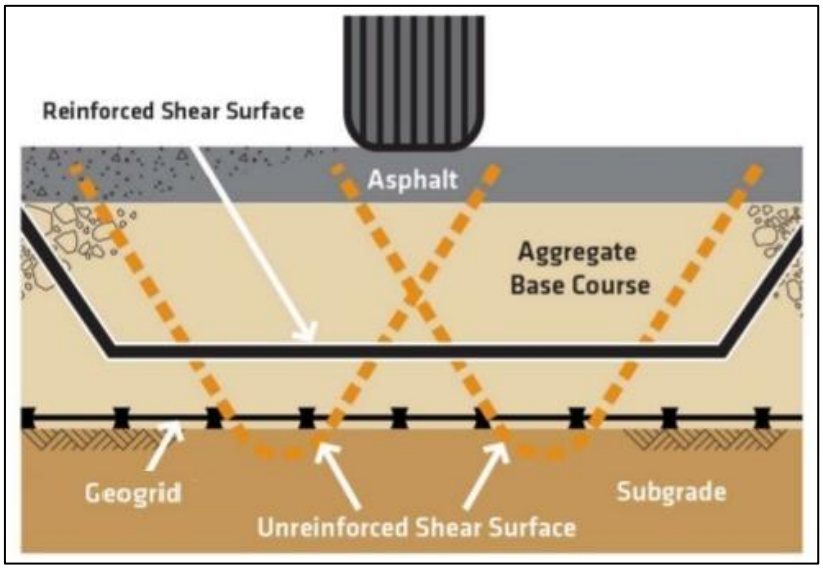

Figure 2.11 Improved bearing capacity mechanism(Stephen Archer, 2013)

2.2.3.3. Tensioned membrane effect

The geosynthetic can also be assumed to act as a tensioned membrane, which supports the wheel loads (Figure 2.12).

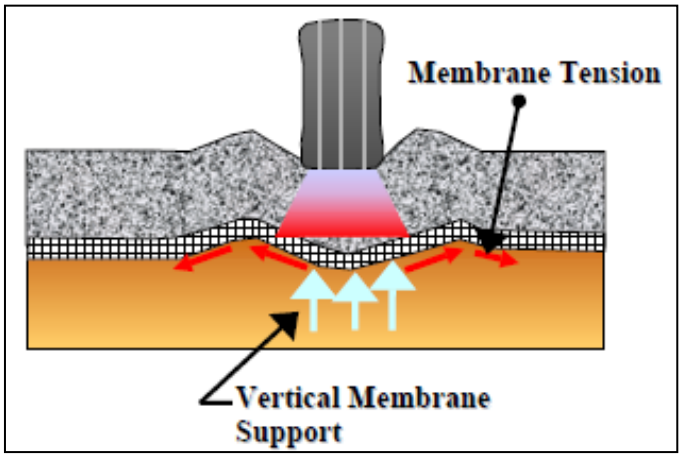

Figure 2.12 Tensioned membrane effect

In this case, the reinforcement provides a vertical reaction component to the applied wheel load. The tensioned membrane effect develops as a result of vertical deformations creating a concave shape in the geosynthetic. The tension developed in the geosynthetic contributes to support the wheel load and reduces the vertical stress on the subgrade.

Higher deformations are required to mobilize the tension of the membrane for decreasing stiffness of the geosynthetic. Each of these functions is inappropriate for permanent paved roads where significant rut depths cannot be tolerated, and where bearing capacity failure is not a permissible failure mechanism.

2.3. Geosynthetics in paved road

The idea to reinforced paved road appeared in the early 1950s in the US and was based on the general concept that if asphalt layer is strong in compression and weak in tension, then reinforcement could be used to provide needed resistance to tensile stresses, in the same manner as reinforced concrete.

For paved road which undergo a small level of permanent deformation, the important aforesaid reinforcing effects observed in unpaved roads are considerably less apparent. It is due because the geosynthetic must undergo tensile strain due either to lateral stress or large permanent deformations to be effective as a reinforcing element.

In order to rehabilitate and/or improve flexible pavement mechanical performance, geosynthetic or metal reinforcements can be introduced between the flexible pavement layers. Geosynthetic materials in widespread use for flexible pavement are geogrids, which, depending on the grid constituent material, the mesh shape and size and the stiffness and position in the pavement structure, are able to increase fatigue resistance, reduce rutting and limit reflective cracking.

Flexible pavements are constructed so that traffic loads are distributed from the surface to underlying layers. Therefore, the purpose of using geosynthetics as reinforcements in layered flexible pavement system is to improve a stress distribution the load over a large areas with increasing of depth and increase the structural or load-carrying capacity of a pavement system by transferring the load to the geosynthetic material.

Usually, vehicular traffic exerts shear and tensile forces on pavements and when these forces generate strains greater than the yield strength of the overlays cracking starts. Asphalt overlays can also suffer fatigue cracking caused by tensile strength in the lower part of them.

Two are the main benefits of using geosynthetics, such as geogrids and geotextiles in the base course layer of flexible pavements. For a given cross-section of the pavement, addition of geosynthetic leads to an increase in serviceability life and reduction in the maintenance cost of the pavement. This alternative is feasible when the maintenance and replacement costs during the service life of the pavement are offset by the high initial cost of using the geosynthetic for a given project. Moreover, if the pavement is designed for same serviceability life as an unreinforced pavement, the addition of geosynthetic may results in the reduction in the thickness of the base course layer. This alternative is feasible if the cost of the geosynthetic is less than the combined cost of the replaced base course material and any construction related costs associated with a reduced base thickness (Perkins and Ismeik, 1997).

There are a lot of parameters that influence the reinforcement system in flexible pavement. They are:

- the number of geosynthetics layers and selected location (on the top of subgrade, on the top of subbase, at the asphalt-base course interface, in asphalt layer);
- the geosynthetics mechanical properties (tensile strength and stiffness, junction strength, etc.);
- the geosynthetics hydraulic properties (permeability, pore size characteristics);
- the durability (survivability, polymer type, chemical, physical and biological environment).

- type of reinforcement mechanism that want to obtain;
- the position of the reinforcement in the pavement structure.

The position of the geogrid in the pavement structure is one of the most widely investigated subjects due to the important effects that it produces in terms of both the reduction in rutting and the reduction in cracking under repeated loading cycles. In particular, the positioning of the reinforcement at different depths in the road pavement provides different reinforcement mechanism, beneficial effects on performance. The geosynthetic can be place at the base, subgrade-base interface and asphalt layer.

In the base reinforcement a geosynthetic can be used as a tensile element at the bottom of a base (or sub base) or within a base course to improve the service life or obtain an equivalent performance with a reduced structural section. Base reinforcement is applicable for the support of vehicular traffic over the life of the pavement and it is designed to address the pavement distress mode of permanent surface deformation or rutting and asphalt fatigue cracking.

The geosynthetic can be place at the sub-base/subgrade interface to increase the support of construction equipment over a weak or low strength subgrade. The primary result of this application is increased bearing capacity. Lateral restraint and/or tension membrane effects may also contribute to load-carrying capacity. Subgrade restraint is the reinforcing component of stabilization.

One of the more serious problems in flexible pavement is reflective cracking. This phenomenon is commonly defined as the propagation of cracks from the movement of the underlying pavement or base course into and through the asphalt layer as a result of load-induced and/or temperature-induced stresses. Increasing traffic loads, inclement weather, and insufficient maintenance funding increase this problem.

With appropriate design and correct installation, many improvements can result from reinforcing asphalt layer: increased tensile strength; increased resistance to reflective cracking and bottom-up fatigue cracking; increased shearing resistance and hence may reduce shoving and flow rutting; increased coherence in the overlay;

Barksdale (1991) concluded that under favorable conditions, moderate to significant levels of reflection cracking in HMA pavement overlays can be delayed two to four years and, in a few instances, as long five years by using a full-width paving fabric interlayer. Favorable conditions for the use of full-width paving fabrics with flexible pavements include:

- the presence of fatigue (load)-related failure frequently evidenced by alligator cracking.
- the HMA overlay must be engineered to be structurally capable of handling the anticipated loadings. A deflection-based procedure should give the overlay thickness determination for each pavement subsection.
- paving fabrics are usually ineffective for controlling thermal cracks, because those cracks are usually ½ to 1 inch or more wide.

2.3.1. Reinforcement of unbound layer

The inclusion of geosynthetics in flexible pavement structures for reinforcement of unbound layer has long been accepted as a means of reducing overall costs and/or extending pavement service life.

Geosynthetics are widely used as reinforcement elements for aggregate base and subbase layers. It is placed at the bottom, within a base course or at the interface between the base and subbase. The reinforcement base/subbase interface is typically used to support vehicular traffic over the life of the pavement structure. Geogrids constitute the majority of geosynthetic products used to provide reinforcement with benefits ranging from reducing aggregate thickness to prolonging the service life of the pavement system. The primary mechanism of geosynthetic granular base reinforcement is the horizontal reinforcement achieved by providing lateral restraint. It is thought that the geogrid interacted with the surrounding materials developing friction forces that would provide a lateral confinement to the system.

Presence of geosynthetic reinforcement at the interface of subgrade and aggregate layer or within the aggregate layer provide two modes of action that are: confinement effect and tensioned membrane effect. Furthermore, the reinforcement can absorb additional shear stresses between the subgrade and the aggregate layer, which would otherwise be applied to the soft subgrade. Granular base reinforced by geogrids could be a crucial choice to ensuring their successful and beneficial application in low to moderate volume roads having thin hot-mix asphalt surfaces and subgrade California Bearing Ratios (CBRs) between 3 to 8%.

According to Christopher et al. (2000), the use of geogrids can result in reduced surface rutting of flexible pavement and aggregate base thickness requirements or extended service live of the pavement.

2.3.2. Reinforcement in asphalt overlays

Most overlays are done predominantly to provide a waterproofing and pavement crack retarding treatment. A minimum thickness of the asphalt overlay may be required to provide an additional support to a structurally deficient pavement.

With an increase in rehabilitation funds and a decline in new road construction, this type of reinforcement appears to be the major contribution that interlayer products may provide in pavement applications. Repairing a deteriorated road using a conventional overlay is rarely a permanent solution. When an overlay is placed over a crack, the crack grows up to the new surface. The causes of crack formation and enlargement in asphalt overlays are numerous but the mechanisms involved may be categorized as: traffic induced, thermally induced and surface initiated. The original cracks reflect in the new surface causing the “reflection cracking ” phenomena.

According to Lytton (1989), the passing of a wheel load over a crack in the existing pavement causes three critical pulses, one maximum bending and two maximum shear stresses (Figure 2.13).

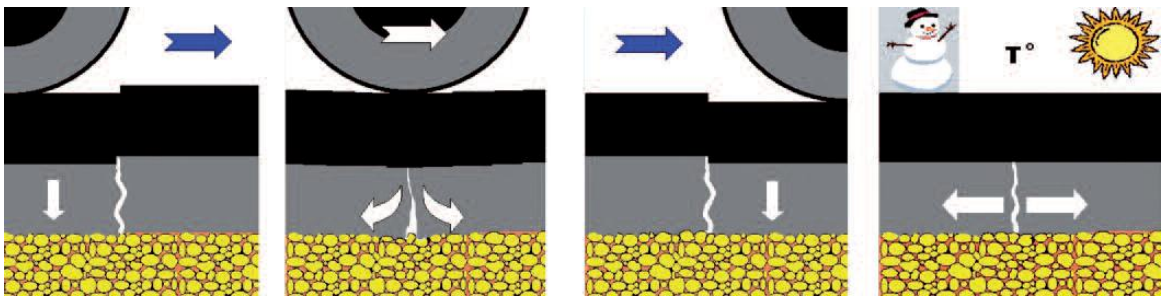

Figure 2.13 Cracking mechanism

The AASHTO Design Guide (1993) suggests that paving geosynthetics can be effective in controlling (reducing) reflection cracking from low and medium severity alligator-cracked pavements and that they may also help control the reflection of thermal cracks. This procedure is typically accomplished by attaching a geosynthetic product to the existing pavement (flexible or rigid) with an asphalt tack coat and then overlaying a hot mix asphalt layer with a specified thickness (Figure 2.14).

Based on earlier work by Lytton (1989) and Al-Qadi (1994,1997), the stress relief failure mode can be summarized as follows:

1) the crack starts to propagate (due to thermal and traffic loading) from its original position upward until it reaches the stress-relieving layer. Due to its low stiffness, the interlayer will exhibit large deformations, which will be accompanied with a dissipation of energy.
2) a second mode of failure that was hypothesized explain that a crack can be initiated near the surface.(16) In this failure mode, the crack starts to propagate upward from its original position until it reaches the stress-relieving layer.
3) from the previous mechanism, it can be concluded that reinforcement effect can only occur if the interlayer is sufficiently stiffer than the surrounding materials. The stiffness of an interface is equal to the material elastic modulus times its thickness.

Figure 2.14 Geosynthetic installation in asphalt layer

Roberts et al. (1996) considered four methods that are commonly employed to reduce reflective cracking:

1. increasing the HMA overlay thickness;
2. performing special treatments on the existing surface;
3. treatments only on the cracks and/or joints;
4. special considerations of the HMA overlay design (reinforcement with geosynthetic).

Methods for controlling reflective cracking and extending the life of overlays consider the importance and effectiveness of overlay thickness and proper asphalt mixture specification. Asphalt mixes have been improved and even modified by adding a variety of materials.

The most basic way to slow down the reflective cracking is to increase the overlay thickness. In general, as the overlay thickness increases, its resistance to reflective cracks increases. Limits on the

thickness of an overlay are the expense of asphalt and the increase in the height of road structure. More and more geosynthetic reinforcements in asphalt overlays have been mostly indicated to minimize fatigue and reflection of cracks

The main functions generally attributed to geosynthetic reinforcements in asphalt layers are described as increase in asphalt fatigue life, thermal and reflective cracking mitigation, with three associated group of mechanisms: strain-relief, waterproofing and reinforcement.

Usually geosynthetic is placed at the bottom of asphalt layer to absorb a large portion of the energy that would otherwise contribute to the reflective cracking. In fact, the addition of a stress-relief interlayer reduces the shear stresses between the existing pavement and the new overlay, creating a break layer that gives the overlay a degree of independence from movements in the existing pavement. For a pavement with geosynthetic reinforcement, whenever a crack starts to form in the pavement overlay, the ribs of the geogrid will develop tensile stress subsequent to the movement or opening of the crack surface. With this, the geogrid can restrain the growth of the opening fracture.

Therefore by incorporating geosynthetics in asphalt layers, the following effects are expected:

- absorption of thermal stresses;
- absorption of traffic loads deformations;
- deviation of reflective cracking;
- providing the waterproofing;
- delaying and reducing the surface cracking reflection.

In general, geosynthetics in asphalt layers have been focused to provide structural improvements to the pavement in the following situations:

1. Because it is a reinforcing material, the elastic stiffness of asphalt layer under traffic load may ultimately be increased, leading to a reduction in vertical stresses that acts in the underlying layers, which implies a reduction of rutting due to the plastic deformation under the action of repeated traffic loads;
2. In the post-cracking stage, by introducing a stiff tensile element at the base of an asphalt overlay;
3. In the maintenance of pavements, especially very cracked wearing surfaces to the point of reconstruction, the application a geogrid reinforcement and a resurfacing asphalt layer, may be the most cost effective alternative;
4. In new pavements, the inclusion of a geosynthetic reinforcement in the asphalt layer within the tensioned area can lead to an increase in fatigue life of the pavement, allowing an asphalt overlay thickness reduction;

2.4. Geosynthetics in unpaved road

Unpaved roads have been extensively used throughout the world for lowcost roads, access roads, etc. Unpaved low volume roads are used extensively for either temporary or permanent transportation purposes, such as haul roads, access roads, rural roads and parking lots. These roads will be subjected to problems like excessive rutting and mud pumping when constructed on weaker subgrade soils, making the road unusable for the traffic.

Many researchers have studied the performance of geosynthetics used in the construction of unpaved roads through full-scale and laboratory model tests.

A vast amount of early research on geosynthetics for reinforcement in unpaved roads has occurred over the last decades. A major advancement in this area was the development of an analytical treatment of unpaved road design with geosynthetic reinforcement, based on the concept of membrane-type reinforcement. The membrane effect refers to the reinforcement provided by a geosynthetic when large rutting is achieved, stretching and allowing the geotextile to provide some vertical (membrane) support.

In the first time, in real unpaved roads geotextiles were used more than geogrids because separation in many cases was the main function required. In these cases, there isn't generally design method. When no design is involved, the aggregate layer thickness and the geotextile are selected on the basis of preceding projects using the same geotextile.

In unpaved roads that are the first phase of construction of paved roads, geotextiles are used if the main concern is separation, whereas geogrids are used more than geotextiles when reinforcement is required, in particular when it is considered important to keep deformations of the aggregate layer as small as possible (Giroud, 2009).

Numerous field trials and full-scale laboratory investigations have illustrated benefits offered by geosynthetics used to reinforce unpaved roads on soft subgrade. In fact, they facilitate compaction (Bloise, 2000), improve the bearing capacity, extend the service life (Cancelli and Montanelli, 2009;Collin et al., 1996), reduce the necessary fill thickness (Bloise, 2000; Cancelli and Montanelli, 2009; Collin et al., 1996; Miura et al., 1990), decrease deformations, and delay rut formation. Furthermore, previous studies (Cancelli and Montanelli,2009; Perkins et al., 1998;Miura et al., 1990) show that reinforcing unpaved roads-over asoft subgrade with geosynthetics could reduce the necessary fill thickness by approximately 30%.

When built on soft foundation soils large deformations can occur that increase maintenance costs and usually lead to periodic interruptions to traffic. The application of geotextiles for the maintenance of unpaved roads has been initiated in the late 1970s.

Geosynthetics have been used in the construction of low-volume, unsurfaced roads on weak and saturated soils to reinforce the base course–subgrade interface. To stabilize weak soil with a geosynthetic for trafficking, the geosynthetic is placed directly on the soil and then covered with aggregate.

In the case of unpaved roads, the need to limit the sagging, in particular the differential ones, and to increase the load bearing capacity of the road base, leads to consider the use of geosynthetics for the construction of a foundation layer reinforced. The base course layer is designed to support and distribute traffic loading to the subgrade. Problems are usually encountered when the subgrade consists of soft clays, silts and organic soils. In fact in this case the road structure is highly heterogeneous: the two materials (granular in the base and cohesive in the subgrade) behave differently, which makes the mechanisms complex and it is complex to analyze the performance of a structure that is progressively modified by load repetition.

The geosynthetic contribution to the performance of an unpaved road is achieved through several mechanisms that take place in the road structure, which consist:

- Separation between base and subgrade;

- Lateral restraint of the base material;
- Improvement of wheel load distribution;
- Tensioned membrane effect.

2.4.1. Separation between base and subgrade

A geosynthetic in unpaved road placed at the interface between the aggregate base course and the subgrade performs the function of separation when it prevents interpenetration of two materials that tend to intermix when they are squeezed together by traffic loads.

Therefore, separation is important to maintain the design thickness and the stability and load-carrying capacity of the base course. In fact, soft subgrade soils are most susceptible to disturbance during the construction phase such as clearing, grubbing, and initial aggregate placement. Therefore,geosynthetics can help minimize subgrade disturbance and prevent loss of aggregate during construction.

In the case of reinforcement unpaved road, separation of the base aggregate and the subgrade soil prevents the loss of aggregate into the subgrade and in the same time prevents intrusion of fine subgrade soil particles into the aggregate base course. This aspect is most important because it only takes a small amount of fines in the base course to significantly reduce its mechanical strength.

Geotextiles (Figure 2.15) are preferred to geogrids when separation is required between the aggregate and the subgrade soils. This is the case when the subgrade soil is very soft and open aggregate is used.

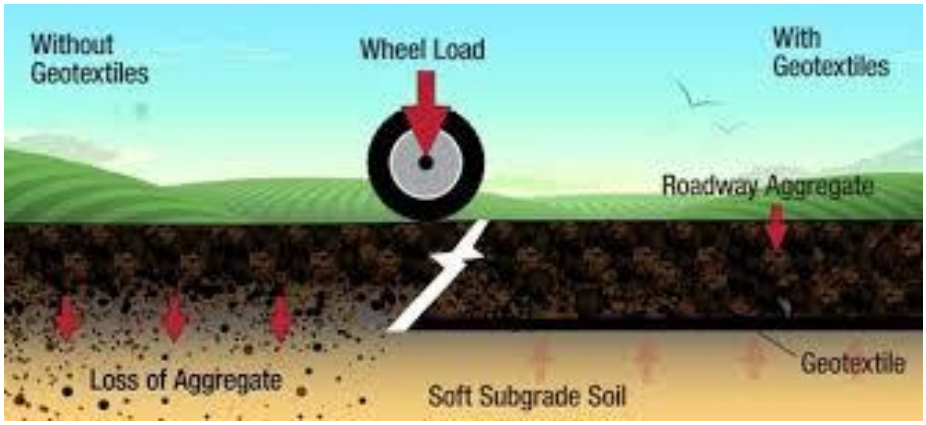

Figure 2.15 Separation phenomena

Among the mechanisms other than separation, the main mechanisms improving unpaved road performance within tolerable deformations (rut depth smaller than 100mm) are improvement of wheel load distribution, lateral restraint of the base material and tension membrane effect. It is also important to underline that the tensioned membrane effect becomes important only when large deformations occur in soft subgrade.

2.4.2. Lateral restraint and improvement of load distribution

A geosynthetic improves load distribution (Figure 2.16) through two mechanisms: by minimizing deterioration of the aggregate layer and by increasing the ability of the aggregate layer to distribute loads.

Geosynthetic reinforcement minimizes deterioration of the aggregate layer by preventing shear failure of the aggregate layer and lateral spreading of aggregate. Shear failure (or bearing capacity failure) of the aggregate layer is rare. Therefore, the main mechanism through which a geosynthetic prevents deterioration of the aggregate layer is by preventing or reducing lateral spreading of aggregate. This is achieved by interlocking between geosynthetic and aggregate.

The interaction due to the geosynthetic interlocking with base aggregate minimizes lateral movement of aggregate particles and increases the modulus of the base course, which leads to a wider vertical stress distribution over the subgrade and consequently a reduction of vertical subgrade deformations.

Thanks to load distribution in the base layer and thanks the use of geosynthetic, the load is applied over a much wider area than the contact area between the wheels and the road surface, which reduces the maximum vertical stress on the subgrade, in fact from the theory of elasticity it is known that, in a two-layer system, the stress distribution on the lower layer depends on the relative moduli of the upper layer and the lower layer. To obtain this mechanism it is essential that the geosynthetic and the granular material closely interact to form a composite system characterized by high tensile stiffness. This interaction is achieved by interlocking in the case of geogrids and confinement in the case of geocells. In the case of geotextiles, the interaction is based on friction, which is less effective than interlocking or confinement. This phenomena depends on the relationship between geosynthetic type and aggregate particle size, and in particular depends on several factors including:

- Geogrid aperture size relative to granular particle size and grading;
- Geogrid aperture shape;
- Shape and stiffness of the geogrid ribs;
- Stiffness (more than strength) and integrity of junctions between ribs.

In particular, the interlocking requires a geogrid with: adequate aperture size relative to the size and grading of the aggregate particles; aperture shape that best interacts with the densest arrangement of the considered aggregate; and optimized stiffness to provide reinforcement at very low deformations of the stabilization structure while having strain compatibility with the aggregate.

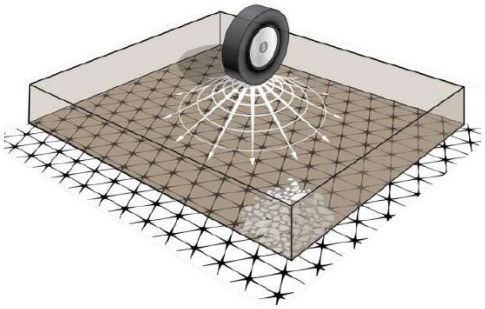

Figure 2.16 Load distribution in unpaved road

2.4.3. Tension membrane effect

This effect has been extensively discussed in the literature because, in early attempts at explaining the performance of unpaved roads, it was thought that the tensioned membrane effect (Figure 2.17) was the main mechanism governing the performance of geosynthetics in unpaved roads. It is known today that this is not the case. In particular in order to develop any benefit from a membrane action, the geosynthetic must be anchored effectively outside the loaded area and significant vertical deformations must occur.

According Giroud and Han (2016) the mechanism of tension membrane can be summarized in the following steps:

1) if the subgrade soil undergoes large deformation because of traffic, the geosynthetic follows the shape of the subgrade and exhibits a concave shape under the wheels.
2) the geosynthetic thus deformed is subjected to tension.
3) the resultant of the geosynthetic tension on the two sides of the concave shape is an upward vertical force that contributes to wheel support.
4) the tension of the geosynthetic on each side of the concave shape laterally transfers the portion of the wheel load supported through the tensioned membrane effect. As a result, smaller vertical stresses are applied to the subgrade beneath the wheels and greater vertical stresses are applied to the subgrade away from the wheels compared to the case without geosynthetic. Thus, thanks to the tensioned membrane effect, the vertical stress distribution on the subgrade is more uniform.

Stress-strain characteristics of the geosynthetic are also important when considering the membrane action. The higher the modulus of the geosynthetic, the less vertical deformation is required to develop the equivalent support from an inclusion of lower modulus.

The tension membrane effect has two principal limitation:

1. the tensioned membrane effect works only with channelized traffic and with important rut;
2. the need for sufficient anchor length for the geosynthetic on each side of the axle.

The mechanisms of lateral confinement effect and tension membrane effect require different depth values of rutting in order to be mobilized. At small permanent deformation magnitudes, the lateral restraint mechanism is developed by the ability of the base aggregate to interlock with the geogrid.

As increasing of permanent deformations (which are often acceptable in unpaved roads), the tension membrane mechanism develops (Calvarano et al., 2016a and 2016b).

From this analysis, it is clear that the tensioned membrane effect requires a high-strength geosynthetic and deep rutting. Calculations show that, for typical rut depths (less than 100mm), the tensioned membrane effect is generally negligible

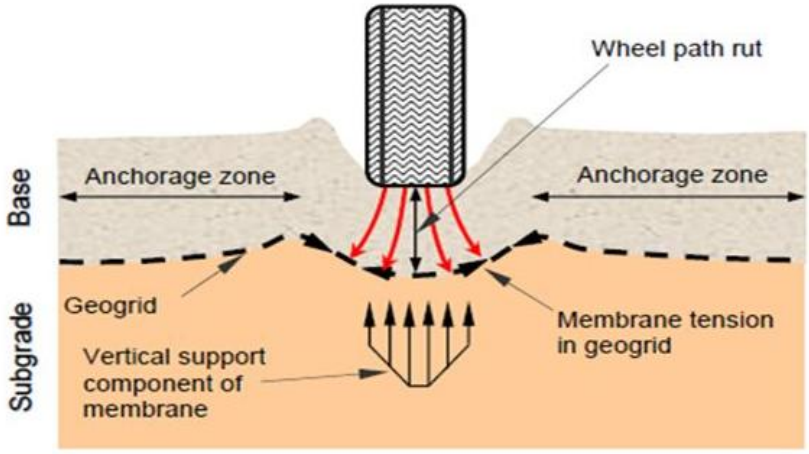

Figure 2.17 Tensioned membrane effect

2.5. Overview of Previous Studies

Through both laboratory and field studies, for unpaved and paved road it has been shown that the inclusion of geosynthetic in pavement section can improve the performance of pavement system by extending the service life or reducing pavement structural thickness with equivalent performance.

This section provides a review on the existing studies of pavement reinforcement by geosynthetic.

2.5.1. Previous study for paved road

Haas et al. (1988) performed laboratory experiments using a stationary plate to which a cyclic load was applied. Testing was performed in a 4.5 m × 1.8 m × 0.9 m box. Cyclic loads were applied through a steel plate with diameter of 30 cm. The variables of the testing program were the base thickness, subgrade strength, and locations of geogrid reinforcement. The surface deflection, the vertical stress at the top subgrade, and the strains in geogrids were measured at intervals of load repetitions. To obtaina weaker subgrade conditions, a peat was blended into the sand to achieve CBR values of 1% and 0.5%. The test results show that the geogrid reinforcement increased the number of load applications to failure by a factor of 3. The base thickness reductions obtain were 25 to 50 percent with inclusion of geogrids (Figure 2.18). Regarding the position of reinforcement it was suggested that the geogrid should be placed at the interface between base course and subgrade for thin base sections and in the midpoint of the thicker bases.

The laboratory experiments performed by Haas et al. (1988) demonstrated the importance of test variables such as geogrid placement position, base course thickness, and subgrade strength. In general, it was shown that reinforced sections carried three times the number of load cycles as compared to a similar control section, and that reinforcement allowed up to a 50% reduction in base course thickness.

The optimum geogrid location was at the bottom of thin bases and at the midpoint for base thicknesses in excess of 250 mm. For very weak subgrades, optimum performance occurred when two layers of geogrid were used.

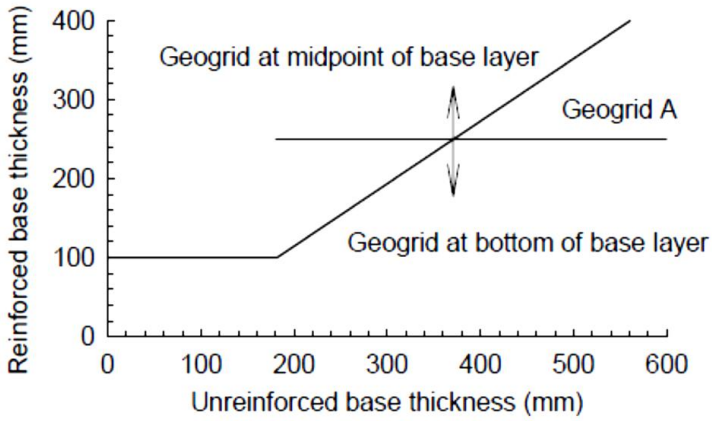

Figure 2.18 Design chart obtain by Haas et al. (1988)

Cancelli et al. (1996)

Cancelli et al. (1996) performed cyclic load plate tests in a laboratory test box (Figure 2.19). For reinforced section a total of five geogrids and one geotextile were used. Due to the relatively small size of the test box (900x900x900 mm^3) the geosynthetics were wrapped upwards around the sides of the box to simulate anchorage. Test box was carried out with a constant thickness of asphalt layer of 75 mm and base course layer with 300 mm .

Additional unreinforced sections used a base layer thickness greater than 300 mmwas used to examine the base layer equivalency that could be attributed to the reinforced section. The moisture content of the sand was kept constant while the density was varied to achieve CBR values ranging from 1% to 18%.

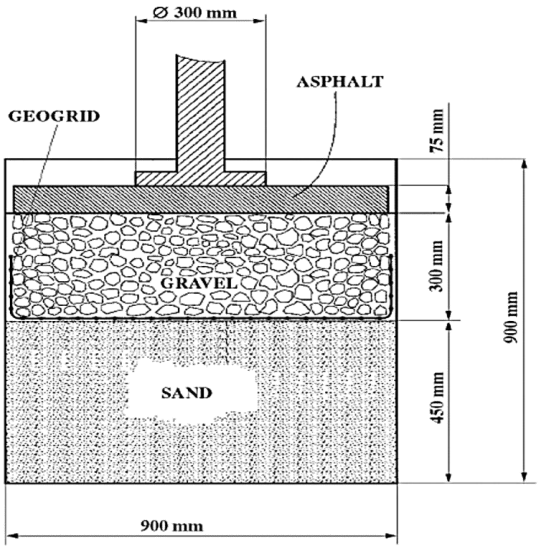

Figure 2.19 Test box used by Cancelli et al. (1996)

For test sections with a subgrade CBR equal to 3% and for a 25 mm rut depth, the authors defined the traffic bearing ratio (TBR) by the following expression:

$$\text{TBR} = N_R\ (geogridreinforcement) / N_{UR}\ (unreinforced)$$

where Nr is the number of cycles to failure of reinforced asphalt concrete and Nur is the number of cycles to failure of unreinforced asphalt concrete.

In particular the TBR values varied from 1.5 to 6.7 (Figure 2.20) decreasing with increasing CBR values.

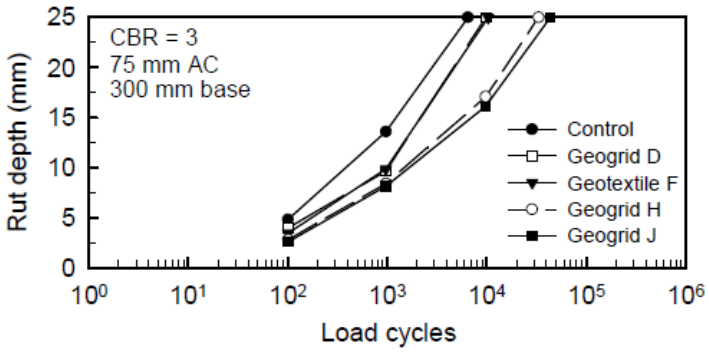

Figure 2.20 Result for CBR=3 by Cancelli et al. (1996)

In the unreinforced sections, very little mixing of the base course and the subgrade occurred for subgrades other than the subgrade with CBR = 1%, indicating that the benefit from the geotextile was most likely due to reinforcement. The improvement in performance due to increased geogrid stiffness decreased as the subgrade strength increased.

Cancelli et al. (1996) demonstrated that by using the most stiffgeogrid of his study the base course thickness could be reduced from approximately 425 mm to 300 mm if the subgrade CBR is equal to 3%. This results in a 30% savings in aggregate base material.

Montanelli et al. (1997)

Montanelli et al. (1997) performed cyclic load plate tests by a laboratory test box. Laboratory tests using a circular loading plate were conducted on pavements built over subgrade with CBR ranging from 1% to 18%.

In this study the authors aimed to quantify the structural contribution of geogrids to pavement systems. In order to make use of the AASHTO design procedure, Montanelli et al. developed a layer coefficient ratio (Figure 2.21) for the granular base, which is equal to the ratio of the reinforced to unreinforced based layer coefficients.

Depending on the subgrade CBR values, the values of this ratio ranged from 2 to 1.5. The layer coefficient ratio value was used as a multiplication factor for the depth of the reinforced base in the equation used to calculate the structural number. This implies that for an equivalent structural number, the unreinforced base could be reduced by 33 to 50%.

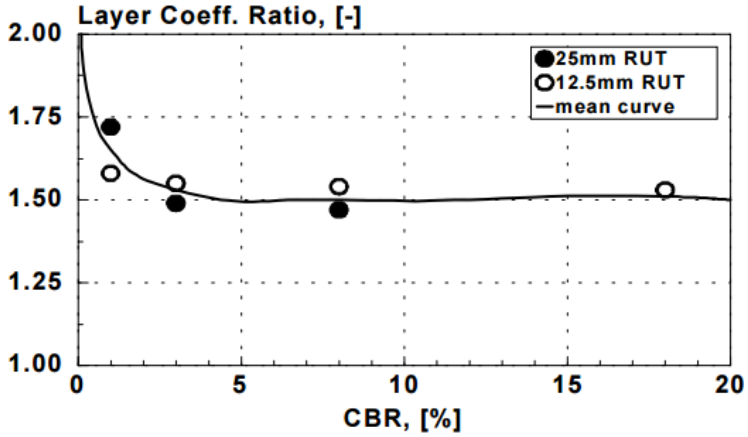

Figure 2.21 Layer coefficient ratio vs CBR

Chang et al. (1998)

In a study conducted by Chang et al. (1998), fiber glass geogrids with ultimate strength of 100 kN/m and 200 kN/m were used as reinforcement materials to evaluate the effect of reinforcement on the fatigue life of asphalt beams. Asphalt beam specimens were placed over two pieces of plywood with a 10 mm gap at center to simulate an existing joint or crack underneath the overlay, with the entire system placed on a rubber base representing the soil foundation (Figure 2.22).

Failure was defined as the time when crack grew throughout the entire cross area of the beam.

The factor of effectiveness of the reinforcement (FER) is defined as follow:

$$FER = \frac{N_{R(reinforced)}}{N_{UR(Unreinforced)}} \qquad \text{(Eq. 2.1)}$$

where N_R is the number of cycles to failure of reinforced asphalt concrete and N_{UR} is the number of cycles to failure of unreinforced asphalt concrete.

A series of testing for a beam reinforced with geogrid of 100 kN/m strength showed a FER of 1.5 to 2.5 times greater than the unreinforced beam for fatigue life. For a beam reinforced with 200 kN/m geogrid, the FER was 5 to 9 times greater.

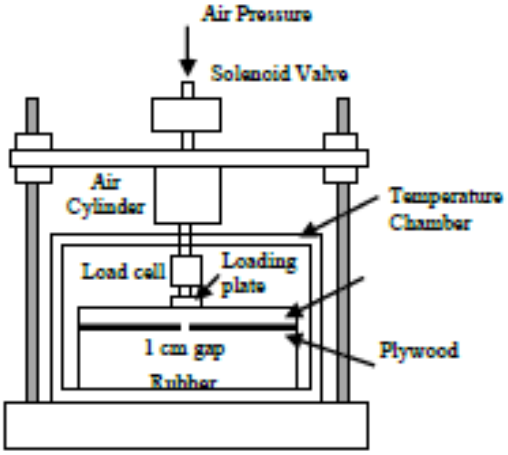

Figure 2.22 Chang et al. (1998) laboratory test

Perkins (1999)

A reinforced concrete box (Figure 2.23) with the dimensions of 2 m × 2 m × 1.5 m was used by Perkins (1999) for the testing. The author applied by means a 30 cm diameter steel plate a series of cyclic load with 40 kN of magnitude. A total of 20 test sections were proposed, including variables of two geogrids and one woven geotextile, subgrade type and strength, base course thickness, and position of geosynthetics.

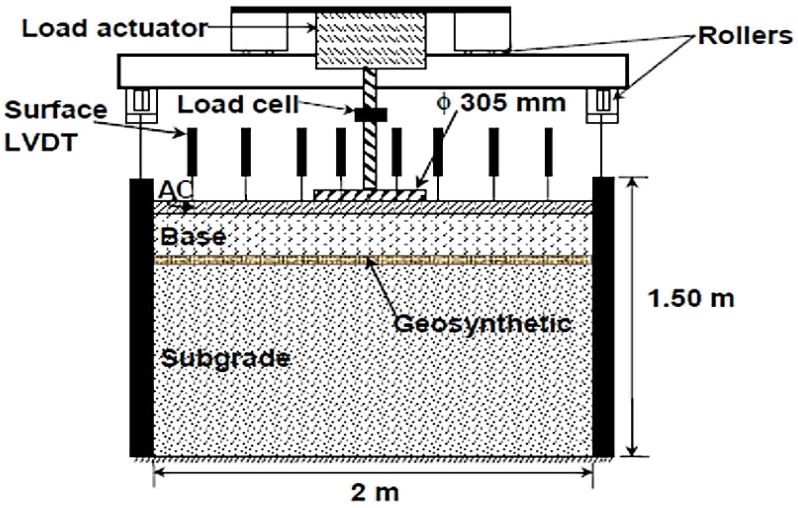

Figure 2.23 Perkins et al. (1998) laboratory test

Pavement surface deformation, strains in geosynthetics, strain and stress in soil, temperature and moisture content were measured using various instruments (Figure 2.24). Geogrids showed substantial improvement for pavements built over a subgrade with CBR of 1.5, while little improvement was found for pavements built over a stronger subgrade with CBR of 20. Between the two geogrid products used in the test, the stiffer one exhibited better performance. The geogrids performed better than the geotextile (Figure 2.25). The position of geogrid placement was considered an important factor affecting the geogrid performance. Significantly better performance was found with the geogrid placed closer to the load in the base, while geogrids showed much less improvements when placed at the bottom of a thicker base.

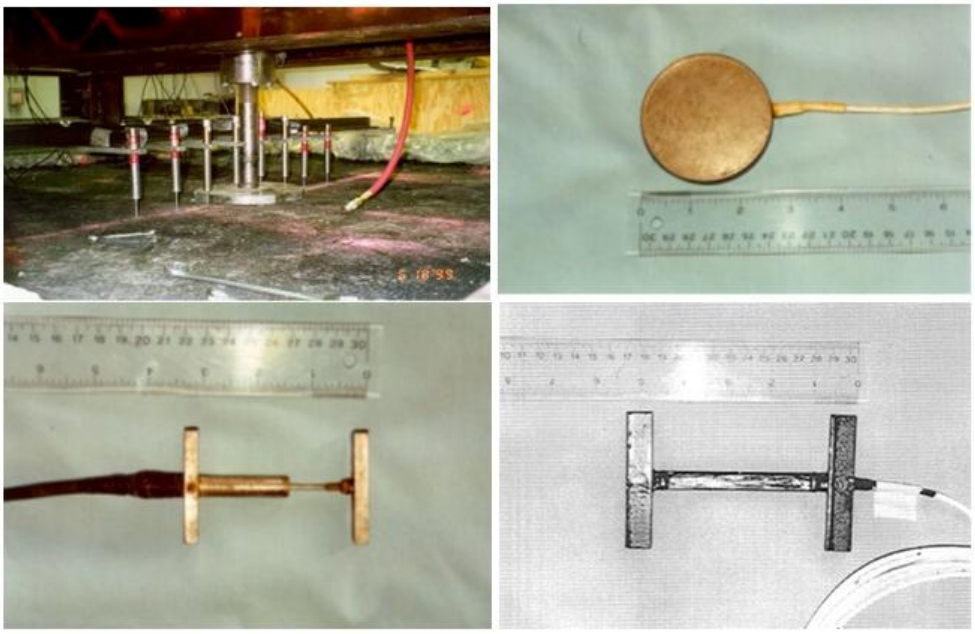

Figure 2.24 Various instruments used by Perkins (1999).

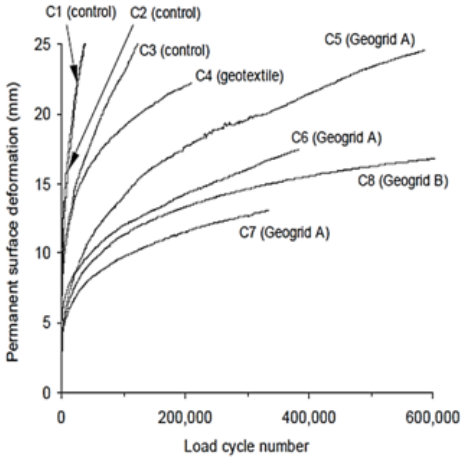

Test Section	Base (mm)	CBR (%)	Geosynt.	Position
C1	300	1.5	Control	-
C2	300	1.5	Control	-
C3	375	1.5	Control	-
C4	300	1.5	GTX	botton
C5	300	1.5	GGEB_A	botton
C6	375	1.5	GGEB_A	botton
C7	300	1.5	GGEB_A	100mm above botton
C8	300	1.5	GGEB_B	botton

Figure 2.25 Result obtain by Perkins (1999)

Montestruque et al. (2004)

The studies were conducted by Montestruque et al. (2004) based on quantitative and qualitative analysis of fatigue tests in asphalt concrete beams with and without polyester geogrid reinforcements (Figure 2.26). Tests were conducted to simulate a cracked pavement after rehabilitation, with the load applied at the two critical positions: on bending and on shearing, with a pre-crack with an opening of 3, 6 and 9 mm.

The geogrid was positioned exactly over the extremity of a pre-crack, with an elastic base as a support. The criterion for the end of the test was considered when the first visible crack appeared on the surface. The improvement that represents the beneficial effect of the geogrid was valued by effective reinforcement factor (FER).

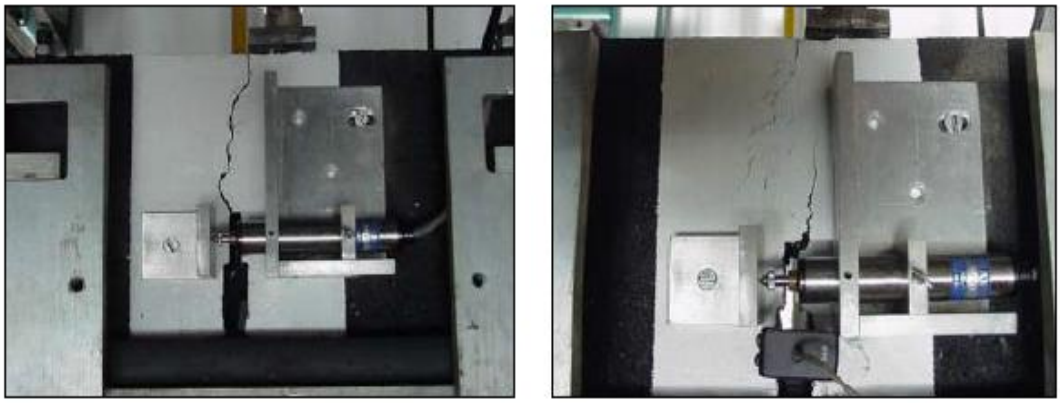

Figure 2.26 Test in asphalt concrete beams (a) unreinforced beam (b) geogrid-reinforced beam

For 3 mm pre-crack opening, tests have demonstrated FER values of 6.14, while 6 and 9 mm pre-crack openings with FER up to 4.6 and 5.11, respectively. After load cycles in the unreinforced beam, micro cracks developed and became more visible, interconnecting to each other, leading to the formation of new cracks of less severity spread over a greater volume of asphalt concrete. In the reinforced beams the growth of the crack was interrupted and a quite different pattern of cracking was observed: micro-cracks have initiated, associated with asphalt fatigue, but without any clear relation to a reflective cracking mechanism.

Furthermore, Montestruque et al. (2012) have evaluated the fatigue behavior (shear mode) of polyester and fiberglass geogrids for the use of pavement rehabilitation. The results obtained showed a superior performance of the polyester grid in comparison to fiberglass material, because it becomes brittle after some load cycles. The fiberglass geogrid broke after 21,000 cycles, while polyester geogrid did not break after 160,000 cycles.

Al-Qadi et al. (2008)

Al-Qadi et al. (2008), in order to study the effectiveness of geogrids on low-volume flexible pavements, carried out full-scale tests on nine pavement sections over a weak subgrade with CBR equal to 4%. Two geogrids, three base thicknesses, and two asphalt layer thicknesses were selected. A total of 173 instruments were installed to measure stresses, strains, deflections, moisture contents, pore-water pressures, and temperature. A unidirectional 44 kN dual-tire load was applied to simulate vehicular field loading conditions. It was found that geogrids are effective in reducing pavement distresses. Based on instrument measurements and visual observation after trenching, was suggested that, thanks the reinforcing mechanisms, the geogrid is effective in reducing horizontal shear deformation of the aggregate layer, In particular in the traffic direction.

The results show furthermore that for a flexible pavement with thin aggregate base, the optimum position of geogrid placement is at the interface between the base course and subgrade. For a thicker base, the optimal location of geogrid is at the upper third of the layer.

Wathugala et al. (1996)

Experimental and numerical studies were performed by Wathugala et al. (2010) to investigate the influence, on the performance of pavements, of synthetic geogrids in the hot mix asphalt layer. Laboratory experiments were conducted in a large box. Numerical modeling analyses were performed by using both two-dimensional and three-dimensional finite element models of the experimental setup.

The laboratory-scale pavement sections were instrumented with pressure cells, displacement gages, and strain gages (Figure 2.27). Test sections were subjected to 1,000,000 load applications at a frequency of 1.2 Hz. Static loading tests were conducted at intervals of 100,000 load applications. In thirteen experiments, glass fiber grids were used as reinforcement in the asphalt layer. After laboratory test several computer analyses of flexible pavement sections (Figure 2.28) were performed by using the finite element method (FEM) at the same loading, boundary and mechanical conditions. The laboratory data were compared with results obtained from the computer analyses. Results from this study show that glass fiber grids can be used to improve the performance of flexible pavement systems. It was also observed that the inclusion of glass fiber grid in the asphalt layer provided resistance to crack propagation. Overall, the flexible pavement sections reinforced with glass fiber grids showed better performance under laboratory test conditions.

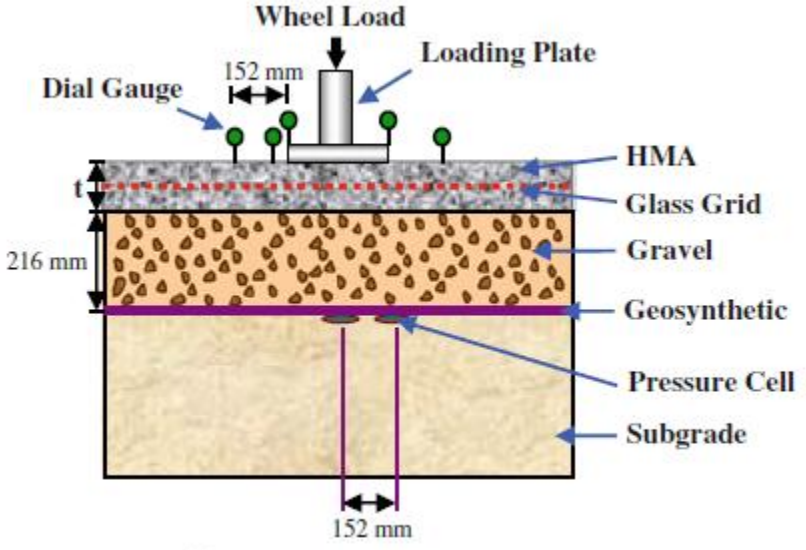

Figure 2.27 Laboratory section test by Wathugala et al. (1996)

.

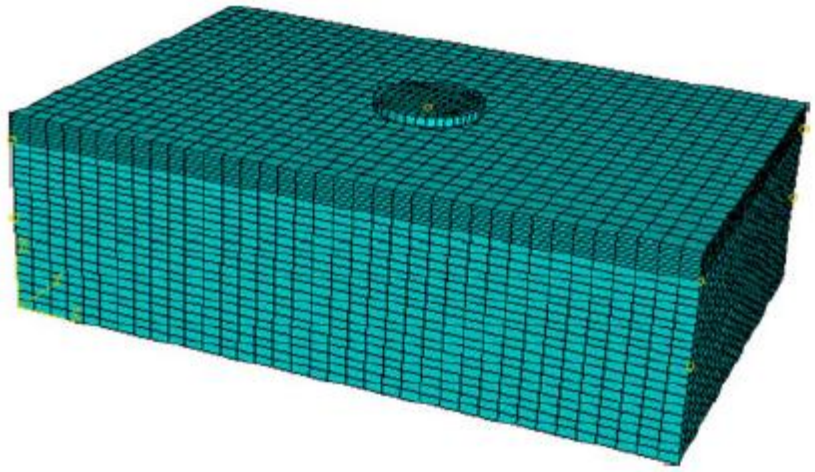

Figure 2.28 Finite element mesh by Wathugala et al. (1996)

Canestrari et al. (2013)

Canestrari et al. (2013) conducted tests in order to investigate the impact of geogrid reinforcement at the interface of asphalt layers. Flexural tests (repeated loading four-point bending) were carried out on double layered asphalt concrete specimens, with reinforced and unreinforced interface using a carbon fiber/fiber-glass geogrid pre-coated with bitumen and a fiber-glass reinforced polymer geogrid.

Figure 2.29 represents the scheme of four point bending test. The results show that geogrid have improved the permanent deformation resistance of the double-layered systems with respect to the unreinforced specimens which reached collapse before the planned test conclusion (36,000 cycles).The use of the reinforcement have reduced the load fraction carried by the AC double-layer and therefore reducing damage accumulation of the AC mixture.

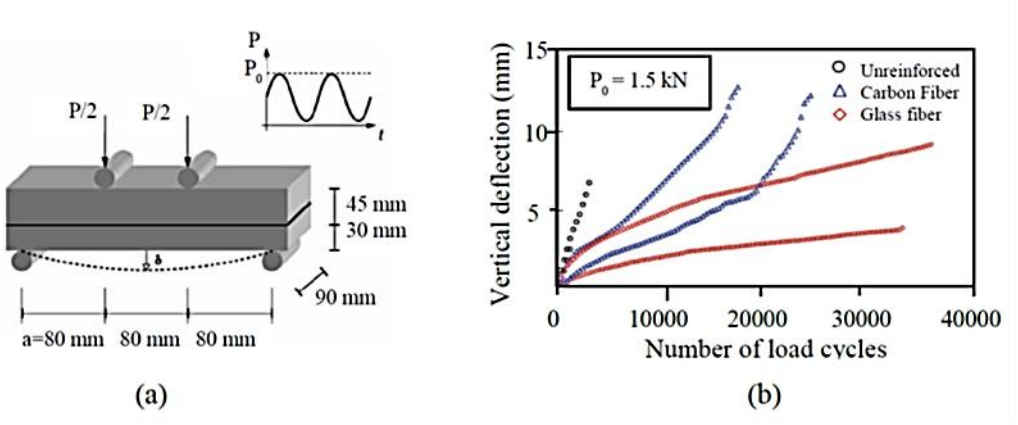

Figure 2.29 Flexural laboratory tests: (a) repeated loading four point bending; (b) permanent deformation results

Bin Yu et al. (2013)

A laboratory simulation of load-induced reflective cracking was carried out by Bin Yu et al. (2013) using the Hamburg wheel tracking (Figure 2.30) to study the development of reflective cracking under repetitive dynamic wheel load. The test ran at loading rate of 52 cycles/min with a load pressure of 0.7

MPa. The criterion for damage was set as the occurrence of cracks at the bottom of surface layer for all the specimens. The shortcoming of this approach was the subjective results (visual observation) and manually recorded number of load repetitions to damage. A fiberglass-polyester interlayer showed a mean value of 39000 cycles to retard reflective cracking, while the control specimen had crack reflected after 7400 cycles. The result show that the fiberglass-polyester has a high resistance to tensile stress and a low elongation rate, revealing that tensile stress and strain were dominant in the reinforced specimens, with a FER of 5.3.

Figure 2.30 Hamburg wheel tracking tester Laboratory tests

Graziani et al. (2014)

Graziani et al. (2014) have recently conducted a study on the structural response of geogrid-reinforced bituminous pavement based on stress-strain measurements carried out using pressure cells and asphalt strain gauges installed inside instrumented pavement sections. Pavement section was constructed to obtain actual response of geogrid-reinforced systems under vehicular loads by installing a fiber glass polymeric geogrid (FP) and a carbon fiber/ fiber glass geogrid (CF) inside a double-layered asphalt surfacing along an in-service road. CF geogrid has an ultimate tensile strength of 111 kN/m and elongation at rupture of 3-4.5%, while FP has a tensile strength of 211 kN/m and elongation at rupture of 3%, both on longitudinal and transversal direction. The pavement response to falling weight deflectometer (FWD) at real scale of truck loads was measured. The double layered asphalt surfacing was composed of a 40 mm thick lower layer and a 50 mm thick upper layer (Figure 2.31).

According to real-scale tests, the same behavior was observed for CF section; however, the presence of the FP geogrid have caused an increase of the measured longitudinal strains. As a result, the more flexible CF geogrid showed better compatibility with the AC double-layered surfacing, reducing the overall strains compared to the unreinforced case, potentially increasing the long-term pavement performance. In particular, the reinforcing effect was not observed in FP geogrid, mainly attributed to a debonding effect (reported by Canestrari et al. 2013), probably related to the high torsional rigidity and thickness of FP geogrid.

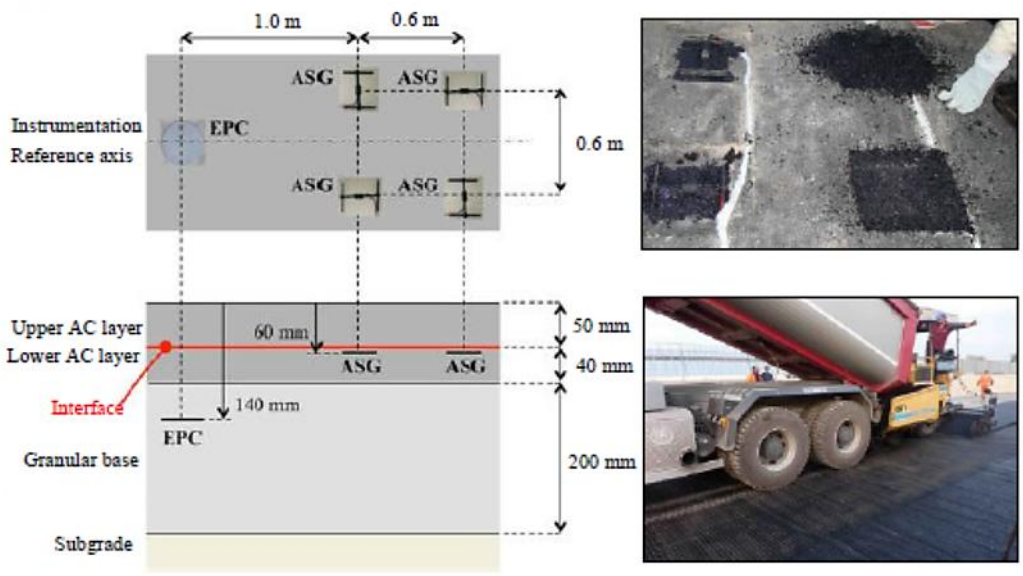

Figure 2.31 Pavement section by Graziani et al. (2014)

2.5.2. Finite element analysis for reinforced pavement system

Dondi (1994)

Dondi (1994) used the commercial program to model a geosynthetic-reinforced pavement. Load was applied to the pavement surface over two rectangular areas measuring 240 mm by 180mm and representing a single pair of dual wheels. Each rectangular area experienced a peak loading pressure of 1500 kPa. Due to the loading geometry, a three-dimensional finite element analysis was performed. Various material models were used for each layer of the road's cross-section, in particular: the base material was assumed to be an elastic perfectly plastic, cohesive, non-associative material using the Drucker–Prager failure criterion; an elastic material model was used for both the hot mixture of asphalt material and the geosynthetic material and the subgrade was assumed to be an elastic perfectly plastic, cohesive Cam-clay type material. In addition, the frictional behavior of the geosynthetic–soil interface was assumed to follow a Mohr–Coulomb elasto-plastic model. Different friction coefficients were used between the geosynthetic and the base and subgrade soils. Sections were analyzed with and without the geosynthetic layer and for two geosynthetics of differing elastic modulus.

The results showed that: a reduction in the shear strain and the stress transmitted to the top of surface; the rut depth of the loaded area reduced 15-20% for the reinforced section as compared with the unreinforced one and the fatigue life for the reinforced section 2 to 2.5 times longer than the unreinforced section.

Wathugala et al. (1996)

Wathugala et al. (1996) used the commercial program ABAQUS to develop a finite element model of a geogrid-reinforced pavement. The select base course and embankment soils were modeled using the constitutive model developed by Desai et al. (1986) and Wathugala and Desai (1993).

This model can account for the nonlinear behavior of soil materials during cyclic loading applications. A geogrid-soil interface model was not incorporated into the overall model. The geogrid was given a thickness of 2.5 mm and the pavement section was analyzed with and without

the geogrid layer. The addition of the geogrid reduced the permanent rut depth by approximately 20% for a single cycle of load. This level of improvement was most likely due to the flexural rigidity of the geosynthetic, which is an artificial feature arising from the material and element model used for the geosynthetic.

Perkins et al. (2000)

Perkins et al. (2000) developed a 3-D finite element model using ABAQUS to predict the behavior of reinforced roadway sections after repeated traffic loading. The material model for the asphalt layer consisted of an elastic-perfectly plastic model. This model allowed for the asphalt layer to deform with the underlying base aggregate and subgrade layers as repeated pavement loads were applied. A material model including elasticity, plasticity, and creep and direction dependency was used for the geosynthetic. The shear interaction between the base and geosynthetic was molded by the Coulomb friction model, which is an elastic-perfectly plastic model. Nominal thicknesses of 75 mm and 300 mm were used for the pavement and subbase, respectively.

The model subgrade had a CBR of 1.5%. Three models were created using generic properties for the asphalt, subbase, reinforcement, and subgrade layers: a typical unreinforced section, a geosynthetic reinforced section, and a perfectly reinforced section where the nodes at the interface of the subbase and subgrade were restricted from horizontal movement to simulate perfect lateral base course restraint. Under a cyclic load of 550 kPa the model simulated the improvement mechanisms associated with geosynthetics.

The result shows that reinforcement reduced the lateral permanent strain at the bottom of the base, as well as the vertical stress on top of the subgrade and the amount of vertical deformation after 10 cycles was significantly reduced in the reinforced model compared to the unreinforced case.

Perkins and Edens (2003)

Perkins and Edens (2003) quantified the benefits of geosynthetic base reinforcement using 3D FEM analysis. Benefits of geosynthetic base reinforcement depend on many factors including structural thicknesses of the pavement section, strength of the subgrade, and properties of the interlayer used. This study shows the development of a design model to quantify the benefits of reinforcement. The design model was formulated by first developing a 3D FE model that simulates reinforced and unreinforced pavement sections. In the developed FE model, elasto-plastic models were used to simulate HMA, base aggregate and subgrade materials. The geosynthetic material was simulated as orthotropic linear elastic. Two reinforcement cases were simulated. In the first case, an infinitely stiff reinforcement was assumed by restricting motion at the bottom of the base. In the second case, the geosynthetic was modeled by membrane elements with varying tensile properties.

Results of the FE model showed the ability of the reinforcement to prevent lateral spreading at the bottom of the aggregate layer in contact with the interlayer. Lateral confinement led to an increase in the

aggregate layer stiffness, a reduction of vertical stress on top of the subgrade, and a reduction of vertical compressive strain in the lower half of the base. The developed model showed that reinforcement benefits increases with the decrease in subgrade strength and increase in geosynthetic tensile modulus.

Saad et al. (2006)

Saad et al. performeda dynamic 3-D FE modeling on geosynthetic-reinforced flexible pavements using the commercial FE program ADINA. The simulations are conducted under a parametric study to investigate the beneficial effects of geosynthetic reinforcement to the fatigue and rutting strain criteria, and to determine how such effects are influenced by the base quality and thickness as well as the subgrade quality. An elastoplastic Drucker-Prager model was used for the aggregate base, instead, a modified CamClay model was used for the subgrade. Both the asphalt concrete and geosynthetic were model as linear elastic. Dynamic load with a triangular wave having duration of 0.1 second was applied to the pavement model. The pavement layers-geosynthetic interface was assumed to be fully bounded.

Three locations of the geosynthetic reinforcement are studied, namely the base–asphalt concrete interface, the base–subgrade interface, and inside the base layer at a height of 1/3 of its thickness from the bottom. A parametric study was carried out to investigate the factors such as base quality and thickness and subgrade quality that influence the reinforcing effectiveness of geosynthetics.

The results show that placing the geosynthetic reinforcement at the base–asphalt concrete interface leads to the highest reduction of the fatigue strain 46–48%. The placement of geosynthetic reinforcement in thin bases is In particular effective; the highest decrease of rutting strain 16–34% occurs when the reinforcement is placed at a height of 1/3 of the base thickness from the bottom.

Faheem and Hassan (2014)

Faheem and Hassan (2014) presents an axisymmetric finite element model (FEM) (Figure 2.32) to analyze the behavior of unreinforced and geogrid reinforced bituminous pavement subjected to static and dynamic loadings. Axisymmetric modeling was chosen in this study because it could simulate circular loading and did not require excessive computational time under dynamic loading. The sand subgrade soil of thickness 1.2 m is overlaid by a 0.40 m layer of crushed gravel as sub-base, 0.30 m crushed gravel as base course and 0.1 m asphalt concrete on top. The bottom of model was fixed in both vertical and horizontal directions. Both edges of the models were restricted against horizontal movement.

The constitute model for the asphalt layer consisted of an linear-elastic model while other layer are modeled with Mohr- Coulomb model.

The model was loaded with an incremental loading and the critical pavement responses such as effective stress and vertical surface deflection were determined for unreinforced and geogrid reinforced flexible pavement.

For the materials and loading conditions used, the following conclusions can be drawn:

1) A significant improvement in pavement behavior is obtained by applying one-layer of geogrid reinforcement. Vertical displacement and effective stress responses are significantly lower for reinforced pavement system.

2) Effect of geogrid axial elastic stiffness is on reinforced pavement behavior is not significant.
3) No significant improvement in pavement system was gained by adding another layer of geogrid to the pavement system.
4) For case of dynamic loading, no significant influence of geogrid reinforcement on pavement behavior was observed.
5) Effect of dynamic loading frequency on pavement behavior is significant only for high stress amplitude.

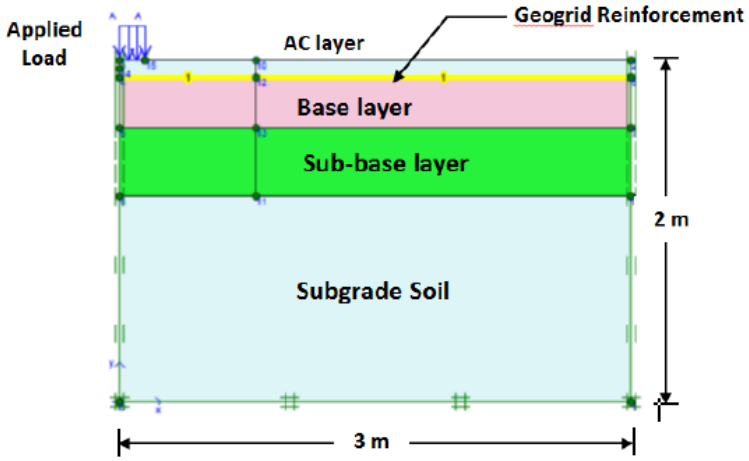

Figure 2.32 Axisymmetric finite element model (FEM)

2.5.3. Previous study for unpaved road

Webster and Watkins (1977)

Webster and Watkins (1977) have conducted a field trial involving seven test sections: one was reinforced with a nonwoven needle punched polyester geotextile, one with a neoprene-coated one-ply woven nylon membrane, and one was left unreinforced to act as a control section. The remaining sections were reinforced with materials other than geosynthetics. The test sections were 9.1 m long, and 3.7 m wide; They comprised a 35 cm thick crushed stone base course placed on a 61 cm thick clay subgrade of undrained shear strength 21-30 kPa in the upper 25 cm and 30-69 kPa below.

Vehicle loading was applied using a 44.5 kN tandem axle dump truck, but analyzed in terms of an equivalent 80.1 kN single axle, dual wheel load. The performance of the sections was evaluated from visual observations, photographs, and deformations of cross-sections recorded at intervals throughout the trafficking period. The sections were trafficked up to an average rut depth of 28 cm, which can be considered as failure. Results showed the performance of the reinforced sections was significantly better than the unreinforced section. The unreinforced section accepted 200 passes, the non-woven geotextile section 2500 passes, and the woven membrane 37000 passes.

This investigation was probably the first clear affirmation that using geosynthetics in construction of unpaved roads on soft ground leads to a significant improvement in terms of traffic load application number.

Bender and Barenberg (1978)

Bender and Barenberg (1978) indicated that unpaved roadway sections constructed using geotextile at the interface of the subgrade and subbase could withstand larger traffic volumes than sections constructed using no geosynthetics. The test used a strip footing and a circular plate to which static and cyclic loads were applied. The result obtain indicate that the reinforced sections showed less rutting under simulated traffic loads. The authors attribute the improved performance of the sections constructed using geotextile to increased distribution of traffic loads over the subgrade, reduced mixing of the subbase and subgrade particles, and limitation of free-flow of water from the subgrade into the subbase.

Webster and Alford (1978)

Webster and Alford (1978) conducted full-scale tests on unpaved roads reinforced by nonwoven geotextiles and geomembranes. The author realize two test section. The first section consisted of 380 mm of well-graded crushed limestone as the base course and a subgrade with CBR of 1. This section was reinforced by a nonwoven geotextile at the base/subgrade interface. Their second test section was constructed from a 150 mm crushed limestone layer on a subgrade of 3.3 CBR reinforced with a geomembrane. Rutting results indicated that geosynthetic reinforcement reduced required base thickness. This study also proved that effects of geosynthetics were more significant when a low strength subgrade was used. Furthermore Webster (1992) conducted tests on six aggregate-surfaced road sections. Test sections included unreinforced section, one geogrid reinforced, and three geotextile reinforced. All sections had 100 mm base course thickness and poorly-graded sand subgrade with a CBR of 10. Geotextile reinforced sections did not perform better than the control section. Therefore, the conclusion was made that lateral movement of aggregates at the aggregate-geotextile interface limits the reinforcement effect of geotextiles.

Austin and Coleman (1993)

Austin and Coleman (1993) conducted a full-scale field study near Greeneville, Mississippi, to evaluate the performance of geogrid and geotextile stabilization of an unpaved road constructed over very soft soil. When the initial investigation of the test site was performed, it was learned that the subgrade soil consisted of a fat clay meeting USCS classification of CH. The CBR value of this soil ranged from 3 to 6%, values which were considered too high to satisfy the objectives of that study.

So the investigators sought to obtain a subgrade with CBR values less than about 1%.

Thus, the test site was flooded for a period of eight months and then drained. This process had the desired effect, reducing the CBR values to between 0.6 and 0.9% in most locations.

The geosynthetics used to stabilize the road section included four types of polypropylene geogrids and geotextiles. The nonwoven polypropylene was used in conjunction with one of the geogrids. The geosynthetics were installed on the test road. Each test section was approximately 6 m wide x 6 m long. The test sections were loaded by a two-axle dump truck with the rear dual-wheel axle loaded to approximately 80 kN. The tire pressures were maintained at 550 kPa. The performance of each test section was based on the number of vehicle passes, that induced surface deflections of 50 mm and 75 mm.

From the results it was clear that the use of geosynthetics significantly improved the performance of each test section compared to the control sections. The research also demonstrated the effectiveness of the geotextile as a separator. The investigators observed that no contamination of the base aggregate occurred at the geotextile-stabilized sections, but that significant contamination occurred at the control sections and the geogrid sections.

The test results suggest that the tensile strength of geogrids may not have a significant influence on their ability to stabilize an unpaved road over weak soil.

Leng and Gabr (2002)

Leng and Gabr (2002) investigated the behavior of geogrid-reinforced aggregates over a soft subgrade. A text box (Figure 2.33) with dimensions of 1.5m x 1.5m x 1.35m was used to evaluate the performance of geogrid base reinforcement under cyclic loading. A cyclic load of 550 kPa a load frequency of 0.67Hz was applied to aggregate base thicknesses of 152 mm and 254 mm using a 305 mm diameter loading plate attached to a hydraulic actuator.

The subgrade material had a CBR of 3 and ranged in thickness from 750 to 900 mm.

During the test, vertical stress at the base-subgrade interface and at varying distance from the centerline of the plate was monitored. Surface deformation was also measured throughout the test.

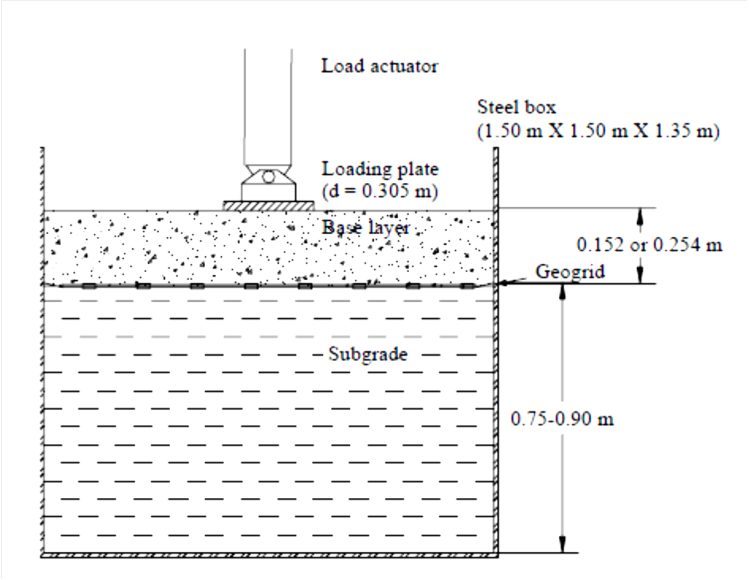

Figure 2.33 Test box and load configuration

Two types of biaxial, polypropylene geogrids (BX1 and BX2) were used in the experimental program. In total, nine cyclic loading tests were conducted to evaluate the effects of reinforcement, geogrid types, and base thickness.

Leng et al. (2002) show that:

1. Geogrid reinforcement effectively decreased surface deformation and improved the stress distribution transferred to the subgrade. As expected, the stronger BX2 performed better than BX1 (Figure 2.34).

2. Results showed that surface permanent deformation quickly increased at the start of the loading cycle and then gradually accumulated with the number of load repetitions. Reinforced sections experienced a slower increase in the rate of surface deformation and reduced surface deformation magnitude.
3. Geogrid successfully decreased the maximum vertical stress at the center of the plate and produced a more uniform stress distribution on the foundation soil.
4. Improvement is related to two mechanisms: lateral confinement of base course and tensile membrane effect of geosynthetics.

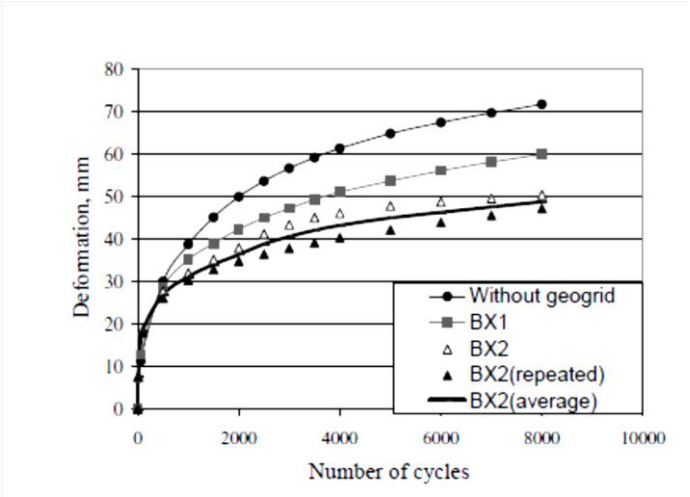

Figure 2.34 Surface deformation with 152 mm aggregate base thicknesses

Leng and Gabr (2005)

Numerical analyses using the finite element program ABAQUS were conducted to investigate the performance of geogrid-reinforced aggregate over soft subgrade.

The asymmetric mesh (Figure 2.35) used has a radius of 0.75 m and a total depth of 0.90 m. It includes 84 elements for the base layer, 14 elements for the geogrid reinforcement at the interface, and 140 elements for the subgrade. A load of 40 kN (pressure 550 kPa), simulating a single wheel load, is applied to a circular area with a radius of 0.152 m on top of the base layer, to simulate load magnitude during the testing program.

Solid elements were selected for the base course and the subgrade. The reinforcement between the base course and the subgrade was simulated by membrane elements with thickness of 0.003m.

The Drucker-Prager model with hyperbolic yield criterion was used for pavement base materials to minimize the unrealistic tensile stresses in the base. The geogrid was modeled as membranes that take tension only. A Coulomb friction model was adopted to simulate the shear resistance behavior of the interface between the base layer and geogrids. A friction coefficient value and allowed elastic slip/relative displacement were assigned to the interface model.

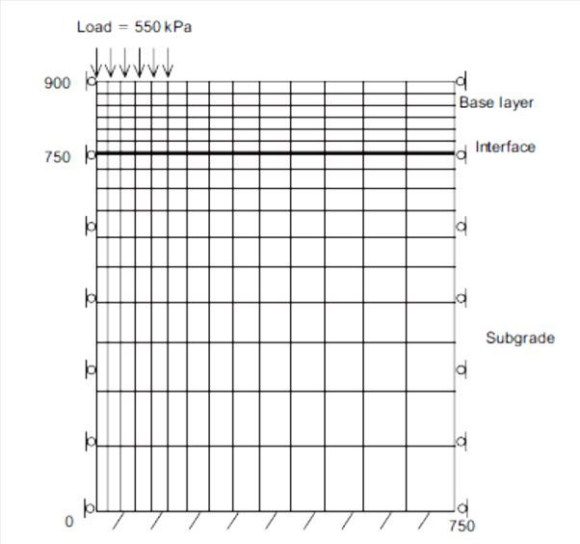

Figure 2.35 Asymmetric mesh for FEM analysis

The results of the numerical study (Figure 2.36) demonstrated that the inclusion of geogrids between base layer and subgrade reduce the surface deformation on the unpaved structure, and improve the stress distribution inside the base layer and subgrade layer.

Furthermore a geogrid with higher tensile modulus and better interface property with base course aggregate shows a better reinforcement effect. As the ABC thickness decreases, or the elastic modulus ratio decreases, the benefit due to geogrid reinforcement becomes more apparent.

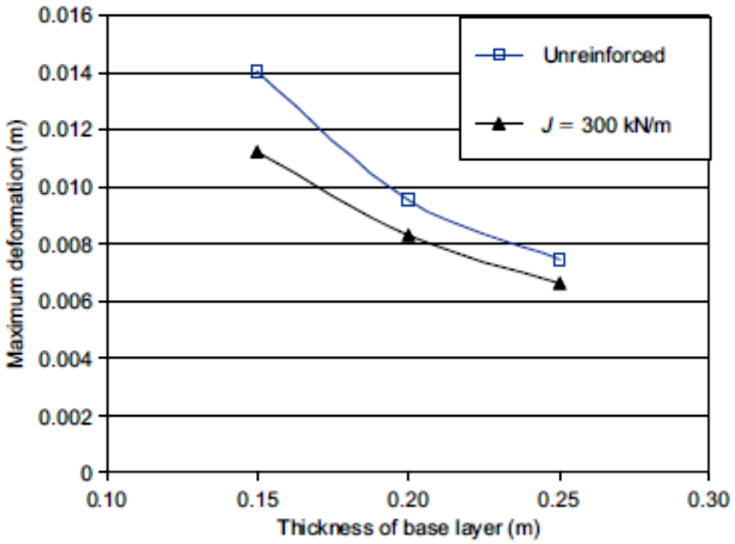

Figure 2.36 Some results obtained by Leng and Gabr (2005)

Klompmaker et al. (2009)

The purpose of the author was to evaluate the reinforcement benefit provided by different geogrids in terms of the number of load cycles to reach a specific permanent rut depth of approximately 75 mm in the aggregate surface layer for each section and Traffic Benefit Ratio (TBR), which is the number of load

cycles for a reinforced section divided by the number of load cycles to reach this same rut depth for a comparable unreinforced test section.

The test sections were instrumented to measure geosynthetic deformation and subgrade pore water pressure response. Test sections were constructed in a 2 m by 2 m by 1.5 m deep box shown in Figure 2.37 and the walls of the box consist of 150 mm thick reinforced concrete. The front wall is removable in order to facilitate excavation of the test sections.

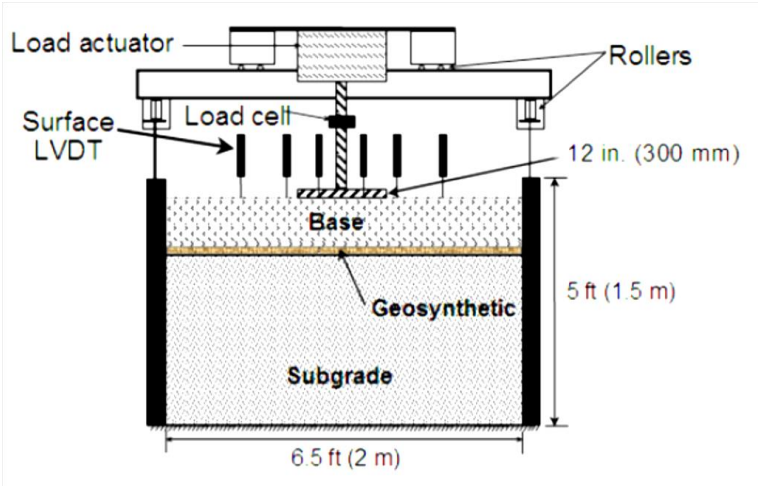

Figure 2.37 Laboratory test box

Each roadway test section was constructed with a nominal cross-section consisting of 300 mm of base course aggregate and 1.1 m of subgrade soil with a CBR = 1. The geosynthetic was placed between the base course and subgrade layers. A control test section having the same cross section without a geogrid was used for comparison to the geogrid stabilized sections.

The geosynthetic materials used in these tests were a welded polypropylene biaxial geogrid and a composite geogrid using a welded polypropylene biaxial geogrid where a needle punched nonwoven geotextile is firmly bonded between the cross laid reinforcement bars.

A cyclic, non-moving load with a peak load value of 40 kN was used to create dynamic wheel loads. The load plate consists of a 300 mm diameter steel plate with a thickness of 25 mm. A 6.4 mm thick, waffled butyl-rubber pad is placed beneath the load plate in order to provide a uniform pressure and avoid stress concentrations along the plate's perimeter

The results (Figure 2.38) show a difference in the performance of the geosynthetics: the geocomposite material performed the best of all materials tested and reached over 850 cycles of loading before reaching 75 mm of rutting and had a TBR value of over 170.

Over 10,000 cycles were required to reach a rut depth of 100 mm. Over 10,000 cycles were required to reach a rut depth of 100 mm. Open geogrids may be at a disadvantage with the type of soil used, as no filter stability between the coarse aggregate and the fine grained subgrade is given, so that the soft subgrade can easily be penetrated by gravel particles from the base course layer until interlock is developed. Regardless, both laid and welded geogrids provided significant improvements in deformation response over the control section with TBR values between 11 and 19.

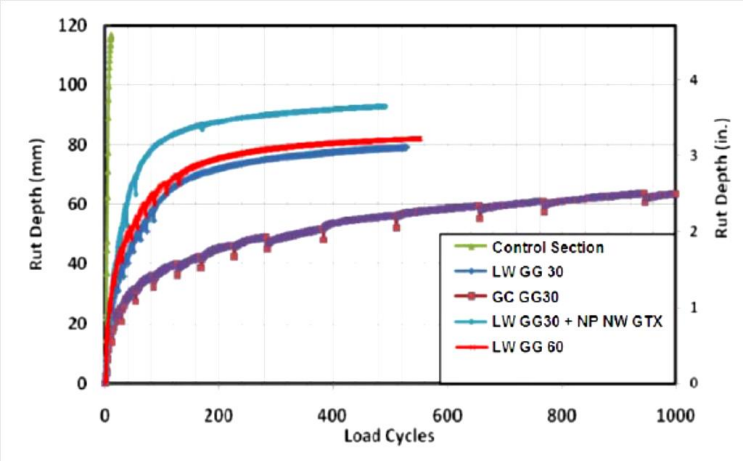

Figure 2.38 Permanent surface deformation vs cyclic load

Christopher & Perkins (2011)

Christopher & Perkins (2011) presents the results of full scale laboratory tests on geogrid reinforcements in unpaved roadway sections over a soft subgrade. Test sections were constructed in a 2 m by 2 m by 1.5 m box shown in Figure 2.39. The side and back walls of the box consist of 150 mm thick reinforced concrete. The load plate consists of a 300 mm diameter steel plate with a thickness of 25 mm. Two geosynthetics were used in this study: a welded polypropylene biaxial geogrid (GG), and a geogrid/geotextile geocomposite (GC). The silt type subgrade material was placed at a moisture content of approximately 35% to produce a CBR value of approximately 1%.

The result show that the geocomposite test was terminated at 100,000 cycles of loading at a maximum permanent rut depth of 30 mm while the geogrid provided 76 to 100 mm of rutting in 1000 cycles (Figure 2.40). This is occur because the subgrade soil can easily be penetrated by gravel particles and thus some of the displacement may be the result of aggregate penetration until interlock is developed.

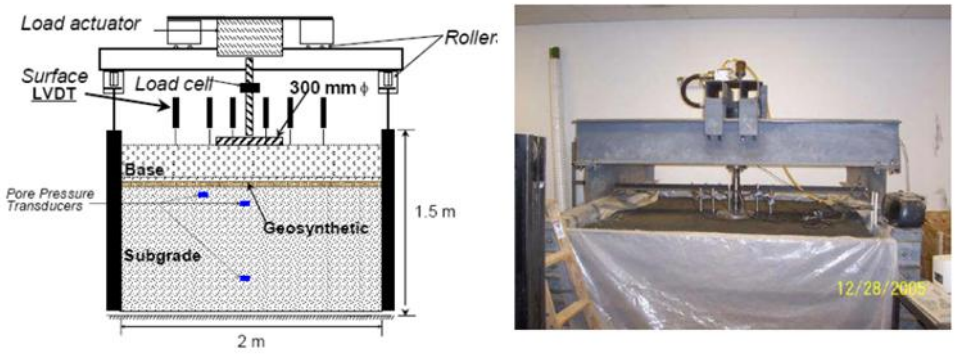

Figure 2.39 Laboratory test box

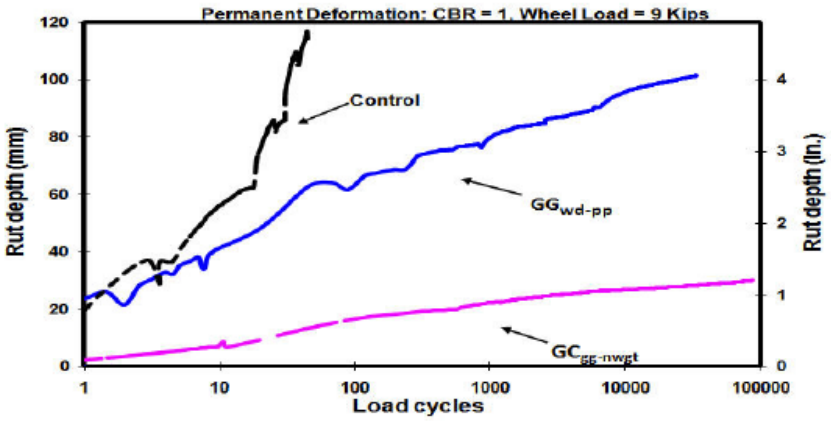

Figure 2.40 Permanent deformation vs load cycles

Wen-Chao Huang (2013)

Wen-Chao Huang (2013) used finite element analysis of a two-layer soil system reinforced at the interface (Figure 2.41) and subjected to surface applied loading to simulate the behavior of soft subgrade when its upper layer has been excavated and substituted with geogrid-reinforced aggregate.

The author verified numerical models by comparing the analysis results with previous studies. The major numerical models in this study were assumed to be a simplified simulation of a geogrid reinforced two-layer system with an aggregate layer above a subgrade layer. The numerical models were applied a quasistatic loading and unloading cycle, in order to monitor the permanent deformation at the surface of the models. Afterwards, thickness of aggregate layer, and subgrade CBR values were varied in order to summarize the outcomes of each case. This approach makes it possible to quantify the effects of geogrid reinforcement and aggregate material in terms of an enhanced California Bearing Ratio (CBR) of a single subgrade clay layer. The results of this study show that the benefit obtained by placing the geogrid and aggregates to improve a soft subgrade can be quantified as an equivalent enhancement of the subgrade CBR. Results indicate that the analysis of geogrid-reinforced two layer system is most effective when the aggregate layer thickness is approximately 100 to 150 mm. Under these circumstances, the aggregate material and the geogrid reinforcement can contribute about 50% improvement of the subgrade material. When the aggregate layer is thicker, such as 300 mm, the geogrid reinforcement may not be as efficient when it is compared to the improvement contributed by the aggregate material.

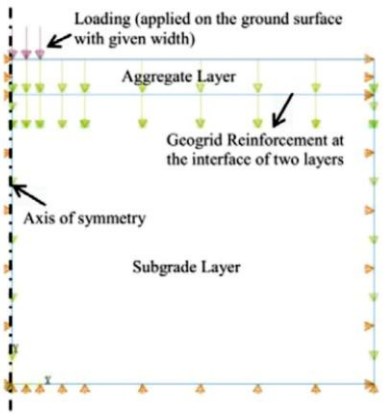

Figure 2.41 Numerical model with geogrid reinforcement

CHAPTER 3

Design method for unpaved road reinforced with geosynthetic

This page has been intentionally left blank

3. Design method for unpaved road reinforced with geosynthetic

3.1. Design method for unpaved roads

Unpaved structures are commonly known as gravel roads. However, it should be acknowledged that the structures are designed for connecting roads in yards, that are tread by heavy axle loads, and to service very remote areas. In fact, it is common to have gravel roads providing service to agricultural and important areas with fairly high traffic volumes. AASHTO (1993) allows unpaved roads to be designed for up to 100,000 equivalent single axle loads (ESALs) and their most relevant distress is related to rutting. Rutting is a permanent deformation that accumulates as the traffic loads increases. Large rutting may cause discomfort to drivers, damage to vehicles, and instability of the vehicles; therefore, excessive rutting should be avoided. For this reasons in many cases it is used the geosynthetic like reinforcement.

Unpaved roads reinforced with geosynthetic usually are realized by a base (made of granular material) resting on subgrade soil (typically a cohesive soil) and a geosynthetic (usually a geogrid) whith reinforcing function included between the base and the subgrade. The geosynthetic contribution to the performance of an unpaved road is achieved through several mechanisms that have been analyzed in Chapter 2.

The reinforcement improves the performance of the structure in different ways. In fact, for a given base layer thickness and a given allowable rut depth, the traffic can be increased, in comparison with the allowable traffic on the same thickness of unreinforced base layer; or, for a given base layer thickness and a given traffic, the rut depth is smaller than respect to unreinforced section.

As with any engineering design, an appropriate design methodology must be utilized when geosynthetics are being considered to provide cost effective alternatives to traditional construction methods. They will primarily help to reduce the aggregate thickness while preserving the quality and performance of the unpaved surface.

Several design methods for unpaved roads incorporating geosynthetics have been published over the last two decades. Some of these many have been developed for specific commercial products, but others are intended to be generic.

Very little is known about the exact method to design a pavement system incorporating an interlayer system, in fact to date, a general analytical design solution has not been found that addresses all of the many variables that impact performance roads and, as a result, that has been validated by experimental data (Perkins and Ismeik, 1997). Another problem lies in the fact that the contribution of most of the geosynthetics is not yet quantifiable.

Design methods can be divided into three broad classes: empirical design methods; semi-theoretical design methods and purely analytical method which includes the finite element methods. In the last case field and laboratory data are used in association with available theory. The experimental test results must be extrapolated to create design procedure. Therefore many empirical design methods are limited by the conditions associated with the experiments of the study, and then to all the restrictions in terms of time, space and investments.

Aim for all design methods in unpaved road are to provide a cost-effective alternative to typical designs and obtain in a reduction of the required layer thicknesses to reach the same level of performance using a geosynthetic reinforcement.

Several design methodologies have emerged for unpaved roads reinforced with geosynthetic. In this chapter, in particular, will be analyzed the following unpaved design method:

- Barenberg et al. (1975);
- Giroud and Noiray (1981);
- Giroud and Han (2004) ;
- Leng and Gabr (2005).

3.2. Method proposed by Barenberg et al. (1975)

Barenberg et al. (1975) developed a simple design procedure based on a laboratory testing program using both a large and a small scale two dimensional model systems of a nonwoven geotextile reinforced unpaved road.

This is a method, that utilizes different bearing capacity factors for unpaved roads with or without a geotextile, focused on the lateral restraint theory offered by geosynthetic. This method assumed a soft cohesive subgrade overlain by a crushed-rock aggregate base and the vertical stress at the interface between the base and the subgrade was calculated using a Boussinesq solution. The Boussinesq solution determines stresses due to an uniform load applied over a circular area of an elastic half space. However, this theory is intended for single-layer elastic systems. The Barenberg system, instead, was no single-layered nor elastic. Therefore, to determining the base course thickness when a geotextile is used in unpaved road, Barenberg (1975), has calculated the vertical stress using the Boussinesq theory, where the allowable stress on the subgrade is not to exceed its bearing capacity. In other words, the bearing capacity value was chosen equal to 6 time the undrained shear strength of the subgrade (Cu), in reinforced system. In the unreinforced one, the same procedure is used but a bearing capacity factor equal to 3.3 rather than 6 was used.

Shear layer theory was developed by Barenberg (1975) and is based on the assumption that a reinforced layer can transmit stresses only by shear deformations. High horizontal stresses develop at the aggregate base-subgrade interface, causing failure. This theory, however, does not take into account plastic deformations, and therefore may not be useful for predicting rut depth or the rate of rut depth development (Bearden,1997).

Based on their results they concluded that the critical stress level to cause excessive permanent deformation was found to be about 3.2*Cu for systems without geotextile and 6*Cu for systems with geotextile, where Cu is the undrained shear strength. These conclusions compare well to Terzaghi's bearing capacity factors for general and local shear failure, respectively.

Barenberg (1975) also has found that geotextile were effective in preventing the intrusion of subgrade soil into the aggregate layer and stabilizing the aggregate. For certain conditions, the use of geotextile was found to result in significant aggregate savings, with approximately a one-third reduction in aggregate thickness but it should be noted that in the research program only one type of geotextile was used.

Furthermore based on work performed by the Army Corps of Engineers was recommended that if the number of load cycles is greater than 10,000, the required aggregate depth should be increased by 10% above that calculated using the critical stress levels given above. This correction factor is purely empirical and should be applied for each increment of 10,000 loads above the initial level of excessive loading, that is the first 10,000 loads.

The design procedure can be schematized as follows:

STEP 1

Determine the wheel load, P, and contact pressure anticipated on the surface of the gravel layer. It is assumed that all loaded areas have uniform pressure over a circular area of radius a calculated by the following expression:

$$a = \sqrt{\frac{P}{\pi p}} \qquad \text{(Eq. 3.1)}$$

where p is the average contact pressure which is assumed to be equal to the tire inflation pressure in kPa for a single wheel or equal about 0.7 to 0.8 times the air pressure of dual tires.

STEP 2

Determine the maximum allowable stress, σ_{all}, for the subgrade:

$$\sigma_{all} = 3.2 \cdot A \cdot c_u \qquad \text{(Eq. 3.2)}$$

where cu is the subgrade undrained shear strength in kPa and A is a coefficient related to the reinforcement effect, in particular A=1 for unreinforced section and A=2 for reinforced one.

STEP 3

Establish the rut geometry (Figure 3.1) including width and maximum rut depth both on the base surface and at the interface with subgrade.

Subgrade rut depth, W, can, for practical purposes, be taken as the base surface rut depth and it can be estimated by the following equation:

$$W = B + 2X \qquad \text{(Eq. 3.3)}$$

Where B= aggregate surface rut width

X = spreading effect of granular layer with and without fabric

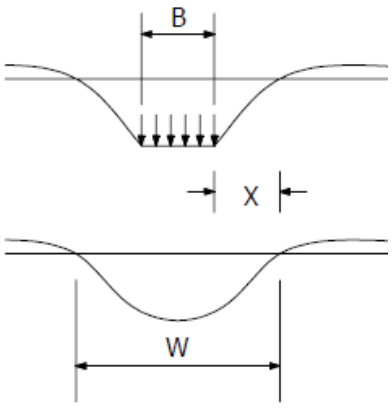

Figure 3.1 Rut geometry (Barenberg 1975)

STEP 4

Determine the average strain in the geotextile from the assumed deformed circular shape (Figure 3.2) according to the following equation:

$$\varepsilon_f = \frac{4\pi R\theta}{135W} - 2 \qquad \text{(Eq. 3.4)}$$

Where R and θ can be estimated by the following equation:

$$\theta = 2tan^{-1}\left(\frac{5d}{3W}\right) \qquad \text{(Eq. 3.5)}$$

$$R = \frac{3W}{8sin\theta} \qquad \text{(Eq. 3.6)}$$

Where d = rut depth

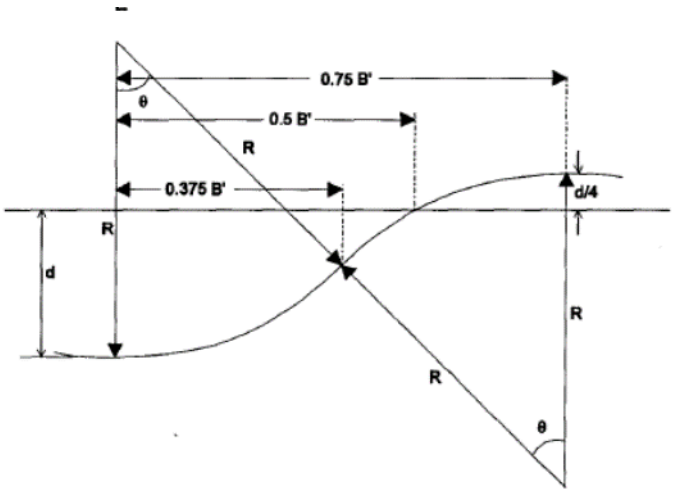

Figure 3.2 Deformed shape of base course-subgrade interface (Barenberg 1975)

STEP 5

It is assumed that the tension in the geosynthetic is:

$$t_f = k\varepsilon_f \qquad \text{(Eq. 3.7)}$$

Where *K*= geosynthetic modulus

STEP 6

The differential normal stress is the normal stress difference between the top and bottom side of the geosynthetic. The summation of the differential normal stress over the geosynthetic in the loaded region is the portion of the applied load that is supported by the geosynthetic . For practical purposes, only the differential stress needs to be calculated and added to the permissible stress on the subgrade to determine the permissible stress on the surface of the geosynthetic.

$$\Delta\sigma_{z-f} = \frac{t_f}{R} \qquad \text{(Eq. 3.8)}$$

Where $\Delta\sigma_{z\text{-}f}$ = differential normal stress across the fabric;

t_f = tension in geosynthetic;

R = radius of circular deflected shape.

STEP 7

Calculate the permissible vertical stress $\sigma_{p\text{-}f}$ on the top of the geosynthetic by summing the maximum permissible stress on the subgrade plus the differential normal stress due to the uplift by the geosynthetic tension:

$$\sigma_{p-f} = \Delta\sigma_{z-f} + 3.2Ac_u \qquad \text{(Eq. 3.9)}$$

STEP 8

Calculate the maximum vertical stress, σ_z, on the fabric using the Boussinesq theory. If the maximum vertical stress on the fabric is greater than the permissible vertical stress on the fabric, is necessary to increase the thickness of the granular layer and return to step 4.

$$\sigma_z = p\left[1 - \left(\frac{1}{1+\left(\frac{a}{z}\right)^2}\right)^{\frac{3}{2}}\right] \qquad \text{(Eq. 3.10)}$$

Where z = aggregate layer thickness

3.3. Method proposed by Giroud e Noiray (1981)

Giroud and Noiray (1981) developed a method that enables to calculate the required thickness of the aggregate base in unpaved road reinforced with geotextile. The results were presented in the form of charts and are applicable only to purely cohesive subgrade soils and roads subjected to low traffic load (less than 10,000 cycles).

This method consider the subgrade to be saturated and to have low permeability and therefore, under quick loading, behave in an undrained manner. This means that the subgrade soil is incompressible, and in terms of total stresses, its friction angle is zero and shear strength is simply the undrained shear strength, Cu. Furthermore, the subgrade is assumed to be homogeneous at least over a thickness sufficient for the development of plastic zone, therefore, an inclusion of geotextile increases the bearing capacity from the elastic to the ultimate bearing capacity, which is considered as change from Terzaghi's local to general shear failure. The aggregate base was assumed to have a CBR greater than 80. The method assumed that the geosynthetic is rough enough to prevent sliding of the aggregate layer along the geotextile surface (that is, a no slip condition).

In addition, Giroud and Noiray (1981) assumed a rectangular contact area and a fixed stress distribution angle. A stress distribution method was used to estimate the vertical stress at the base-subgrade interface. In fact, the aggregate base was assumed to provide a pyramidal load distribution in function of its mechanical characteristics, and based on this assumption, the uniform normal stresses, at the bottom of the aggregate base, were developed (Figure 3.3).

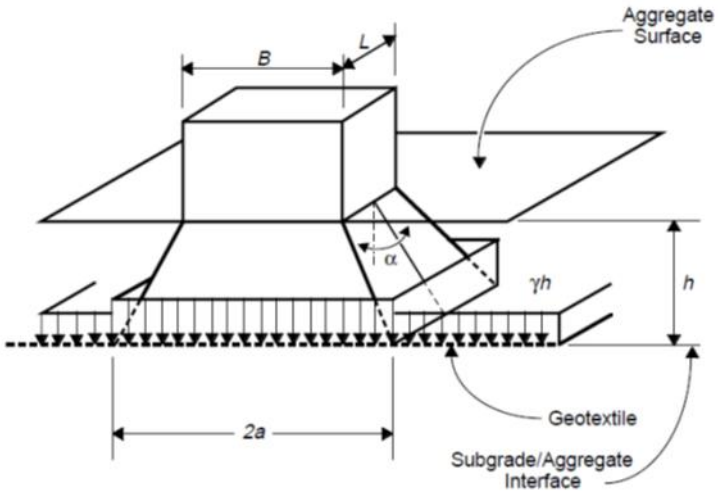

Figure 3.3 Wheel load distribution by aggregate layer to subgrade (Giroud and Noiray 1981)

Giroud and Noiray (1981) initially considered the same "lateral restraint reinforced mechanism" that Barenburg et al. (1975) have proposed, but added to this "tensioned membrane reinforced mechanism," which is a function of the geotextile modulus. According to Giroud e Noiray (1985) the membrane support offered by the geosynthetic can be described as follows.

In the case of wheel loadings on a geotextile reinforced unpaved road, the normal stress applied through the aggregate and onto the geotextile is greater than the normal stress applied through the geotextile and onto the subgrade. The stress against its aggregate face is higher than the stress against its subgrade face. This stress difference is attributed to membrane support.

The resulted overall effect of the "tensioned membrane" mechanism, a different shaped contact area, and a liberal stress distribution can recommend thin granular surface course layers when high modulus geotextiles are utilized, as compared to Barenberg's design method.

Giroud and Noiray (1981) found that for typical geotextiles, the reduction of aggregate thickness resulting from the use of a geotextile generally ranged from 20-60% for a subgrade soil with a CBR=1 and a number of passages between 1,000 and 10,000. Furthermore, the smaller the geotextile tensile modulus, the larger the required thickness of the aggregate layer.

The design procedure can be schematized as follows:

STEP 1

Determine the axle load, P, that is considered to be evenly distributed between the four wheels

$$P = 4A_C p_c \quad \text{(Eq. 3.11)}$$

where P = axle load

A_c = contact area of a tire

p_c = tire inflation pressure assumed to be equal to the average value of the actual contact pressure (non-uniformly distributed) between each tire and the base layer.

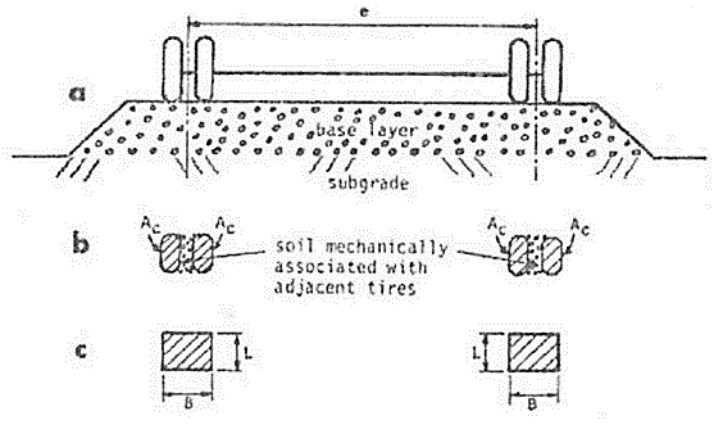

Figure 3.4 Vehicle axle and contact area (Giroud and Noiray, 1981)

For dual wheel axle configurations shown in Figure 3.4:

Contact Area ≈ 2Ac

$$Ac \approx 2*Ac*\sqrt{2} \quad \text{(Eq. 3.12)}$$

And

$p_c = p_{ec}$, where p_{ec} is the "equivalent contact pressure" of an equivalent contact area on the aggregate base:

$$P = 2LBp_{ec} \quad \text{(Eq. 3.13)}$$

$$p_{ec} = \frac{p_c}{\sqrt{2}} \quad \text{(Eq. 3.14)}$$

It assumes a rectangular form for contact area with dimension BxL (Figure 3.4c). The above dimensions depend on the tire pressure p_c, therefore two different cases are proposed:

On highway trucks:

$$P = \frac{B}{\sqrt{2}} \quad \text{(Eq. 3.15)}$$

Off highway trucks:

$$L = \frac{B}{2} \quad \text{(Eq. 3.16)}$$

So using previous equations B is equal to:

On highway trucks:

$$B = \sqrt{\frac{P}{p_c}} \quad \text{(Eq. 3.17)}$$

Off highway trucks:

$$B = \sqrt{\frac{P\sqrt{2}}{p_c}} \quad \text{(Eq. 3.18)}$$

STEP 2

The normal stress distribution from top of the aggregate base, p_{ec}, until at the base-subgrade interface is assumed to be of pyramidal type (Figure 3.5). In fact, the aggregate base was assumed to provide a pyramidal load distribution in function of its mechanical characteristics, and based on this assumption, the uniform normal stresses, at the bottom of the aggregate base, are developed as a function of the chosen pyramidal load distribution angle. Experiments suggested that the tangent of this angle was between 0.5 and 0.7, while theoretical solutions yielded values for the tangent of the angle between 0.47 and 0.64. Preliminary calculations have shown that the value of the calculated aggregate thickness is not significantly influenced by the angle of load distribution if the tangent is between 0.5 and 0.7. So, the equations relating the vertical equilibrium at the base-subgrade interface are :

without geotextile

$$p_{ec}LB = (B + 2h_o tan\alpha_0)(L + 2h_o tan\alpha_0)(p_0 - \gamma h_0) \qquad \text{(Eq. 3.19)}$$

with geotextile

$$p_{ec}LB = (B + 2htan\alpha)(L + 2htan\alpha)(p - \gamma h) \qquad \text{(Eq. 3.20)}$$

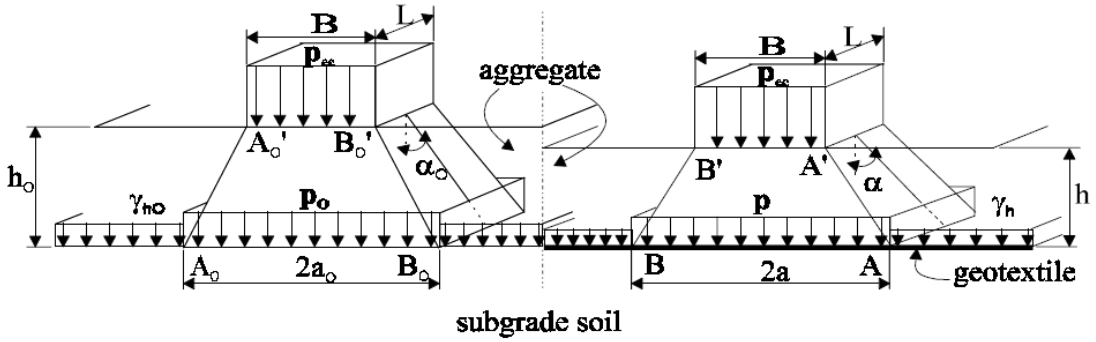

Figure 3.5 Pyramidal load distribution in both unreinforced and reinforced sections (Giroud and Noiray, 1981)

Therefore, an expression for stress on top of the geotextile can be generated using previous equations:

$$p = \frac{P}{2(B+2htan\alpha)(L+2htan\alpha)} + \gamma h \qquad \text{(Eq. 3.21)}$$

Where tanα= 0.5-0.7

STEP 3

Determine the stress at the plastic limit, q_p, that was assumed to be:

$$q_p = (\pi + 2)c_u \qquad \text{(Eq. 3.22)}$$

where c_u = undrained shear strength of the subgrade that was assumed to be:

$$c_u = f_c CBR \quad \text{(Eq. 3.10)} \qquad \text{(Eq. 3.23)}$$

Where f_c=30 for silt and clay saturated conditions

f_c= 20.5 for clayey sand

STEP 4

Due to the assumed failure mechanism with 45° angles in the plastic zone (Figure 3.6), the depth of the plastic zone, H_p, provides the minimum thickness of the base layer and can be expressed as:

$$H_p = a\sqrt{2} \qquad \text{(Eq. 3.24)}$$

From Figure 3.6 2a = B + 2htan α , so the plastic zone height can be rewritten as:

$$H_p = \frac{2a+2h\tan\alpha}{2}\sqrt{2} = \frac{B+2h\tan\alpha}{\sqrt{2}} \qquad \text{(Eq. 3.25)}$$

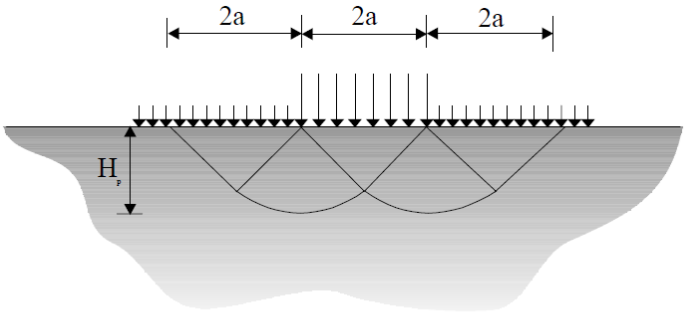

Figure 3.6 Plastic zone (Giroud and Noiray 1981)

STEP 5

The actual stress on the subgrade, p*, and the stress reduction due to the geotextile, p_g, is given by:

$$p^* = p - p_g \qquad \text{(Eq. 3.26)}$$

Where p_g is a tension in the geotextile.

Considering the limiting condition p*=qp, so:

$$p - p_g = (\pi + 2)c_u \qquad \text{(Eq. 3.27)}$$

STEP 6

To determine p_g this method assume that the deformed shape of the geotextile consists of parabolas and that the subgrade is incompressible; thus, the volume of the subgrade displaced downwards equals the volume heaved upwards (Figure 3.7).

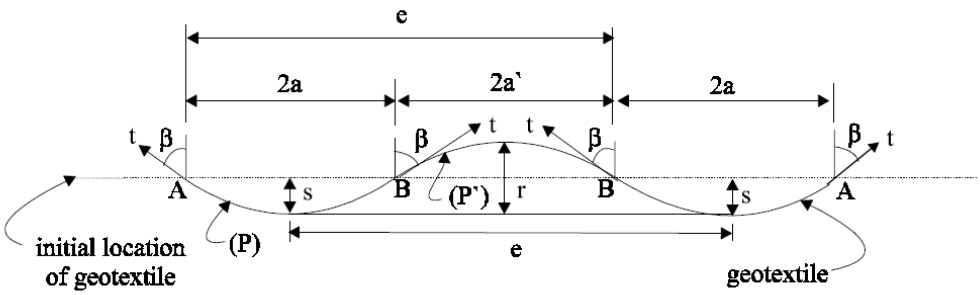

Figure 3.7 Hypothesis of subgrade incompressible

It is possible to considerer two cases: the parabola horizontal distance between the wheel loads ,a', is greater than that beneath the wheel load, a, (i.e. a' > a); the parabola horizontal distance underneath the wheel load is greater than that between the wheel load (i.e. (i.e. a > a'). From the geometry of a curved geotextile:

$$2a = B + 2h\tan\alpha \qquad \text{(Eq. 3.28)}$$

$$2a' = e - B - 2h\tan\alpha \qquad \text{(Eq. 3.29)}$$

If a'>a

$$s = \frac{ra'}{a+a'} \qquad \text{(Eq. 3.30)}$$

If a>a'

$$s = \frac{2ra^2}{2a^2+3aa'-a'^2} \qquad \text{(Eq. 3.31)}$$

If a'>a determine Geotextile elongation as:

$$\varepsilon = \frac{b+b'}{a+a'} - 1 \qquad \text{(Eq. 3.32)}$$

If a>a' determine Geotextile elongation as:

$$\varepsilon = \frac{b}{a} - 1 \qquad \text{(Eq. 3.33)}$$

To determine b and b' the equations are:

$$\frac{b}{a} - 1 = \frac{1}{2}\left[\frac{a}{2s}\ln\left(\frac{2s}{a} + \sqrt{1+\left(\frac{2s}{a}\right)^2}\right) - 2 + \sqrt{1+\left(\frac{2s}{a}\right)^2}\right] \qquad \text{(Eq. 3.34)}$$

$$\frac{b'}{a'} - 1 = \frac{1}{2}\left[\frac{a'}{2(r-s)}\ln\left(\frac{2(r-s)}{a'} + \sqrt{1+\left(\frac{2s}{a'}\right)^2}\right) - 2 + \sqrt{1+\left(\frac{2(r-s)}{a'}\right)^2}\right] \qquad \text{(Eq. 3.35)}$$

Knowing the relationship between load, t, and strain, ε , for a geotextile:

$$t = K\varepsilon \qquad \text{(Eq. 3.36)}$$

the following expression for p_g can be derived:

$$p_g = \frac{K\varepsilon}{a\sqrt{1+\left(\frac{a}{2s}\right)^2}} \qquad \text{(Eq. 3.37)}$$

STEP 7

Whereas the limit condition, in the case of a single traffic load, the aggregate layer thickness, h, is determined by following equations:

$$h = \frac{-(B+L)+\sqrt{(B+L)^2-4\left(BL-\frac{P}{2\left[(\pi+2)c_u+\frac{K\varepsilon}{a\sqrt{1+\left(\frac{a}{2s}\right)^2}}\right]}\right)}}{4tg\alpha} \qquad \text{(Eq. 3.38)}$$

STEP 8

With the purpose of keeping each type of traffic load, the authors have proposed to add to the thickness h just calculated an incremental thickness Δh:

$$\Delta h = h_0' - h_0 \qquad \text{(Eq. 3.39)}$$

Where h_0' is the thickness of the base layer required for a unreinforced section, subjected to a number of traffic load equal to N, and is calculated as:

$$h_0^{'} = \frac{125{,}70 \cdot \log N + 496{,}50 \cdot \log(1000P) - 294{,}14 \cdot r - 2412{,}42}{(1000c_u)^{0{,}63}} \qquad \text{(Eq. 3.40)}$$

And h_0 is the thickness of the base layer required for a unreinforced section, subjected to a singol traffic load, and is calculated as:

$$h_0 = \frac{-(B+L)+\sqrt{(B+L)^2-4\cdot(B\cdot L-\frac{P}{2\cdot\pi\cdot Cu})}}{4\cdot\tan\alpha_0} \qquad \text{(Eq. 3.41)}$$

STEP 9

Calculate the thickness of the base layer reinforced using the equation:

$$h' = h + \Delta h \qquad \text{(Eq. 3.42)}$$

3.4. Method proposed by Giroud e Han (2004)

Giroud and Han method is a theoretically based design method for determine out the thickness of the base course of unpaved road by considering the important parameters such as: traffic volume, wheel loads, tire pressure, subgrade strength, rut depth, and influence of the presence of a reinforcing geosynthetic geotextile or geogrid on the failure mode of the unpaved road.

The method introduce in addition to the factors considered by the Giroud and Noiray (1981) methods, the strength of base course material, the variations of the stress distribution angles through the base course, and the aperture stability modulus "strength" property of the geogrid.

Different from the Giroud and Noiray Method, the Giroud and Han Method assumed a circular tire contact area and considered the effect of the base course stiffness, which is empirically correlated to the California Bearing Ratio of the base. This is an important feature of the Giroud and Han method. Another significant difference between the Giroud and Noiray method and the Giroud and Han method is the consideration of the stress distribution angle. In the Giroud and Noiray method, the stress distribution angle is fixed while in the Giroud and Han method, the stress distribution angle changes with the number of passes, the thickness of the base, the radius of the contact area, and the geosynthetic reinforcement, which make this design method more realistic.

The method has based on the limit equilibrium bearing capacity theory with a modification to consider the benefit of the tension membrane effect.

The method was developed, calibrated, and validated with data from full-scale, field and laboratory tests considering different geogrids. These tests were run for both reinforced and unreinforced conditions. The tests yielded data for pressures on the subgrade and deformations at the surface as functions of the number of load cycles for the various combinations of reinforcement and base thickness. The pressure data was used to estimate the load distribution angle and to quantify the effects of base reinforcement and thickness on both the initial angle and on the changes in the angle with continued applications of load.

Different bearing capacity factors were considered for unreinforced, geotextile-reinforced, and geogrid-reinforced bases.

The subgrade soil is assumed to be saturated and exhibit undrained behavior under traffic loading. The subgrade soil modulus is used based on correlation between the CBR and the resilient modulus for fine grained soils. In the formulation of the design method, the ratio of the resilient modulus of base course to subgrade soil is limited to 5.

This method assume the failure of the unpaved roads considering the shear failure or the excessive deformation of the subgrade. The formulation of the design method is based on a typical surface rut depth of 75 mm which is a serviceability criterion. Also It allows the analysis for rut depths between 50 and 100 mm.

The aperture stability modulus was the stiffness property selected by the authors to characterize the property of geogrid. The aperture stability modulus is obtained by measuring the in-plane torsional behavior directly across the junction of a biaxial geogrid. It is a direct measure of the in-plane stiffness and stability of the ribs and junctions of the geogrid. The method was calibrated using data for stiff biaxial geogrids with aperture stability modulus of 0.32 and 0.65 N-m/deg (Christopher, 2010).

The main parameters and relationships are discussed in the below sessions.

3.4.1. Base layer and wheel load

The base course has a uniform thickness. It is assumed that only one layer of geogrid is used as reinforcement and it is assumed to be placed at the base-subgrade interface.

A minimum base course thickness is taken to be 0.10 m in this method . This minimum base thickness is necessary to ensure the constructability of the base course, to minimize disturbance of the subgrade soil during trafficking and to provide sufficient anchorage for the geogrid.

The wheel load, P, is considered to be half of the axle load, P . The relationship between wheel load and tire contact pressure is as follows:

$$P=p*A \qquad \text{(Eq. 3.43)}$$

where P= wheel load, A= tire contact area and p= tire contact pressure.

The tire contact area is replaced in this theoretical study by a circular area called the equivalent tire contact area. The equivalent tire contact area has the same surface area as the tire contact area, and its radius r is equal to:

$$r = \sqrt{\frac{P}{\pi p}} \qquad \text{(Eq. 3.44)}$$

3.4.2. Properties of base and subgrade materials

In this method the base course material quality is assumed to be sufficient to preclude a failure within the base course and the base course material is characterized by its California bearing ratio, noted CBR_{bc}.

Using CBR of the base layer it is possible to calculate the resilient modulus of the layer using the following relationship:

$$E_{bc} = \mathrm{f_c CBR_{bc}^{0.3}} \qquad \text{(Eq. 3.45)}$$

where E_{bc}= base course resilient modulus, CBR_{bc}=base course California Bearing Ratio; and f_{EBC}= factor equal to 36 (MPa)

The value of c_u can also be approximately deduced from the CBR value of the subgrade soil using the relationship proposed by Giroud and Noiray (1981):

$$c_u = \mathrm{f_c CBR_{sg}} \qquad \text{(Eq. 3.46)}$$

where c_u= undrained cohesion of the subgrade soil, CBR_{sg}= California Bearing Ratio of the subgrade soil; and f_C= factor equal to 30 (kPa).

Furthermore, the subgrade resilient modulus can be calculated as:

$$E_{bc} = \mathrm{f_{ESG} CBR_{sg}} \qquad \text{(Eq. 3.47)}$$

where E_{sg}= subgrade soil resilient modulus and f_{ESG}= factor equal to 10.35(MPa).

So, the modulus ratio of base to subgrade soil can be calculated using the following equation:

$$\frac{E_{bc}}{E_{sg}} = \frac{3.48\mathrm{CBR_{bc}^{0.3}}}{\mathrm{CBR_{sg}}} \qquad \text{(Eq. 3.48)}$$

3.4.3. Bearing capacity factor

The bearing capacity factor N_c= 3.14 is adopted for unreinforced unpaved roads and it is consistent with the widely used method by Giroud and Noiray (1981).

The theoretical value of the ultimate bearing capacity factor for axisymmetric conditions and maximum shear stress of 5.71 is adopted for the geogrid reinforced unpaved roads. For the case when the base course is separated by a geotextile and there is no interlock, Giroud and Han adopted the value of 5.14 initially proposed by Giroud and Noiray (1981), which is the ultimate bearing capacity factor for plain-strain conditions and zero shear stress at the base-subgrade interface.

Summarizing in this design method the values that are used for the bearing capacity factor are: i) N_c=3.14 for unreinforced unpaved roads; ii) N_c=5.14 for geotextile-reinforced unpaved roads; iii) and N_c=5.71 for geogrid-reinforced unpaved roads.

3.4.4. Effect of base and subgrade resilient modulus on stress distribution angle

The ratio of tangents of the stress distribution angle is a function of the ratio of base to subgrade resilient modulus . The correlation is:

$$\tan\alpha_1 = \tan\alpha_0 \left[1 + 0.204\left(\frac{E_{bc}}{E_{sg}} - 1\right)\right] \qquad \text{(Eq. 3.49)}$$

where α_1= stress distribution angle, α_0= stress distribution angle for a reference medium defined by E_{bc}=E_{sg} ; and E_{bc} and E_{sg} moduli of base course and subgrade soil, respectively.

3.4.5. Effect of traffic on stress distribution angle

Unpaved roads deteriorate under repeated loading. As a result, the stress distribution angle decreases with increasing number of load applications. This phenomenon was measured in laboratory cyclic plate loading tests by Gabr (2001). The correlation is:

$$\frac{1}{\tan\alpha} = \frac{1+k\log N}{\tan\alpha_1} \qquad \text{(Eq. 3.50)}$$

Then combining the effect of base and subgrade resilient modulus on stress distribution angle with the effect of traffic is obtained:

$$\frac{1}{\tan\alpha} = \frac{1+k\log N}{\tan\alpha_0[1+0.204(R_E-1)]} \qquad \text{(Eq. 3.51)}$$

Whereas previous relations and using the results obtained from the experimental tests, the authors obtained the following equation for the calculation of the thickness of the reinforced base layer:

$$h = \frac{0.868+\left(0.661-1.006J^2\right)\left(\frac{r}{h}\right)^{1.5}\log N}{[1+0.204(R_E-1)]}\left[\sqrt{\frac{\frac{P}{\pi r^2}}{\left(\frac{s}{f_s}\right)\left[1-0.9\exp\left(-\left(\frac{r}{h}\right)^2\right)\right]N_c c_u}} - 1\right] r \qquad \text{(Eq. 3.52)}$$

Where h = required base course thickness;

J = geogrid aperture stability modulus (m-N/degree), that in the unreinforced case is J=0;

N = number of axle passes;

P = wheel load;

r = radius of the equivalent tire contact area;

CBR_{sg} = California bearing ratio of the subgrade;

CBR_{bc} = CBR of the base course;

s = allowable rut depth;

f_s = factor equal to 75 mm;

f_c = factor equal to 30 kPa;

R_E=Modulus ratio = E_{bc}/E_{sg}

N_c = bearing capacity factor.

3.4.6. Limit case bearing capacity

It is important to check capacity of subgrade soil to support wheel load without reinforcement

$$P_{h=0,unreinf} = \left(\frac{s}{f_s}\right)\pi r^2 N_c c_u \qquad \text{(Eq. 3.53)}$$

Where P_h = support capacity of subgrade.

If $P < P_{h=0,\ unreinf}$ the subgrade soil can support the wheel load and a minimum thickness of 4 in. (100 mm) base course is recommended to prevent disturbance of the subgrade. If $P > P_{h=0,\ unreinf}$ the use of reinforcement is required and the solution continues to the next step.

3.5. Method proposed by Leng e Gabr (2005)

The authors have conducted a study to investigate the behavior of reinforced unpaved structure under cyclic load through laboratory testing, theoretical and finite element analyses.

The authors have realized fourteen laboratory large-scale cyclic load plate tests on unpaved road sections with two base course thicknesses and several geosynthetic reinforcements placed between base layer and subgrade. Results indicated that reinforcement improved stress distribution transferred to the subgrade, decreased degradation of base course and surface deformation accumulation and stiffer geogrids showed better stress attenuation effect and reduced plastic surface deformation as compared with lower modulus geogrids.

Subsequently performance of geogrid-reinforced test sections was simulated using the FEM program ABAQUS. FEM results indicated that geogrid reinforcement can provide lateral confinement at the bottom of the base layer by improving interface shear resistance and increasing mean stress at the bottom of the base layer. Based on results obtained both laboratory and FEM analysis was developed a new unpaved road design procedure, considering in particular the geogrid reinforcement mechanisms, degradation of base course, and mobilization of subgrade bearing capacity. This method, in fact,

incorporates base course property, mobilization of subgrade bearing capacity with rutting, degradation of base course stress attenuation with cyclic load, and the effect of reinforcement inclusion.

The authors used an elastic layer method to back-analyze the vertical stresses on subgrade with data from previous cyclic plate load tests performed in the laboratory and the degradation of unpaved sections was expressed as a reduction in base course–subgrade elastic modulus ratio (E1/E2) with an increasing number of cycles or a decrease in stress distribution angle of base course.

With this method the authors tend to exceed the two shortcomings presents in previous methods .

1) The performance of aggregate under cyclic load was not clearly explained;

2) The degradation of aggregate layer was not explicitly considered.

The following paragraphs aim to analyzed of the various factors that influence the method proposed by Leng and Gabr.

3.5.1. Equivalent thickness for base course layer

For a two-layer unpaved road section, the base course layer is transformed to an equivalent layer with the same modulus as the underlying subgrade. To keep the same stiffness as the original layer, the equivalent thickness, h_e, is specified as follows:

$$h_e = h\left(\frac{E_1(1-\mu_2^2)}{E_2(1-\mu_1^2)}\right)^{\frac{1}{3}} \qquad \text{(Eq. 3.54)}$$

where

h = base course thickness,

E1 = base course elastic modulus,

E2 = subgrade elastic modulus,

μ1 = Poisson's ratio of base course

μ2 = Poisson's ratio of subgrade.

The maximum interface vertical stress (σ c) underneath the center of a circular loaded area was expressed as follows:

$$\sigma_c = p\left(1 - \frac{h_e^3}{(a^2-h_e^2)^{\frac{1}{5}}}\right) \qquad \text{(Eq. 3.55)}$$

where

p = contact pressure

a = radius of contact area

3.5.2. Base layer degradation analysis

The authors consider that during the application of loads traffic from the base layer undergoes two types of deterioration, due to the degradation of the elastic modulus of the base layer and to decrease the angle of the load distribution through the base layer.

With an assumption that base course thickness remains relatively constant during cyclic loading, the authors obtain the degradation coefficient (λ1) of the elastic modulus ratio as follows:

$$\lambda_1 = \frac{\left(\frac{E_1}{E_2}\right)_N}{\left(\frac{E_1}{E_2}\right)_1} = \frac{1}{1+k_1 \log N} \qquad \text{(Eq. 3.56)}$$

where

(E1/E2)N = elastic modulus ratio at the Nth load cycle;

(E1/E2)1 = initial elastic modulus ratio under first load cycle;

k_1 = constant representing the degradation rate of the elastic modulus ratio.

Another factor considered in the definition of the method is the stress distribution angle that can be used to represent load distribution through the base layer.

Occurs that the stress distribution angle suffer a degradation from number of traffic load repetition and the coefficient, λ2, can be express in terms of stress distribution angle decrease, with the number of traffic loads:

$$\lambda_2 = \frac{\tan\alpha_N}{\tan\alpha_1} = \frac{1}{1+k_2 \log N} \qquad \text{(Eq. 3.57)}$$

where

α_N = stress distribution angle at the N^{th} load cycle,

α_1 = initial stress distribution angle, and

k_2 = a constant.

The k_2 value is indicative of the degradation of stress distribution angle.

3.5.3. Contribution of geogrid reinforcement

By laboratory tests the authors support that the performance of geogrid-reinforced base course largely depends on the interaction of geogrid and aggregate (interlock effect), that is affected by geogrid aperture size, rib thickness, junction strength, and geogrid tensile modulus. Results by tests have indicated that both tensile modulus of geogrid reinforcement and interface friction coefficient between geogrid and base aggregate have an effect on the stress transferred to subgrade as well as surface deformation.

Through the regression analysis the degradation parameters k_1 and k_2 can be empirically correlated to the 2% tensile strength of geogrids (J_t) as follows:

Degradation parameter of elastic modulus ratio:

$$k_1 = \left(\frac{a}{h}\right)^{0.72} (1.04 - 0.00045 J_t^{3.7}) \qquad \text{(Eq. 3.58)}$$

Degradation parameter of the stress distribution angle:

$$k_2 = \left(\frac{a}{h}\right)^{0.81} (0.58 - 0.000046 J_t^{4.5}) \qquad \text{(Eq. 3.59)}$$

As a result of these considerations the design procedure can be schematized as follows:

STEP 1

Determine subgrade undrained shear strength. The empirical relationship between subgrade undrained shear strength used in this method was proposed by Giroud and Noiray (1981):

$$C_u = 30\ CBR_{sb}\ (kPa) \qquad \text{(Eq. 3.60)}$$

STEP 2

Calculate the subgrade modulus. The most widely used relation of subgrade resilient modulus (E2) and CBR is the one developed by Heukelom and Klomp (1962):

$$E_2\ (MPa) = 10*CBR_{sb} \qquad \text{(Eq. 3.61)}$$

STEP 3

Calculate the base course modulus. The empirical relationship of base course modulus and base course CBR value used by Leng and Gabr is represented in a design method proposed by Tensar Earth Techologies, Inc. (2001).

$$E_1 = 36\ CBR_{bs}{}^{0.3}\ (MPa) \qquad \text{(Eq. 3.62)}$$

So, with the correlation equations of modulus and CBR value for subgrade and base course, the modulus ratio E_1/ E_2 can be expressed as:

$$\frac{E_1}{E_2} = \frac{36CBR_{bc}^{0.3}}{10CBR_{sg}} = \frac{3.6}{CBR_{sg}^{0.7}}\left(\frac{CBR_{bc}}{CBR_{sg}}\right)^{0.3} \qquad \text{(Eq. 3.63)}$$

STEP 4

Determine the critical subgrade deformation, r_{cr}, relative to number of load cycles as follows:

$$r_{rcr} = 0.025(0.125\log N + 1.5) \qquad \text{(Eq. 3.64)}$$

The mobilized subgrade bearing capacity ratio (m) can be adjusted according to design rutting criterion (r) used for the design as follows:

$$m = \left[1 - e^{-0.78\left(\frac{a}{h}\right)h}\right]\frac{r}{r_{cr}} < 1 \qquad \text{(Eq. 3.65)}$$

STEP 5

This method assumed that one loaded wheel contacting the unpaved road surface on a circular area, the vertical stress distributed on the subgrade layer need to be less than or equal to mobilized bearing capacity of subgrade in order to prevent the rutting failure and the bearing capacity failure of subgrade, so the balance equation was expressed as follows:

$$\sigma_c = \frac{P}{\pi(a+h\tan\alpha_N)^2} < mN_c c_u \qquad \text{(Eq. 3.66)}$$

where

σ_c = additional vertical stress on top of the subgrade,

P = single wheel load,

a = radius of the loaded area,

α_N = stress distribution angle at the design load cycles N,

m = mobilized subgrade bearing capacity ratio

Nc = subgrade bearing capacity factor (3.8 for the unreinforced case, 6 for the geogrid-reinforced case)

C_u = subgrade undrained shear strength.

STEP 6

The required thickness of base layer, h, can be expressed as:

$$h = \frac{1}{\tan\alpha_N}\left(\sqrt{\frac{P}{\pi m N_c c_u}} - a\right) \qquad \text{(Eq. 3.67)}$$

Assuming that the wheel load is uniformly distributed on the contact area ($P = p\pi a^2$), and the degradation of base layer can be determined as $\tan \alpha_N = \tan \alpha_1/[1 + k_2 \log N]$, the required base layer thickness and a/h can be determined as following:

$$h = \frac{a[1+k_2 \log N]}{\tan\alpha_1}\left(\sqrt{\frac{P}{\pi m N_c c_u}} - 1\right) \qquad \text{(Eq. 3.68)}$$

Where tan α1 is a function of initial E_1/E_2 and a/h; degradation coefficient k_2 is related to a/h and the geogrid property (the average value of transversal and longitudinal 2% geogrids tensile strength, J_t).

For this reasons an iteration scheme is necessary in order to solve the equations. So the required base layer thickness (h) in this method is a function of:

1) the modulus ratio of base layer and subgrade (E_1/E_2);
2) the undrained shear strength of subgrade (Cu);
3) the geogrids tensile strength (J_t),;
4) the bearing capacity factor (N_c);
5) the single wheel load (P);
6) the radius of loaded area (a);
7) the number of traffic load cycles (N).

CHAPTER 4

Analysis and discussion of results obtained by unpaved roads design methods and by unpaved roads FEM implementations

This page has been intentionally left blank

CHAPTER 4

4. Analysis and discussion of results obtained by unpaved roads design methods and by unpaved roads FEM implementations

4.1. Parameters used for the implementation of unpaved roads design procedures

For all unpaved roads design procedure, previously described in Chapter 3, a set of different input values has been considered. The goal of the following analysis is to evaluate the effects that each design parameter has on each unpaved road procedure. In addition, a comparison between the above mentioned design methods has been done.

In particular, the input variables considered by Barenberg (1975), Giroud and Noiray (1981), Giroud and Han (2004) and Leng and Gabr (2005) design methods are related to the subgrade mechanic characteristics, the geogrid mechanical characteristics, the traffic loads conditions and the allowable rut depth. All these design parameters are listed below:

- allowable rut depth;
- base California Bearing Ratio, CBR_b [%];
- subgrade California Bearing Ratio , CBR_S [%] or subgrade undrained shear strength, C_u [kN/m];
- number of vehicular or wheel passes, N_{cycles} [-];
- tire contact pressure, P_c[kN/m];
- mechanical reinforcement characteristics (in terms of tensile load or tensile stiffness at 2% of deformations, $J_{2\%}$ [kN/m] or geogrid aperture stability modulus, J_{AS} [mN/°]).

Due to the relatively high number of considered values as input, the methods have been implemented in Matlab (2009) environment and the obtained results have been reported in the form of graphs to better analyze the dependence of the various methods on these input values and to make a more accurate comparison between the different design procedures proposed.

With respect to the allowable rut depth values a serviceability criteria offered by AASHTO design guidelines (1993) has been used. It considers allowable rut depths from 13 to 75 mm. In the case of unpaved access roads, allowable rut depths greater than 75 mm are sometimes used, such as 100 mm. Thus, based on the above considerations, for each unpaved roads design method, three allowable rutting values have been used for the implementation.

Moreover the subgrade mechanical proprieties have been chosen in agreement to AASHTO design guidelines (1993) In fact, for unpaved roads, geosynthetics with reinforcement function are required only for weak subgrade characterized by California Bearing Ratio (CBR) less than 3,or undrained shear strength (C_u) less than 90÷120 kPa.

The analyses of all methods presented in Chapter 3 were focused on the use of different extruded bi-oriented geogrids as reinforcement commercially available. They are characterized by different mechanical proprieties (in terms of tensile load or tensile stiffness at 2% of deformations, $J_{2\%}$[kN/m] or geogrid aperture stability modulus, J_{AS} [mN/°]) and they were placed at the bottom of base course layer.

About the axles and loads design parameters, the wheel load (P) is the load applied by one of the wheels, in the case of single-wheel axle, or the load applied by a set of two wheels, in the case of dual-wheel axles and it is considered to be half of the axle load (P_{Axle}). In this analysis P_{Axle} =80 kN, so P=40 kN and a tire contact pressure (P_c) equal to 556 kPa, were assumed. The traffic, being vehicular traffic channelized, has been assumed characterized by the number of passes (N_{cycles}) of a given axle during the road design life. The analysis conducted expected a maximum number of load applications equal to 10000.

4.2. Unpaved roads design procedure by Barenberg et al. (1975): analysis of results and discussion

The focus of this section is a parametric analysis of design curves, obtained by Barenberg (1975) design procedure, with respect to the thickness required for the base layer, both in the unreinforced and reinforced configuration, and to the improvement offered by the use of a reinforcement geosynthetic expressed in terms of percentage reductions of the reinforced base layer thickness, compared to the unreinforced one.

In particular, as widely discussed in Chapter 3, the authors developed a design procedure to determine the thickness of the base layer, including the membrane effect, based on the limit equilibrium bearing capacity theory. Some assumptions have been done: occurrence of significant rutting, reinforcement deflected shape as circular arc, separation function provided by the reinforcement and no slip occurrence at the interface. The limit equilibrium bearing capacity theory is based on selecting an aggregate base thickness so that the vertical stress applied to the interface geosynthetic-subgrade purified the amount of the wheel load which is supported by the reinforcement, if exists, is below the theoretical limits for subgrade shear failure (or bearing capacity). Being the failure mode of the unreinforced system characterized by local shear failure, whereas the one of a geosynthetic-reinforced system by a general shear failure, Barenberg et al. proposed a bearing capacity factor value, Nc, equal to 3.3 and 6.0 for unreinforced and reinforced systems, respectively.

About design parameters related to geosynthetic mechanical properties, allowable depth ruts, sub-grade mechanical characteristics and traffic conditions are given in Table 4.1.

Six extruded bi-oriented geogrids, commercially available, of different tensile stiffness were selected. Geogrids mechanical properties were investigated by means of the wide-width tensile tests (according to EN ISO 10319). Tensile modules at 2% (in transverse direction along which the geogrids carry the higher mechanical characteristics) varying from 315 kN/m to 2100 kN/m were chosen in the implementation of this design procedure. It is important to emphasize that the geogrids' tensile stiffness was reduced by a factor equal to 1.1 in order to take into account the working conditions in site.

Based on the serviceability criteria offered by AASHTO design guidelines three allowable rutting values equal to 0.025m, 0.075m and 0.100 m were chosen.

Further in this analysis Cu values varying from 5 kN/m^2 to 80 kN/m^2 were assumed according to AASHTO design guidelines that suggest the use of geosynthetics with reinforcement function only in presence of weak subgrade characterized by undrained shear strength (Cu) less than 90÷120 kPa.

About the traffic conditions the previously reported consideration were applied, having clear in mind that the theory used by Barenberg et al. (1975) is based on static loading (i.e., up to 100 vehicle passes).

Table 4.1 Design parameters of Barenberg et al. (1975) design method

Allowable rut, r [m]	**Geogrid Stiffness, $J_{2\%}$ [kN/m]**	**Undrained shear strength, Cu [kN/m^2]**
0.025	315	5
0.075	530	10
0.100	750	15
	1017	25
	1630	50
	2100	60
		80

Figure 4.1 a ÷ Figure 4.1 c show the design curves related to the reinforced and unreinforced base course layer thickness, for fixed rut depth (r = 0.025m, 0.075m, 0.100m) and different values of the subgrade undrained shear strength (C_u= 5 ÷ 80 kN/m^2). Each curve is referred to a reinforcement geogrid with different tensile stiffness ($J_{2\%}$= 315 ÷2100 kN/m).

For both the reinforced and unreinforced conditions, the base course layer thickness decreased with the increasing of the subgrade undrained shear strength.

Moreover, the unreinforced base course layer thickness appeared to be independent on the rutting. These results highlight that this design procedure does not take intrinsically into account the mechanic characteristics of base aggregate course, which influence the rut depth magnitude together with the wheel load. In fact, the allowed rut depth variation in the reinforced configuration appeared to be relevant only to mobilize the membrane effect.

The Barenberg et al. (1975) method, thus, overlooks the base course layer mechanical properties. Hence, the conservative nature of the method, characterized by the determination of the subgrade allowable pressure based on the Boussinesq theory, can be deduced.

Analyzing the design curves related to the reinforced base layer thickness for the allowable rut depth limit values (i.e., r= 0.025 m in Figure 4.1 a, and r= 0.100m in Figure 4.1 c), it is evident that the geogrid stiffness has no effect on the design of the reinforced base course layer thickness when the rut depth is equal to the minimum allowable value (r= 0.025 m). This behavior can be ascribed to the permanent superficial deformations caused by the channelized vehicular traffic, which need to be deep enough to activate the membrane support.

On contrary, for higher allowable rut depth values (r=0.075 m e r=0.100 m) the geosynthetic appears to supply more support to the vertical pressure due to the vehicular traffic. In particular, it works proportionally to its tensile strength, reducing the vertical pressure on the subgrade and consequently reducing the reinforced base course layer thickness, when compared to the unreinforced configuration. In

fact, the design curves for different values of tensile strength appear clearly distinguished between each other.

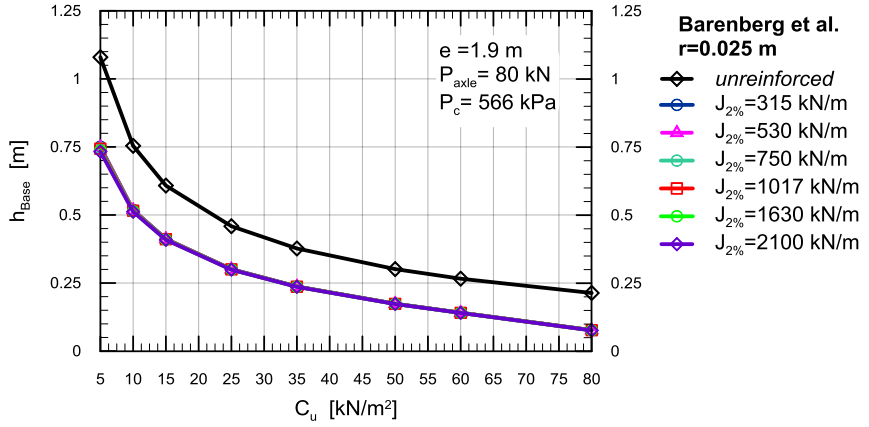

(a)

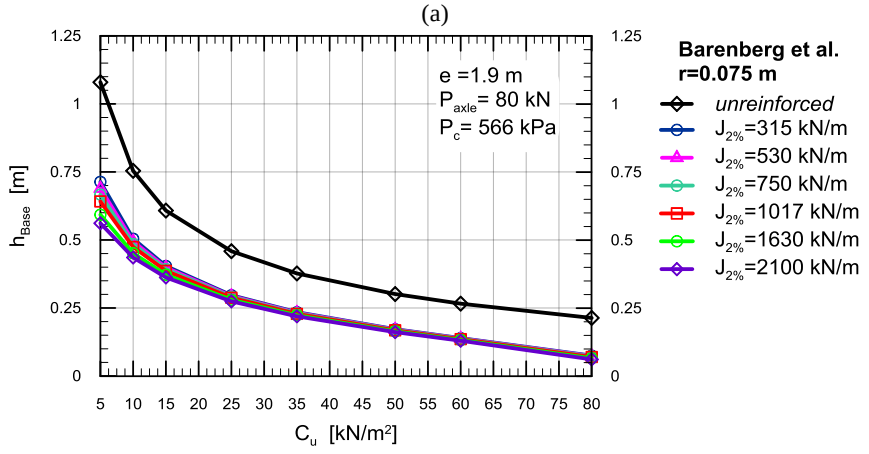

(b)

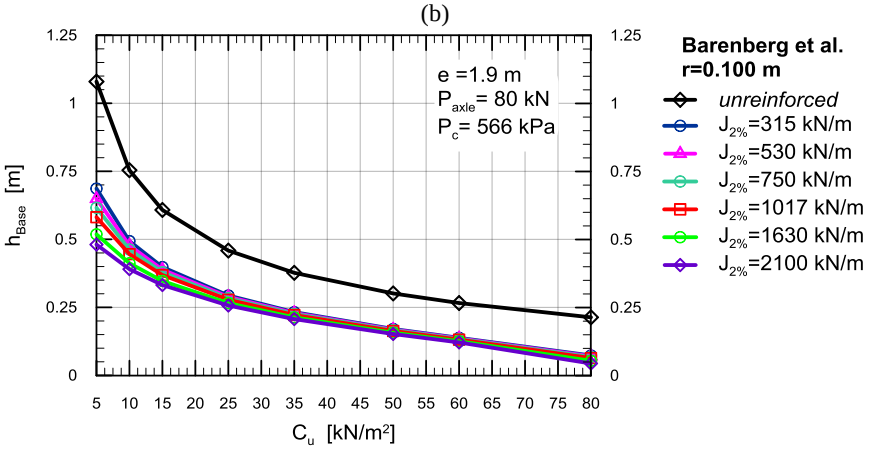

(b)

Figure 4.1 Unpaved roads design procedure by Barenberg et al. (1975): unreinforced and reinforced base aggregate thickness versus subgrade undrained shear strength, for each geogrids chosen and for a fixed allowable rut depth equal to: a) 0.025m; b) 0.075m; and c) 0,100m.

In addition, the geogrid stiffness for $C_u > 35$ kN/m^2 is shown to have once again no effect on the reinforced base course layer thickness since the reinforcement contribution, regardless of the reinforcement stiffness, decreases with the increasing of the mechanical characteristics of the subgrade, which result to be able to carry the vehicular traffic load independently.

To confirm what previously discussed, in Table 4.2 are summarized some results of the simulations in terms of unreinforced and reinforced base aggregate thickness ($h_{B,UNR}$ and $h_{B,R}$, respectively) and in terms of percentage reduction of the reinforced base layer thickness, for extreme values of subgrade undrained shear strength, geogrid tensile stiffness and allowable rut depth.

Table 4.2 Results of Barenberg et al. (1975) unpaved roads design procedure in terms of unreinforced and reinforced base aggregate thickness, reduction and percentage reduction of the reinforced base layer thickness, for extreme values of geogrid tensile stiffness and allowable rut depth and varying the subgrade undrained shear strength

Undrained shear strength Cu [kN/m2]	Allowable rut depth r [m]	Tensile stiffness $J_{2\%}$ [kN/m]	$h_{B,UNR}$ [m]	$h_{B,R}$ [m]	$\Delta h_{reinf.}$ [m]	$\Delta h_{reinf.}$ [%]
5	0.025	315	1.08	0.75	0.33	30.46
5	0.025	2100	1.08	0.73	0.35	32.12
35	0.025	315	0.38	0.24	0.14	37.07
35	0.025	2100	0.38	0.24	0.14	37.40
60	0.025	315	0.27	0.14	0.12	47.00
60	0.025	2100	0.27	0.14	0.13	47.28
5	0.100	315	1.08	0.69	0.39	37.11
5	0.100	2100	1.08	0.48	0.60	38.50
35	0.100	315	0.38	0.23	0.14	38.33
35	0.100	2100	0.38	0.21	0.17	45.11
60	0.100	315	0.27	0.14	0.13	48.09
60	0.100	2100	0.27	0.12	0.14	54.45

Therefore, the decrease in $h_{B,UNR}$ and $h_{B,R}$ is observed as the subgrade undrained shear strength increases. In the reinforced configuration the geosynthetic stiffness has no effect on the design base thickness if r=0.025 m and if C_u > 35 kN/m2 (see Figure 4.1a and Figure 4.1c for comparison). The former behavior is due to the rut depths, and consequently the plastic deformations in the subgrade surface, which have to be great enough to develop membrane type support. The latter behavior is due to the influence of each reinforcement mechanism, which goes down with stronger subgrade conditions.

On the other hand, for weak subgrade and for increasing rut magnitude (r>0.025 m and if Cu < 35 kN/m^2, see Figure 4.1a and Figure 4.1c), the decrease of vertical stresses transferred to the subgrade with consequent improvement in terms of lower reinforced base thickness is observed thanks to the geogrid reinforcement achieving higher values of deformation, so higher tensile stresses are mobilized proportionately to geogrids' stiffness.

In order to understand the r and J variables influence and relevance on the Barenberg et al. (1975) method some considerations are reported below.

In Figure 4.2 a and Figure 4.2 b are reported the design curves for the reinforced and unreinforced base course layer thickness for fixed values of the geogrid tensile stiffness (respectively for $J_{2\%}$ equal to 315

kN/m and 2100 kN/m) with varying subgrade undrained shear strength (Cu= 5 ÷ 80 kN/m^2) and for three different allowable rut depth values (r=0.025m, 0.075m, 0.100m).

According to what previously observed, the effects that r and $J_{2\%}$ have on the Barenberg et al. (1975) method can be appreciated if the subgrade is weak, which means C_u<35 kN/m^2.

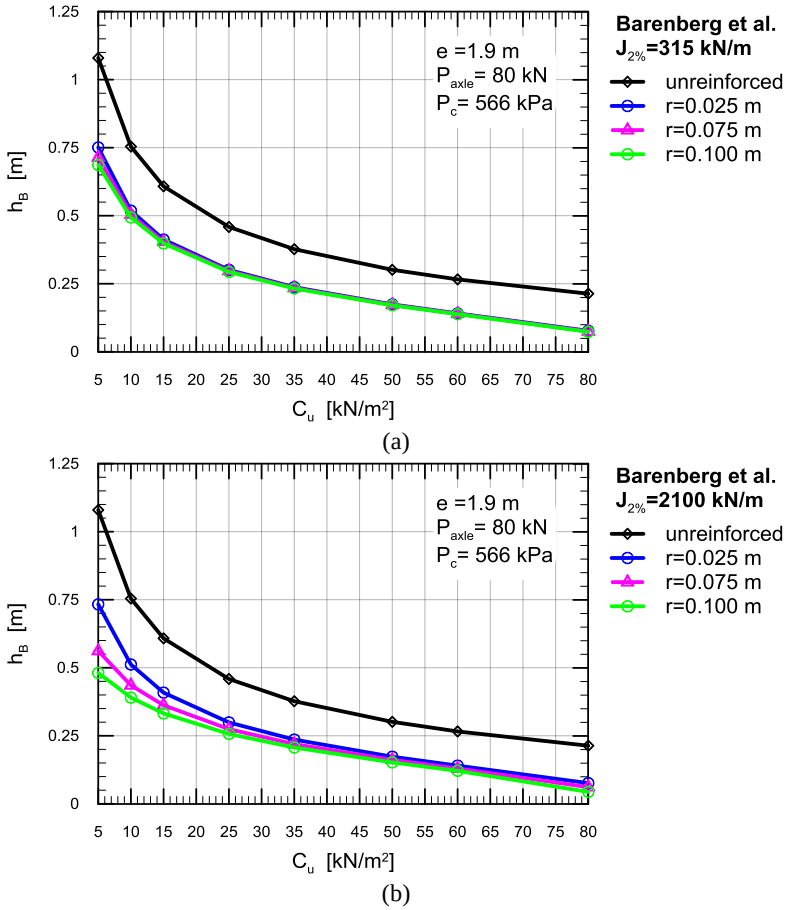

Figure 4.2 Unpaved roads design procedure by Barenberg et al. (1975): unreinforced and reinforced base aggregate thickness varying the subgrade undrained shear strength, for each allowable rut depth values and for a fixed geogrid tensile stiffness a) J2%=315 kN/m; b) J2%=2100 kN/m.

Given the reduction of the required thickness with the increase of the subgrade undrained shear strength, some considerations can be drawn comparing the results obtained for the geogrid tensile stiffness limit values, i.e. 315 and 2100 kN/m.

The base course layer thickness is not affected by the rut depth in the examined range when the geogrid reinforcement is characterized by the minimum tensile stiffness ($J_{2\%}$ =315 kN/m). This behavior could be explained by the incapacity of the geogrids with low values of tensile stiffness (i.e., J2%= 315 kN/m) to offer an efficient support. This result is confirmed by the reinforced base aggregate thickness values obtained and reported in Table 4.3)

When the geogrid placed at the base--subgrade interface has higher mechanical characteristics ($J_{2\%}$=2100 kN/m) and C_u<35 kN/m, small enough allowable rut depth to let work the geosynthetic which is able to support to the vertical pressure due to the vehicular traffic are observed. In other words, thanks to its

higher tensile stiffness, the geogrid reinforcement develops tensile tensions larger than the ones of the previous case (J=315 kN/m), which increase proportionally to the assumed rutting. Therefore, the design curves for each allowable rutting appear to be clear and distinct, highlighting the influence of the parameter on the Barenberg et al. (1975) method. This result is confirmed by the reinforced base aggregate thickness values obtained and reported in Table 4.3)

In addition, considering the same design condition (in terms of geogrid tensile stiffness and subgrade mechanical proprieties), the increasing of allowable rut depth produces an improvement in terms of higher reinforced base layer thickness percentage reduction, $\Delta h_{B,R}$ [%], (see Table 4.3), with consequent saving of aggregate material needed for the construction.

Table 4.3 Results of Barenberg et al. (1975) unpaved roads design procedure in terms of unreinforced and reinforced base aggregate thickness and reduction and percentage reduction of the reinforced base layer thickness, for extreme values of geogrid tensile stiffness and varying the subgrade undrained shear strength and allowable rut depth.

Undrained shear strength Cu [kN/m2]	**Allowable rut depth r [m]**	**Tensile stiffness $J_{2\%}$ [kN/m]**	**$h_{B,UNR}$ [m]**	**$h_{B,R}$ [m]**	**$\Delta h_{reinf.}$ [m]**	**$\Delta h_{reinf.}$ [%]**
5	0.025	315	1.08	0.75	0.33	30.46
5	0.075	315	1.08	0.71	0.37	33.90
5	0.100	315	1.08	0.69	0.39	36.42
35	0.025	315	0.38	0.24	0.14	37.07
35	0.075	315	0.38	0.23	0.14	37.77
35	0.100	315	0.38	0.23	0.14	38.33
60	0.025	315	0.27	0.14	0.12	47.00
60	0.075	315	0.27	0.14	0.13	47.60
60	0.100	315	0.27	0.14	0.13	48.09
5	0.025	2100	1.08	0.73	0.35	32.12
5	0.075	2100	1.08	0.56	0.52	47.99
5	0.100	2100	1.08	0.48	0.60	55.47
35	0.025	2100	0.38	0.24	0.14	37.40
35	0.075	2100	0.38	0.22	0.16	41.80
35	0.100	2100	0.38	0.21	0.17	45.11
60	0.025	2100	0.27	0.14	0.13	47.28
60	0.075	2100	0.27	0.13	0.14	51.22
60	0.100	2100	0.27	0.12	0.14	54.45

In order to better analyze the different effect caused by the allowable rutting, r, and by the geogrid tensile stiffness J_2%, on the Barenberg et al.(1975) method, the results obtained have been plotted keeping constant the subgrade mechanical characteristics.

In particular, to evaluate the sensitivity of the Barenberg et al.(1975) model on the values of r and $J_{2\%}$ the analysis was done considering each variable individually.

First, the effect of the variable $J_{2\%}$ was analyzed. Figure 4.3a ÷ Figure 4.3b show the design curves related to both unreinforced and reinforced base layer thickness varying the geogrid tensile stiffness ($J_{2\%}$ from 315 kN/m to 2100 kN/m) for three different allowable rut depth values (r=0.025m, 0.075m, 0.100 m) keeping constant the subgrade undrained shear strength. Specifically, two Cu values equal to 5 and 35 kN/m^2 were chosen, since the reinforcement does not offer better performances for Cu>35 kN/m^2, as previously seen.

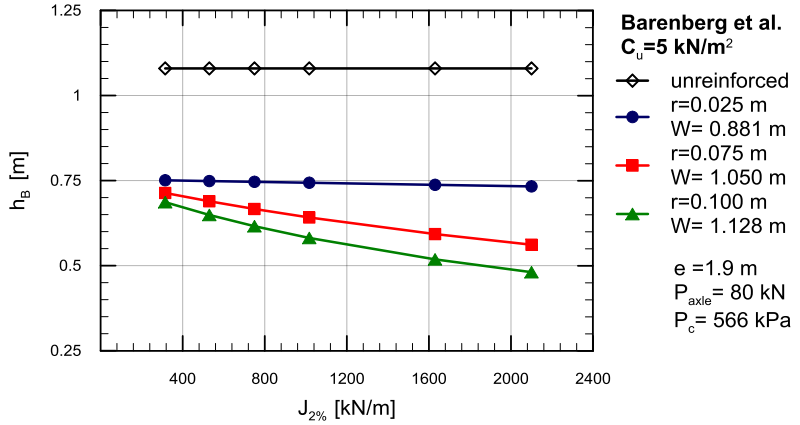

(a)

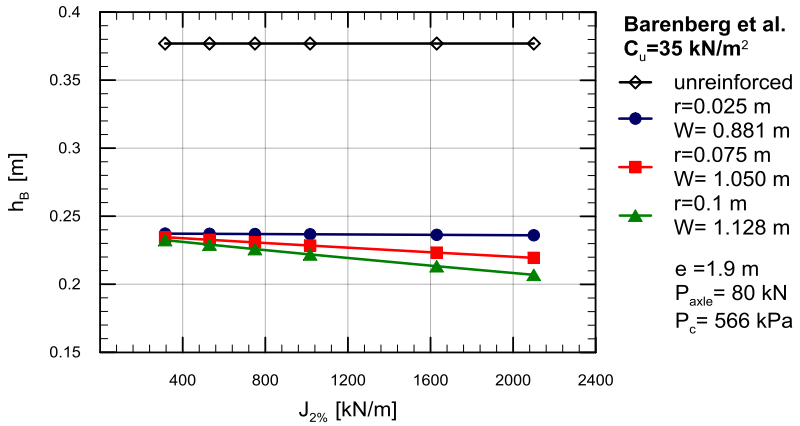

(b)

Figure 4.3 Unpaved roads design procedure by Barenberg et al.: unreinforced and reinforced base aggregate thickness varying the geogrid tensile stiffness, for each allowable rut depth values and for a fixed subgrade undrained shear strength a) Cu=5 kN/m^2; b) Cu=35 kN/m^2.

In addition, the design curves representing the percentage reduction of reinforced base course layer thickness have been plotted varying the geogrid tensile stiffness for each allowable rut depth. It is noteworthy that for the subgrade undrained shear strength minimum value (Cu= 5 kN/m^2) the percentage differences are more evident (Figure 4.4 a) whereas the presence of a stronger subgrade allows to support the vehicular load without the introduction of the reinforcement (i.e., C_u= 35 kN/m^2, see Figure 4.4 b).

It is evident that, at the same design condition (in terms of rutting and subgrade mechanical proprieties), the geogrid membrane support increases proportionally to the geogrids' tensile stiffness. This is confirmed by the improvement offered by the use of stiffer geogrids that lead to larger percentage

reduction of the reinforced base layer thickness with consequent saving of aggregate material needed for the base coarse construction.

Let focus the attention on the curve relating the maximum value of rutting, i.e. r = 0.100m (Figure 4.3a and Figure 4.4b, green line) for which the differences are larger because the rutting is deep enough to let the geogrid reinforcement provide the highest membrane support. It can be noticed that by increasing the geogrids' tensile stiffness from 315 kN/m to 2100 kN/m the base thickness reduces from 0.69 m to 0.48m, which implies a reduction in absolute terms of 0.21m (Figure 4.3a and Table 4.4). Therefore, an improvement is obtained in terms of saving of about 30%. in the aggregate material required for the reinforced base layer construction

In addition, at the same design conditions (in terms of traffic assumptions, subgrade mechanical characteristics, allowable rutting), the efficiency to use a reinforcement with better tensile properties is shown in Figure 4.4 and Table 4.4. Considering the iso-rutting curves relating the maximum allowable rut depth (r = 0.100m, green line in Figure 4.4b) an improvement of performances has been observed by using a stiffer reinforcement (Table 4.4). In particular the percentage reduction of reinforced base aggregate layer thickness varied from 36.42% to 55.47% .

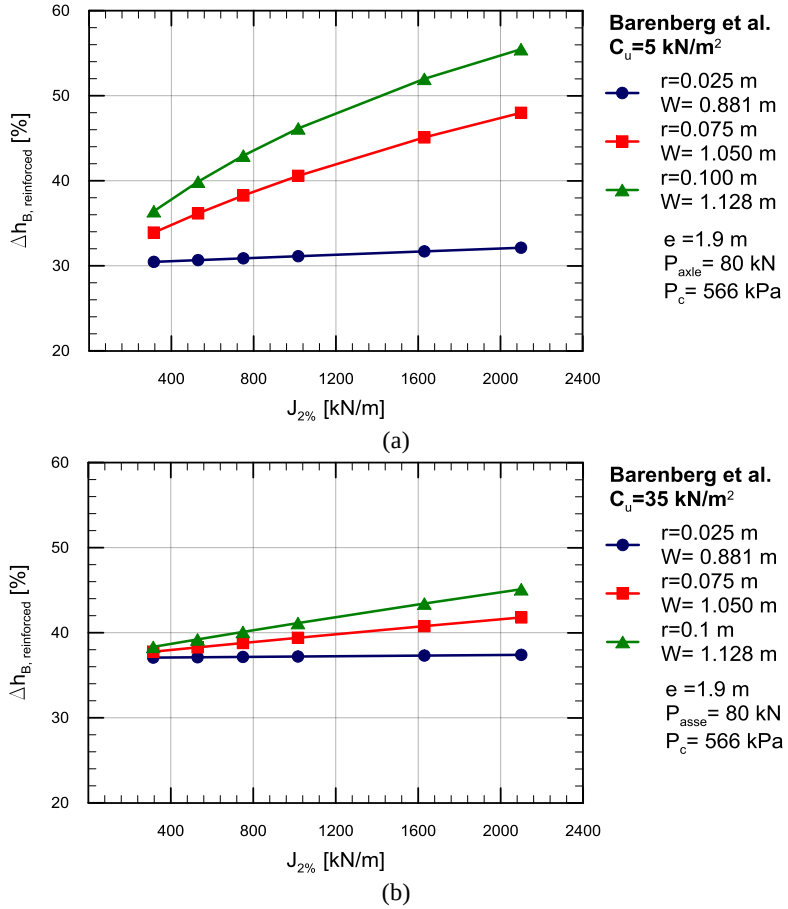

Figure 4.4 Unpaved roads design procedure by Barenberg et al.: percentage reduction of the reinforced base layer thickness varying the geogrid tensile stiffness, for each allowable rut depth values and for a fixed subgrade undrained shear strength a) Cu=5 kN/m^2; b) Cu=35 kN/m^2.

The same analysis has been repeated for Cu= 35 kN/m^2 obtaining the same comparable and negligible reduction of the geogrid reinforced base course layer thickness, both in terms of absolute and percentage reductions (Figure 4.3b, Figure 4.4b and Table 4.4). This result confirms that the reinforcement geogrids tensile stiffness affects the base thickness only if the subgrade is weak enough, in particular for the design conditions proposed in this study (i.e. for Cu < 35 kN/m^2).

Table 4.4 Results of Barenberg et al. unpaved roads design procedure in terms of unreinforced and reinforced base aggregate thickness, reduction and percentage reduction of the reinforced base layer thickness, for extreme values of geogrid tensile stiffness for each and allowable rut depth and for the subgrade undrained shear strength equal to 5 kN/m2 and 35 kN/m2.

Undrained shear strength Cu [kN/m2]	Allowable rut depth r [m]	Tensile stiffness $J_{2\%}$ [kN/m]	$h_{B,UNR}$ [m]	$h_{B,R}$ [m]	$\Delta h_{reinf.}$ [m]	$\Delta h_{reinf.}$ [%]
5	0.025	315	1.08	0.75	0.33	30.46
5	0.025	2100	1.08	0.73	0.35	32.12
5	0.075	315	1.08	0.71	0.37	33.90
5	0.075	2100	1.08	0.56	0.52	47.99
5	0.100	315	1.08	0.69	0.39	36.42
5	0.100	2100	1.08	0.48	0.60	55.47
35	0.025	315	0.38	0.24	0.14	37.07
35	0.025	2100	0.38	0.24	0.14	37.40
35	0.075	315	0.38	0.23	0.14	37.77
35	0.075	2100	0.38	0.22	0.16	41.80
35	0.100	315	0.38	0.23	0.14	38.33
35	0.100	2100	0.38	0.21	0.17	45.11

In a second step, the comparison has been done keeping constant $J_{2\%}$ and analyzing the effect of the rut depth on the design base layer thickness.

Figure 4.5 shows the design curves related to both unreinforced and reinforced base layer thickness varying the allowable rut depth values (from r=0.025 m to r=0.100 m), for each geogrid tensile stiffness (from $J_{2\%}$=315 kN/m to $J_{2\%}$=2100 kN/m) and for fixed Cu=5kN/m^2.

It is evident that, at the same design condition (in terms of geogrid tensile stiffness and subgrade mechanical proprieties), the geogrid offers higher membrane support for larger allowable rut depth. In fact, by increasing the rutting the geosynthetic is more stretched and mobilizes higher tensile stresses, so that the vertical component of this tensile resistance further helps to support the applied wheel loads. In this case the attention should be focused on the design curve corresponding to the stiffest geogrid ($J_{2\%}$= 2100 kN/m, brown line in Figure 4.6) which provides the greatest membrane support and gives the largest differences. As can be observed in Table 4.4, the reinforced base course layer thickness reduces from 0.73m to 0.48m as the rut depth increases from 0.025m to 0.100m, resulting in a base thickness reduction of 0.25m (Figure 4.5 and Table 4.4). This leads to reduce of about the 34% the amount of the aggregate material required to the reinforced base layer construction.

In addition, at the same design conditions, the efficiency to allow deeper rutting is shown in Figure 4.6 and Table 4.4. As it can be observed the stiffest geogrid ($J_{2\%}$ = 2100 kN/m, brown line in Figure 4.6) implies an improvement of performances, in terms of absolute and percentage reductions of reinforced base aggregate layer thickness, from 32.12% to 55.47% by allowing a deeper rut depth (Table 4.4).

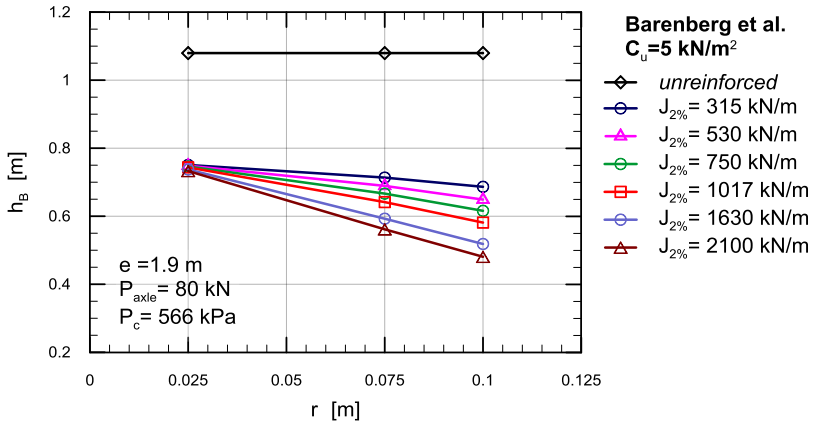

Figure 4.5 Unpaved roads design procedure by Barenberg et al.: unreinforced and reinforced base aggregate thickness varying the allowable rut depth values, for each geogrid tensile stiffness and for a fixed subgrade undrained shear strength equal to 5 kN/m^2

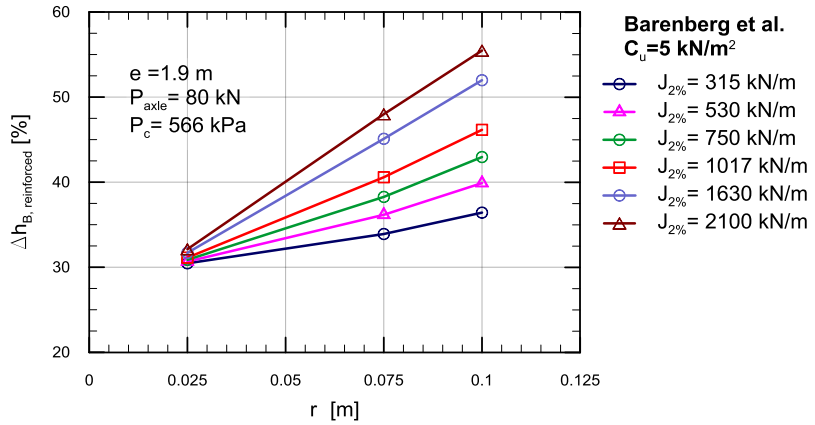

Figure 4.6 Unpaved roads design procedure by Barenberg et al.: percentage reduction of the reinforced base layer thickness varying the allowable rut depth values, for each geogrid tensile stiffness and for a fixed subgrade undrained shear strength equal to 5 kN/m^2

Moreover, the unreinforced base course layer thickness appears to be independent on the rutting. These results highlight that the Barenberg et al. (1975) design procedure does not take into account the mechanical characteristics of the base aggregate course layer, which influence the rut depth magnitude together with the wheel load. This is confirmed by the horizontality of the unreinforced design curve in Figure 4.5 (black line).

Since the variation of the rut depth for fixed subgrade undrained shear strength produces only slightly higher reductions of the reinforced base course layer thickness (34%) than those obtained varying the geogrid tensile stiffness (30%), it could be concluded that the effect of the two design parameters r and J on the Barenberg et al. (1975) model is comparable.

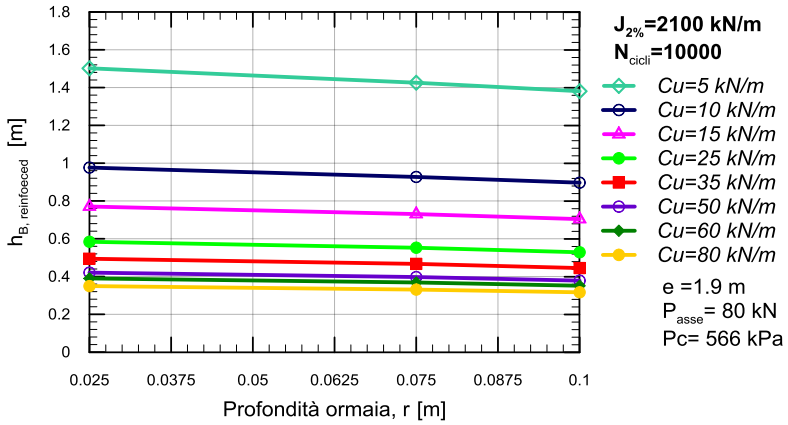

Figure 4.7 Unpaved roads design procedure by Barenberg et al.: unreinforced and reinforced base aggregate thickness varying the allowable rut depth values, for each subgrade undrained shear strength and for a fixed geogrid tensile stiffness equal to 2100 kN/m

Finally, Figure 4.7 and Figure 4.8 plot the unreinforced and reinforced base aggregate thickness as a function of the subgrade undrained shear strength. In Figure 4.7 different values for the allowable rut depth values are considered keeping constant the geogrid tensile stiffness ($J_{2\%}$ = 2100 kN/m). In Figure 4.8 different values for the geogrid tensile stiffness are considered keeping constant the allowable rut depth (r=0.100 m).

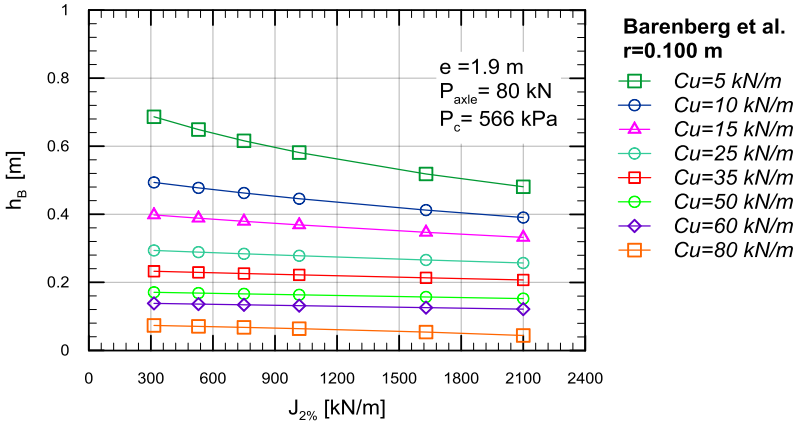

Figure 4.8 Unpaved roads design procedure by Barenberg et al.: unreinforced and reinforced base aggregate thickness varying the geogrid tensile stiffness, for each subgrade undrained shear strength and for a fixed allowable rut depth values equal to 0.100 m

Since the Barenberg et al. (1975) method takes into account the membrane function of reinforcement, the dependency of the required aggregate layer on rut depth and reinforcement tensile modulus are reflected on the results. In particular, the results obtained confirm that reinforcement benefits generally increase with the increasing of the allowable rut depth (Figure 4.7) and with the use of stiffer geogrids (Figure 4.8).

Furthermore, as undrained subgrade shear strength increases, the design base thickness and the effect of the rutting and the benefits offered by reinforcements decrease, as it is confirmed by the horizontality of the design curve in Figure 4.7 and Figure 4.8 for Cu > 35 kN/m^2.

4.3. Unpaved roads design procedure by Giroud and Noiray (1981): analysis of results and discussion

The focus of this section is a parametric analysis of the design curves obtained by Giroud and Noiray (1981) unpaved roads design procedure. The authors, as done by Barenberg et al. (1975), take into account the membrane effect as reinforcement mechanism as well as the limit equilibrium bearing capacity theory, widely discussed in Chapter 3. Since the required thickness of unreinforced and reinforced unpaved roads is a function of traffic loading, subgrade shear strength and geosynthetics properties, the following assumptions have been done: undrained soft saturated clay subgrade; granular base with a CBR ≥80%; pyramidal stress distribution with a fixed stress distribution angle (in order to estimate the vertical stress at the interface base-subgrade); reinforcement well anchored outside the loaded area, in order to avoid slippage, parabolic deformed shape of the reinforcement. So, chosen an allowable rut depth the strain in the reinforcement, and hence the reinforcement tension (tensioned membrane effect), could be calculated. This procedure is also based on limit equilibrium bearing capacity theory with modifications to include the benefit offered by reinforcement, which was taken into account using an enhanced bearing capacity factor. For unreinforced unpaved roads a bearing capacity factor, N_c, equal to 3.14, which is the elastic limit for a saturated undrained subgrade, was proposed. On contrary, for geotextile-reinforced unpaved road, on the assumption that the geotextile provides mainly a separation function, N_c equal to 5.14 was assumed. Finally, for the case of reinforce consisting in a geogrid, which offers improved interface shear resistance due to interlocking, as compared to a geotextile, a bearing capacity factor even more amplified equal to 5.71 was chosen.

Besides, for the Giroud and Noiray (1981) method a parametric analysis of design curves relating to the thickness required for the base layer, both in the unreinforced and reinforced configuration, and the evaluation of the improvement offered by the use of a reinforcement geosynthetic expressed in terms of percentage reductions of the reinforced base layer thickness, compared to the unreinforced one, were performed.

The design parameters (Table 4.5) related to the geosynthetic mechanical properties, the allowable depth ruts and the subgrade mechanical characteristics, are the same considered for the Barenberg et al. (1975) method. For traffic conditions, unlike the Barenberg et al. (1975) theory based on static loading (i.e., up to 100 vehicle passes), the Giroud and Noiray (1981) method takes into account the effect of vehicular load in terms of magnitude (P_{axle}) and number of wheel passes (N_{cycles}). In this analysis N_{cycles} up to a maximum of 10000 vehicle passes have been considered. Additionally, since the geogrid reinforcement improves the load distribution angle more than the geotextile, thanks to geogrid-aggregate interlocking mechanism, Giroud and Noiray (1981) suggested a load distribution improvement ratio ($tan\alpha/tan\alpha_0$) variable between 1.1 and 2.5 (Giroud et al., 1985). This ratio depends on the expected degree of confinement and separation that the geogrid provides to the road layer system. Therefore, this ratio could be considered as a linear function of the tensile load at 2% of deformation

$$tan\alpha/tan\alpha_0 = 1.1 + 0.0005 \cdot J_{2\%} \qquad \text{(Eq. 4.1)}$$

where: tanα is the stress distribution angle in the reinforced base layer; tanαo is the stress distribution angle in the unreinforced base layer that could be considered constant for all unpaved roads constructed with unbound aggregate and equal to 0.6÷0.7.

Table 4.5 Design parameters of Giroud and Noiray (1981) design method

Allowable rut, r [m]	**Geogrid Stiffness, $J_{2\%}$ [kN/m]**	**Undrained shear strength, Cu [kN/m^2]**	**N_{cycles} [-]**
0.025	315	5	100
0.075	530	10	250
0.100	750	15	500
	1017	25	750
	1630	50	1000
	2100	60	5000
		80	7500
			10000

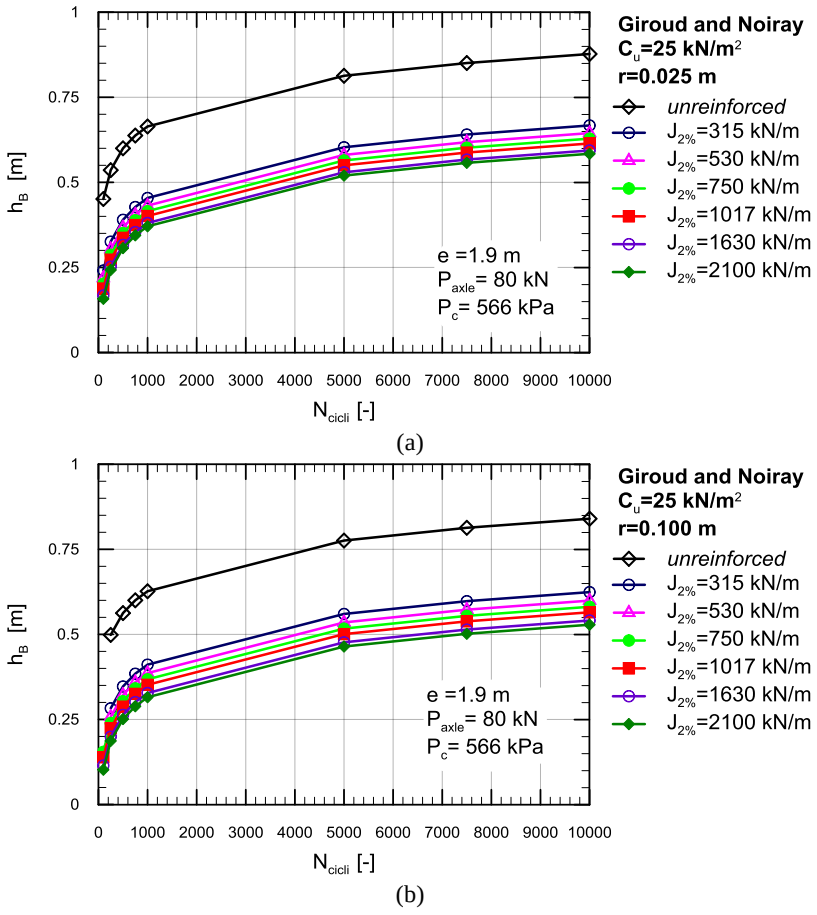

Figure 4.9 Unpaved roads design procedure by Giroud and Noiray: unreinforced and reinforced base aggregate thickness versus number of wheel passes for a fixed value subgrade undrained shear strength (Cu=25 kN/m^2) and for each geogrids chosen, when the allowable rut depth is: a) 0.025 m; b) 0.1 m.

In Figure 4.9 a ÷ Figure 4.9 b are shown the design curves related to the base layer thickness required versus the number of vehicular load cycles (N_{cycles} = from 100 to 10000) and for the extreme values of allowable rut depth (r=0.025m,0.100 m, respectively) for fixed value of the undrained shear strength (Cu= 25 kN/m^2) for both an unreinforced and a reinforced unpaved road section. Each curve is characterized by a different value of the geogrid tensile modulus (i.e. $J_{2\%}$ varying from 315 to 2100 kN/m).

Since the Giroud and Noiray (1981) method considers the effect of traffic conditions, it can be seen how both the unreinforced and reinforced base layer thickness, at the same subgrade mechanical characteristics and for each allowable rut assumed, increases as the number of wheel load cycles (N_{cycles} = 100 ÷ 10000) increases and the geogrid mechanical proprieties decrease.

It is evident that the base thickness rate growth is more pronounced in the first load cycles ($N_{cycles} \leq$ 1000) and settles back down after a number of repetitions beyond a certain threshold (e.g. $N_{cycles} \geq 5000$). This might be explained considering that for too large base thickness (obtained for a higher number of wheel repetitions) the repeated loads on the road surface do not lead to the subgrade limit pressure, so that further load cycles are uninfluential on the response of the road unpaved structure.

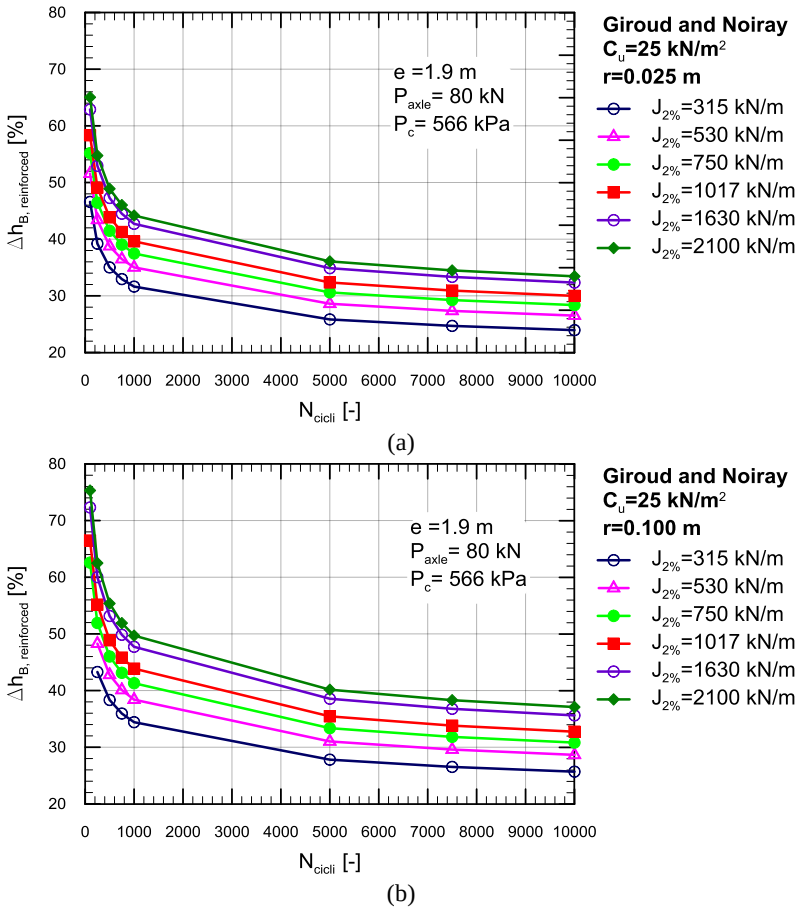

Figure 4.10 Unpaved roads design procedure by Giroud and Noiray (1981): percentage reduction of base aggregate thickness versus number of wheel passes for a fixed value subgrade undrained shear strength (Cu=25 kN/m^2) and for each geogrids chosen, when the allowable rut depth is: a) 0.25 m; b) 0.1m;.

Moreover, all depth values of rutting (r = 0.025 m ÷ 0.100 m) are large enough to let the geosynthetic layer work providing a reinforcement support proportionally to its own mechanical

characteristic (Figure 4.9 a ÷ Figure 4.9 b). Then, by increasing the rut depth, the membrane mechanism that requires the achievement of higher values of geosynthetic deformation could be activated.

In addition, the design curves for each geogrids with different tensile stiffness appear to be clear and distinct. In other words, at the same design conditions it can be observed the decrease of the reinforced base thickness with the increase of the geogrids' mechanical properties with consequent saving of aggregate material needed for its construction.

Figure 4.10 a and Figure 4.10 b show the improvement offered by the reinforcement, in terms of percentage reduction of the reinforced base layer thickness in comparison with the thickness required when the base layer is unreinforced. The results, Moreover, confirm that higher efficiency is reached when the reinforcement, placed at based-substrate interface, has higher mechanical proprieties. Consequently, the related benefits consist in saving of aggregate material needed for the base layer construction. From a more careful analysis based on the comparison between the graphics of Figure 4.10 a and Figure 4.10 b it can be observed that the percentage reduction of the reinforced base layer thickness increase with the increase of the allowable rut. This behavior could be explained considering that the more the rutting increases the more the geosynthetic deforms the greater is the membrane support offered.

Some of these results are summarized in Table 4.6

Table 4.6 Results of Giroud and Noiray (1981) unpaved roads design procedure in terms of: unreinforced and reinforced base aggregate thickness and percentage reduction of the reinforced base layer thickness, when the subgrade undrained shear strength is equal to 25 kN/m^2 and varying the number of wheel passes. The limit values of allowable rut depth and the geogrids' tensile stiffness were selected.

N_{cycles} [-]	C_u [kN/m^2]	r [m]	$J_{2\%}$ [kN/m]	$h_{B,UNR}$ [m]	$h_{B,R}$ [m]	$\Delta h_{reinf.}$ [%]
100	25	0.025	315	0.45	0.24	46.58
100	25	0.025	2100	0.45	0.16	65.05
100	25	0.100	315	0.41	0.20	52.15
100	25	0.100	2100	0.41	0.10	75.31
1000	25	0.025	315	0.66	0.45	31.63
1000	25	0.025	2100	0.66	0.37	44.17
1000	25	0.100	315	0.63	0.41	34.42
1000	25	0.100	2100	0.63	0.32	49.70
10000	25	0.025	315	0.88	0.67	23.95
10000	25	0.025	2100	0.88	0.58	33.44
10000	25	0.100	315	0.84	0.62	25.68
10000	25	0.100	2100	0.84	0.53	37.09

At the same value of rut depth (r = 0.075m), Figure 4.11 a ÷ Figure 4.11 c show the design curves related to the thickness of the base layer, reinforced and not, for different values of vehicular load cycles (N_{cycles} = from 100 to 10000) and for each type of geogrid characterized by increasing values of the tensile modulus ($J_{2\%}$ = 315 ÷ 2100 kN / m).

Figure 4.11 a ÷ Figure 4.11 c, respectively, refer to a subgrade undrained shear strength equal to 5, 35 and 80 kN/m^2.

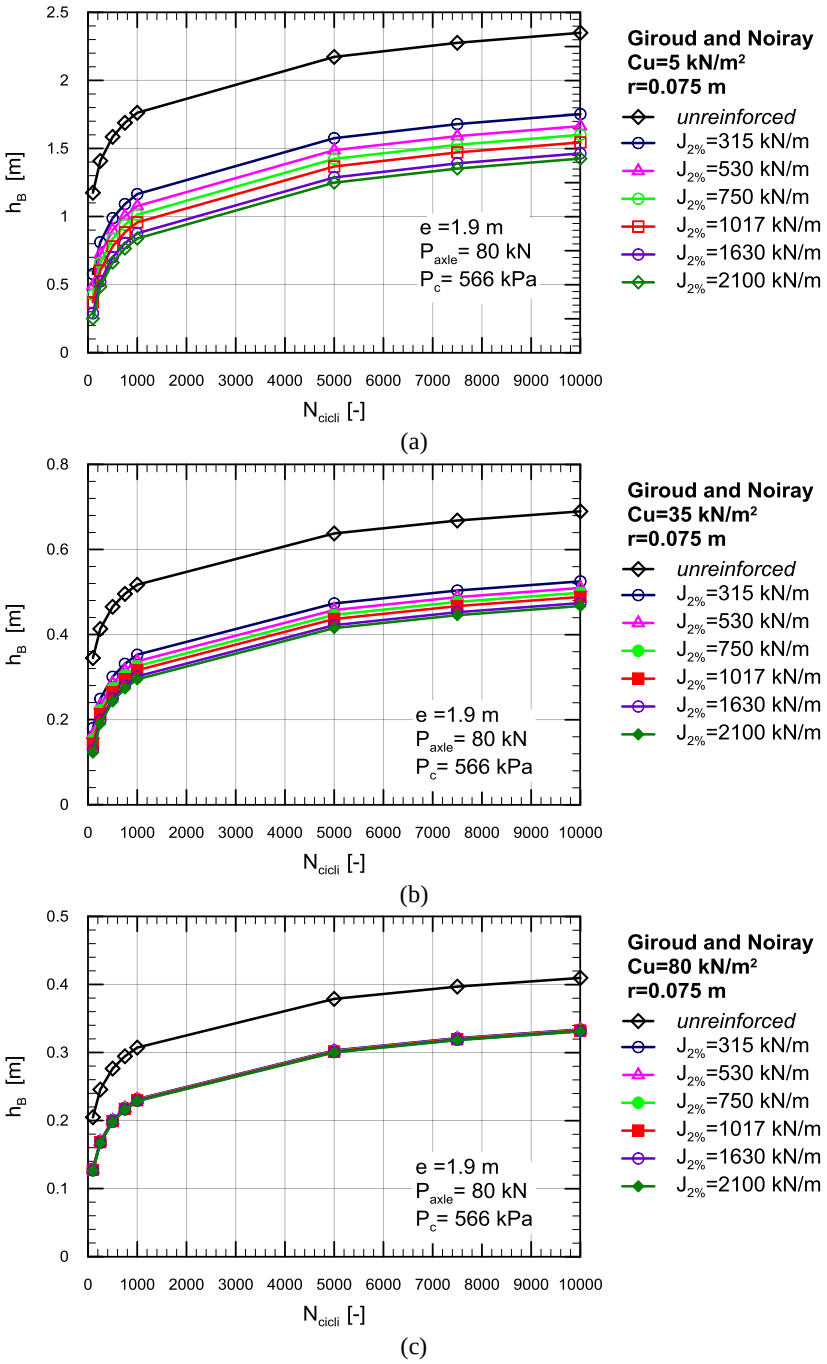

Figure 4.11 Unpaved roads design procedure by Giroud and Noiray (1981) : unreinforced and reinforced base aggregate thickness versus number of wheel passes for a fixed value of the allowable rut depth and for each geogrids chosen, when the subgrade undrained shear strength is: a) Cu=5 kN/m^2; b) Cu=35 kN/m^2; c) Cu=80 kN/m^2.

Table 4.7 summarizes the unreinforced and reinforced base aggregate thickness and percentage reduction of the reinforced base layer thickness at the same value of allowable rut depth (i.e. r = 0.075 m) for different values of wheel passes and subgrade undrained shear strength, considering for the geogrids' tensile stiffness the limit values.

As expected, the decrease of the unreinforced and reinforced base thickness with the increasing of the subgrade bearing capacity is observed. Moreover, the improvement offered by the use of a

reinforcement geogrid with greater mechanical properties becomes negligible as the subgrade undrained shear strength increases. This result is confirmed by the design curves for each geogrid type that are closer to each other and almost overlap with the increasing of Cu. This result can be explained considering that if the subgrade is strong enough it can support the traffic load reduction as well as the geogrid, which use become useless in this case.

Table 4.7 Results of Giroud and Noiray (1981) unpaved roads design procedure in terms of: unreinforced and reinforced base aggregate thickness and percentage reduction of the reinforced base layer thickness, at the same values of allowable rut depth equal to 0.075 m, varying the number of wheel passes and the subgrade undrained shear strength. The limit values of geogrids' tensile stiffness the were selected.

N_{cycles} [-]	C_u [kN/m^2]	r [m]	$J_{2\%}$ [kN/m]	$h_{B,UNR}$ [m]	$h_{B,R}$ [m]	$\Delta h_{reinf.}$ [%]
100	5	0.075	315	1.17	0.58	50.85
1000	5	0.075	315	1.76	1.16	33.90
10000	5	0.075	315	2.35	1.75	25.42
100	5	0.075	2100	1.17	0.25	78.66
1000	5	0.075	2100	1.76	0.84	52.43
10000	5	0.075	2100	2.35	1.43	39.32
100	35	0.075	315	0.34	0.18	47.74
1000	35	0.075	315	0.52	0.35	31.82
10000	35	0.075	315	0.69	0.52	23.86
100	35	0.075	2100	0.34	0.12	64.56
1000	35	0.075	2100	0.52	0.29	43.04
10000	35	0.075	2100	0.69	0.47	32.28
100	80	0.075	315	0.20	0.13	36.99
1000	80	0.075	315	0.31	0.23	24.65
10000	80	0.075	315	0.41	0.33	18.49
100	80	0.075	2100	0.20	0.13	38.42
1000	80	0.075	2100	0.31	0.23	25.61
10000	80	0.075	2100	0.41	0.33	19.21

Furthermore, a more careful analysis of the previous base thickness design curves, reinforced and unreinforced, leads to confirm the following considerations.

At the same design conditions (in terms of traffic conditions, rutting and subgrade mechanical characteristics) greater efficiency is observed in terms of percentage reduction of reinforced base aggregate layer thickness if the reinforcement placed at the base-subgrade interface is stiffer. The improvements are shown to be proportional to the mechanical properties of the reinforce. In particular, the above percentage reductions are the greatest if the subgrade is the weakest. It is precisely in this case that the use of a reinforcement geosynthetic is required so to let the base layer better distribute the vehicular load on the subgrade compatibly with its limit bearing capacity.

On contrary, if the subgrade is characterized by the highest mechanical characteristics (Cu =80 kN/m^2) the use of a geogrid is unnecessary, according to AASHTO design guidelines, because the subgrade is stiff enough as confirmed by the overlapping of the reinforced base thickness curves.

The above considerations on the effect of the mechanical characteristic of the subgrade on the Giroud and Noiray (1981) unpaved roads design procedure is further corroborated by the results shown in Figure 4.12 a ÷ Figure 4.12 b, which report the design curves related to the reinforced and unreinforced base course layer thickness versus the subgrade undrained shear strength (Cu= 5 ÷ 80 kN/m^2), at the same traffic conditions (i.e., N_{cycles}=10000) and for extreme rut depth value (r = 0.025m and 0.100m). Each curve is reeferred to a geogrid with different tensile stiffness ($J_{2\%}$= 315 ÷2100 kN/m).

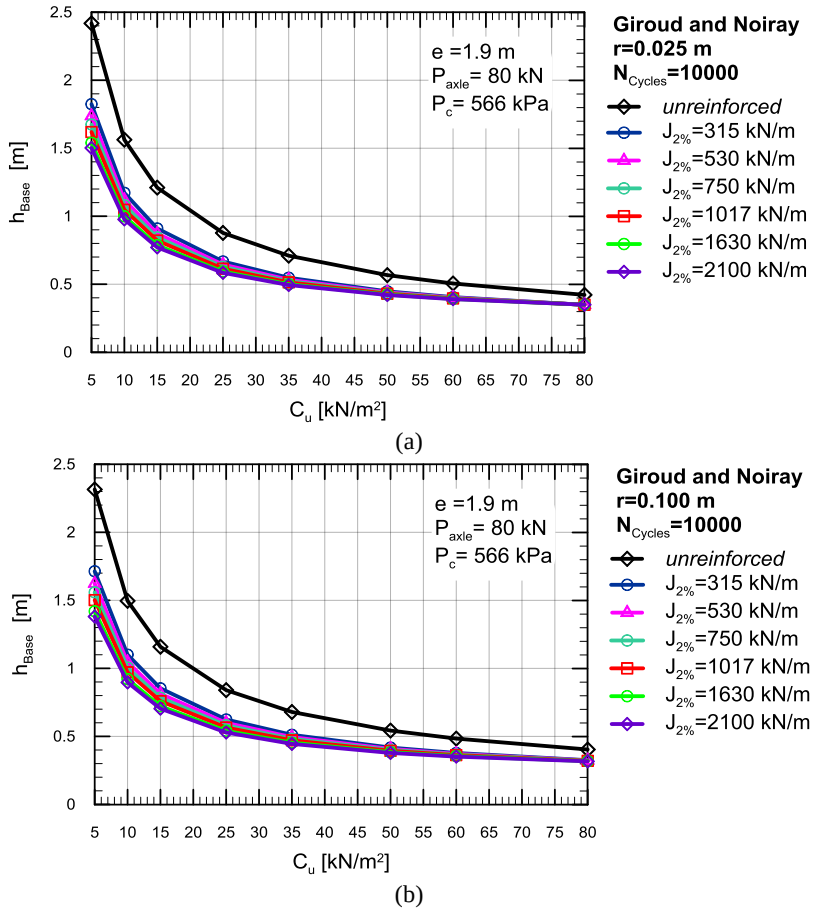

Figure 4.12 Unpaved roads design procedure by Giroud and Noiray (1981) : unreinforced and reinforced base aggregate thickness versus subgrade undrained shear strength, at the same traffic conditions (Ncycles=10000), for each geogrids chosen and for extremal allowable rut depth values: a) r= 0.025m; b) 0.100m.

Therefore, as expected, the reinforced and unreinforced base layer thickness decreases as the subgrade undrained shear strength increases.

All allowable rut depth values (Figure 4.12 a and Figure 4.12 b) are large enough to let the geosynthetic support the vertical pressure due to the vehicular traffic proportionally to its tensile stiffness. In fact, the design curves for different values of tensile strength appear clearly distinguished between each other. In addition, the geogrid stiffness, for Cu> 50 kN/m^2, has no effect on the reinforced base course layer thickness since the reinforcement contribution, regardless of the reinforcement stiffness, decreases with the

increasing of the mechanical characteristics of the subgrade, which results to be able to carry the vehicular traffic load independently.

By a careful analysis of these figures it can be highlighted that the unreinforced base course layer thickness is affected by the rutting for given traffic conditions and subgrade mechanical properties, contrary to the Barenberg et al. (1975) method. These results highlight that the Giroud and Noiray (1981) design procedure takes intrinsically into account the mechanic characteristics of base aggregate course, which influence the rut depth magnitude together with the wheel load. On the other hand, in the reinforced configurations, larger allowed rut depth leads to more mobilized membrane effect.

Table 4.8 Results of Giroud and Noiray (1981) unpaved roads design procedure in terms of unreinforced and reinforced base aggregate thickness, absolute reduction and percentage reduction of the reinforced base layer thickness, at the same traffic conditions (Ncycles=10000), for extreme values of geogrid tensile stiffness and allowable rut depth and varying the subgrade undrained shear strength

N_{cycles} [-]	Undrained shear strength Cu [kN/m2]	Allowable rut depth r [m]	Tensile stiffness $J_{2\%}$ [kN/m]	$h_{B,UNR}$ [m]	$h_{B,R}$ [m]	$\Delta h_{reinf.}$ [m]	$\Delta h_{reinf.}$ [%]
10000	5	0.025	315	2.42	1.82	0.59	24.57
10000	5	0.025	2100	2.42	1.50	0.92	37.89
10000	25	0.025	315	0.88	0.67	0.21	23.95
10000	25	0.025	2100	0.88	0.58	0.29	33.44
10000	50	0.025	315	0.57	0.45	0.12	21.03
10000	50	0.025	2100	0.57	0.42	0.15	25.79
10000	80	0.025	315	0.42	0.35	0.07	17.39
10000	80	0.025	2100	0.42	0.35	0.07	17.08
10000	5	0.100	315	2.32	1.71	0.60	25.99
10000	5	0.100	2100	2.32	1.38	0.93	40.36
10000	25	0.100	315	0.84	0.62	0.22	25.68
10000	25	0.100	2100	0.84	0.53	0.31	37.09
10000	50	0.100	315	0.54	0.42	0.12	23.02
10000	50	0.100	2100	0.54	0.38	0.16	30.29
10000	80	0.100	315	0.40	0.33	0.08	19.45
10000	80	0.100	2100	0.40	0.32	0.09	21.56

To confirm what previously discussed, in Table 4.8 are summarized some results of the simulations in terms of unreinforced and reinforced base aggregate thickness ($h_{B,UNR}$ and $h_{B,R}$, respectively) and in terms of percentage reduction of the reinforced base layer thickness, for extreme values of subgrade undrained shear strength, geogrid tensile stiffness and allowable rut depth.

In addition, Figure 4.13 a and Figure 4.13 b show, for both reinforced and unreinforced case, the base course layer thickness design curves varying the subgrade undrained shear strength (Cu= 5 ÷ 80

kN/m^2) for each allowable rut depth values (r=0.025m, 0.075m, 0.100m), considering the extremal values of the geogrid tensile stiffness ($J_{2\%}$ = 315 kN/m and $J_{2\%}$ = 2100 kN/m, respectively).

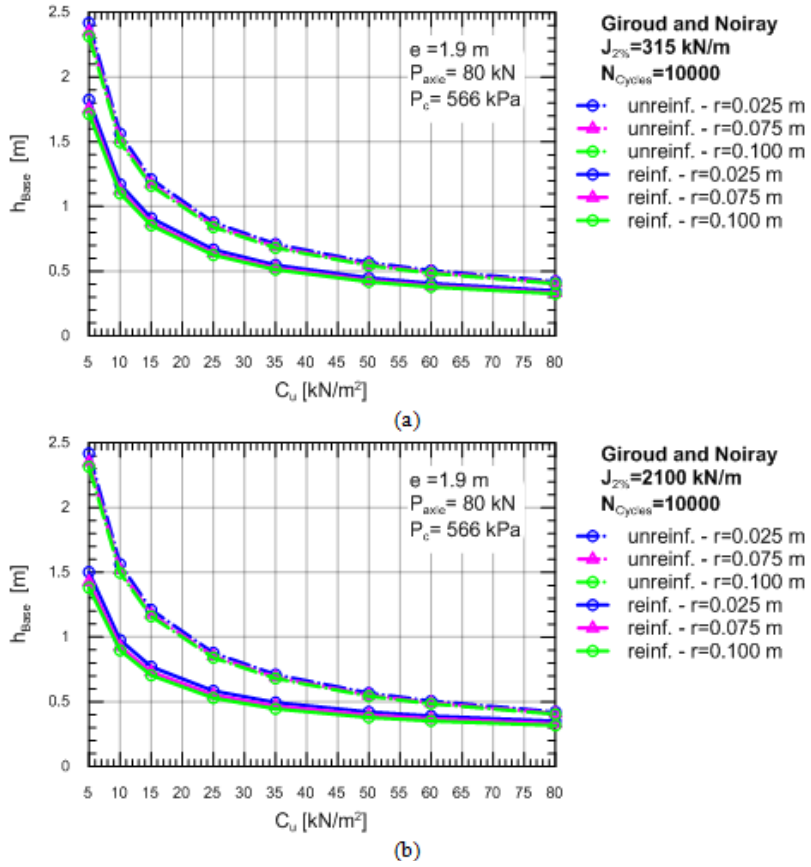

Figure 4.13 Unpaved roads design procedure by Giroud and Noiray (1981) : unreinforced and reinforced base aggregate thickness varying the subgrade undrained shear strength, for each allowable rut depth values and for a fixed geogrid tensile stiffness a) $J_{2\%}$=315 kN/m; b) $J_{2\%}$=2100 kN/m.

Given the reduction of the required thickness with the increasing of the subgrade undrained shear strength, comparing the results obtained for the geogrid tensile stiffness limit values, i.e. 315 and 2100 kN/m, some considerations could be drawn:

- the base course layer thickness is not affected by the rut depth in the examined range when the geogrid reinforcement is characterized by the minimum tensile stiffness (e.g., $J_{2\%}$ =315 kN/m). To explain this behavior it should be taken in mind that if the geogrid is characterized by low values of tensile stiffness (i.e., $J_{2\%}$= 315 kN/m) it is not able to offer an efficient support, as it is confirmed by the results reported in Table 4.9;
- when the geogrid placed at the base-subgrade interface has higher mechanical characteristics (e.g., $J_{2\%}$=2100 kN/m), small allowable rut depth are enough to let the geosynthetic support the vertical pressure due to the vehicular traffic. In other words, thanks to its large tensile stiffness, the geogrid reinforcement develops tensile tensions larger than the ones previously observed (i.e. for J=315 kN/m), which increase proportionally to the assumed rutting. Therefore, the design curves for each allowable rutting appear to be clear and distinct, highlighting the influence of the parameter on the Giroud and Noiray (1981) method, as confirmed by the results presented in Table 4.9;

- in addition, at the same design conditions (in terms of geogrid tensile stiffness and subgrade mechanical proprieties), the increasing of the allowable rut depth produces a slight improvement in terms of percentage reduction of the reinforced base layer thickness, $\Delta h_{B,R}$ [%], (see Table 4.9), with consequent negligible saving of aggregate material needed for its construction.

Table 4.9 Results of Giroud and Noiray (1981) et al. unpaved roads design procedure in terms of unreinforced and reinforced base aggregate thickness, absolute and percentage reduction of the reinforced base layer thickness , at the same traffic conditions (Ncycles=10000), for extremal values of geogrid tensile stiffness and varying the subgrade undrained shear strength and allowable rut depth.

N_{cycles} [-]	Undrained shear strength Cu [kN/m2]	Allowable rut depth r [m]	Tensile stiffness $J_{2\%}$ [kN/m]	$h_{B,UNR}$ [m]	$h_{B,R}$ [m]	$\Delta h_{reinf.}$ [m]	$\Delta h_{reinf.}$ [%]
10000	5	0.025	315	2.42	1.82	0.59	24.57
10000	5	0.075	315	2.35	1.75	0.60	25.42
10000	5	0.100	315	2.32	1.71	0.60	25.99
10000	25	0.025	315	0.88	0.67	0.21	23.95
10000	25	0.075	315	0.85	0.64	0.21	24.93
10000	25	0.100	315	0.84	0.62	0.22	25.68
10000	60	0.025	315	0.51	0.41	0.10	19.81
10000	60	0.075	315	0.49	0.39	0.10	20.91
10000	60	0.100	315	0.48	0.38	0.11	21.85
10000	5	0.025	2100	2.42	1.50	0.92	37.89
10000	5	0.075	2100	2.35	1.43	0.92	39.32
10000	5	0.100	2100	2.32	1.38	0.93	40.36
10000	25	0.025	2100	0.88	0.58	0.29	33.44
10000	25	0.075	2100	0.85	0.55	0.30	35.19
10000	25	0.100	2100	0.84	0.53	0.31	37.09
10000	80	0.025	2100	0.42	0.35	0.07	17.08
10000	80	0.075	2100	0.41	0.33	0.08	19.21
10000	80	0.100	2100	0.40	0.32	0.09	21.56

To better analyze the different effect caused by the allowable rutting, r, and by the geogrid tensile stiffness J_2%, on the Giroud and Noiray (1981) method, the results obtained have been plotted for fixed subgrade mechanic characteristics.

In particular to evaluate the sensitivity (or weight) of r and $J_{2\%}$, on the design procedure the effect of the two variables has been studied individually.

First, the effect of the variable $J_{2\%}$ was analyzed. Figure 4.14 a÷ s Figure 4.14 b show the design curves related to both unreinforced and reinforced base layer thickness varying the geogrid tensile stiffness ($J_{2\%}$ from 315 kN/m to 2100 kN/m) for three different allowable rut depth values (r=0.025m, 0.075m, 0.100 m) keeping constant the subgrade undrained shear strength. Specifically, two Cu values equal to 5 and 60

kN/m^2 have been chosen, since the reinforcement does not offer better performance if the subgrade is strong (i.e. Cu>50 kN/m2, as previously seen).

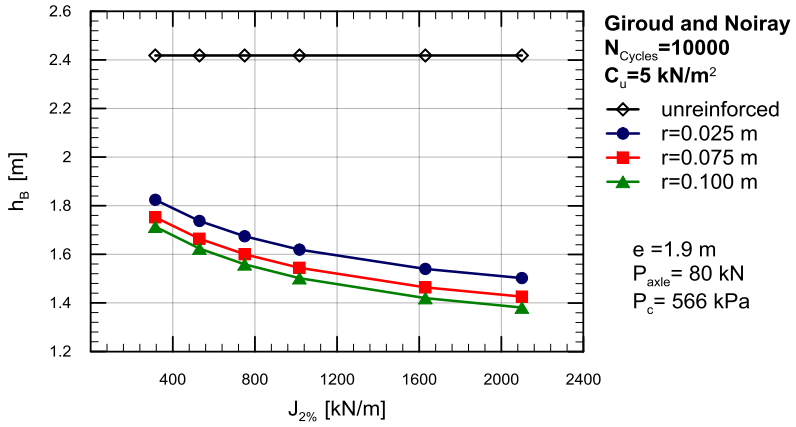

(a)

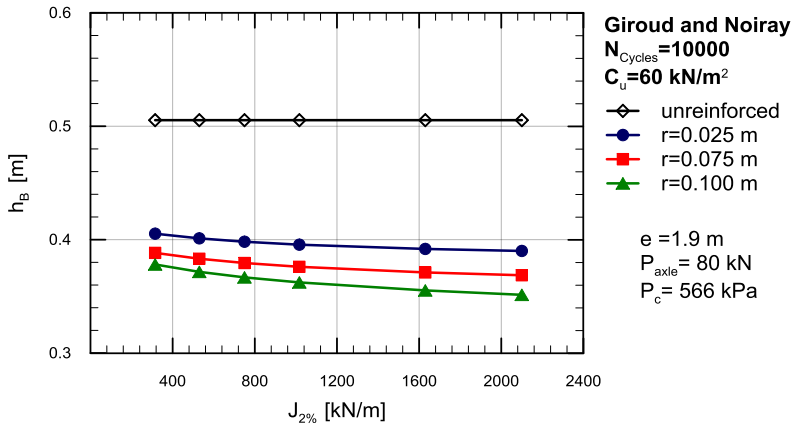

(b)

Figure 4.14 Unpaved roads design procedure by Giroud and Noiray (1981) unreinforced and reinforced base aggregate thickness varying the geogrid tensile stiffness, at the same traffic conditions (N_{cycles}=10000), for each allowable rut depth values and for a fixed subgrade undrained shear strength a) Cu=5 kN/m^2; b) Cu=60 kN/m^2.

In addition, the design curves representing the percentage reduction of reinforced base course layer thickness have been plotted considering the minimum value of the subgrade undrained shear strength (Cu= 5 kN/m^2), for which the percentage differences are more evident (Figure 4.15 a), and the subgrade undrained shear strength equal to 60 kN/m^2, which corresponds to a stronger subgrade which is able to support alone the vehicular load (see Figure 4.15 b).

It is evident that, at the same design condition (in terms of rutting and subgrade mechanical proprieties), the geogrid membrane support increases proportionally to the geogrids' tensile stiffness. This is confirmed by the improvement offered by the use of stiffer geogrids that lead to larger percentage reduction of the reinforced base layer thickness with consequent saving of aggregate material needed for the base coarse construction.

Let focus the attention on the curve relating the maximum value of rutting, i.e. r = 0.100m (Figure 4.14 a and Figure 4.15 a, green line) for which the differences are larger because the rutting is deep enough

to let the geogrid reinforcement provide the highest membrane support. It can be noticed that by increasing the geogrids' tensile stiffness from 315 kN/m to 2100 kN/m the base thickness reduces 1.71 m to 1.38 m, which implies a reduction in absolute terms of 0.21m (Figure 4.14 a and Table 4.10). Therefore, an improvement is obtained in terms of saving of about 19% in the aggregate material required for the reinforced base layer construction (Figure 4.15 a and Table 4.10).

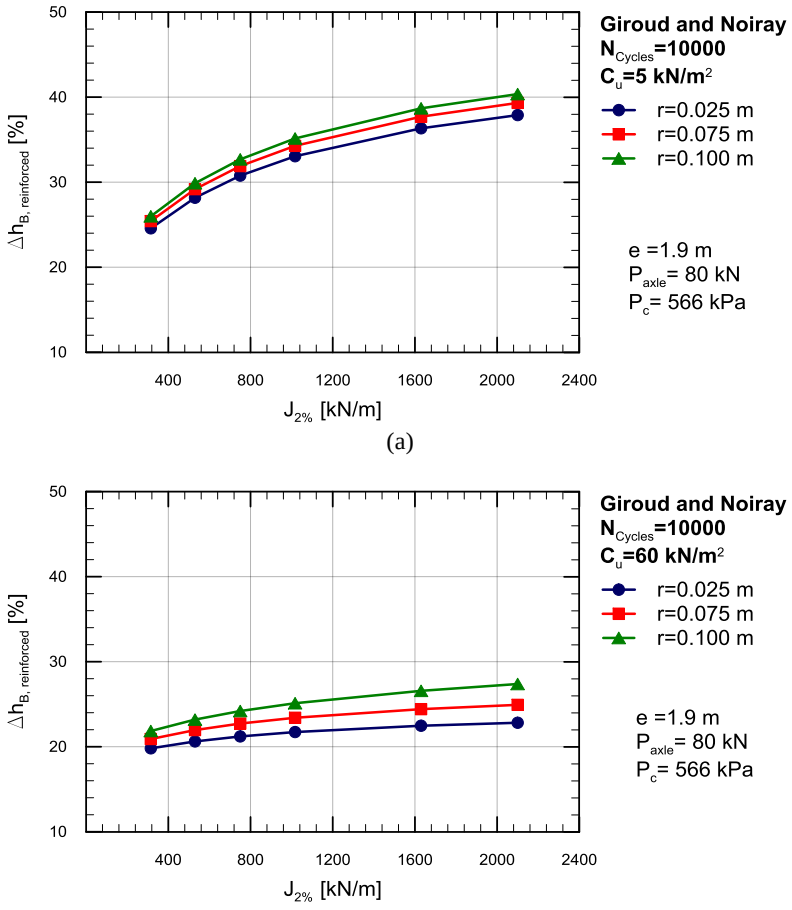

Figure 4.15 Unpaved roads design procedure by Giroud and Noiray (1981) percentage reduction of reinforced base aggregate thickness varying the geogrid tensile stiffness, at the same traffic conditions (N_{cycles}=10000), for each allowable rut depth values and for a fixed subgrade undrained shear strength a) Cu=5 kN/m^2; b)) Cu=60 kN/m^2.

In addition, at the same design conditions (in terms of traffic assumptions, subgrade mechanical characteristics, allowable rutting), the efficiency to use a reinforcement with better tensile properties is shown in Figure 4.15 a and Table 4.10. Once again, considering the iso-rutting curves relating the maximum allowable rut depth (r = 0.100m, green line in Figure 4.15a) an improvement of performances has been observed by using a stiffer reinforcement (Table 4.10). In particular the percentage reduction of reinforced base aggregate layer thickness varied from 36.42% to 55.47% as observed in Table 4.10.

The same analysis has been repeated for Cu = 60 kN/m^2 obtaining the same comparable and negligible reduction of the geogrid reinforced base course layer thickness, both in terms of absolute and percentage reductions (Figure 4.14 b, Figure 4.15 b and Table 4.10).

This result confirms that the use of reinforcement geogrids is justified only if the subgrade is enough weak. In particular at the design conditions propose in this study for Cu < 50 kN/m^2.

In a second step, the comparison has been done keeping constant $J_{2\%}$ and analyzing the effect of the rut depth on the design base layer thickness.

Figure 4.16 shows the design curves related to both unreinforced and reinforced base layer thickness varying the allowable rut depth values (from r=0.025 m to r=0.100 m), for each geogrid tensile stiffness (from $J_{2\%}$=315 kN/m to $J_{2\%}$=2100 kN/m) and for a weak subgrade (i.e. Cu=5kN/m^2), which lead to the greatest differences.

It is evident that, at the same design conditions (in terms of geogrid tensile stiffness and subgrade mechanical proprieties), the geogrid offers higher membrane support for larger allowable rut depth. In fact, by increasing the rutting the geosynthetic is more stretched and mobilizes higher tensile stresses, so that the vertical component of this tensile resistance further helps to support the applied wheel loads.

Table 4.10 Results of Giroud and Noiray (1981) unpaved roads design procedure in terms of unreinforced and reinforced base aggregate thickness, reduction and percentage reduction of the reinforced base layer thickness, at the same traffic conditions (N_{cycles}=10000), for extreme values of geogrid tensile stiffness for each and allowable rut depth and for the subgrade undrained shear strength equal to 5 kN/m^2 and 60 kN/m^2.

N_{cycles} [-]	Undrained shear strength Cu [kN/m2]	Allowable rut depth r [m]	Tensile stiffness $J_{2\%}$ [kN/m]	$h_{B,UNR}$ [m]	$h_{B,R}$ [m]	$\Delta h_{reinf.}$ [m]	$\Delta h_{reinf.}$ [%]
10000	5	0.025	315	2.42	1.82	0.59	24.57
10000	5	0.025	2100	2.42	1.50	0.92	37.89
10000	5	0.075	315	2.35	1.75	0.60	25.42
10000	5	0.075	2100	2.35	1.43	0.92	39.32
10000	5	0.100	315	2.32	1.71	0.60	25.99
10000	5	0.100	2100	2.32	1.38	0.93	40.36
10000	60	0.025	315	0.51	0.41	0.10	19.81
10000	60	0.025	2100	0.51	0.39	0.12	22.82
10000	60	0.075	315	0.49	0.39	0.10	20.91
10000	60	0.075	2100	0.49	0.37	0.12	24.92
10000	60	0.100	315	0.48	0.38	0.11	21.85
10000	60	0.100	2100	0.48	0.35	0.13	27.38

In this case the attention should be focused on the design curve corresponding to the stiffest geogrid ($J_{2\%}$= 2100 kN/m, brown line in Figure 4.17) which provides the greatest membrane support and gives the largest differences. As can be observed in Table 4.10, the reinforced base course layer thickness reduces from 1.50 m to 1.38 m as the rut depth increases from 0.025m to 0.100m, resulting in a base thickness reduction of 0.12m (brown line in Figure 4.16 and Table 4.10). This leads to reduce of about the 8% only the amount of the aggregate material required to the reinforced base layer construction. Moreover, the unreinforced base course layer thickness appeared to be dependent on the rutting. These results

highlight that this design procedure takes into account the mechanical characteristics of the base aggregate course, which influence the rut depth magnitude together with the wheel load.

In addition, at the same design conditions (in terms of traffic assumptions, subgrade mechanical characteristics, geogrid tensile stiffness), the efficiency to allow deeper rutting is shown in Figure 4.17 and Table 410. As it can be observed the stiffest geogrid ($J_{2\%}$ = 2100 kN/m, brown line in Figure 4.17) implies an improvement of performances, in terms of percentage reductions of reinforced base aggregate layer thickness, which slightly increase from 37.89% to 40.36% by allowing a deeper rut depth (Figure 4.17 and Table 4.10).

Eventually, in the Giroud and Noiray (1981) design procedure the variation of the rut depth for the weakest subgrade undrained shear strength produces improvement (8%) only slightly higher than those obtained varying the geogrid tensile stiffness (19%), highlighting that the geogrid tensile properties affect this design procedure more than the allowable rut depth.

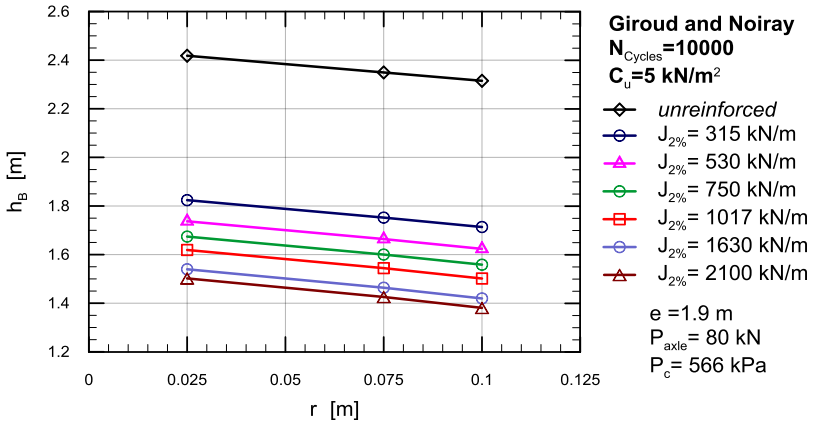

Figure 4.16 Unpaved roads design procedure by Giroud and Noiray (1981) : unreinforced and reinforced base aggregate thickness varying the allowable rut depth values, at the same traffic conditions (N_{cycles}=10000),for each geogrid tensile stiffness and for a fixed subgrade undrained shear strength equal to 5 kN/m^2

Finally, Figure 4.18 and Figure 4.19 plot the unreinforced and reinforced base aggregate thickness as a function of the subgrade undrained shear strength. In Figure 4.18 different values for the allowable rut depth values are considered keeping constant the geogrid tensile stiffness ($J_{2\%}$ = 2100 kN/m). In Figure 4.19 different values for the geogrid tensile stiffness are considered keeping constant the allowable rut depth (r=0.100 m).

Since the Giroud and Noiray (1981) method takes into account the membrane function of the reinforcement, the dependency of the required aggregate layer on the rut depth and reinforcement tensile modulus are reflected on the results. In particular, the reinforcement benefits generally increase as the allowable rut depth increases (Figure 4.18) and with the use of stiffer geogrids (Figure 4.19).

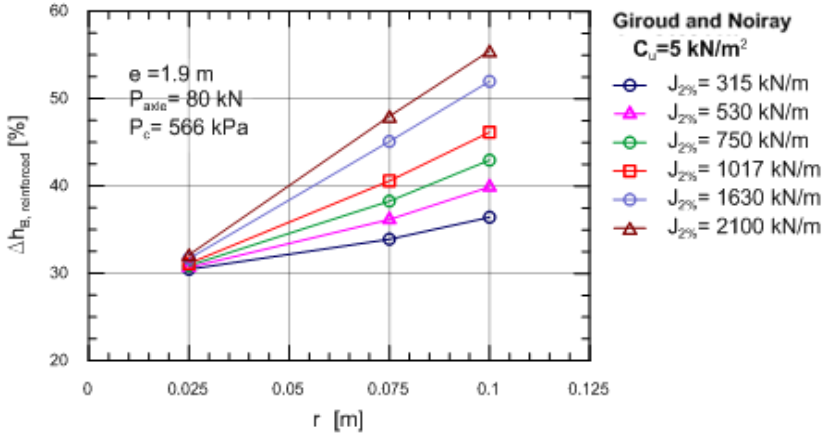

Figure 4.17 Unpaved roads design procedure by Giroud and Noiray (1981): percentage reduction of the reinforced base layer thickness varying the allowable rut depth values, at the same traffic conditions (N_{cycles}=10000), for each geogrid tensile stiffness and for a fixed subgrade undrained shear strength equal to 5 kN/m^2

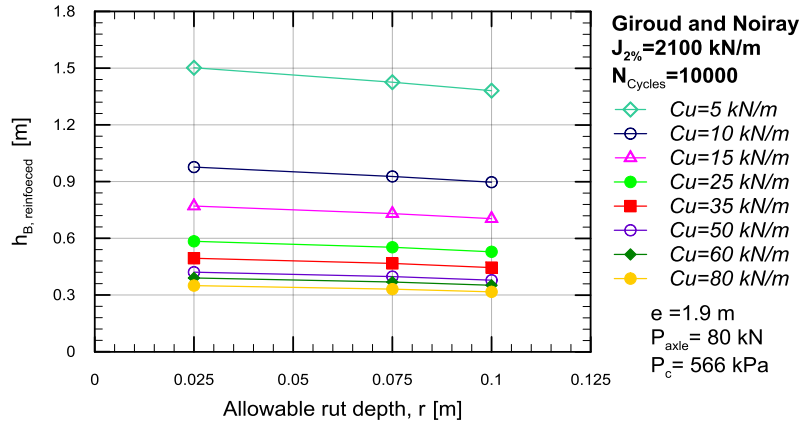

Figure 4.18 Unpaved roads design procedure Giroud and Noiray (1981): unreinforced and reinforced base aggregate thickness varying the allowable rut depth values, at the same traffic conditions (N_{cycles}=10000), for each subgrade undrained shear strength and for a fixed geogrid tensile stiffness equal to 2100 kN/m

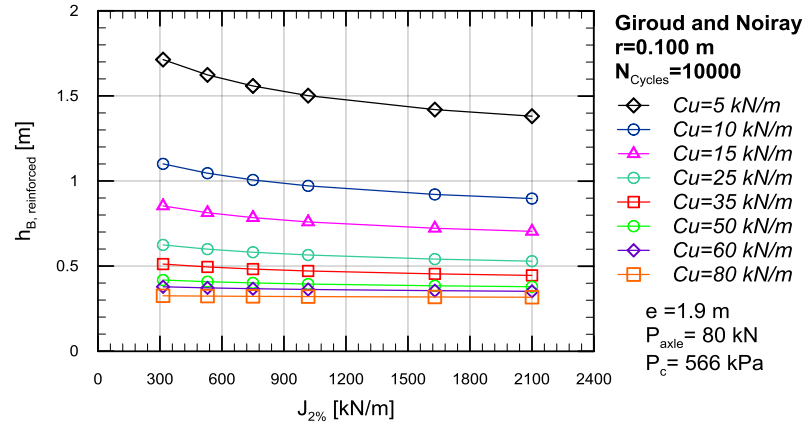

Figure 4.19 Unpaved roads design procedure by Giroud and Noiray (1981): unreinforced and reinforced base aggregate thickness varying the geogrid tensile stiffness, at the same traffic conditions (N_{cycles}=10000), for each subgrade undrained shear strength and for a fixed allowable rut depth values equal to 0.100 m

Moreover, as undrained subgrade shear strength increases, so decrease the design base thickness, the effect of the rutting and the benefits offered by reinforcements, as confirmed by the horizontality of the design curves in Figure 4.18 and Figure 4.19 for Cu > 50 kN/m^2.

4.4. Comparison between Barenberg et al. (1975) and Giroud and Noiray (1981) unpaved roads design procedures: analysis of results and discussion

This section is dedicated to the comparison between Barenberg et al. (1975) and Giroud and Noiray (1981) unpaved roads design procedures based on the careful analysis of the obtained results.

All the design parameters related to the geogrids' mechanical properties, the allowable rut depth, the subgrade mechanical characteristics and the traffic conditions are listed in Table 4.11.

As previously said, six bi-oriented geogrids, commercially available, of different tensile stiffness were selected. Geogrids mechanical properties were investigated by means wide-width tensile tests (according to EN ISO 10319). Tensile modules at 2% of deformation, $J_{2\%}$ [kN/m], (in transverse direction along which the geogrids carry the higher mechanical characteristics) varying from 315 kN/m to 2100 kN/m and reduced by factor of 1.1 to take into account the working conditions in site, were chosen in the implementation of the analyzed design procedures.

Table 4.11 Design parameters

Allowable rut, r [m]	Geogrid Stiffness, J2% [kN/m]	Undrained shear strength, Cu [kN/m2]	Ncycles* [-]
0.025	315	5	100
0.075	530	10	250
0.100	750	15	500
	1017	25	750
	1630	50	1000
	2100	60	5000
		80	7500
			10000

* Giroud and Noiray (1981) unpaved roads design procedures

As already said, the serviceability criteria offered by AASHTO design guidelines (AASHTO 1993) considers allowable rut depths from 13 to 75 mm. In the case of unpaved access roads, allowable rut depths greater than 75 mm, such as 100 mm, are sometimes used. Thus, for the analyses previously performed three allowable rutting values equal to 0.025m, 0.075m and 0.100 m were chosen.

Moreover, according to AASHTO design guidelines that suggests the use of geosynthetics with reinforcement function only when the subgrade is weak and characterized by a subgrade undrained shear strength (C_u) less than 90÷120 kPa, in this analysis Cu varying from 5 kN/m^2 to 80 kN/m^2 were assumed.

About the axles and loads design parameters, the wheel load (P) is the load applied by one of the wheels, in the case of single-wheel axle, or the load applied by a set of two wheels, in the case of dual-wheel axles and it is considered to be half of the axle load (P_{Axle}). In this analysis P_{Axle} =80 kN, so P=40 kN and a tire contact pressure (P_c) equal to 556 kPa, were assumed. The traffic, being vehicular traffic channelized, has been assumed characterized by the number of passes (N_{cycles}) of a given axle during the

road design life. The theory used by Barenberg et al. (1975) is based on static loading (i.e., up to 100 vehicle passes) while the Giroud and Noiray (1981) method, which takes into account the traffic conditions, extends the value of N_{cycles} up to a maximum of 10000 vehicle passes. In function of the above reported considerations, the comparison between these two design methods has been done considering for the Giroud and Noiray (1981) procedure a low number of vehicle passes equal to 100 (i.e., $N_{cycles,G\text{-}N}$= 100).

The comparison between the considered design procedures have been carried out also in terms of their sensitivity to the design parameter (i.e. geosynthetic stiffness, allowable rut depth and subgrade undrained strength).

Figure 4.20 shows the design curves related to the reinforced base aggregate layer thickness varying the geogrid tensile stiffness ($J_{2\%}$ from 315 kN/m to 2100 kN/m) for three different allowable rut depth values (r=0.025m, 0.075m, 0.100 m) keeping constant the subgrade undrained shear strength (i.e., Cu=5 kN/m^2).

In addition, the analysis is conducted in terms of Base Course Reduction factor (BCR), which is defined, at equivalent traffic capacity, as the percent reduction in the reinforced base layer thickness with respect to the unreinforced layer thickness, with the same aggregate materials, corresponding to the same defined failure state (in terms of rutting):

$$BCR = \left[\left(h_{B,unreinf.} - h_{B,reinf.}\right)/h_{B,unreinf.}\right] \cdot 100 \qquad \text{(Eq 4.2)}$$

In particular, Figure 4.21 shows the improvement offered by the reinforcement in unpaved roads, for different values of reinforcement tensile stiffness and for fixed subgrade mechanical characteristic (i.e., Cu =5 kN/m^2, which lead to more evident differences).

In order to take into account the influence of $J_{2\%}$ an iso-rutting curve relative to the maximum allowable rut depth (r= 0.100 m, curve in green for which the greatest differences are shown because the rutting is enough deep to let the geogrid reinforcement providing the highest membrane support) is analyzed.

In particular, for each allowable rut depth, the reinforced base layer thickness obtained by Giroud and Noiray (1981) procedure are less than the ones provided by Barenberg et al. (1975) (Figure 4.21). This behavior highlights the conservative nature of the Barenberg et al. (1975) method that to determine the vertical stress at the base-subgrade interface does not take into account the base course layer mechanical properties since is based on the theory of elasticity of Boussinesq.

Moreover, the trend of the reinforced base thickness curves reflects the weight of the geogrids' tensile properties on the design method. Decreasing the Giroud and Noiray (1981) iso-rutting curves with a greater gradient than Barenberg et al. (1975) ones (Figure 4.21), it can be observed that $J_{2\%}$ affects more the former design procedure than the latter. In fact, the use of a stiffer reinforcement geogrid ($J_{2\%}$ from 315 kN/m to 2100 kN/m) leads to a percentage reduction of the reinforced base layer thickness for Barenberg et al. (1975) and Giroud and Noiray (1981) procedures, respectively, of about 30%. (the reinforced base thickness reduces from 0.69 m to 0.48 m, see Table 4.12) and of about 60% (the reinforced base thickness reduces from 0.54 m to 0.21 m, see Table 4.12). Therefore, the choice of a reinforcement geosynthetic with

better tensile properties results in the reduction of about 50% for the amount of granular material required for the construction of the reinforced base layer which implies, consequently to halve the costs for its realization.

In addition, at the same design conditions (in terms of traffic assumptions, subgrade mechanical characteristics, allowable rutting), the employment of a stiffer reinforcement provides higher BCR values both in Barenberg et al. (1975) and in Giroud and Noiray (1981) procedures improving the performances of the geogrid-reinforced unpaved roads (Figure 4.21 and Table 4.12). As it can be observed in Figure 4.21, higher values of BCR are related to the Giroud and Noiray (1981) method.

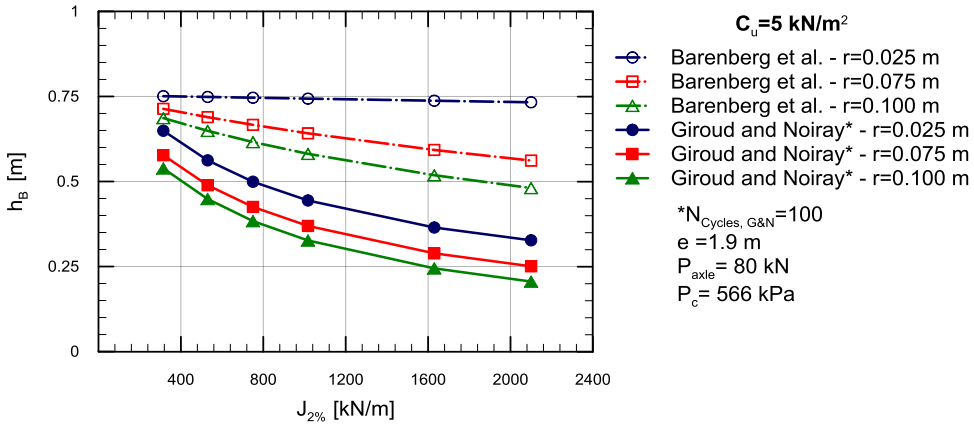

Figure 4.20 Comparison between Barenberg et al. (1975) et al. and Giroud and Noiray (1981) ($N_{cycles,G-N}$= 100) unpaved roads design procedure: Iso-rutting curves relating to the reinforced base aggregate thickness varying reinforcement stiffness, at the same traffic conditions (NcyclesG-N=100) and subgrade undrained shear strength (at C_u = 5 kN/m^2)and for each allowable rut depth

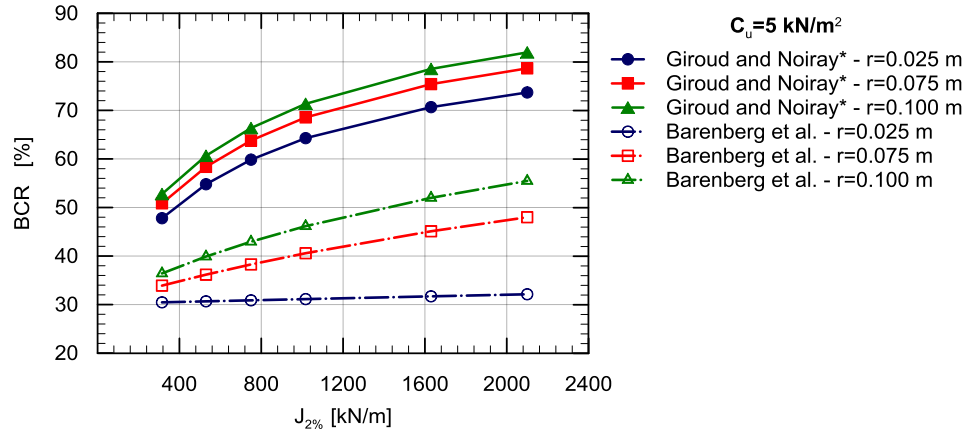

Figure 4.21 Comparison between Barenberg et al. (1975) et al. and Giroud and Noiray (1981) ($N_{cycles,G-N}$= 100) unpaved roads design procedure: Iso-rutting curves Base Course Reduction factor (BCR) varying reinforcement stiffness, at the same traffic conditions ($N_{cyclesG-N}$=100) and subgrade undrained shear strength (at Cu = 5 kN/m^2).

On the other hand, to investigate the effect of the rut depth the comparison between the two design methods is conducted for fixed $J_{2\%}$. In the present analysis the highest value of the geogrid stiffness (i.e. $J_{2\%}$= 2100 kN/m) which provides the greatest membrane support gives the largest differences.

As it can be observed in Table 4.12 and in Figure 4.20, the choice of deeper allowable rutting leads to a percentage reduction of the reinforced base layer thickness for Barenberg et al. (1975) et al. and Giroud

and Noiray (1981) procedures, respectively, of about 34% (the reinforced base thickness reduces from 0.73 m to 0.48 m, see Table 4.12) and of about 36% (the reinforced base thickness reduces from 0.33 m to 0.21 m, see Table 4.12). Therefore, the weight of r on the design procedures considred is comparable.

Moreover, considering separately the procedures, for fixed subgrade mechanical properties, the sensitivity (or weight) of Barenberg et al. (1975) unpaved reinforced design procedure to the two variables $J_{2\%}$ [kN/m] and r [m] is the same. On the other hand, for the Giroud and Noiray (1981) method, the geosynthetics tensile stiffness has more weight than the allowable rutting.

Table 4.12 Results of Barenberg et al. (1975) et al. and Giroud and Noiray (1981) unpaved roads design procedures in terms of unreinforced and reinforced base aggregate thickness, reduction and percentage reduction of the reinforced base layer thickness, at the same traffic conditions ($N_{cycles\ G\text{-}N}$ =100), for each geogrid tensile stiffness and allowable rut depth when the subgrade undrained shear strength is equal to 5 kN/m^2.

Design Procedure	N_{cycles} [-]	Undrained shear strength Cu [kN/m2]	Allowable rut depth r [m]	Tensile stiffness $J_{2\%}$ [kN/m]	$h_{B,UNR}$ [m]	$h_{B,R}$ [m]	BCR [%]
Barenberg et al. (1975)	-	5	0.025	315	1.08	0.75	30.46
	-	5	0.025	750	1.08	0.75	30.87
	-	5	0.025	2100	1.08	0.73	32.12
	-	5	0.075	315	1.08	0.71	33.90
	-	5	0.075	750	1.08	0.67	38.27
	-	5	0.075	2100	1.08	0.56	47.99
	-	5	0.100	315	1.08	0.69	36.42
	-	5	0.100	750	1.08	0.62	42.95
		5	0.100	2100	1.08	0.48	55.47
Giroud and Noiray (1981)	100	5	0.025	315	1.24	0.65	47.79
	100	5	0.025	750	1.24	0.50	59.85
	100	5	0.025	2100	1.24	0.33	73.69
	100	5	0.075	315	1.17	0.58	50.85
	100	5	0.075	750	1.17	0.43	63.80
	100	5	0.075	2100	1.17	0.25	78.66
	100	5	0.100	315	1.14	0.54	52.77
	100	5	0.100	750	1.14	0.38	66.36
	100	5	0.100	2100	1.14	0.21	81.95

In addition, a parametric sensitivity analysis on the rut depth (Figure 4.22 a), on the reinforcement tensile stiffness (Figure 4.22 b) and on the subgrade undrained shear strength (Figure 4.22 c) is proposed. For each figure, just one design parameter varies. Since both design methods, aiming at obtaining the reinforced base thickness layer of an unpaved road system, consider the membrane action of reinforcement, the dependency of the required aggregate layer on the rut depth and on reinforcement tensile modulus are reflected on the results. In particular, results confirm that reinforcement benefits generally increase the allowable rut depth increases (Figure 4.22 a) and the geogrids becomes stiffer (Figure 4.22 b). Further, as

the undrained subgrade shear strength increases, so the design base thickness decreases as well as the benefits offered by the reinforcement (Figure 4.22 c).

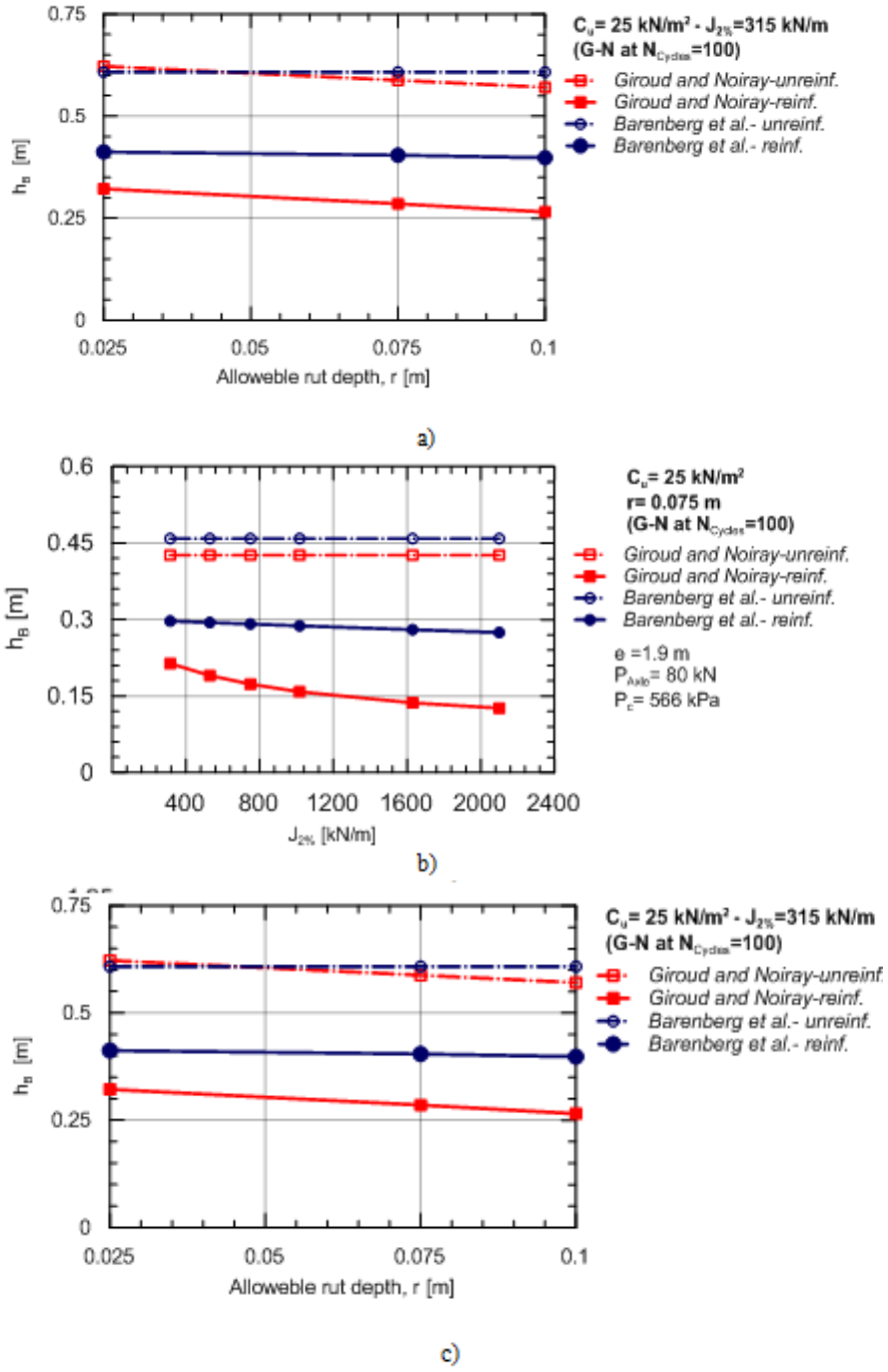

Figure 4.22 Comparison between design procedures proposed by Barenberg et al. (1975) et al. and by Giroud and Noiray (1981) : a) influence of rut depth; b) influence of the reinforcement tensile stiffness; c) influence of the undrained subgrade shear strength.

It is interesting to note how the value of the unreinforced base thickness by Barenberg et al. (1975) procedure is independent of the rutting value (Figure 4.22 a) since the authors does not take into account the base mechanical characteristics.

A more accurate analysis shows that greater values of reinforced base thickness are obtained by Giroud and Noiray (1981) method, highlighting the conservative nature of the Barenberg et al. (1975) model (Figure 4.22 a, Figure 4.22 b and Figure 4.22 c). Similarly, greater sensitivity of the Giroud and Noiray (1981) procedure to the geosynthetic tensile module is seen (Figure 4.22 b).

The amount of improvement due to reinforcement effect can be related to a Performance Index (PI) which is defined as follows:

$$PI = 1 - \left[\left(h_{B,unreinf.} - h_{B,reinf.}\right)/h_{B,unreinf.}\right] \qquad \text{(Eq. 4.3)}$$

It's important to note that the best performance due to the reinforcement effect corresponds to lower values of PI (e.g. PI=0.1 means 90% of Base Course Thickness Reduction).

In Figure 4.23 PI is plotted versus Cu, for fixed design conditions (in terms of equivalent traffic capacity, allowable rut depth and geogrid tensile properties). In the range of undrained subgrade shear strength chosen, generally Giroud and Noiray (1981) design procedure shows higher PI than Barenberg et al. (1975) method, registering larger differences for lower Cu values. It is noteworthy that when the reinforced base layer is too high the reinforcement works less. The differences in the results from the procedures are probably due to the way of each method to estimate the pressure on the substrate surface. Barenberg et al. (1975) consider a load distribution according to the Boussinesq theory, overlooking the base mechanical characteristics. On contrary, Giroud and Noiray (1981) use a trapezoidal distribution of pressures taking into account the base aggregate layer mechanical proprieties. This aspect stresses once again the more conservative nature of the Barenberg et al. (1975) design procedure.

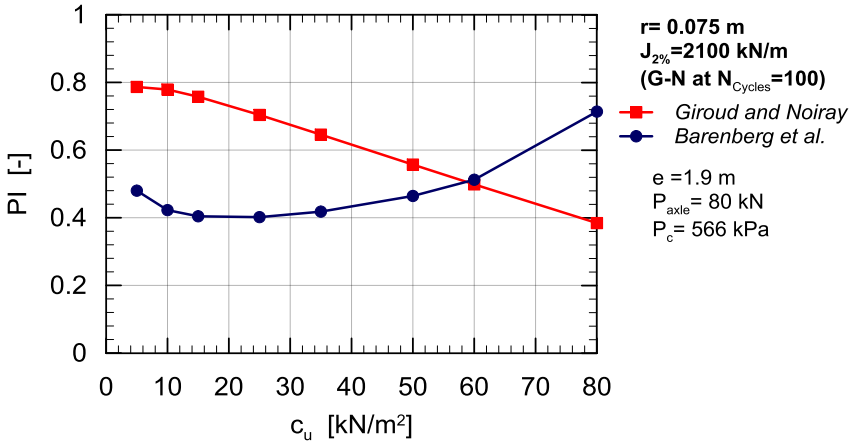

Figure 4.23 Comparison between design procedures proposed by Barenberg et al. (1975) et al. and by Giroud and Noiray (1981) in term Performance Index (PI).

4.5. Unpaved roads design procedure by Giroud and Han (2004): analysis of results and discussion

Giroud and Han (2004) modified the Giroud and Noiray (1981) method giving further headways to the previous unpaved road design method. As it has been widely discussed in Chapter 3, Giroud and Han (2004) approach is based on determining the base aggregate thickness as a function of the stresses at the base-subgrade interface and of the subgrade bearing capacity. The authors take into account: the effects of

degradation in the base course strength; the number and size of load cycles (axle passes); the mechanical geogrid properties; how the load distribution angle, within the base course, decreases with time. They also performed the calibration and validation of the theoretical results with empirical data from laboratory full-scale test sections monitoring unpaved roads.

As previously done, a parametric analysis of the design curves related to the thickness required for the base layer, both in the unreinforced and reinforced configuration, and the evaluation of the improvement offered by the use of a reinforcement geosynthetic in terms of percentage reductions of the reinforced base layer thickness, compared to the unreinforced one, was performed for the Giroud and Han (2004) method as well.

Table 4.13 Design parameters of Giroud and Han (2004) design method

Allowable rut, r [m]	**Geogrid aperture stability modulus, J_{AS} [mN/°]**	**CBRs [%]**	**N_{cycles} [-]**
0.050	0.28	0.5	1
0.075	0.32	1	10
0.100	0.41	1.3	100
	0.48	1.5	250
	0.58	2	500
	0.65	2.5	750
	0.75	3	1000
		3,5	5000
			7500
			10000

In the reinforced sections seven bi-oriented geogrids, commercially available, were selected, each characterized by different geogrid aperture stability modulus, J_{AS}, (m-N/degree), varying from 0.28 a 0.75 Nm, and placed at the bottom of the base course layer.

As previously mentioned, the serviceability criteria offered by AASHTO design guidelines (AASHTO 1993) considers allowable rut depths from 13 to 75 mm. In the case of unpaved access roads, allowable rut depths greater than 75 mm, such as 100 mm, are sometimes used. Thus, for the analyses previously performed three allowable rutting values equal to 0.050m, 0.075m and 0.100 m were chosen.

Moreover, according to AASHTO design guidelines, geosynthetics with reinforcement function are recommended only for weak subgrades, characterized by California Bearing Ratio (CBRs) less than 3÷4%, or alternatively subgrade undrained shear strength (C_u) less than 90÷120 kPa. In the present analysis, CBR varying from 0.5% to 3.5% were used. About the axles and loads design parameters, the wheel load (P) is the load applied by one of the wheels, in the case of single-wheel axle, or the load applied by a set of two wheels, in the case of dual-wheel axles and it is considered to be half of the axle load (P_{Axle}). In this analysis P_{Axle} =80 kN, so P=40 kN and a tire contact pressure (P_c) equal to 556 kPa, were assumed. The traffic, being vehicular traffic channelized, has been assumed characterized by the number of passes (N_{cycles})

of a given axle during the road design life. The analysis conducted expected a maximum number of load applications equal to 10000.

The above reported design parameters regarding the geosynthetic mechanical properties, allowable rut depths, subgrade mechanical characteristics, traffic conditions are given in Table 4.13.

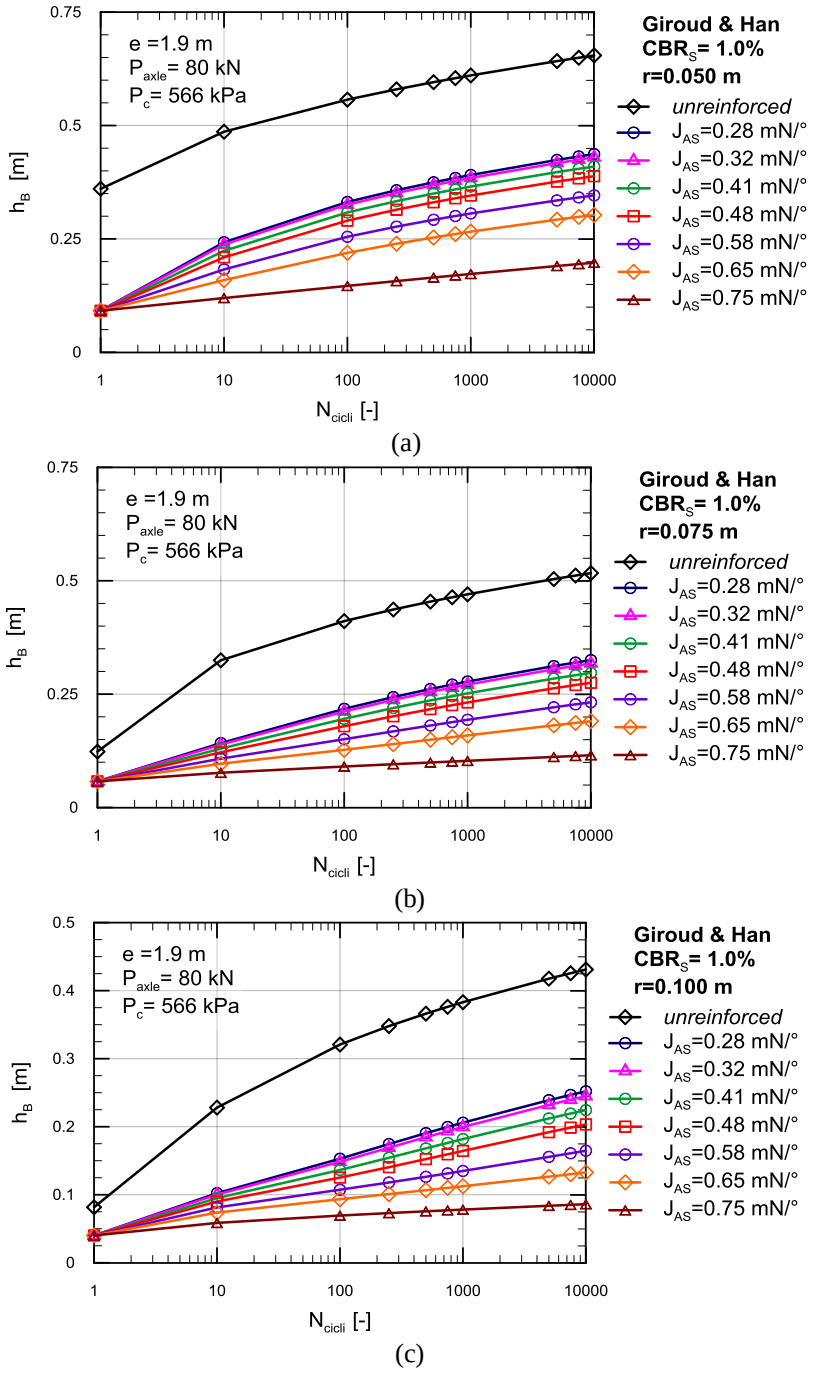

Figure 4.24 Unpaved roads design procedure by Giroud and Han: unreinforced and reinforced base aggregate thickness versus number of wheel passes for fixed value of Subgrade CBR (CBRs=1%) and for each geogrids chosen, when the allowable rut is: a) 0.050 m; b) 0.075m; c) 0.100 m.

In Figure 4.24 a ÷ Figure 4.24 c illustrate the design curves related to the base layer thickness required for both unreinforced and reinforced unpaved road section versus the number of vehicular load

cycles (N_{cycles} = from 1 to 10000) for fixed value of the subgrade CBR (CBR= 1%) and for each value of allowable rut depth assumed (r equal to 0.050m, 0.075m, 0.100m). Each curve is referred to different geogrid aperture stability modulus values (i.e. J_{AS} varying from 0.28 ÷0.75 Nm / °).

The method of Giroud and Han (2004), as well as the method of Giroud and Noiray (1981), moves away from the static condition assumed by the Barenberg et al. (1975) model and, therefore, considers the effect of the number of vehicular load cycles on the unreinforced and reinforced base layer thickness. Therefore, in Figure 4.24 a ÷ Figure 4.24 c the required thickness for both unreinforced and reinforced base layer is shown to increase as the number of wheel load cycles increase (N_{cycles} = 1 ÷ 10000) and the geogrid mechanical proprieties decrease considering the same subgrade mechanical characteristics and for each allowable rut assumed.

Moreover, all depth values of rutting chosen (r = 0.050 m ÷ 0.100 m) are large enough to let the geosynthetic layer work providing a reinforcement support proportionally to its own mechanical characteristic (Figure 4.24 a ÷ Figure 4.24 c). This result suggests that the main reinforcement mechanism is due to the lateral restraint of the base soil, which develops for more reduced rut depth, and it is, therefore, always the first mechanism to be activated. Then, by increasing the rut depth, the membrane mechanism, that requires higher values of geosynthetic deformation to be achieved, can take over. Therefore, the design curves for each geogrids with different aperture stability modulus appear to be clear and distinct. In other words, at the same design conditions the decrease of the reinforced base thickness as the geogrids' mechanical properties increase is observed with consequent saving of aggregate material needed for its construction.

Figure 4.25 a ÷ Figure 4.25 c show the improvement offered by the reinforcement, in terms of percentage reduction of the reinforced base layer thickness in comparison with the thickness required when the base layer is unreinforced. The results, moreover, confirm that there is higher efficiency when the reinforcement, placed at based-substrate interface, has higher mechanical proprieties. Consequently, the benefits are in terms of saving of aggregate material needed for the base layer construction. From a more careful analysis carried out comparing between them the graphics of Figure 4.25 a ÷ Figure 4.25 c it can be observed that the percentage reduction of the reinforced base layer thickness increases as the allowable rut increases. Some of these results are summarized in Table 4.14

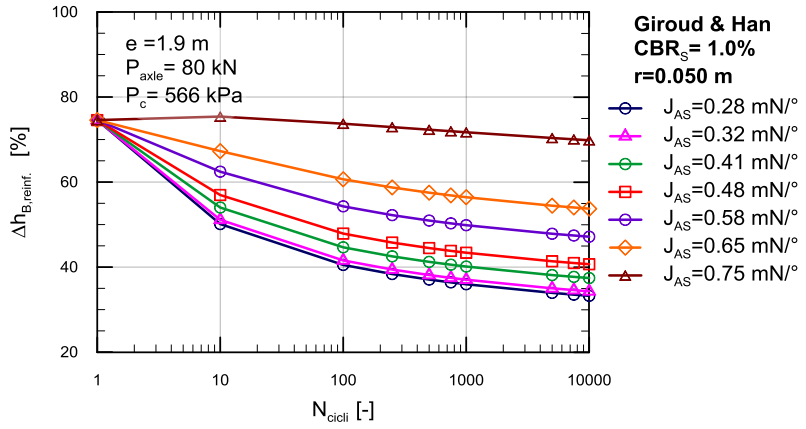

(a)

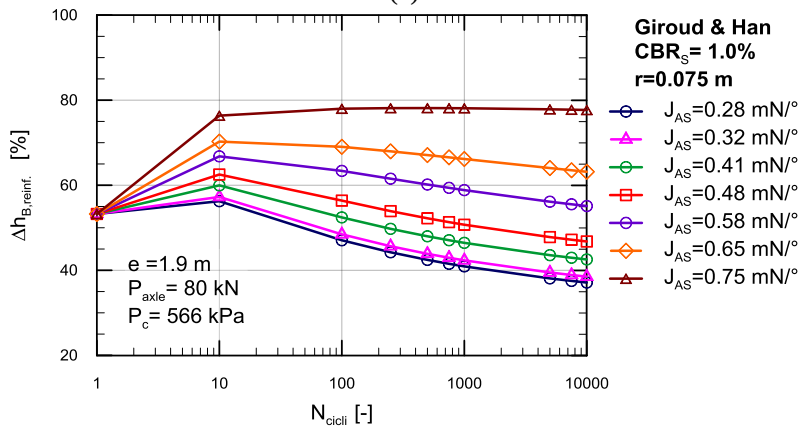

(b)

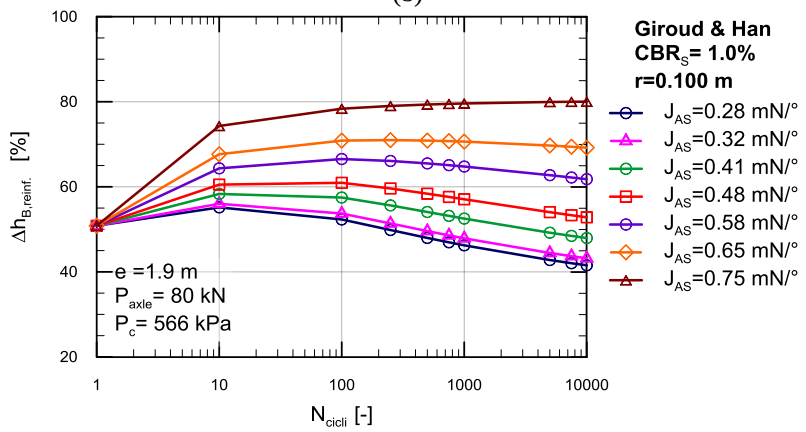

(c)

Figure 4.25 Unpaved roads design procedure by Giroud and Han: percentage reduction of the reinforced base layer thickness versus number of wheel passes for fixed value of Subgrade CBR (CBRs=1%) and for each geogrids chosen, when the allowable rut is: a) 0.050 m; b) 0.075m;c) 0.100 m.

Table 4.14 Results of Giroud and Han unpaved roads design procedure in terms of: unreinforced and reinforced base aggregate thickness and percentage reduction of the reinforced base layer thickness, when the subgrade CBR is equal to 1.0% and varying the number of wheel passes, the allowable rut depth and the geogrids' aperture stability modulus

N [-]	CBR [%]	r [m]	J_{AS} [mN/°]	$h_{B,UNR}$ [m]	$h_{B,R}$ [m]	$\Delta h_{reinf.}$ [%],
100	1	0.050	0.28	0.557	0.331	40.51
100	1	0.050	0.48	0.557	0.290	47.88
100	1	0.050	0.65	0.557	0.219	60.65
100	1	0.075	0.28	0.411	0.218	47.06
100	1	0.075	0.48	0.411	0.179	56.39
100	1	0.075	0.65	0.411	0.127	69.03
100	1	0.100	0.28	0.321	0.153	52.32
100	1	0.100	0.48	0.321	0.125	60.94
100	1	0.100	0.65	0.321	0.093	70.86
1000	1	0.050	0.28	0.610	0.391	35.97
1000	1	0.050	0.48	0.610	0.346	43.38
1000	1	0.050	0.65	0.610	0.266	56.43
1000	1	0.075	0.28	0.470	0.278	40.92
1000	1	0.075	0.48	0.470	0.232	50.71
1000	1	0.075	0.65	0.470	0.159	66.17
1000	1	0.100	0.28	0.383	0.206	46.24
1000	1	0.100	0.48	0.383	0.164	57.07
1000	1	0.100	0.65	0.383	0.113	70.63
10000	1	0.050	0.28	0.655	0.437	33.24
10000	1	0.050	0.48	0.655	0.388	40.68
10000	1	0.050	0.65	0.655	0.303	53.74
10000	1	0.075	0.28	0.517	0.325	37.11
10000	1	0.075	0.48	0.517	0.275	46.77
10000	1	0.075	0.65	0.517	0.190	63.16
10000	1	0.100	0.28	0.431	0.252	41.54
10000	1	0.100	0.48	0.431	0.203	52.82
10000	1	0.100	0.65	0.431	0.133	69.19

In order to investigate the effect of the allowable rut depth, r, on the Giroud and Han (2004) model, in Figure 4.26 are reported the design curves related to both the unreinforced and reinforced base layer thickness varying the allowable rut depth for a fixed number of vehicular repetitions (N_{cycles} = 10000) and subgrade CBR value (CBR = 1%). Each curve refers to a geogrid with different values of J_{AS} (i.e. J_{AS} = 0:28 ÷ 0.75 Nm/°). It is noteworthy that as the allowable rut depth increases the required base layer thicknesses decrease. This behavior could be explained by considering that the main reinforcement mechanisms that take place are the lateral confinement effect and the tension membrane effect. They require different depth values of rutting in order to be mobilized. At small permanent deformation magnitudes, the lateral restraint

mechanism is developed by the ability of the base aggregate to interlock with the geogrid. As the permanent deformations (which are often acceptable in unpaved roads) increase the tension membrane mechanism develops. So, if the geosynthetic has a sufficiently high tensile modulus, tensile stresses are mobilized in the reinforcement, and a vertical component of this tensile membrane resistance further helps to support the applied wheel loads.

These results also confirm that the use of geogrids with higher mechanical characteristics, for each value of rut depth assumed, is more effective since it provides higher support to the vehicular load.

It follows that, at the same design conditions, (i.e., subgrade CBR and traffic conditions) the improvements obtained by the use of reinforcement geogrid in terms of the percentage reduction thickness required for the base layer increase as the allowable rut depth increases and proportionally to the mechanical characteristics of the geogrid used (see Figure 4.27 and Table 4.15).

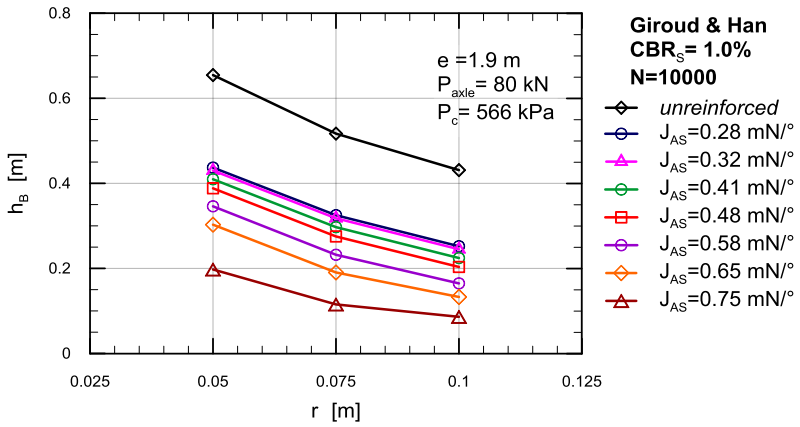

Figure 4.26 Unpaved roads design procedure by Giroud and Han: unreinforced and reinforced base aggregate thickness versus allowable rut depth for fixed value of subgrade CBR (CBRs=1%) and the number of wheel passes (N_{cycles}=10000) and for each geogrids chosen.

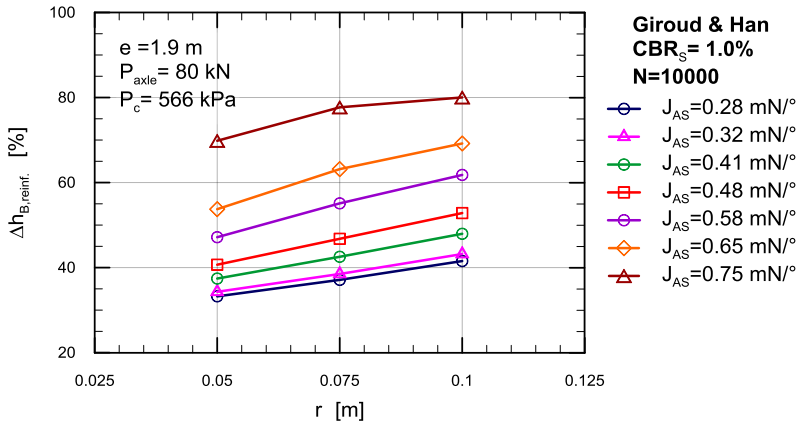

Figure 4.27 Unpaved roads design procedure by Giroud and Han: percentage reduction of the reinforced base layer thickness versus allowable rut depth for fixed value of subgrade CBR (CBRs=1%) and the number of wheel passes (N_{cycles}=10000) and for each geogrids chosen.

In particular, when the geogrid with the maximum mechanical characteristic (i.e., J_{AS} = 0.75 mN/° which provides the greatest reinforcement support and, thus, gives the greatest differences) is used, it can be observed that the reinforced base course layer thickness reduces from 0.197m to 0.086m as the rut depth

increases from 0.050m to 0.100m, resulting in a base thickness reduction of 0. 0.111m (Figure 4.26 and Table 4.15). This leads to an improvement in terms of less aggregate material required to the reinforced base layer construction of about 56%. Therefore, the choice of a greater allowable rut depth results in saving about twice the amount of granular material required for the construction of the reinforced base layer.

In addition, considering the same design conditions and the geogrid with highest mechanical properties (J_{AS} = 0.75 mN/°), allowing a deeper rutting leads to an improvement of performances, in terms of percentage reductions of reinforced base aggregate layer thickness, which increase from 69.83% to 80.02% (Figure 4.27 and Table 4.15).

Table 4.15 Results of Giroud and Han unpaved roads design procedure in terms of unreinforced and reinforced base aggregate thickness and percentage reduction of the reinforced base layer thickness, when the subgrade CBR is equal to 1.0% and varying the number of wheel passes, the allowable rut depth and the geogrids' aperture stability modulus

N [-]	CBR [%]	r [m]	J_{AS} [mN/°]	$h_{B,UNR}$ [m]	$h_{B,R}$ [m]	$\Delta h_{reinf.}$ [%],
10000	1	0.0500	0.28	0.655	0.437	33.24
10000	1	0.0500	0.32	0.655	0.430	34.31
10000	1	0.0500	0.41	0.655	0.410	37.42
10000	1	0.0500	0.48	0.655	0.388	40.68
10000	1	0.0500	0.58	0.655	0.346	47.15
10000	1	0.0500	0.65	0.655	0.303	53.74
10000	1	0.0500	0.75	0.655	0.197	69.83
10000	1	0.0750	0.28	0.517	0.325	37.11
10000	1	0.0750	0.32	0.517	0.318	38.50
10000	1	0.0750	0.41	0.517	0.297	42.54
10000	1	0.0750	0.48	0.517	0.275	46.77
10000	1	0.0750	0.58	0.517	0.232	55.11
10000	1	0.0750	0.65	0.517	0.190	63.16
10000	1	0.0750	0.75	0.517	0.115	77.69
10000	1	0.1000	0.28	0.431	0.252	41.54
10000	1	0.1000	0.32	0.431	0.245	43.19
10000	1	0.1000	0.41	0.431	0.224	47.95
10000	1	0.1000	0.48	0.431	0.203	52.82
10000	1	0.1000	0.58	0.431	0.165	61.80
10000	1	0.1000	0.65	0.431	0.133	69.19
10000	1	0.1000	0.75	0.431	0.086	80.02

In order to investigate the effect of the geogrids' mechanical proprieties on the Giroud and Han (2004) model in Figure 4.28 are plotted the design curves related to both the unreinforced and reinforced base layer thickness, for different aperture stability modulus values (i.e. J_{AS} from 0.28 to 0.75 mN/°),

keeping constant the number of vehicular repetitions (N_{cycles} = 10000) and the subgrade CBR value (i.e. 1%). Each curve refers to different allowable rut depths (r = 0:050 ÷ 0.100 m).

Given the reduction of the required thickness with the increasing of the allowable rut depth, as previously seen, the results obtained show that geosynthetics with higher mechanical properties are more effective, at the same design conditions (i.e., subgrade CBR and traffic conditions). This is more evident when considering the maximum value of the rut depth (r=0.100m) since the reinforcement mechanism is due to the combination of the membrane effect and the lateral confinement effect (see Figure 4.28).

Let focus the attention on the curve related to the maximum value of rutting (i.e. r = 0.100m) (Figure 4.28, green line) for which the differences are larger because the rutting is enough deep to let the geogrid reinforcement provide the highest membrane support. It can be noticed that by increasing the geogrids' aperture stability modulus from 0.28 to 0.75 mN/° the base thickness reduces from 0.252 m to 0.086 m, resulting in a reduction in absolute terms of 0.166 m (Figure 4.28 a and Table 4.15). Therefore, this leads to an improvement in terms of less aggregate material required to the reinforced base layer construction of about 66%. Thus, the choice of the stiffest geogrid results in saving about two-thirds of the amount of granular material required for the construction of the reinforced base layer, which implies, consequently, to halve the costs for its realization.

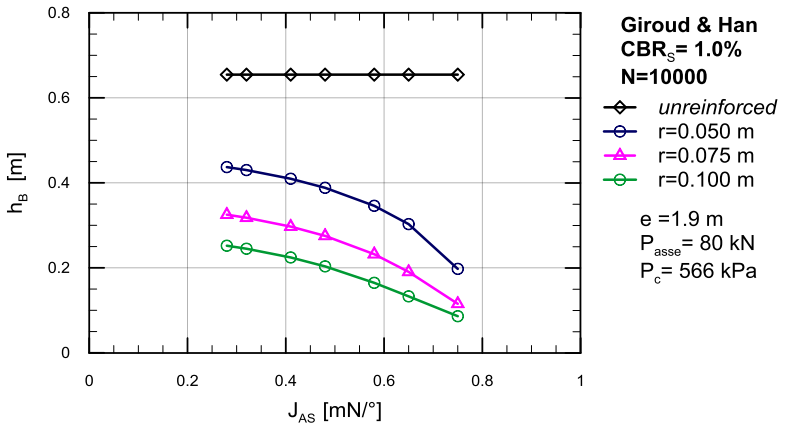

Figure 4.28 Unpaved roads design procedure by Giroud and Han: unreinforced and reinforced base aggregate thickness versus geogrid aperture stability modulus for fixed value of subgrade CBR (CBRs=1%) and the number of wheel passes (N_{cycles}=10000) and for each allowable rut depth chosen.

It may be also interesting to evaluate the percentage reduction of the reinforced base thickness, Δh_{reinf}. [%], obtained by the use of geogrid, considering the same design conditions previously described. In particular, for the maximum allowable rut depth (i.e., r = 0.100m), which leads to greater differences, the aperture stability modulus increases from 0:28 mN/° to 0.75 mN/° yielding to a more efficient use of the reinforcement, with consequent increase of the percentage reduction of the reinforced base thickness required from 41.54% to 80.02%. (see Table 4.15).

Summarizing the obtained results it follows that, the sensitivity (or weight) of Giroud and Han (2004) to the design variables J_{AS} [mN/°] and r [m] in unpaved reinforced design procedure is different although the subgrade mechanical properties and the traffic conditions are the same. In fact, the geogrid aperture stability modulus has more weight than the allowable rutting.

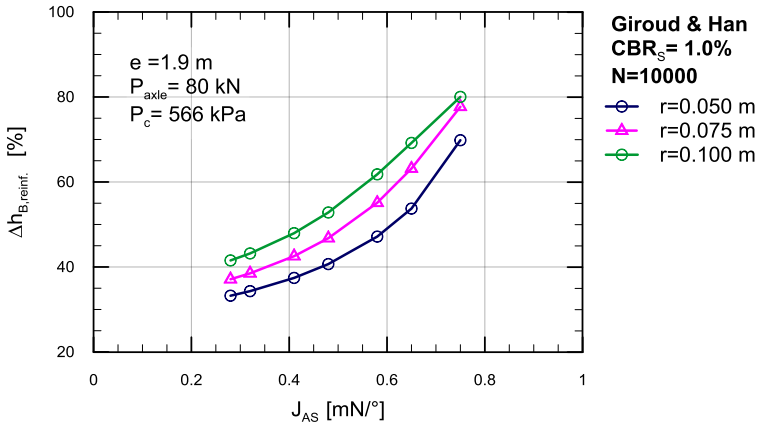

Figure 4.29 Unpaved roads design procedure by Giroud and Han: percentage reduction of the reinforced base layer thickness versus geogrid aperture stability modulus for fixed value of subgrade CBR (CBRs=1%) and the number of wheel passes (N_{cycles}=10000) and for each allowable rut depth chosen.

Finally, to analyze the influence of the substrate mechanical characteristics, in Figure 4.30a ÷ Figure 4.30c are shown the unreinforced and reinforced base aggregate thickness as a function of the subgrade CBR (from 0.5% to 3.5%), keeping constant the allowable rut depth (r=0.075m) and varying the geogrids chosen (characterized by increasing values J_{AS} from 0:28 mN/° to 0.75 mN/°). For the analysis three values of the number of wheel passes equal to 100, 1000 and 10000 were chosen.

As expected, the increase of the required base aggregate thickness is observed as the number of vehicular load passes increase. Anyway, at the same traffic conditions, in Figure 4:30 a ÷ Figure 4:30 c the decrease of the base layer thickness, reinforced and not, is observed as the subgrade mechanical characteristic increase and the geogrid mechanical characteristics becomes higher. In particular, Giroud and Han (2004) design procedure requires, for unpaved roads, the use of geosynthetics with reinforcement function only for weak subgrade characterized by California Bearing Ratio (CBR) less than 2.5%÷3.0%, in agreement with the AASHTO regulations (1993).

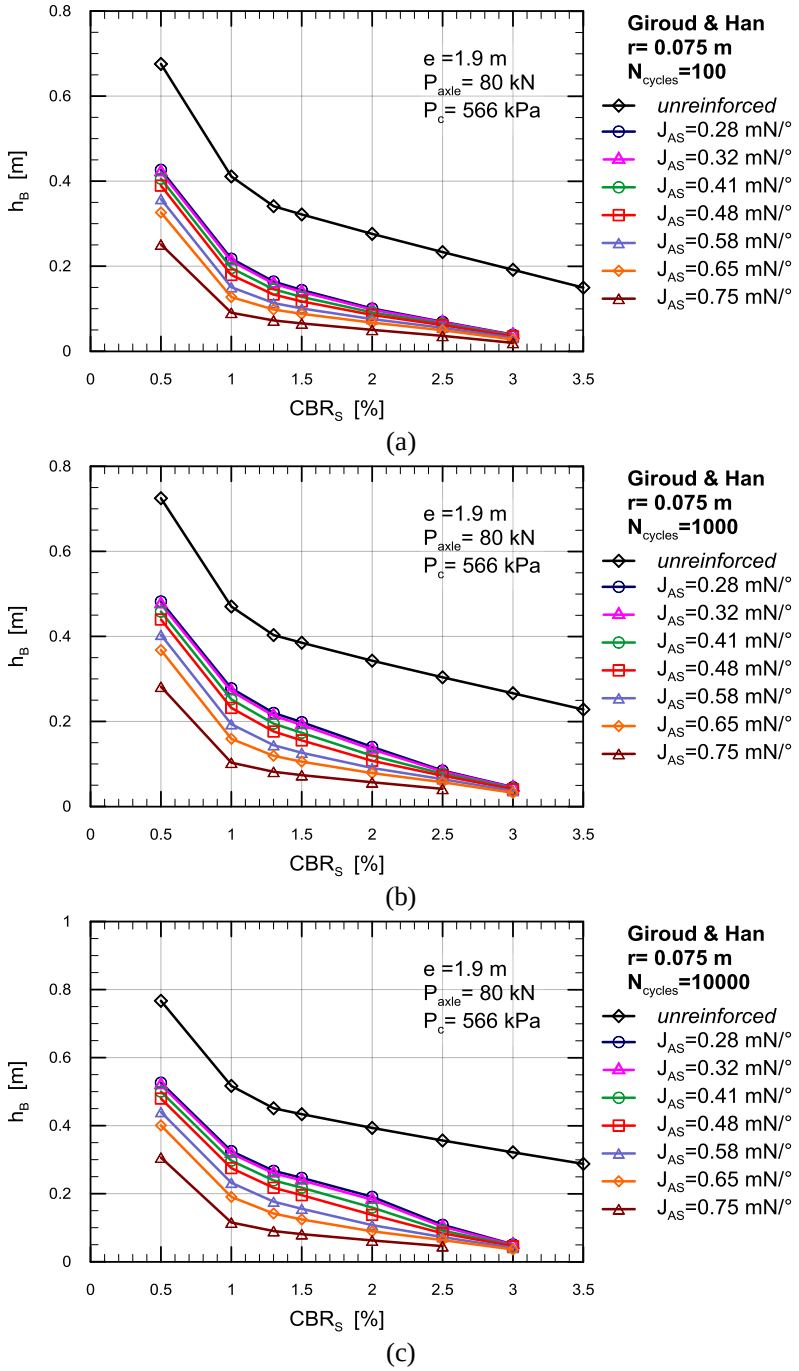

Figure 4.30 Unpaved roads design procedure by Giroud and Han: unreinforced and reinforced base aggregate thickness versus subgrade CBR at the same value of allowable rut depth (r=0.075m) for each geogrids chosen and at the same number of wheel passes: a) N_{cycles}= 100; b) N_{cycles}= 1000; c) N_{cycles}= 10000.

4.6. Unpaved roads design procedure by Leng and Gabr (2005): analysis of results

Leng and Gabr (2005) proposed further developments in the geosynthetic-reinforced unpaved roads design. Their model takes into account the degradation of base course with cyclic loading, in addition to the base course properties, the mobilization of subgrade bearing capacity with rutting and the contribution of geogrid reinforcement. In their model, the degradation of unpaved road depends on the base

course-subgrade elastic modulus ratio (E1/E2) and the load distribution angle degradation with the increasing of number of wheel load repetitions. Definitely, the highlight of the Leng and Gabr (2005) design procedure is to consider the unpaved road section as a two-layer system, where a stiffer soil layer (aggregate base course) rests on a softer layer (subgrade). For a given loading condition, the base with a high modulus reduces drastically the stress on the subgrade, under the wheel loading, in comparison with the case of elastic, isotropic and homogeneous semi-infinite half space. Therefore, for the two-layer unpaved road section, the authors replace the base course layer of thickness *h*, having elastic parameters E1 and υ_1, by an equivalent layer thickness h_e with the same modulus and Poisson's ratio of the underlying subgrade (E2 and υ_2, respectively).

As previously done, a parametric analysis of design curves related to the thickness required for the base layer, both in the unreinforced and reinforced configuration, and of the improvement offered by the use of a reinforcement geosynthetic expressed in terms of percentage reductions of the reinforced base layer thickness, compared to the unreinforced one, was performed for the Leng and Gabr (2005) method too, varying the input data.

In particular.in the reinforced sections, five extruded bi-oriented geogrids, commercially available, of different mechanical characteristic were selected. Geogrids mechanical properties were investigated by means of wide-width tensile tests (according to EN ISO 10319). The design tensile load at 2% of deformation, $J_{2\%}$, was selected as the average value of the tensile load measured at 2% ($J_{M,2\%}$) of deformation both in transverse direction ($J_{TD,2\%}$) and longitudinal or machine direction ($J_{MD,2\%}$). In other words, for the geogrids chosen in the simulation $J_{M,2\%}$ varies from 4.75 kN/m to 7.5 kN/m (Table 4.16).

As previously mentioned, the serviceability criteria offered by AASHTO design guidelines (AASHTO 1993) considers allowable rut depths from 13 to 75 mm. In the case of unpaved access roads, allowable rut depths greater than 75 mm, such as 100 mm, are sometimes used. Thus, three allowable rutting values equal to 0.050m, 0.075m and 0.100 m were chosen.

Moreover, according to AASHTO design guidelines, geosynthetics with reinforcement function in unpaved roads are recommended only for weak subgrades, characterized by California Bearing Ratio (CBRs) less than 3÷4%, or alternatively subgrade undrained shear strength (C_u) less than 90÷120 kPa. In the present analysis, CBR varying from 0.5% to 3.5% was used. About the axles and loads design parameters, the wheel load (P) is the load applied by one of the wheels, in the case of single-wheel axle, or the load applied by a set of two wheels, in the case of dual-wheel axles and it is considered to be half of the axle load (P_{Axle}). In this analysis P_{Axle} =80 kN, so P=40 kN and a tire contact pressure (P_c) equal to 556 kPa, were assumed. The traffic, being vehicular traffic channelized, has been assumed characterized by the number of passes (N_{cycles}) of a given axle during the road design life. The analysis conducted expected a maximum number of load applications equal to 10000.

All the design parameters in terms of geosynthetic mechanical properties, allowable rut depths, subgrade mechanical characteristics and traffic conditions are summarized in Table 4.17.

Table 4.16 Mechanical properties of the geogrids, commercially available, used in Leng and Gabr (2005) design procedures.

Geogrid	Direction	Tensile Strength at 2% of Strain (kN/m)	Average Tensile Strength at 2% of Strain (kN/m)
GG1	MD	4	4.75
	TD	5.5	
GG2	MD	4.1	5.35
	TD	6.6	
GG3	MD	6	6.70
	TD	7.4	
GG3	MD	7	7.00
	TD	7	
GG5	MD	6	7.50
	TD	9	

Table 4.17 Design parameters of Leng and Gabr (2005) design method

Allowable rut, r [m]	Geogrid aperture stability modulus, $J_{M,2\%}$ [kN/m]	CBRs [%]	N_{cycles} [-]
0.050	4.75	0.5	1
0.075	5.35	1	10
0.100	6.7	1.3	100
	7	1.5	250
	7.5	2	500
		2.5	750
		3	1000
			5000
			7500
			10000

In Figures 4.31 a ÷ Figures 4.31 c show the design curves related to the base layer thickness required for both the unreinforced and reinforced unpaved road section versus the number of vehicular load cycles (N_{cycles} = from 1 to 10000) for fixed subgrade CBR (CBR= 1%) and for each value of allowable rut depth assumed (r equal to 0.050m, 0.075m, 0.100 m). Each curve refers to a geogrid characterized by different tensile load at 2% of deformations (i.e. $J_{M,2\%}$ varying from 4.75 kN/m to 7.5 kN/m).

The method of Leng and Gabr (2005), as well as the Giroud and Noiray (1981) and the Giroud and Han (2004) methods, moves away from the static condition assumed by the Barenberg et al. (1975) model and, in addition, considers the effect of the number of vehicular load cycles on the unreinforced and reinforced base layer thickness. Is can be observed in Figure 4.31a ÷ Figure 4.31c that the required thickness for both unreinforced and reinforced base layer increases as the number of wheel load cycles (N_{cycles} = 1 ÷ 10000) increase and the geogrid mechanical proprieties increase, given the same subgrade mechanical characteristics and for each allowable rut assumed.

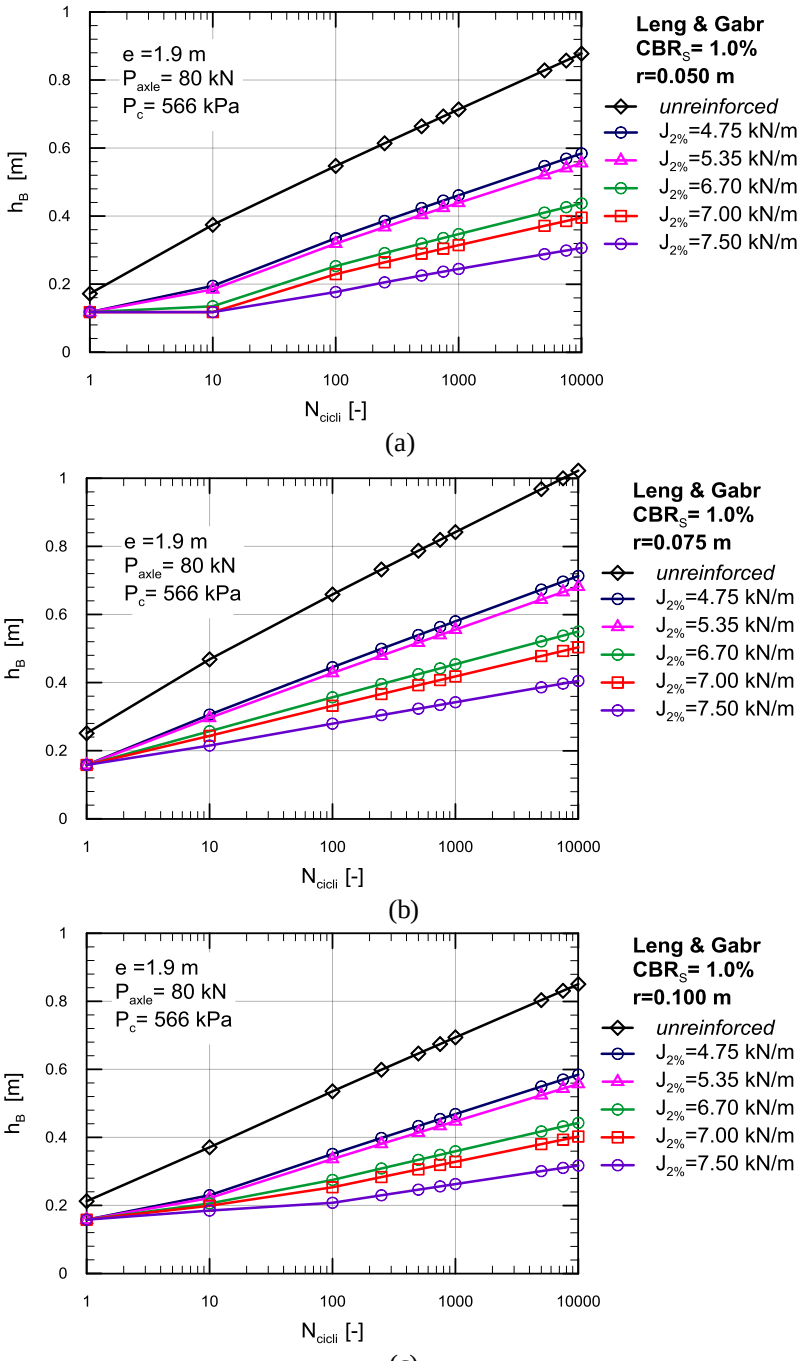

Figure 4.31 Unpaved roads design procedure by Leng and Gabr: unreinforced and reinforced base aggregate thickness versus number of wheel passes for fixed value of Subgrade CBR (CBRs=1%) and for each geogrids chosen, when the allowable rut is: a) 0.050 m; b) 0.075m; c) 0.100 m.

Moreover, all depth values of rutting chosen (r = 0.050 m ÷ 0.100 m) are large enough to let the geosynthetic layer work providing a reinforcement support proportionally to its own mechanical characteristic (Figure 4.31 a ÷ Figure 4.31 c). This suggests that the lateral restraint of the base soil, which develops for more reduced rut depth, is the main mechanism of reinforcement and it is, therefore, the first mechanism to be activated. Then, by increasing the rut depth, the membrane mechanism that requires higher values of geosynthetic deformation to be achieved, can take over. Therefore, the design curves for each geogrid with different tensile stiffness appear to be clear and distinct. In other words, at the same

design conditions the decrease of the reinforced base thickness as the geogrids' mechanical properties increase is observed with consequent saving of aggregate material needed for its construction.

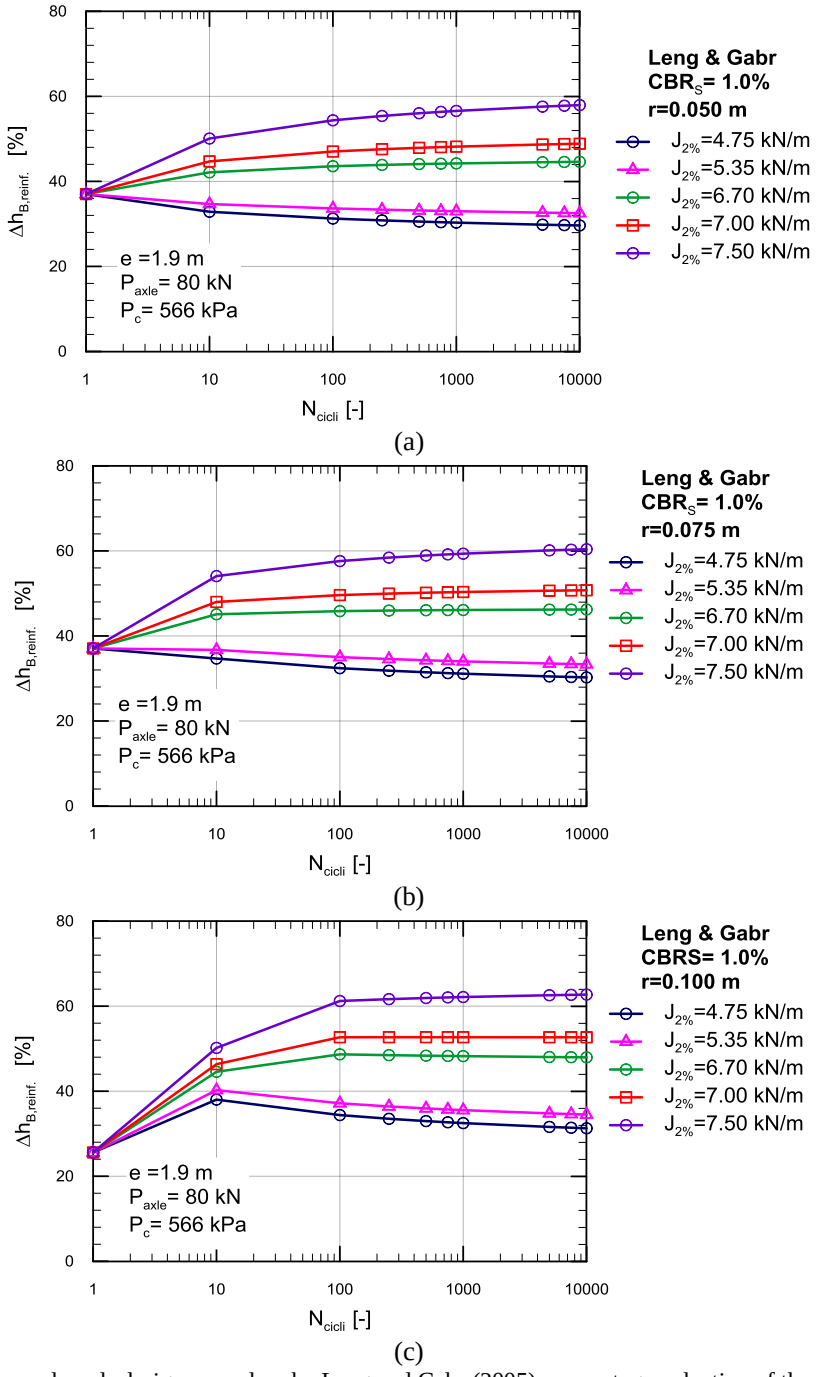

Figure 4.32 Unpaved roads design procedure by Leng and Gabr (2005): percentage reduction of the reinforced base layer thickness versus number of wheel passes for fixed value of Subgrade CBR (CBRs=1%) and for each geogrids chosen, when the allowable rut is: a) 0.050 m; b) 0.075m; c) 0.100 m.

Figure 4.32 a ÷ Figure 4.32 c show the improvement offered by the reinforcement, in terms of percentage reduction of the reinforced base layer thickness in comparison with the thickness required when the base layer is unreinforced. The results confirm that there is higher efficiency when the reinforcement, placed at based-substrate interface, has higher mechanical proprieties. Consequently, the benefits gained

consist in the saving of aggregate material needed for the base layer construction. From a more careful analysis based on the comparison between them of the graphics of Figure 4.32 a ÷ Figure 4.32 c the percentage reduction of the reinforced base layer thickness to increase as the allowable rut increases can be observed. Some of these results are summarized in Table 4.18

Table 4.18 Results of Leng and Gabr unpaved roads design procedure in terms of: unreinforced and reinforced base aggregate thickness and percentage reduction of the reinforced base layer thickness, when the subgrade CBR is equal to 1.0% and varying the number of wheel passes, the allowable rut depth and the geogrids' aperture stability modulus

N [-]	CBR [%]	r [m]	$J_{2\%}$ [kN/m]	$h_{B,UNR}$ [m]	$h_{B,R}$ [m]	$\Delta h_{reinf.}$ [%],
100	1	0.050	4.75	0.877	0.603	31.26
100	1	0.050	6.70	0.877	0.495	43.56
100	1	0.050	7.50	0.877	0.400	54.36
100	1	0.075	4.75	0.659	0.445	32.42
100	1	0.075	6.70	0.659	0.357	45.84
100	1	0.075	7.50	0.659	0.279	57.61
100	1	0.100	4.75	0.535	0.351	34.38
100	1	0.100	6.70	0.535	0.275	48.67
100	1	0.100	7.50	0.535	0.208	61.22
1000	1	0.050	4.75	1.102	0.768	30.30
1000	1	0.050	6.70	1.102	0.614	44.23
1000	1	0.050	7.50	1.102	0.478	56.57
1000	1	0.075	4.75	0.842	0.580	31.12
1000	1	0.075	6.70	0.842	0.454	46.10
1000	1	0.075	7.50	0.842	0.342	59.35
1000	1	0.100	4.75	0.694	0.468	32.50
1000	1	0.100	6.70	0.694	0.359	48.25
1000	1	0.100	7.50	0.694	0.263	62.15
10000	1	0.050	4.75	1.323	0.931	29.63
10000	1	0.050	6.70	1.323	0.733	44.60
10000	1	0.050	7.50	1.323	0.556	57.93
10000	1	0.075	4.75	1.022	0.713	30.25
10000	1	0.075	6.70	1.022	0.550	46.22
10000	1	0.075	7.50	1.022	0.405	60.40
10000	1	0.100	4.75	0.850	0.584	31.28
10000	1	0.100	6.70	0.850	0.443	47.96
10000	1	0.100	7.50	0.850	0.317	62.72

In order to investigate the effect of the allowable rut depth, r, on the Leng and Gabr (2005) model in Figure 4.33 the design curves related to both the unreinforced and reinforced base layer thickness are shown as functions of the allowable rut depth, for a fixed number of vehicular repetitions (N_{cycles} = 10000)

and of the subgrade CBR value (CBR = 1%). Each curve refers to geogrids with different values of $J_{M,\%}$ (i.e. $J_{M,2\%}$ varying from 4.75 kN/m to 7.5 kN/m). It can be observed that as the allowable rut depth increases smaller base layer thicknesses are required.

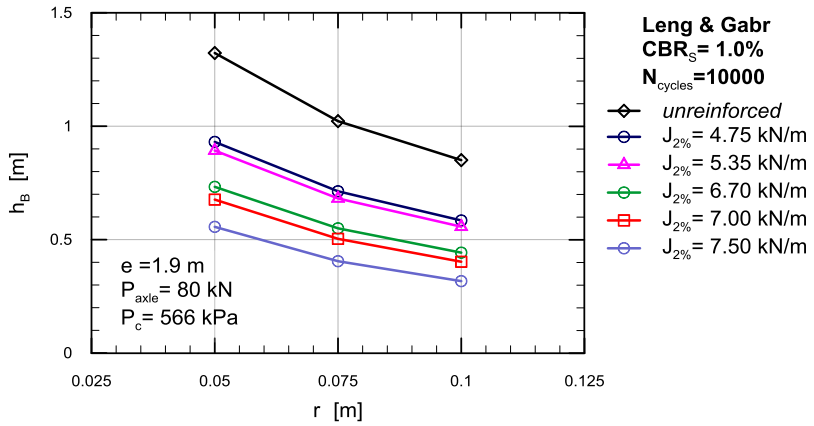

Figure 4.33 Unpaved roads design procedure by Leng and Gabr: unreinforced and reinforced base aggregate thickness versus allowable rut depth for fixed value of subgrade CBR (CBRs=1%) and the number of wheel passes (N_{cycles}=10000) and for each geogrids chosen.

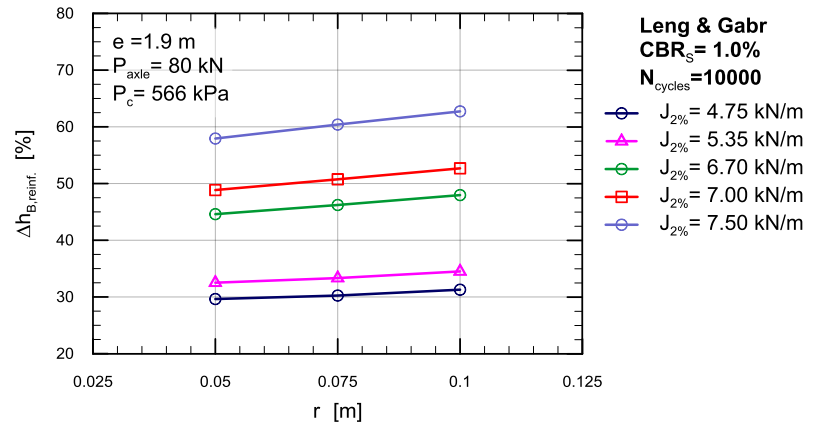

Figure 4.34 Unpaved roads design procedure by Leng and Gabr: percentage reduction of the reinforced base layer thickness versus allowable rut depth for fixed value of subgrade CBR (CBRs=1%) and the number of wheel passes (N_{cycles}=10000) and for each geogrids chosen.

This behavior could be explained by considering that the main reinforcement mechanisms that take place are the lateral confinement effect and the tension membrane effect. They require different depth values of rutting in order to be mobilized. At small permanent deformation magnitudes, the lateral restraint mechanism is developed by the ability of the base aggregate to interlock with the geogrid. As the permanent deformations (which are often acceptable in unpaved roads) increase the tension membrane mechanism develops. So, if the geosynthetic has a sufficiently high tensile modulus, tensile stresses are mobilized in the reinforcement, and a vertical component of this tensile membrane resistance further helps to support the applied wheel loads.

These results also confirm that the use of geogrids with higher mechanical characteristics, for each value of rut depth assumed, is more effective since it provides higher support to the vehicular load.

It follows that, at the same design conditions, (i.e., subgrade CBR and traffic conditions) the improvements obtained by the use of reinforcement geogrid in terms of the percentage reduction thickness required for the base layer increase as the allowable rut depth increases and proportionally to the mechanical characteristics of the geogrid used (see Figure 4.34 and Table 4.19).

In particular, when the geogrid with the maximum mechanical characteristic (i.e., $J_{2\%}$ = 7.5 kN/m which provides the greatest reinforcement support and, thus, gives the greatest differences) is used, it can be observed that the reinforced base course layer thickness reduces from 0.556m to 0.317m as the rut depth increases from 0.050m to 0.100m, resulting in a base thickness reduction of 0.239m (Figure 4.33 and Table 4.15). This leads to an improvement in terms of less aggregate material required to the reinforced base layer construction of about 43% and, consequently, to the saving in the amount of granular material required for the construction of the reinforced base layer.

Table 4.19 Results of Leng and Gabr unpaved roads design procedure in terms of unreinforced and reinforced base aggregate thickness and percentage reduction of the reinforced base layer thickness, when the subgrade CBR is equal to 1.0% and varying the number of wheel passes, the allowable rut depth and the geogrids' aperture stability modulus

N [-]	CBR [%]	r [m]	$J_{2\%}$ [kN/m]	$h_{B,UNR}$ [m]	$h_{B,R}$ [m]	$\Delta h_{reinf.}$ [%],
10000	1	0.050	4.75	1.323	0.931	29.63
10000	1	0.050	5.35	1.323	0.893	32.52
10000	1	0.050	6.70	1.323	0.733	44.60
10000	1	0.050	7.00	1.323	0.676	48.85
10000	1	0.050	7.50	1.323	0.556	57.93
10000	1	0.075	4.75	1.022	0.713	30.25
10000	1	0.075	5.35	1.022	0.682	33.33
10000	1	0.075	6.70	1.022	0.550	46.22
10000	1	0.075	7.00	1.022	0.504	50.74
10000	1	0.075	7.50	1.022	0.405	60.40
10000	1	0.100	4.75	0.850	0.584	31.28
10000	1	0.100	5.35	0.850	0.557	34.50
10000	1	0.100	6.70	0.850	0.443	47.96
10000	1	0.100	7.00	0.850	0.402	52.68
10000	1	0.100	7.50	0.850	0.317	62.72

In addition, considering the same design conditions and the geogrid with highest mechanical properties (i.e., $J_{2\%}$ = 7.5 kN/m), allowing a deeper rutting leads to an improvement of performances, in terms of percentage reductions of reinforced base aggregate layer thickness, which increase from 57.93% to 62.72% (Figure 4.34 and Table 4.19). In order to investigate the effect of the geogrids 'mechanical proprieties on the Leng and Gabr (2005) model in Figure 4.35 the design curves related to both the unreinforced and reinforced base layer thickness are reporting as a function of the tensile stiffness, $J_{M,2\%}$; (from 4.75 to 7.50 kN/m), keeping constant the number of vehicular repetitions (N_{cycles} = 10000), and of the subgrade CBR value (CBR = 1%). Each curve refers to one allowable rut depth (r = 0:050 ÷ 0.100 m).

Given the reduction of the required thickness with the increasing of the allowable rut depth, as previously seen, the results obtained show that geosynthetics with higher mechanical properties are more effective, at the same design conditions (i.e., subgrade CBR and traffic conditions). This is more evident when considering the maximum value of the rut depth (r=0.100m) since the reinforcement mechanism is due to the combination of the membrane effect and the lateral confinement effect (see Figure 4.35 and Table 4.19).

Let focus the attention on the curve related to the maximum value of rutting (i.e. r = 0.100m) (Figure 4.35, green line) for which the differences are larger because the rutting is enough deep to let the geogrid reinforcement provide the highest membrane support. It can be noticed that by increasing the geogrids' tensile stiffness from 4.75 to 7.50 kN/m the base thickness reduces from 0.584 m to 0.317 m, resulting in a reduction in absolute terms of 0.267 m (Figure 4.35 a and Table 4.19). Therefore, this leads to an improvement in terms of less aggregate material required to the reinforced base layer construction of about 43%. Thus, the choice of the stiffest geogrid results in a saving of the amount of granular material required for the construction of the reinforced base layer, which implies, consequently, to halve the costs for its realization.

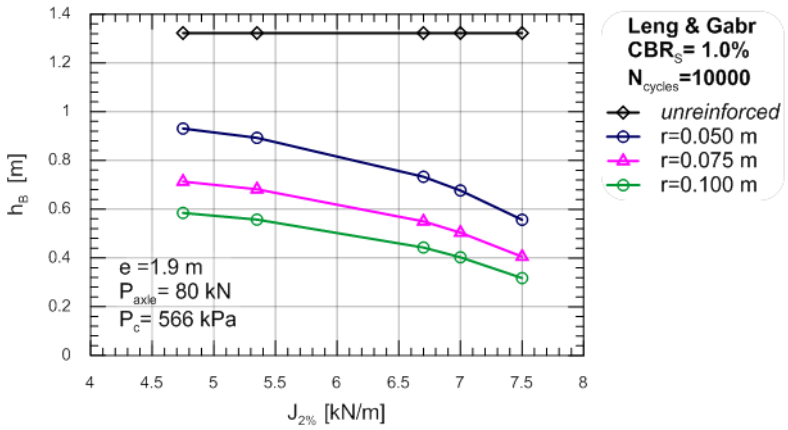

Figure 4.35 Unpaved roads design procedure by Leng and Gabr: unreinforced and reinforced base aggregate thickness versus geogrid tensile load at 2% of deformations, for fixed value of subgrade CBR (CBRs=1%) and the number of wheel passes (N_{cycles}=10000) and for each allowable rut depth chosen.

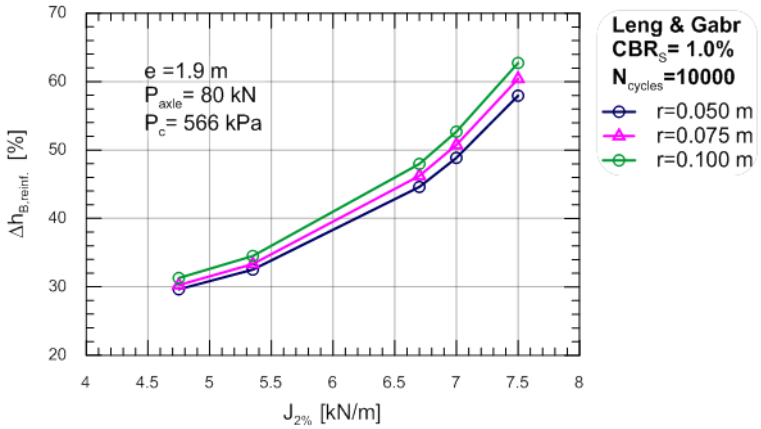

Figure 4.36 Unpaved roads design procedure by Leng and Gabr: percentage reduction of the reinforced base layer thickness versus geogrid tensile load at 2% of deformations, for fixed value of subgrade CBR (CBRs=1%) and the number of wheel passes (N_{cycles}=10000) and for each allowable rut depth chosen.

It may be also interesting to evaluate the percentage reduction of the reinforced base thickness, $\Delta h_{reinf.}$ [%], obtained by the use of geogrid, considering the same design conditions previously described. In particular, for the maximum allowable rut depth (i.e., r = 0.100m), which leads to greater differences, the geogrid tensile load at 2% of deformations increases from 4.75 to 7.50 kN/m yielding to a more efficient use of the reinforcement, with consequent increase of the percentage reduction of the reinforced base thickness required from 31.28% to 62.72%. (see Figure 4.36 and Table 4.19).

Summarizing the obtained results it follows that, the sensitivity (or weight) of in Leng and Gabr (2005) to the design variables $J_{2\%}$ [kN/m] and r [m] in unpaved reinforced design procedure is comparable when the subgrade mechanical properties and the traffic conditions are the same.

Finally, to analyze the influence of the substrate mechanical characteristics, Figure 4.37a ÷ Figure 4.37c show the unreinforced and reinforced base aggregate thickness varying the subgrade CBR (from 0.5% to 3.5%), for fixed value of allowable rut depth (r=0.075m) and for each geogrid chosen (characterized by increasing values of $J_{2\%}$ from 4.75 to 7.50 kN/m). To this scope, three values of the number of wheel passes were chosen (i.e. 100, 1000 and 10000).

As expected, the increase in the required base aggregate thickness becomes evident as the number of vehicular load passes increase. Anyway, at the same traffic conditions, the decrease of the base layer thickness, reinforced and not, as the subgrade mechanical characteristic increase and using geogrids with higher mechanical characteristics in shown in Figure 4.37 a ÷ Figure 4.37 c.

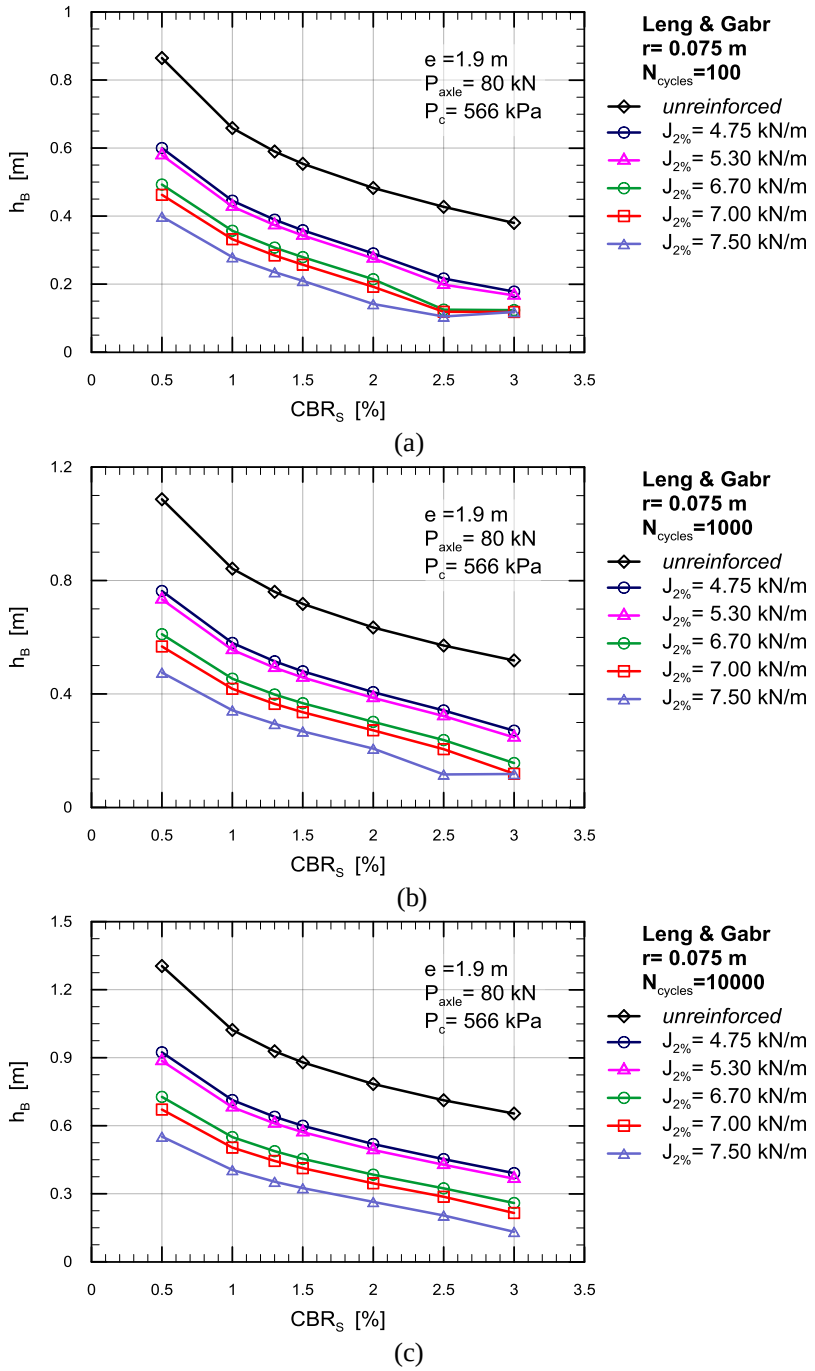

Figure 4.37 Unpaved roads design procedure by Leng and Gabr: unreinforced and reinforced base aggregate thickness versus subgrade CBR at the same value of allowable rut depth (r=0.075m) for each geogrids chosen and for a number of wheel passes equal to: a) 100; b) 1000; c) 10000.

4.7. Comparison between Giroud and Han (2004) and Leng and Gabr (2005) unpaved roads design procedures: analysis of results

This section is dedicated to the comparison between the Giroud and Han (2004) and the Leng and Gabr (2005) unpaved roads design procedures, through a careful analysis of the obtained results.

In particular, in this comparison three extruded bi-oriented geogrids with different mechanical properties, were selected. Their mechanical characteristics, summarized in Table 4.20, are expressed in

terms of aperture stability modulus, J_{AS} [mN/°], as done by Giroud and Han (2004), and in terms of geogrid tensile load at 2% of deformation, $J_{2\%}$ [kN/m], as done by Leng and Gabr (2005).

Table 4.20 Mechanical properties of the geogrids, commercially available, used in design procedures.

Geogrid	Direction	Tensile Strength at 2% of Strain (kN/m)	Average Tensile Strength at 2% of Strain $J_{M,2\%}$ (kN/m)	Tensile Strength at 5% of Strain (kN/m)	Geogrid Stiffness, $J_{2\%}$ (kN/m)	Geogrid Stiffness, $J_{5\%}$ (kN/m)	Aperture Stability Modulus, J_{AS} (m-N/deg)
GG1	MD	4.1	5.35	8.5	205	170	0,32
	TD	6.6		13.4	330	268	0,32
GG2	MD	6	6.70	11.7	300	234	0.48
	TD	7.4		14.6	370	292	0.48
GG3	MD	6	7.00	11.8	300	236	0.65
	TD	9		19.6	450	392	0.65

The others design parameters related to the allowable rut depths, subgrade mechanical characteristics and traffic conditions are given below.

According to the serviceability criteria offered by AASHTO design guidelines (AASHTO 1993), three allowable rutting values equal to 0.050m, 0.075m and 0.100 m were chosen.

Moreover, geosynthetics with reinforcement function in unpaved roads are recommended only for weak subgrades, characterized by California Bearing Ratio (CBRs) less than 3%, thus, in the present analysis, CBR varying from 0.5% to 3% was used. About the axles and loads design parameters, the wheel load (P) is the load applied by one of the wheels, in the case of single-wheel axle, or the load applied by a set of two wheels, in the case of dual-wheel axles and it is considered to be half of the axle load (P_{Axle}). In this analysis P_{Axle} =80 kN, so P=40 kN and a tire contact pressure (P_c) equal to 556 kPa, were assumed. The traffic, being vehicular traffic channelized, has been assumed characterized by the number of passes (N_{cycles}) of a given axle during the road design life. The analysis conducted expected a maximum number of load applications equal to 10000.

Generally, the required thickness for both unreinforced and reinforced base layer, considering the same subgrade mechanical characteristics and allowable rut depth, is seen to increase as the number of wheel load cycles (N_{cycles} = 1 ÷ 10000) increase and the geogrid mechanical proprieties decrease (Figure 4.38 and Figure 4.39).

In addition, Figure 4.40 shows the increase in unreinforced and reinforced base aggregate thickness ($h_{B,unrenif}$ and $h_{B,reinf}$) with the increase of the number of vehicular load cycles and with the decrease of the geogrid mechanical properties (respectively in terms of geogrid tensile stiffness, for the Leng and Gabr (2005) method, and in terms of aperture stability modulus for the Giroud and Han (2004) one), keeping constant the design conditions (i.e., subgrade CBR and allowable rut depth).

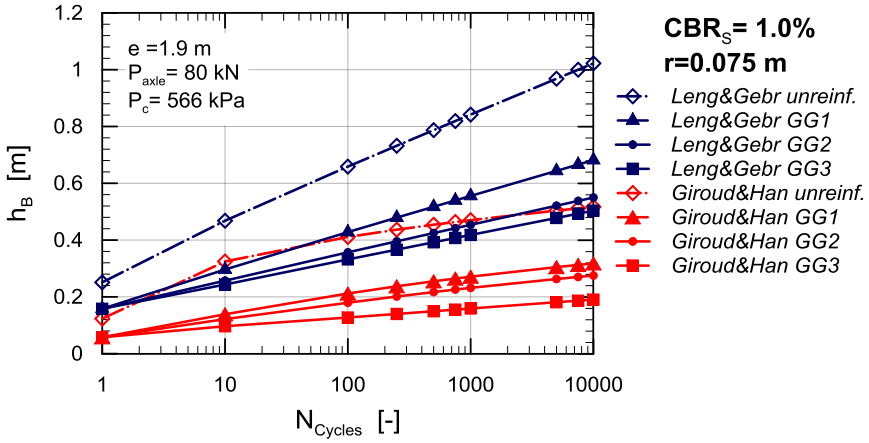

Figure 4.38 Comparison between Giroud and Han and Leng and Gabr unpaved road design procedures: reinforced base aggregate thickness versus number of wheel passes for fixed value of Subgrade CBR (CBRs=1%) and for extremal values of geogrids' mechanical properties, when the allowable rut depth is 0.075 m

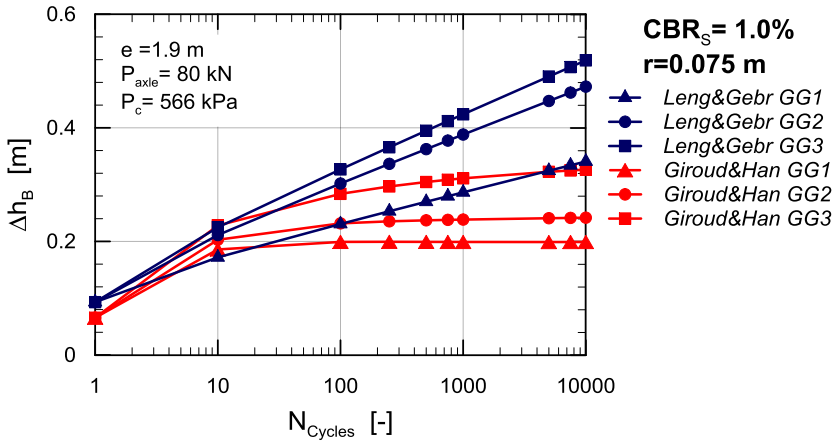

Figure 4.39 Comparison between Giroud and Han and Leng and Gabr unpaved road design procedures: unreinforced and reinforced base aggregate thickness reduction versus number of wheel passes for fixed value of Subgrade CBR (CBRs=1%) and for each geogrids chosen, when the allowable rut depth is 0.075 m

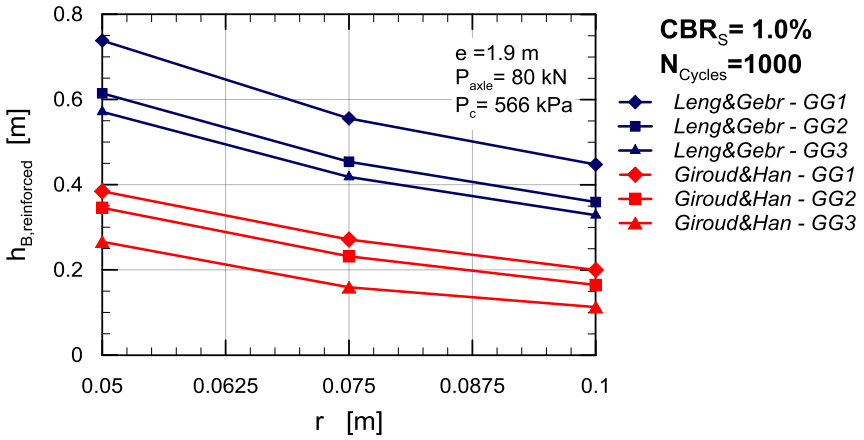

Figure 4.40 Comparison between Giroud and Han and Leng and Gabr unpaved road design procedures: reinforced base aggregate thickness reduction versus allowable rut depth, at the same traffic conditions (N_{cyles}=1000), for fixed value of Subgrade CBR (CBRs=1%) and for each geogrids chosen

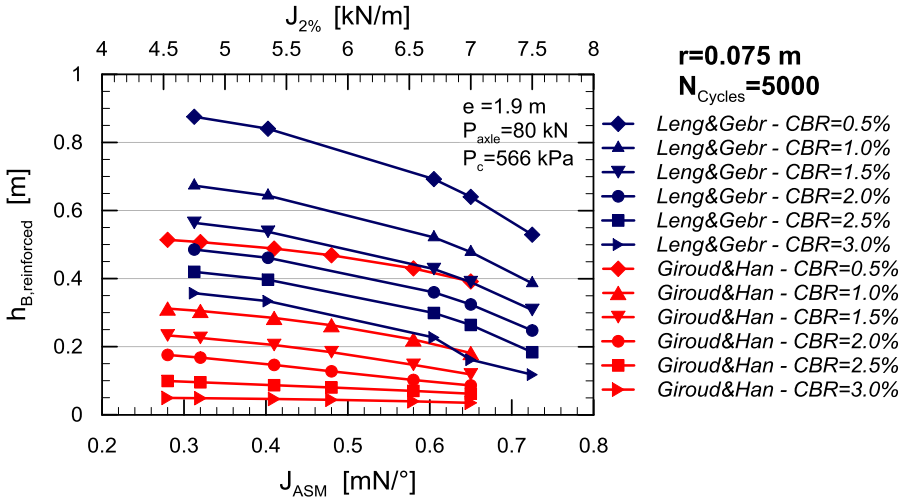

Figure 4.41 Comparison between Giroud and Han and Leng and Gabr unpaved road design procedures: reinforced base aggregate thickness reduction varying the geogrids' mechanical properties, at the same traffic conditions (N_{cyles}=1000) and allowable rut depth and for each Subgrade CBR chosen

Furthermore, Figure 4.39 shows that the highest improvement offered by the reinforcement, in terms of reduction of the reinforced base layer thickness, is offered by Leng and Gabr (2005) method. The results, moreover, confirm that there is higher efficiency when the geosynthetic, placed at based-substrate interface, possesses higher mechanical characteristics. The consequence is more benefits in terms of saving of aggregate material needed for the base layer construction.

For both the proposed design method the aggregate base thickness increase with the increase of the rutting, and all the depth values of rutting chosen (r = 0.050 m ÷ 0.100 m) appear to be large enough to let the geosynthetic layer work providing a reinforcement support proportional to its own mechanical characteristic (Figure 4.40). This suggests that the reinforced base performances better thanks to the lateral restraint of the base soil, which develops for more reduced rut depths, and it is, therefore, always the first mechanism to be activated. Then, by increasing the rut depth, the membrane mechanism that requires higher values of geosynthetic deformation to be achieved could take over.

Figure 4.41 confirms that, at equivalent traffic capacity and serviceability conditions, the geogrid benefits increase as the subgrade mechanical proprieties decrease and by using stiffer geogrids.

By analyzing the results obtained by different combinations of the design parameter (i.e., traffic conditions, CBR subgrade, geogrid mechanical characteristics and allowable rutting; Figure 4.38 ÷ Figure 4.40) it becomes evident that the Leng and Gabr (2005) design procedure is more conservative with respect to the Giroud and Han (2004) one. The reason is probably the former design procedure takes into account the degradation of the stress distribution angle with the number of cycles as well as the effect of the wheel load repetitions on the degradation of the elastic modulus ratio (E1/E2). This ratio is very important because it governs the distribution of the vertical stresses on subgrade and consequently the amount of the vertical subgrade deformation developed.

Therefore, the amount of improvement thanks to the reinforcement effect has been related to a Performance Index (PI), previously defined in Eq. 4.3.

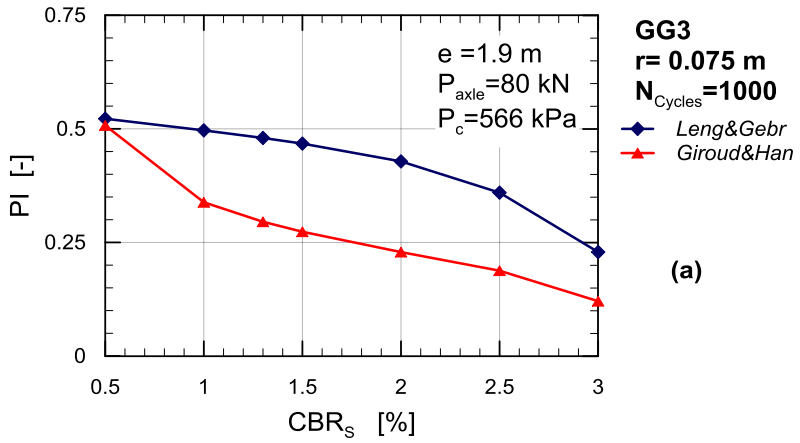

Figure 4.42 Comparison between Giroud and Han and Leng and Gabr unpaved road design procedures in term Performance Index (PI).

Figure 4.42 reports PI versus subgrade CBR, for the same design conditions in terms of equivalent traffic capacity, allowable rutting and geosynthetic reinforcement used. It is noteworthy that the Leng and Gabr (2005) design procedure is associated to higher PI than Giroud and Han (2004) method with average differences of about 40%.

Finally, in Figure 4.43, the above discussed procedures are compared with field data offered by Fannin and Sigurdsson (1966). Field tests were performed using a geogrid with $J_{2\%}$=4.75 kN/m placed on a subgrade characterized by a CBR of about 1.3%. It can be noted that, both in the case of unreinforced and reinforced base layer, the aggregate base thickness by Leng and Gabr (2005) design procedure and by Giroud and Han (2004) method represent respectively the upper and lower bound limits of the experimental field data.

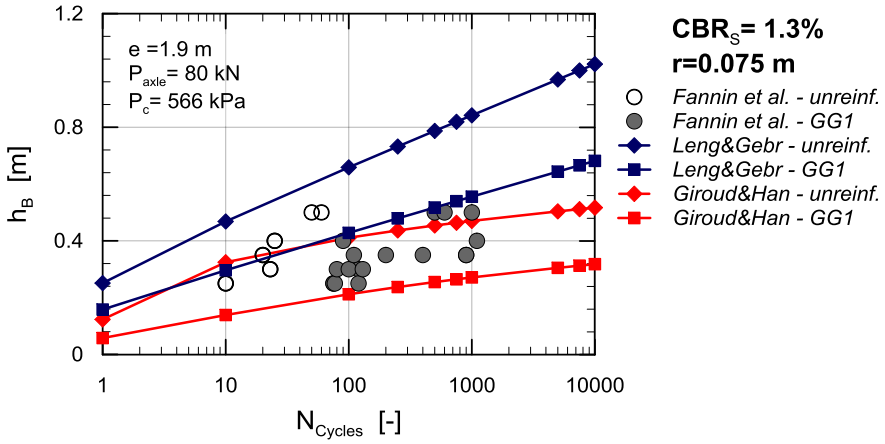

Figure 4.43 Comparison between theoretical results obtained by above procedures and experimental field data obtained by Fannin (1966).

Anyway, both the models have a limitation consisting in their calibration, which was carried out exclusively using two geogrids' types (GG1 and GG3). Therefore, it would be necessary a more wide experimental investigation on different types of geogrids to obtain a wide database in order to make the design method more general and applicable to any type of reinforcement geogrid. In addition, since

interlocking likely plays a key role in the behavior of unpaved roads, it can be said that the shape and mainly the scale effect can affect deeply the behavior of unpaved roads, too. Therefore, a more complete calibration should be developed taking into account, in addition to the geogrid mechanical properties, the average size of the base particles (D_{50}) together with the size of the geogrid openings and the rib thickness and profile. These aspects could be further potential research subjects.

4.8. 3D-FEM analysis of a reinforced unpaved road

After having carefully analyzed the unpaved roads reinforced by means of geosynthetics design procedures a 3D-FEM analysis has been performed by using the ABAQUS software and considering an unpaved road section reinforced by means of a geogrid, then compared to a non-reinforced one in order to evaluate the benefits offered by the geogrid in terms of reduction of the rut depth.

Many problems in engineering and science involve complicated systems of differential equations which are too difficult to exactly solve due to their complex geometry. Finite element analysis, which has evolved over the past three decades, involves a method of breaking up a continuum into discrete, coupled components that approximate the overall solution. The geometric domain is broken into these non-overlapping coupled components called elements. These elements are represented by a linear combination of polynomial functions with undetermined coefficients, which form the approximate numerical solution to the governing differential equations. The undetermined coefficients are represented by nodes, which are located on the element. The solutions are found at these nodes using the polynomial functions and prescribed boundary conditions.

Because the local form of the solution needs to be kept simple, accuracy is increased by making the elements as small as possible. This makes the approximation defined by a larger number of equations, which increases with every increase in the number of elements used. However, it reduces the differential equation into many algebraic equations, which leads to the possibility of solving more complicated problems. Although finite element analysis was originally done with personally written computer programs to carry out the analysis, there are many commercially available computer programs now which eliminate the need to write an individual code.

ABAQUS, like ANSYS or PLAXIS, are the general-purpose finite element programs that can provide proper analyses of various engineering problems. Although pavement structural modeling has developed widely in recent years, pavement analysis with general-purpose programs has not been applied to unpaved road modeling frequently.

ABAQUS is used in the automotive, aerospace, and industrial products industries. The product is popular with academic and research institutions due to the wide material modeling capability, and the program's ability to be customized. It performs static and/or dynamic analysis and simulation of complex engineering and non-engineering problems. It can deal with bodies with various loads, temperatures, contacts, impacts, and other environmental conditions. ABAQUS also provides a good collection of multiphasic capabilities, such as coupled acoustic-structural, piezoelectric, and structural-pore capabilities, making it attractive for production-level simulations where multiple fields need to be coupled.

ABAQUS was initially designed to address non-linear physical behavior; as a result, the package has an extensive range of material models.

Every complete finite-element analysis in ABAQUS consists of 3 separate stages:

- Pre-processing or modeling: This stage involves creating an input file which contains an engineer's design, in this case the unpaved road section, for a finite-element analyzer (also called "solver").
- Processing or finite element analysis: This stage produces an output visual file.
- Post-processing or generating report, image, animation, etc. from the output file.

ABAQUS conducts a geometric model analysis. This analysis has three stages: (1) a consideration of applicable geometry; (2) a consideration of material properties; and (3) and the generated mesh. The first stage of analysis occurs with ABAQUS creating an input file of the relevant geometry. The second stage takes the input file and performs the initial analysis by sending data through simulation. The data is then recorded and the output file generated. The third stage involves this output file being modified for specific visualization. This stage is where the analysis has been finalized for viewing.

Each of these stages can be further examined through a specific implementation of modules. ABAQUS has 11 modules (Figure 4.44) that are commonly known as: part module, property module, assembly module, steps module, interaction module, load module, mesh module, job module, sketch module and visualization module. As it is shown in the picture, ABAQUS cae has 11 modules which will be used one after the other in order to modeling, loading, defining boundary conditions and finally analysis and after show the results.

Several numerical studies were performed to analyze pavement sections and assess the improvements due to the geosynthetic reinforcement. Most of the numerical studies were performed using the finite element method. Different constitutive models were used to determine the model that is most capable of representing the stresses and deformations in a reinforced pavement.

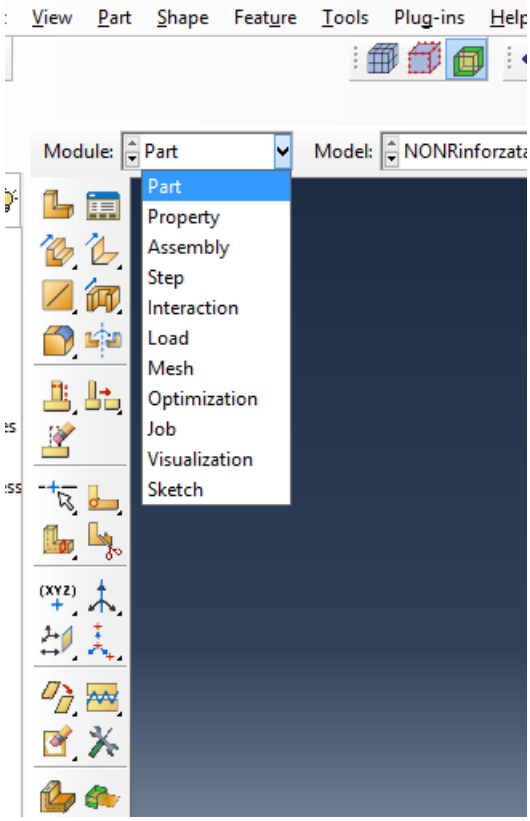

Figure 4.44 ABAQUS modules

Dondi (1994) used ABAQUS software package to conduct a three dimensional finite element analysis to model the geosynthetic reinforced pavements. The results of this study indicated that the use of the reinforcement resulted in an improvement in the bearing capacity of the subgrade layer and a reduction in the shear stresses and strains on top of it. In addition, the vertical displacements (rutting) was also reduced by 20 to 30 % due to the intrusion of geosynthetic reinforcement.

Nazzal et al. (2010) developed a finite-element model with ABAQUS software package to investigate the effect of placing geosynthetic reinforcement within the base course layer on the response of a pavement structure. Finite-element analyses were conducted on different unreinforced and geosynthetic reinforced pavement sections. The results of this study demonstrated the ability of the modified critical state two-surface constitutive model to predict, with good accuracy, the response of the considered base course material at its optimum field conditions when subjected to cyclic as well as static loads. The results of the finite-element analyses showed that the geosynthetic reinforcement reduced the lateral strains and rutting within the base course and subgrade layers. Furthermore, the inclusion of the geosynthetic layer resulted in a significant reduction in the vertical and shear strains at the top of the subgrade layer.

Work conducted in the end of the research aims at numerically analyzing the performance of base course layer reinforced with geosynthetic placed over soft subgrade. Road engineers often cite the problem of soft subgrade as one of the main causes of construction and maintenance difficulty base course layer placed on a poor subgrade is prematurely subject to excessive permanent deformation during and after construction, and hence cannot achieve the expected performance. If, at the time of construction of the base course and throughout the life of the pavement, moisture control such as drainage or drying is not practical

or insufficient, the soft subgrade soil may become difficult to compact, unable to sustain heavy construction equipment traffic, or render compaction effort of the overlaying aggregate ineffective. For pavement built on such a poor subgrade, excessive permanent deformation, rutting, and cracking can be expected.

The finite element modeling approach offers the best method of analysis for multilayered pavement systems. Three-dimensional and two-dimensional or axisymmetric finite element models have different element formulation and consider different directional components of stresses and strains. Three-dimensional finite element analysis can consider all three directional response components and should predict more accurate pavement responses.

An 3D Finite Element Method (FEM) analysis using the computer program ABAQUS is conducted to model reinforced and unreinforced unpaved road, by modelling its dimensions, layers' characteristics and different meshing, to compare an unreinforced section with a reinforced section in terms of surface rutting. The numerical results obtained from section reinforced with geogrid has compared with unreinforced sections to evaluate the improvement offered by geogrid in terms of reduction of surface rut.

Despite the fact that it requires considerably more computational time and computer memory, the 3D analysis is still considered superior to the 2D. The necessity for adopting the 3D analysis arises from the following advantages:

1) It better reflects the complex behavior of the composite pavement system materials under different configurations traffic loads;

2) It is preferred when verifying numerical model results with laboratory or field test results;

3) It allows the simulation of the loaded wheel rectangular footprint [Bassam Saad, 2005].

To create an unpaved rod section in ABAQUS many attributes, such as stratigraphy, boundary conditions, material properties, and loads were modeled as closely as possible to those present in the literature. In the following paragraphs are described all the steps to realize the finite element analysis using ABAQUS software.

4.9. 3D FEM modeling of unpaved structure

As mentioned in the research objective, FEM was used in this study to understand geosynthetic behavior in unpaved road and to evaluate the improvement offered by geosynthetic in terms of reduction of surface rut. A 3-D FE model was constructed using the software ABAQUS through these module:

- Part module;
- Material property module;
- Assembly and interaction module;
- Load and boundary module;
- Mesh module;
- Job module.

4.9.1. Part Module

The part module is the base element of ABAQUS. The part module creates each of the parts that the assembly module later uses to assemble. The part is created using the tools section of the software. The part is not specific to the ABAQUS tools and may also be exported from certain CAD software packages.

The unpaved section (Figure 4.45) create in 3-D ABAQUS software consisted of base course layer placed on a poor subgrade layer with a geogrid to reinforcement placed between base and subgrade.

To model the unpaved road 2 parts were instanced, simulating 5 m wide and 5m long layers with different thickness, in particular: base course thickness is 0.2 m and subgrade thickness is 0.9 m.

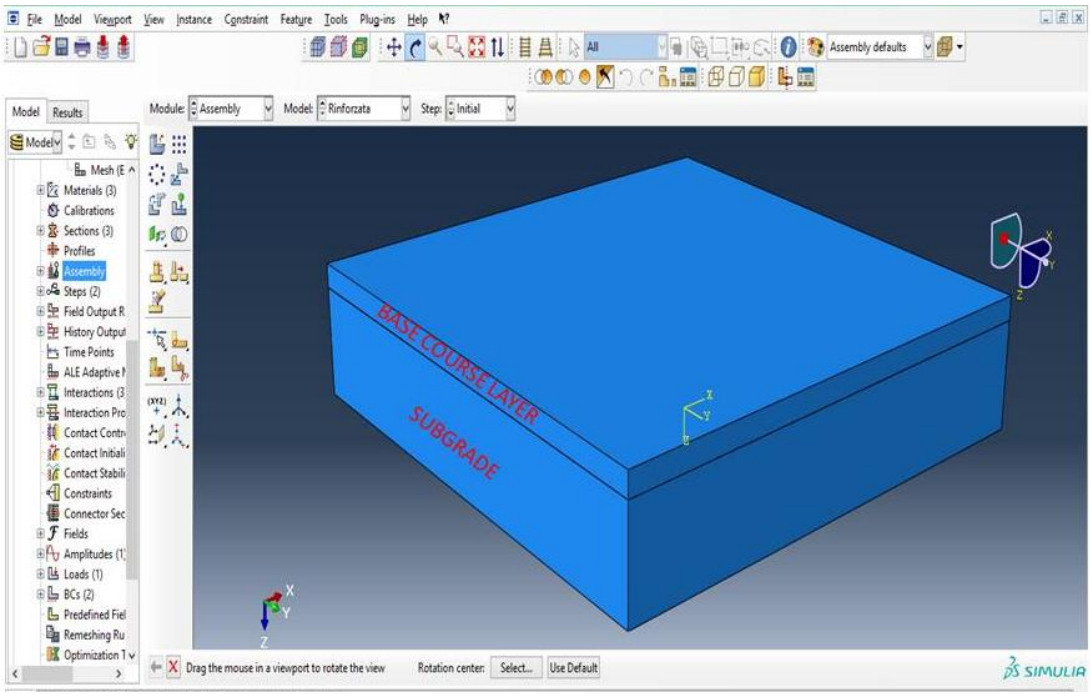

Figure 4.45 Unpaved road system created in ABAQUS CAE

Base course layer and subgrade were modelled by using 3D deformable solid homogeneous elements.

The geogrid, placed between the base course and the subgrade, has been modelled as 5 m wide layer with a thickness of 0.003 m and with open meshes (Figure 4.46).

Model dimensions have been selected to reduce any edge effect error, keeping the elements' sizes within acceptable limits.

Geogrid was modelled by using 3D membrane elements that have a tensile modulus transmitting tensile force only.

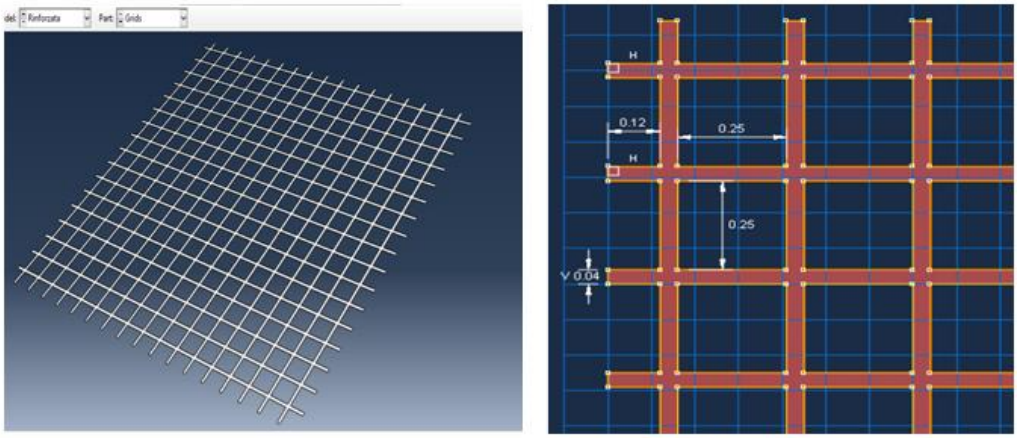

Figure 4.46 Geogrid element realized in part module

4.9.2. Material property module

Different material models need to be employed to describe the behavior of different materials and the geogrid interface in the unpaved system. The following section will describe the models' parameters used in the finite element analysis. The materials data required for the simulations have been assumed to represent realistic material properties.

Unpaved roads usually experience relatively large deformation under traffic load, while base course and subgrade showing significant plastic behaviors. So nonlinear constitutive models are needed to simulate behaviors of granular materials under large deformation. For unpaved roads with aggregate base course over subgrade, traditional linear elastic method or nonlinear elastic methods can't simulate yielding due to tensile stress generated at the bottom of the base course layer.

Plastic deformation of aggregate base course layer has a defining role in determining pavement performance. A majority of rutting in subgrade layer happens due to permanent deformation of the base course layer. Therefore, an accurate model should consider plastic behavior of the layers. There are 13 plasticity models in ABAQUS: plastic, cap plasticity, cast iron plasticity, clay plasticity, concrete damage plasticity, concrete smeared cracking, crushable foam, Drucker Prager, Mohr Coulomb plasticity, porous metal plasticity, creep, swelling, and viscous. For unpaved roads Drucker Prager and Mohr Coulomb plasticity are the most common models that have been used for the base course and subgrade layer.

Based on previous analyses an extended Drucker-Prager model with hyperbolic yield criterion is used in this research. The model is available in Abaqus/Standard.

Drucker-Prager models are used to model frictional materials such as granular-like soil, rock, and asphalt concrete. Drucker-Prager model can also be used to model materials in which compressive yield strength is greater than the tensile yield strength. They allow materials to harden or soften isotropically and allow volume change with inelastic behavior (ABAQUS, 2014). Yield criteria for Drucker-Prager models are based on the shape of the yield surface in the meridional plane. The yield surface can have a linear form, hyperbolic form, or general exponent form (Figure 4.47)

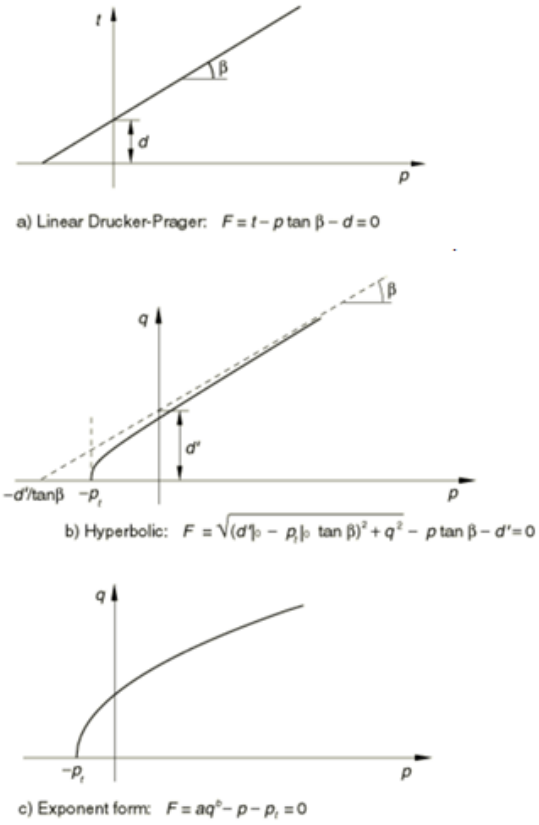

Figure 4.47 Yield surface in Drucker-Pracker model

The hyperbolic yield criterion is a continuous combination of maximum tensile stress condition of Rankine (tensile cut-off) and the linear Drucker-Prager condition at high confining stress, as shown in Figure 4.47 b). The yielding criterion is expressed as:

$$F = \sqrt{(d'_{|o-p_t|}tan\beta)^2 + q^2} - ptan\beta - d' = 0 \qquad \text{(Eq. 4.4)}$$

Where, p and q are the two stress invariants, $p_{t|0}$ is the initial hydrostatic tension strength of the material, $d_{'|0}$ is the initial v1alue of d' (a hardening parameter related to the initial yielding stress), and β is the slope of the yield surface in the p-q stress plane.

In a triaxial compression test, p = 1/3(σ1+2σ3), q = σ1-σ3. The extended Drucker-Prager model parameters (β and initial compression yielding stress σ0c) can be derived from Mohr-Coulomb model parameters (φ and c). For the material with low friction angle (less than 22°), parameters can be determined as follows:

$$\beta = tan^{-1}\left(\frac{6sen\varphi}{3-sen\varphi}\right) \qquad \text{(Eq. 4.5)}$$

$$\sigma_c^0 = 2c\left(\frac{cos\varphi}{1-sen\varphi}\right) \qquad \text{(Eq. 4.6)}$$

For the material with high friction angle, the above equations may provide a poor match with the Mohr-Coulomb parameters, and β can be approximated as equal to φ value.

The hyperbolic model provides a nonlinear relationship between deviatoric and mean stress at low confining pressures, which may provide a better match for the triaxial experimental data. Isotropic hardening and unassociated flow rules are also used. Flow potential (G) is chosen in these models as a hyperbolic function as follows(Hibbitt, Karlsson & Sorensen, Inc., 2001):

$$G = \sqrt{(\varepsilon\sigma Io - tan\psi)^2 + q^2} - ptan\psi \qquad \text{(Eq. 4.7)}$$

Where, ψ is the dilation angle measured in the p-q plane at high confining pressure; σ|0 is the initial equivalent yield stress; and ε is a parameter, referred to as the eccentricity, that defines the rate at which the function approaches the asymptote (the flow potential approaches to a straight line as the eccentricity approaches to zero). The function asymptotically approaches the linear Drucker-Prager flow potential at high confining stress and intersects the hydrostatic pressure axis at 90°(ABAQUS, 2014).

A linear elastic model instead was used to describe the behavior of geogrid material since the induced strain in the geogrid is very small (<1%) and is considered within the linear elastic range of the geogrid layer.

Based on previous studies the mechanical characteristics used for the various layers are shown in Table 4.21

Table 4.21 Mechanical characteristics using for unpaved section

	Base	*Subgrade*	*Geogrid*
Modulus of elasticity [Pa]	50 e^6	10 e^6	100 e^9
Poisson's ratio	0.35	0.35	0.42
Friction angle [°]	40	20	
Angle of dilation [°]	10	0	
Initial tension [kPa]	150	43.6	

4.9.3. Assembly and interaction module

After defining the geometry and the mechanical properties of the various parts the assembly and features interface assignment have been done.

The parts from the part module are combined in the assembly module. Each of the parts created has a specific place in the system that the assembly module combines. When placed appropriately, the parts constitute the assembly section. The assembly-specific combination is formed with a one-way negotiation on how each part aligns selected vertices, edges, or faces; this is also done through rotation or translation of the part (ABAQUS 2014). In the assembly model geogrid was placed on the top of subgrade like shown in Figure 4.48 .

The interface mechanical characteristics are very important because they significantly affect the response of the model depending on the type of contact that is considered.

The interaction between the geogrid and the adjacent soil layers, including aggregate base and subgrade layers, is complex. This mechanism involves the upward movement of fine subgrade particles into the apertures of geogrid reinforcement. At the same time, the aggregate material becomes locked inside the

grids and the geogrid apertures prevent the downward movement of the aggregate. With proper soil compaction efforts, geogrid reinforcement and the effect of aggregate interlocking with the geogrid can prevent the upward movement of subgrade particles.

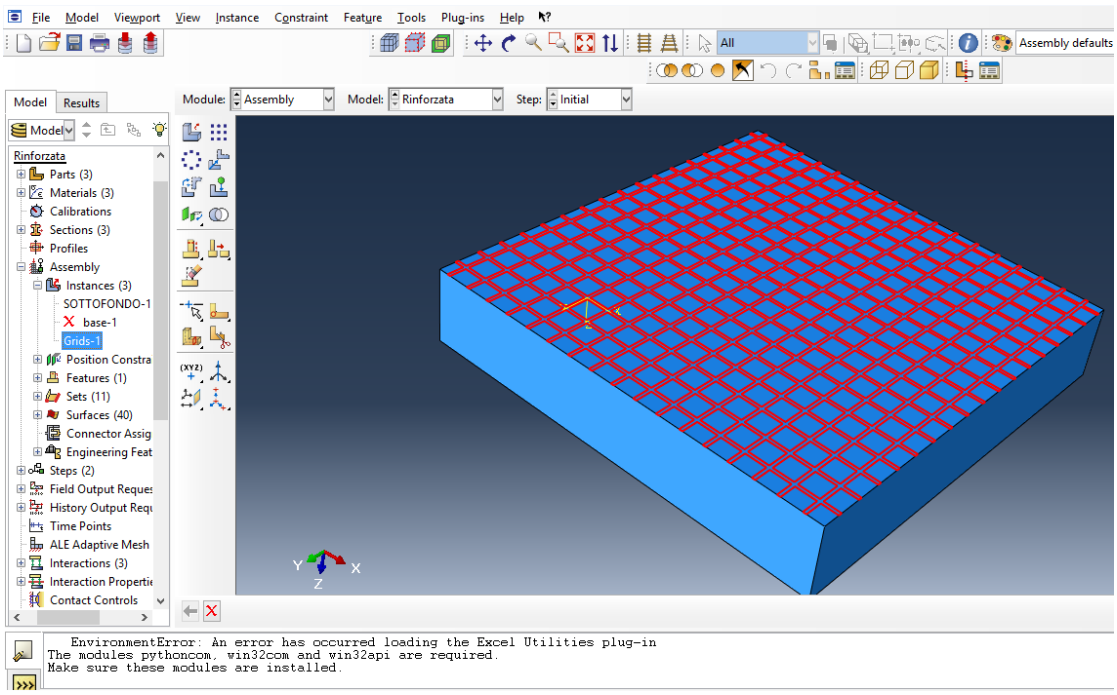

Figure 4.48 Geogrid placed at the top of subgrade in assembly module

So as regards the behavior at the interface between geogrid and soil and between base course and subgrade the interaction is constituted by the tangential and normal component.

For the normal component, the hard contact type behavior has been considered while in the tangential direction a Coulomb friction model was used to simulate the shear-resistance interaction between geogrid reinforcement and soil.

An friction coefficients of 0.5, corresponding to interface friction angles of approximately 27°, were used for the interface between the geogrid and base course aggregate and an elastic slip of 0.001 m was selected to represent the magnitude of elastic shear displacement allowed along the interface between geogrid and aggregate. The same features have been used for all interface.

4.9.4. Load and boundary module

The traffic load is considered as the main factor in designing the unpaved roads system. This includes axial loads, configuration of axles, tire contact areas, number of load repetitions, vehicle speed.

Heavy vehicles, such as trucks, significantly influence pavement distresses and failure. Regarding loading can be considered two parameters: loading duration and loading area. For loading duration, equivalent, instantaneous, and moving loading are the most common methods. Equivalent loading disregards the unloading period and applies load for the accumulative loading time. Instantaneous load assumes that load is applied on a specific area (typically at the center of the top layer) for a specific loading

time and then the load is removed to model unloading time. For loading area, wheel load can be applied on the wheel area, entire wheel path, or equivalent circular/semicircular area. In this model the traffic load has been applied in correspondence of the central part of the unpaved section, simulating a cyclic load of a twin wheel of a heavy vehicle having an axle of 80 kN. The load has been simulated as a uniform load pressure of 550 kPa that acting on a 20x20cm rectangular area (Figure 4.49).

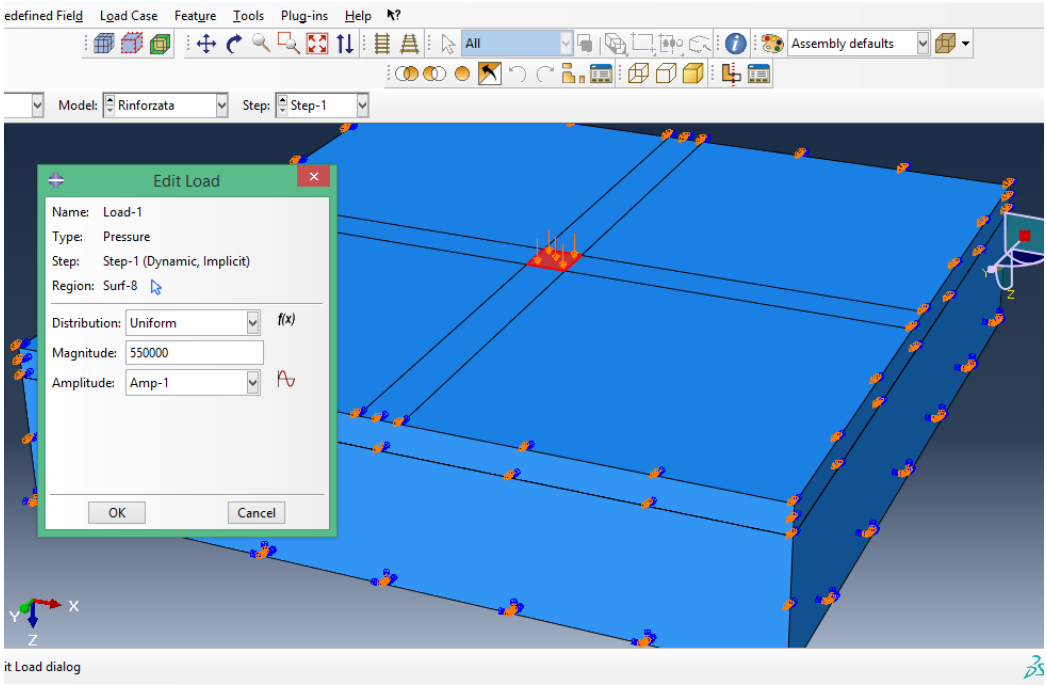

Figure 4.49 Load pressure applied

It was simulates a quasi-static loading and unloading cycle by applying pressure mentioned above. This approach reveals the maximum stresses and deformation under peak load and permanent (i.e., plastic) deformation after unloading. The application of the load impulse time is 0.01 s that is followed by 0.01 s unloading time. Loading pattern is shown in Figure 4.50.

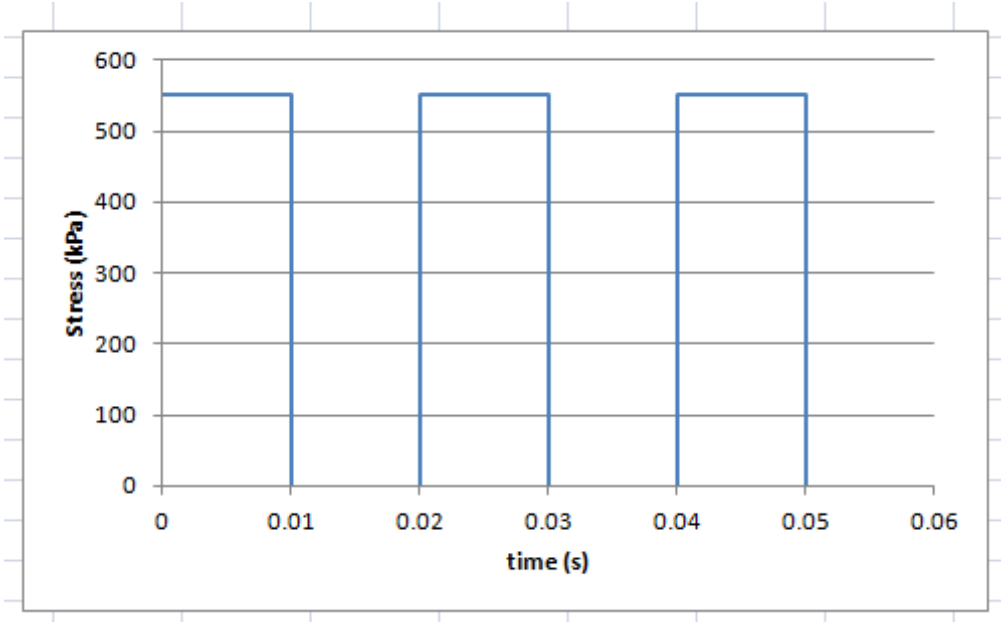

Figure 4.50 Loading pattern used to traffic load simulation

Since the boundary conditions have a significant influence in predicting the response of the model and given the size adopted, the model has been constrained at the bottom (U1 = U2 = U3 = UR1 = UR2 = UR3 = 0); X-Symm (U1 = UR2 = UR3 = 0) on the sides parallel to y-axis; and Y-Symm (U2 = UR1 = UR3 = 0) on the sides parallel to x-axis (Figure 4.51).

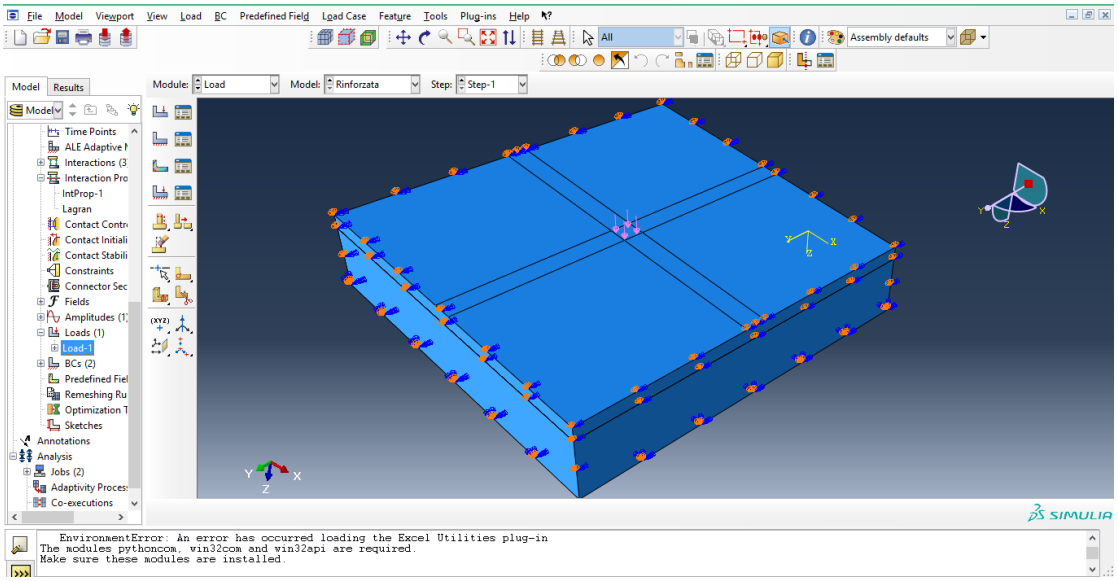

Figure 4.51 Load area and boundary conditions

4.9.5. Mesh module

The parts and assemblies created are generated into meshes within the mesh module. The mesh module has various levels of automation to ensure the mesh meets the needs of the analysis

One of the first considerations in creating a finite element model mesh is what element type to use. In ABAQUS five aspects of an element characterize its behavior: family, degrees of freedom, number of nodes, formulation, and integration. In Figure 4.52 it is shown the element families that are used most commonly in a stress analysis.

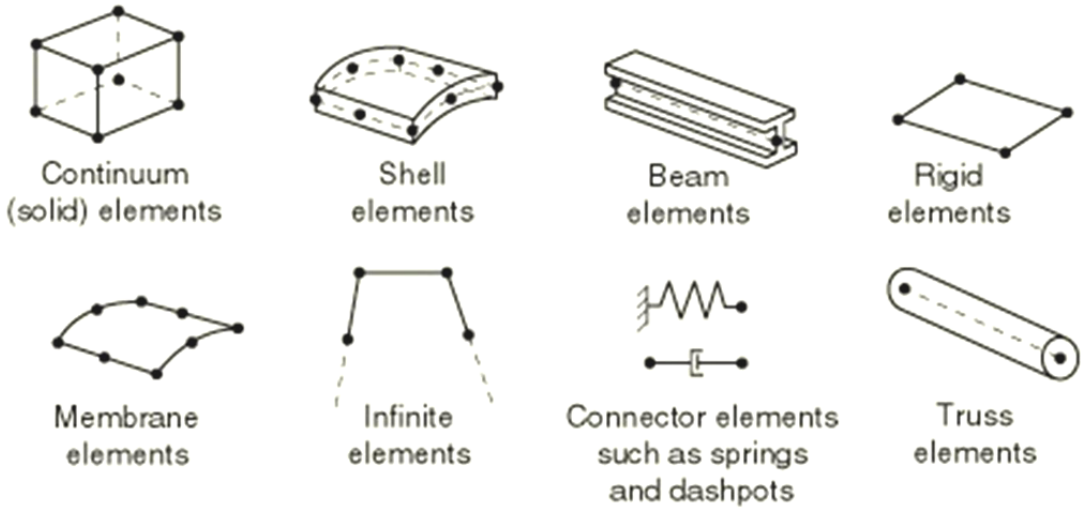

Figure 4.52 Element families in ABAQUS

For elements with nodes only at their corners linear interpolation is used between the nodes, making these linear or first-order elements while elements with midside nodes use quadratic interpolation and are called quadratic or second-order elements (Figure 4.53).

Figure 4.53 Linear and quadratic elements

Previous study indicate that increasing the number of elements in the model mesh to predict maximum rut depth on the top of base course increased computational time. Therefore, maximum element size of 10 cm was selected for base course and subgrade sections realized to reduce the computational costs and 3D eight-node first-order brick elements with reduced integration, C3D8R, to improve the rate of convergence were chosen (Figure 4.54).

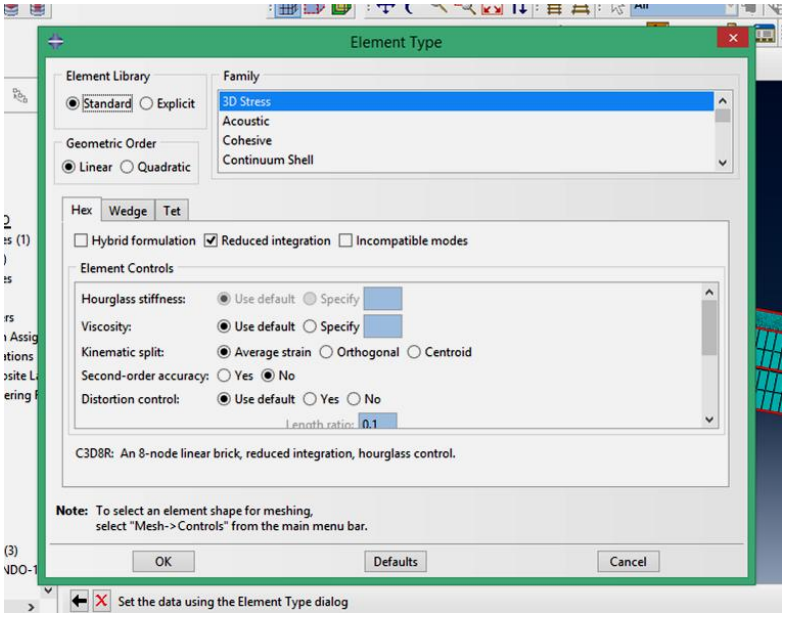

Figure 4.54 Element mesh for base course and subgrade

As shown above in Figure 4.52 there are two element types that could apply for the geogrid element: shell and membrane elements.

Shell elements are curved structural elements of constant thickness, which is small compared to the other two dimensions. The basic approach is that by integrating over the thickness, a two dimensional model is formulated on the midsurface of the shell, which approximates the three dimensional model. There are two different theories associated with shell elements, membrane theory and bending or general theory.

The membrane elements, which follow membrane theory, are used to represent thin surfaces that offer in-plane strength but no bending stiffness, for this reason the geogrid was simulated like membrane element M3D4 (ABAQUS, 2014) (Figure 4.55).

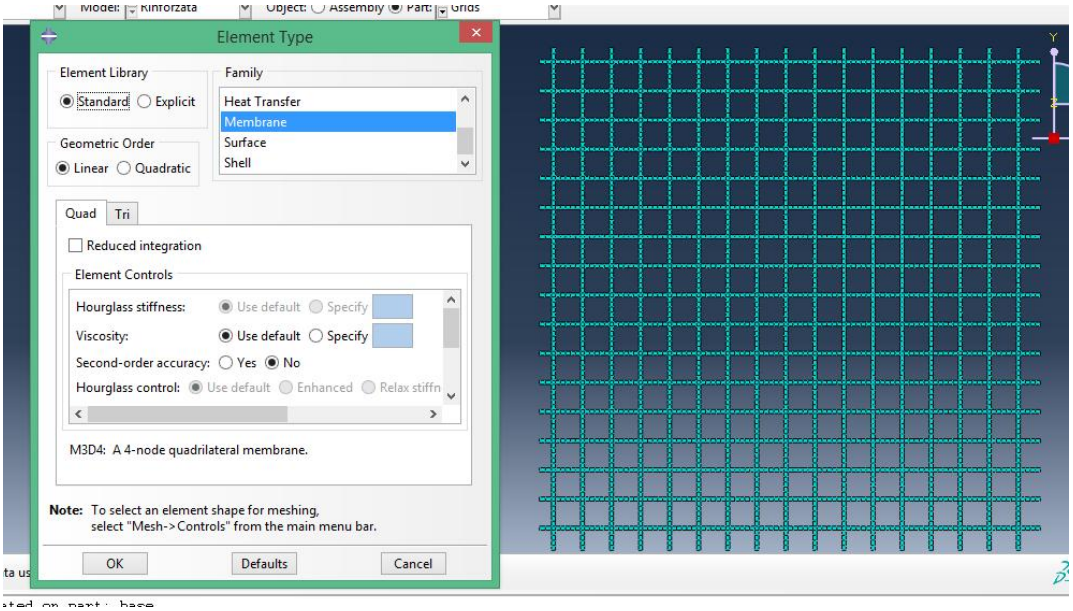

Figure 4.55 Element mesh for geogrid

4.9.6. Job module

The job module is used to analyze a model once all tasks involved in defining a model (such as defining the geometry of the model, assigning section properties, and defining contact etc.) are finished. In the Job module a job is created and submitted to Abaqus/Standard or Abaqus/Explicit for analysis, and for monitoring its progress. In the end made all previously described forms the work has been created to get the results.

4.9.7. Results and discussion

This part of the study analyzes the improvement offered by a geogrid reinforcement placed at the interface between the aggregate base course and the subgrade in terms of surface vertical displacements reduction, by means of the finite element analysis of a two-layer system.

The pavement behavior has been simulated under 500 traffic loads and the vertical displacements have been considered as a response of the traffic load applied.

Figures 4.56 and 4.57 shown the vertical surface displacement computed using the finite element analysis for an unreinforced and a geogrid reinforced section respectively after 500 load cycles.

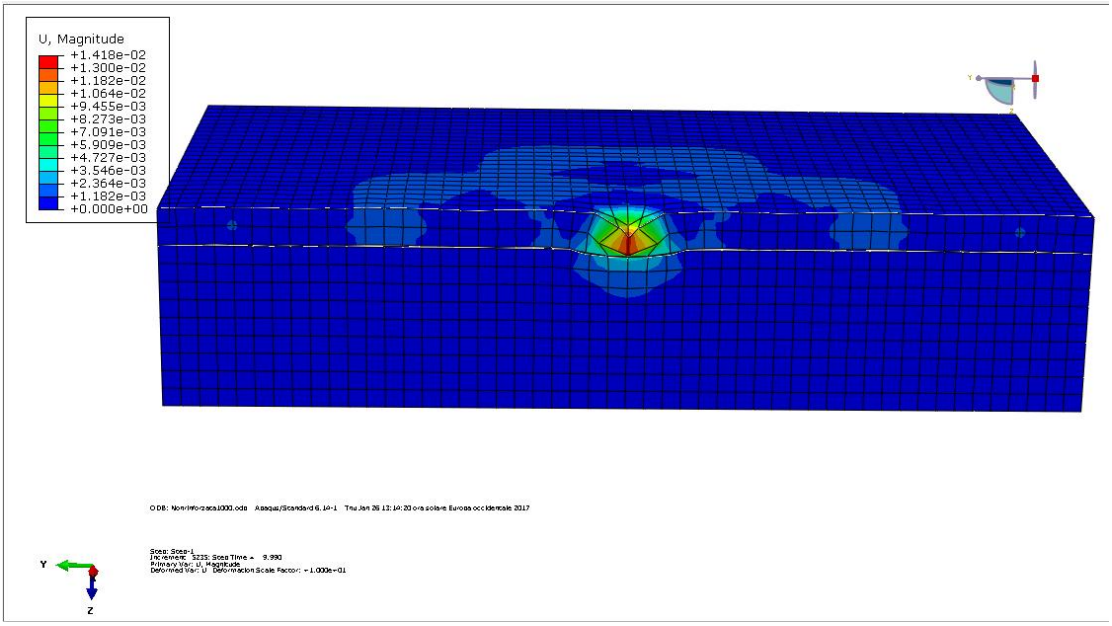

Figure 4.56 Vertical surface displacements computed using finite element analysis for unreinforced test section

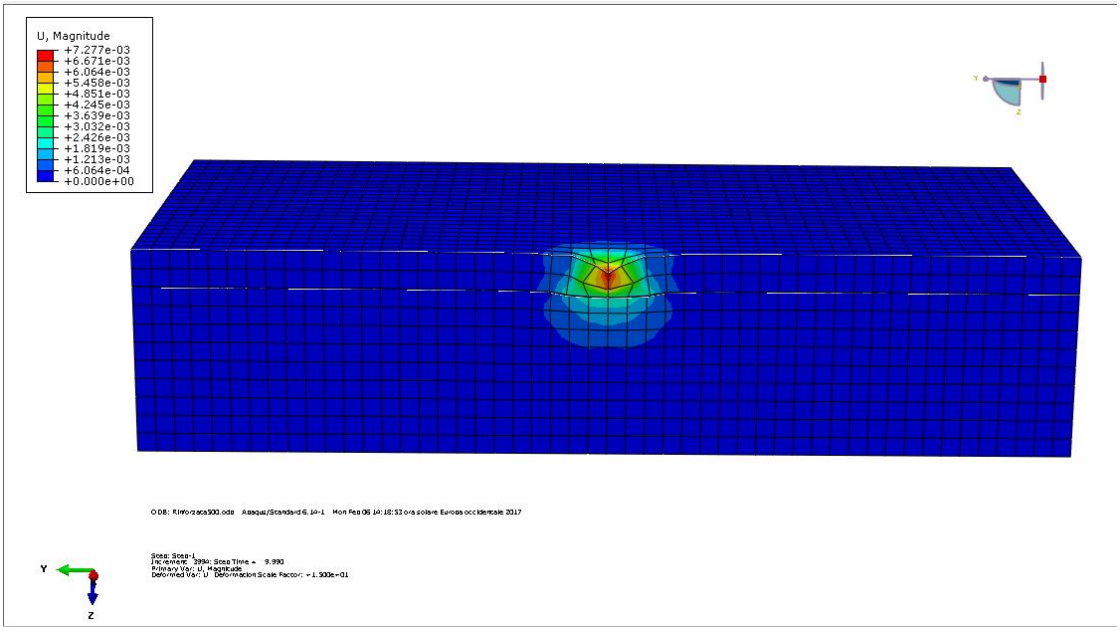

Figure 4.57 Vertical surface displacements computed using finite element analysis for reinforced test section

When examining the vertical displacements after 500 traffic load it can be observed that the results for the geogrid-reinforced test section are lower than the results obtained for the unreinforced test section. The final magnitude of the maximum surface displacements U was 7.27 mm (Figure 4.57) for the reinforced section and 14.1 mm (Figure 4.56) for the unreinforced section.

Figure 4.58 shows the geogrid configuration after 500 traffic load.

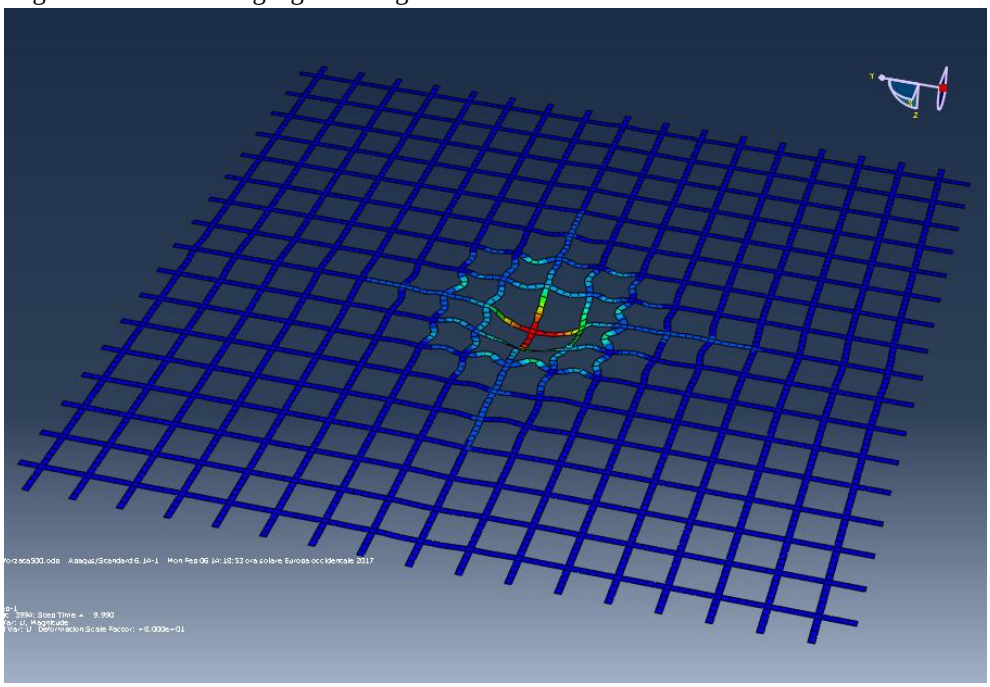

Figure 4.58 Geogrid configuration after 500 traffic load

The comparison between the reinforced (using a geogrid with tensile modulus of 100MPa) and the unreinforced rut depth (Figure 4.59) highlights that the maximum surface displacements of the base course

layer (at the center of the load area) thanks to the presence of the reinforcement was approximately the 51%.

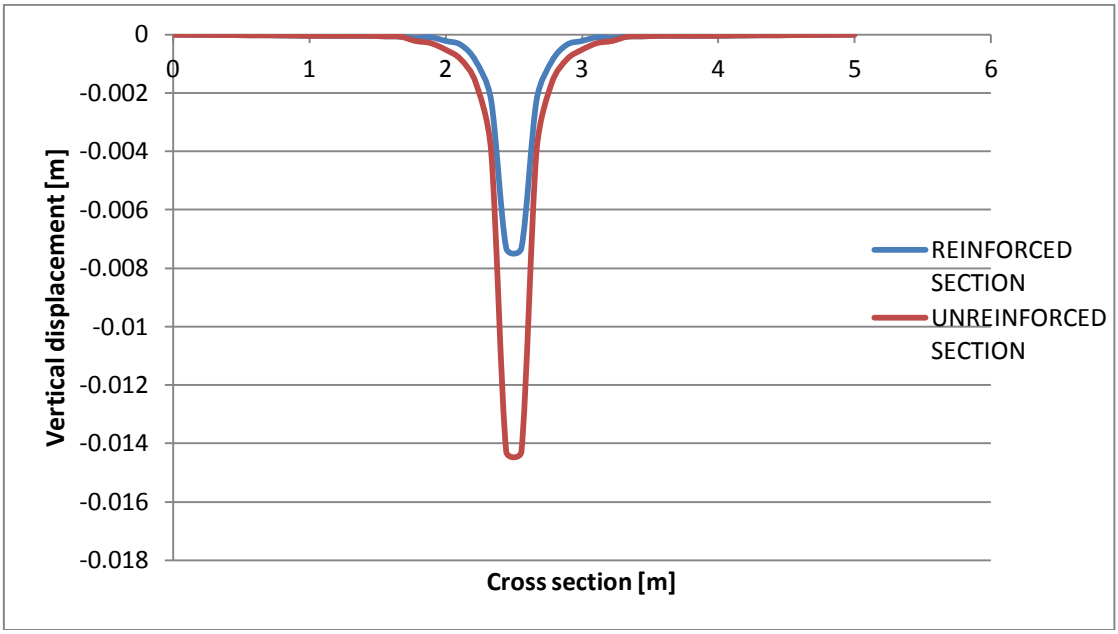

Figure 4.59 Rut evolution on the cross section

Conclusions

In the present thesis, the main road pavement degradations have been initially described highlighting the importance of the traditional maintenance operations, which should be planned and frequently done, and presenting the latest prevention techniques.

Then, different studies available in literature with respect to the reinforcement by means of geosynthetic of unpaved and paved roads systems have been introduced, after a wide presentation of the geosynthetics types employed for civil engineering applications, focusing on those used for roads pavement.

Moreover, several reinforced pavement road design procedures aiming at estimating the base course thickness of unpaved roads have been summarized and analyzed. In particular, a parametrical analysis on the Barenberg (1975), Giroud and Noiray (1981), Giroud and Han (2004) and Leng and Gabr (2005) methods has been developed varying the design parameters, such as traffic conditions, wheel loads, tire pressure, base and subgrade mechanical characteristic, allowable rut depth and geosynthetic tensile properties, in the reinforced configuration.

In general, for all the design procedures implemented it can be observed that:

- For both the reinforced and unreinforced configurations, the base course layer thickness and the benefits offered by the reinforcement decrease with the increasing of the subgrade mechanical characteristics (in terms of undrained shear strength or CBR). This result can be explained considering that if the subgrade is strong enough it can support alone the repeated vehicular traffic loads.
- Considering the same traffic conditions, geogrid tensile properties and subgrade mechanical characteristics, the increasing of allowable rut depth produces an improvement in terms of reduction of the base layer thickness. In fact, by increasing the rut the geosynthetic is more stretched and mobilizes higher tensile stresses, so that the vertical component of this tensile resistance further helps to support the applied wheel loads.
- Moreover, at equal traffic conditions, allowable rut and subgrade mechanical proprieties, the geogrid membrane support increases proportionally to the geogrids' tensile stiffness with a consequent saving of aggregate material needed for the base construction.
- For the design methods that consider the effect of traffic cyclic load (Giroud and Noiray (1981), Giroud and Han (2004) and Leng and Gabr (2005)) the unreinforced and reinforced base layer thickness, considering the same subgrade mechanical characteristics and for each allowable rut and geogrid mechanical properties, increase as the number of wheel load cycles ($N_{cycles} = 100 \div 10000$) increases.

In particular, based on the parametrical analysis carried out on the implementation of Barenberg et al. (1975) unpaved roads design procedure, the following conclusions can be drawn:

- The unreinforced base course layer thickness appears to be independent on the rut. This result confirms that the design procedure does not take intrinsically into account the mechanical characteristics of the base aggregate course, which influence the rut depth magnitude together with the wheel load. In fact, the allowed rut depth variation in the reinforced configuration appeared to be relevant only to mobilize the membrane.
- The Barenberg et al. (1975) method overlooking the base course layer mechanical properties shows its conservative nature, characterized by the determination of the pressure at base-subgrade interface based on the Boussinesq theory.
- The geogrid stiffness has no effect on the design of the reinforced base course layer thickness when the rut depth is equal to the lowest allowable value (r= 0.025 m). This behavior is due to the fact that this value of rutting is not deep enough to activate the membrane support.
- On contrary, for higher allowable rut depth values (r=0.075 m e r=0.100 m) the geosynthetic appears to supply more support to the vertical pressure due to the vehicular traffic. In particular, it works proportionally to its tensile strength, reducing the vertical pressure on the subgrade and consequently reducing the reinforced base course layer thickness when compared to the unreinforced configuration. In fact, the design curves for different values of tensile strength appear clearly distinguished between each other.
- In addition, the geogrid stiffness for Cu> 35 kN/m^2 is shown to have no effect on the reinforced base course layer thickness since the reinforcement contribution, regardless of the reinforcement stiffness, decreases with the increasing of the mechanical characteristics of the subgrade, which results to be able to carry the vehicular traffic load independently.
- Since the variation of the rut depth for fixed subgrade undrained shear strength produces only slightly higher reductions of the reinforced base course layer thickness (34%) than those obtained varying the geogrid tensile stiffness (30%), it could be concluded that the effect of the two design parameters r and $J_{2\%}$ on the Barenberg et al. (1975) model is comparable.

About the parametrical analysis carried out on the Giroud and Noiray (1981) unpaved roads design procedure, the following conclusions can be done:

- All allowable rut depth values are large enough to let the geosynthetic support the vertical pressure due to the vehicular traffic proportionally to its tensile stiffness.
- The use of reinforcement geogrids is justified only if the subgrade is enough weak. In fact, the geogrid stiffness, for Cu> 50 kN/m^2, has no effect on the reinforced base course layer thickness since the reinforcement contribution, regardless of the reinforcement stiffness, decreases with the increasing of the mechanical characteristics of the subgrade, which results to be able to carry the vehicular traffic load independently.
- By a careful analysis, it can be highlighted that the unreinforced base course layer thickness is affected by the rutting for given traffic conditions and subgrade mechanical properties. These results point out that the Giroud and Noiray (1981) design procedure takes intrinsically into

account the mechanical characteristics of the base aggregate course (assuming that the use of geogrid reinforcement improves the load distribution angle proportionally to its tensile properties), influencing the rut depth magnitude together with the wheel load. In the reinforced configurations, larger allowed rut depth lead to more mobilized membrane effects.

- The variation of the rut depth for the weakest subgrade undrained shear strength produces improvements (8%) higher than those obtained varying the geogrid tensile stiffness (19%), highlighting that the geogrid tensile properties affect this design procedure more than the allowable rut depth.
- In addition, the comparison between the Barenberg et al. (1975) and the Giroud and Noiray (1981) design methods by means of the Performance Index (PI) highlighted that, generally, the first design procedure performs better than the second does. In fact, higher PI have been obtained for the Giroud and Noiray (1981) procedure than for the Barenberg et al. (1975) method, with the largest differences for the lowest Cu values. This happens because the reinforced base layer obtained by Barenberg et al. (1975) is too high, thus the reinforcement works less. Probably this depends upon the estimation of the pressure on the substrate surface: Barenberg et al. (1975) consider a load distribution according to the Boussinesq theory and do not take into account the base mechanical characteristics, while Giroud and Noiray (1981) adopt a trapezoidal distribution of pressures taking into account the base aggregate mechanical proprieties.

The parametrical analysis carried out on the implementation of Giroud and Han (2004) design procedure led to the following considerations:

- The method takes into account the degradation of the base aggregate course mechanical characteristics by increasing the number of cyclic wheel loads, which negatively affects the amount of the wheel load distribution at base-subgrade interface and, thus, the amount of surface permanent deformations.
- The geosynthetic layer works providing a reinforcement support proportional to its own mechanical characteristic for all the depth values of rutting chosen (r = 0.050 m ÷ 0.100 m). This behavior could be explained by considering that the main reinforcement mechanisms that take place are the lateral confinement effect and the tension membrane effect. They require different depth values of rutting in order to be mobilized. At small permanent deformation magnitudes, the lateral restraint mechanism is developed by the ability of the base aggregate to interlock with the geogrid. As the permanent deformations (which are often acceptable in unpaved roads) increase the tension membrane mechanism develops. So, if the geosynthetic has a sufficiently high tensile modulus, tensile stresses are mobilized in the reinforcement, and a vertical component of this tensile membrane resistance further helps to support the applied wheel loads.

  The sensitivity of Giroud and Han (2004) unpaved reinforced design procedure on the design variables J_{AS} [mN/°] and r [m] is different. In fact, at the same design conditions, in terms of subgrade mechanical properties and traffic conditions, the geogrid aperture stability modulus has more weight than the allowable rutting.

Finally, with respect to Leng and Gabr (2006) design procedures, it could be said that:

- The procedure proposes further development in geosynthetic-reinforced unpaved roads design. In fact Leng and Gabr (2006) design procedure takes into account the effect of wheel load repetitions on degradation of elastic modulus ratio (E1/E2), in addition to the degradation of the stress distribution angle with number of cycles. This assumption makes the method more realistic because E1/E2 ratio governs how vertical stresses are distributed on the subgrade and consequently the amount of vertical subgrade deformation developed.
- The design variables, i.e. allowable rut depth and geogrids' tensile stiffness, have comparable weight on the unpaved reinforced design procedure proposed by Leng and Gabr (2006) when the subgrade mechanical properties and the traffic conditions are the same.
- The Leng and Gabr (2006) design procedure shows higher PI than the Giroud and Hann (2004) method, with average differences of about 40%.
- Comparing the results obtained with experimental field data offered by Fannin and Sigurdsson (1966), it is noteworthy that the base thickness obtained by the Leng and Gabr (2006) model and by the Giroud and Han (2004) method represent, respectively, the upper and lower bound limits of the experimental field data both in the case of unreinforced and reinforced base layers.
- Finally, all the design models have a limitation consisting in their calibration, carried out exclusively on two geogrids' types. Therefore, it would be necessary a more wide experimental investigation on different types of geogrids to obtain a wide database in order to make the design methods more general and applicable to any type of reinforcement geogrid. In addition, since the interlocking likely plays a key role in the behavior of unpaved roads, the shape and mainly the scale effect appear to be very important in the behavior of unpaved roads, too. Therefore, a more complete calibration should be developed taking into account the average size of the base particles (D_{50}) with respect to the size of the geogrid openings and to the rib thickness and profile, too. These could be further research subjects.

The last step of the present work consisted in the 3D-FEM analysis performed by using the ABAQUS software in order to evaluate the benefits offered by the geogrid in terms of reduction of the rut depth. In the analysis a number of traffic loads equal to 500 simulated through an instantaneous load has been considered. Different material models have been considered for the two layers and for the geogrid in order to better represent the real behavior. Further, the interaction at the interface between geogrid and soil and between base course and subgrade is constituted by the tangential and normal component.

Based on the results of the 3D-FEM analysis, it can be concluded that the use of the geogrid as reinforcement lead to better performances in terms of rut depth reduction of the 51% in the reinforced configuration with respect to the unreinforced case. In fact, 7.27 mm rut depths have been obtained after 500 traffic load for the reinforced configuration, whereas 14.1 have been obtained for the unreinforced configuration. It can be concluded that the presence of the geogrid leads to the reduction of the rut depth

produced by the traffic loads, thus it extends the time lag between two successive maintenance operations on the infrastructure, with a consequent saving of money and energy.

This page has been intentionally left blank

References

A New Design Method for Geosynthetic-Reinforced Unpaved Roads (Draft), Tensar Earth Technologies, Inc., March, 2001.

AASHTO Guide for the Design of Pavement Structures, American Association of State Highway and Transportation Officials, 1993.

ABAQUS (2014). User's Manual. Version 6.14. Providence, RI.

Ainalem Nega, Hamid Nikraz, Sujeewa Herath, and Behzad Ghadimi (2015) "Distress Identification, Cost Analysis and Pavement Temperature Prediction for the Long-Term Pavement Performance for Western Australia", IACSIT International Journal of Engineering and Technology, Vol. 7, No.4.

Al.Qadi et al. (2008) "Synthesis on Use of Geosynthetics in Pavements and Development of a Roadmap to Geosynthetically-Modified Pavements".

Al-Qadi, I. L., Brandon, T. L., Valentine, R.J., and Smith, T. E.(1994), "Laboratory Evaluation of Geosynthetic Reinforced Pavement Sections," Transportation Research Record 1439,Transportation Research Board, Washington DC, pp. 25-31.

Al-Qadi, I.L., Brandon, T., and Bhutta, S. (1997). "Geosynthetic Stabilized Flexible Pavements." Proc., Geosynthetics '97, Long Beach, USA, Vol. 2, 647-661.

Al-Qadi, I.L., Brandon, T., and Lacina, B. (1994). "How Do Geosynthetics Improve Pavement's Performance." Proc., Materials Engineering Conference, No. 804, Infrastructure: New Materials and Methods of Repair, 606-616.

Angelica M. Palomino, Xiaochao Tang and Shelley M. Stoffels (2010) "Determination of Structural Benefits of PennDOT-Approved Geogrids in Pavement Design FINAL REPORT".

ASTM D4439 - 15a Standard Terminology for Geosynthetics.

Austin and Coleman (1993). "A field evaluation of geosynthetic-reinforced haul roads over soft foundation soils." Proceedings of the Conference Geosynthetic, Vancouver, BC, Vol. 1: 65-80.

Barenberg, E. J., Dowland, James H. Jr., and Hales, John H.(1975) Evaluation of Soil Aggregate Systems with Mirafi Fabric. Civil Engineering Studies, Department of Civil Engineering, University of Illinois, Report No UILU-ENG-75- 2020, 52 pp.

Barksdale, R.D.(1991) “Fabrics in Asphalt Overlays and Pavement Maintenance” NCHRP Synthesis 171, National Cooperative Highway Research Program, National Research Council, Washington, D.C..

J. Bearden and J. Labuz, (1997) “Fabric for reinforcement and separation in unpaved roads”, The Minnesota Department of Transportation.

Berg, R. R., Christopher, B. R., and Perkins, S. (2000) “Geosynthetic reinforcement of the aggregate base/subbase courses of pavement structures.” Geosynthetic Materials Association White Paper II, Geosynthetic Materials Association, Roseville, Minnesota.

Bin Yu, Qing Lu and Jun Yang (2013) “Evaluation of anti-reflective cracking measures by laboratory test” Journal International Journal of Pavement Engineering Volume 14, 2013 - Issue 6.

Bloise, N., Ucciardo, S. (2000) “On site test of reinforced freeway with high-strength geosynthetics” Second European Geosynthetics Conference, vol. 1. Bologna, pp. 369–371.

Calvarano L. S., Palamara R., Leonardi G., Moraci N. (2016). Unpaved road reinforced with geosynthetics. Procedia Engineering, 158 pp 296-301, ISSN: 1877-7058- DOI:10.1016/j.proeng.2016.08.445, Ed. Elsevier.

Calvarano L.S., Palamara R., Leonardi G., 2016. Reinforced unpaved roads: parametrical analysis of design procedures. 6th European Geosynthetics Congress (EUROGEO6). Accepted for printing.

Cancelli, A., Montanelli, F., Rimoldi, P. and Zhao, A., 1996, “Full Scale Laboratory Testing on Geosynthetics Reinforced Paved Roads”, Earth Reinforcement,Proceedings of the International Symposium on Earth Reinforcement, Fukuoka, Kyushu, Japan, November 1996, pp.573-578.

Cancelli, A., Montanelli, F. (1999) “In-ground test for geosynthetic reinforced flexible paved roads”, Geosynthetics Conference, vol. 2. Boston, pp. 863–878.

Canestrari, F.; Belogi, L.; Ferrotti, G.; Graziani A. (2013) “Shear and flexural characterization of grid-reinforced asphalt pavements and relation with field distress evolution”, Materials and Structures. Ed. RILEM.

Carlos A. Lopez, P.E (2004) “Manual: Pavement Marking Handbook”, Texas Department of Transportation.

Chang D.T.-T.; Lai R.-Q.; Chang J.-Y.; and Wang Y.-H. (1998) “Effects of geogrid in enhancing the resistance of asphalt concrete to reflection cracks”, ASTM STP 1348, American Society for Testing and Materials, p. 39-51.

Christopher B. R., (2010) “Geogrids in roadway and pavement systems” NAUE GmbH & Co. KG, Global Synthetics Pty Ltd.

Collin J.G., Kinney T.C., Fu X. (1996) “Full scale highway load test of flexible pavement systems with geogrid reinforced base courses”, Geosynthetics International, 3 pp. 537–549.

Dondi, G., (1994). “Three-dimensional finite element analysis of a reinforced paved road.” Proceedings of the Fifth International Conference on Geotextiles, Geomembrane and Related Products, Singapore, pp. 95-100.

Eisenmann, J. and Hilmar, A. (1987),” Influence of wheel load and inflation pressure on the rutting effect of asphalt pavements - Experiments and theoretical investigations”, Proceedings of the Sixth International conference on structural design of asphalt Pavements, Vol. 1, Ann Arbor, Michigan.

Elhakeem, A. and T, Hegazy., (2005). Improving Deterioration Modeling using Optimized Transition Probability Matrices for Markov Chains. 84th Annual Meeting of the Transportation Research Board , Paper No.12-2878, Washington, D.C.

Faheem and Hassan (2014) “2d plaxis finite element modeling of asphalt-concrete pavement reinforced with geogrid” Journal of Engineering Sciences Assiut University Faculty of Engineering Vol. 42 No. 6 November 2014 PP. 1336 – 1348

Fannin, R. J., and O. Sigurdsson (1966). “Field Observations on Stabilization of Unpaved Roads with Geosynthetics”. Journal of Geotechnical Engineering, Vol. 122, pp. 544–553.

Federal Highway Administration (1998) “Pavement Condition Index Distress Identification Manual for Asphalt and Surface Treatment Pavements”. ‖ Federal Highway Administration, United States Department of Transportation.

Federal Highway Administration (FHWA) (1989), 'Pavement Management Systems Manual', FHWA, Washington, D.C.

Francken, L., Vanelstraete, A. and de Bondt, A.H. (1997) “Modelling and Structural Design of Overlay Systems.” RILEM Report 18: Prevention of Reflective Cracking in Pavements, Vanelstraete, A. and Francken, L. (editors). E & FN Spon, London, 84–103.

Giroud, J. P., and Noiray, L. (1981). Geotextile-reinforced unpaved road design. Journal of Geotechnical and Geoenvironmental Engineering, 107, No. 9, 1233-1254.

Giroud, J. P. (2009) "An assessment of the use of geogrids in unpaved roads and unpaved areas." Jubilee Symposium on Polymer Geogrid Reinforcement. Identifying the Direction of Future Research, ICE, London, 8th September.

Giroud, J. P., and Han, J. (2004). Design method for geogrid-reinforced unpaved roads. I: Development of design method. Journal of Geotechnical and Geoenvironmental Engineering, 130, No. 8,775-786.

Graziani A., Pasquini E., Ferrotti G., Virgili A. and Canestrari F. (2014) "Structural response of grid-reinforced bituminous pavements" materials and structures journal .

Haas, R ., Hudson, W.R. and Zaniewski, J. (1994): "Modern Pavement Management". Kriegler Publishing Company, Malabar, Florida.

Haas, R., Walls, J. and Carroll, R. G. (1988). Geogrid reinforcement of granular bases in flexible pavements. Transportation Research Record, 1188,19-27.

Heukelom, W. and Klomp, A.J.G. (1962), "Dynamic Testing as a Means of Controlling Pavements During and After Construction", Proc. of the First International Conference on Structural Design of Asphalt Pavements, University of Michigan, pp. 667-679.

Johanns, M., & Craig, J. (2002). Pvement Maintenance Manual. In N. D. o. Roads (Ed.). United State of America: Nebraska Department of Roads.

Johnson M. (2000) "Best practices handbook on asphalt pavement maintenance", llnivcrsity of Minnesota Center for Transportation Studies.

Klompmaker J. and Partridge A. (2009) "Improvement of Long Term Performance of Temporary and Permanent Traffic Areas Using Composite Geogrid Reinforcement" GIGSA GeoAfrica 2009 Conference Cape Town 2 - 5 September 2009

Koerner, R. M. (1990) "Designing With Geosynthetics, Third Edition", Prentice-Hall Inc. NJ.

Leng, J. & Gabr, M.A., 2005. Deformation-resistance Model for Geogrid-Reinforced Unpaved Road. Journal of the Transportation Research Board, No. 1975, Transportation Research Board of the National Academies, Washington, D.C., 2006, pp. 146–154.

Lytton, R.L. (1989). "Use of Geotextiles for Reinforcement and Strain Relief in Asphalt Concrete." Geotextiles and Geomembranes, Vol. 8, 217-237.

Miura N., Sakai A., Taesiri Y., Yamanouchi T., Yasuhara K. (1990) "Polymer grid reinforced pavement on soft clay ground Geotextiles and Geomembranes", 9 (1), pp. 99–123.

Montanelli, F., Zhao, A. and Rimoldi, P., 1997, "Geosynthetic-Reinforced Pavement System: Testing and Design", Proceedings of Geosynthetics '97, IFAI, Vol. 2, Long Beach, California, USA, March 1997, pp. 619-632.

Montestruque, G. M. V.; Rodrigues R.; Nods M.; Elsing A. (2004) " Stop of reflective crack propagation with the use of PET geogrid as asphalt overlay reinforcement", Proceedings 5th RILEM International Conference Cracking in Pavement, Mitigation, Risk Assessment and Prevention. Limoges, France, pp. 231-238.

Muhammad Ali Mubaraki (2010) "Predicting Deterioration for the Saudi Arabia Urban Road Network".

Nazzal, M. D., Abu-Farsakh, M. Y. and Mohammad, L. N., (2010). "Implementation of a critical state two-surface model to evaluate the response of geosynthetic reinforced pavements." International Journal of Geomechanics, Vol. 10, No. 5, p202-212.

Nirmal Dhakala, Mostafa A. Elseifia, Zhongjie Zhangb (2016) "Mitigation strategies for reflection cracking in rehabilitated pavements – A synthesis" International Journal of Pavement Research and Technology Volume 9, Issue 3 Pages 228–239.

Oddur Sigurdsson (1991) "Geosynthetic Stabilization of Unpaved Roads on Soft Ground :a Field Evaluation".

Perkins, S.W., and Ismeik, M.(1997) "A synthesis and evaluation of geosynthetic-reinforced base layers in flexible pavements: part 2." Geosynthetics International. 4, 605-621.

Perkins, S.W., Ismeik, M., Fogelsong, M.L., Wang, Y., Cuelho, E.V. (1998) "Geosynthetic-reinforced pavements—overview and preliminary results", Sixth International Conference on Geosynthetics, vol. 2. Atlanta, pp. 951–958.

Perkins, S.W. (1999). "Geosynthetic Reinforcement of Flexible Pavements: Laboratory Based Pavement Test Sections." Report No. FHWA/MT-99-001/8138, U.S. Department of Transportation, Federal Highway Administration, Washington, D.C.

Perkins, S. W. (2000). “Mechanistic-empirical modeling and design model development of geosynthetic reinforced flexible pavements.” Montana Department of transportation, Helena, Montana, Report No. FHWA/MT-01-002/99160-1A.

Perkins, S.W., and Edens M.Q. (2003) “Finite Element and Distress Models for Geosynthetic-reinforced Pavements” International Journal of Pavement Engineering 3(4):239-250

Roberts, F.L., P.S. Kandhal, E.R. Brown, D.Y. Lee, and T.W. Kennedy (1996) “Hot Mix Asphalt Materials, Mixture Design and Construction”,NAPA Research and Education Foundation, Lanham, Maryland.

Robinson, R., Danielson, U., & Snaith, M. (1998). ROAD MAINTENANCE MANAGEMENT CONSEPTS AND SYSTEMS. New York: Palgrave.

Saad, B., Mitri, H., and Poorooshasb, H., (2005). “Three-Dimensional Dynamic Analysis of Flexible Conventional Pavement Foundation”. In Journal of Transportation Engineering.

Salman Ahmed Bhutta (1998) “Mechanistic-Empirical Pavement Design Procedure For Geosynthetically Stabilized Flexible Pavements”.

Siriwardane, H.; Gondle, R.; Bora K. (2010) “Analysis of flexible pavements reinforced with geogrids”, Geotechnical and Geological Engineering. Vol. 28, p. 287-297.

Stephen Archer, P.E. Texas Department of Transportation Austin “Geosynthetic Reinforcement for Shoulder Widening & Rehabilitation Project” 0-6748 Best Practices, July 2, 2013.

U.S. Federal Highway Administration, (2000) “Insights into Pavement Preservation”.

Wathugala, G. W., and Desai, C. S. (1993) “Constitutive model for cyclic behavior of clays. I: theory.” Journal of Geotechnical Engineering, Vol.119 (4): 714‑729.

Wathugala, G. W., Huang, B., and Pal, S. (1996).“Numerical simulation of geosynthetic reinforced flexible pavement.” Transportation Research Record 1534, Transportation Research Board, national Research Council, Washington, DC, USA, pp.58-65.

Webster, S.L., (1992) “Geogrid Reinforced Base Courses For Flexible Pavements For Light Aircraft, Test Section Construction, Behavior Under Traffic, Laboratory Tests, and Design Criteria”, Technical Report GL-93-6, U.S. Army Corps of Engineers, Waterways Experiment Station, Vicksburg, Mississippi, USA.

Webster, S. L., and Alford, S. J. (1978). “Investigation of construction concepts for pavements across soft ground.” Technical Report S-78-6. U.S. Army Corps of Engineers Waterways Experiment Station, Vicksburg, Miss.

Webster, S. L., and Watkins, J. E. (1977) “Investigation of construction techniques for tactical bridge approach roads across soft ground : final report. (No. Tech Rpt. S-77-1). United States. Army. Corps of Engineers.; Soils and Pavements Laboratory (U.S.).

Wen-Chao Huang (2014). ”Improvement evaluation of subgrade layer under geogrid-reinforced aggregate layer by finite element method” International Journal of Civil Engineering, Vol. 12, No. 3, Transaction B: Geotechnical Engineering, July 2014.

Wilde W James., Thompson Luke, and Wood Thomas J. (2014) “Cost-Effective Pavement Preservation Solutions for the Real World” Center for Transportation Research and Implementation Minnesota State University, Mankato.

Web site
www.pavementinteractive.org
www.lgam.info
www.tenax.net
www.geofabrics.co.nz